WARSAW UNIVERSITY OF TECHNOLOGY

DISCIPLINE OF ENGINEERING AND TECHNOLOGY

FIELD OF AUTOMATION, ELECTRONIC, ELECTRICAL ENGINEERING

AND SPACE TECHNOLOGIES

Ph.D. Thesis

Kamil Jan Możdżyński, M.Sc.

Fault-tolerant and resistant to grid voltage distortion 4-leg DC/AC converter applied to Power Electronics Transformer

Supervisor

prof. PhD. eng. Mariusz Malinowski

Assistant Supervisor

PhD. eng. Sebastian Styński

WARSAW 2025

Acknowledgements

I would like to extend my heartfelt thanks to my wife Ewelina, and to my family and friends, for their spiritual support, motivation, and constant encouragement. Your presence meant the world to me, especially in moments of hardship and exhaustion.

A special word of gratitude goes to my Supervisor, Prof. Mariusz Malinowski, and Assistant Supervisor PhD. Sebastian Styński for their invaluable support, valuable guidance, patience and assistance at every stage of my research work. Their knowledge, commitment, and openness to my ideas had a huge impact on the shape of the final version of this dissertation.

I am truly grateful to all members of the research team for their support and collaboration throughout the course of this project.

I am also deeply grateful to Prof. Remigiusz Rak for the opportunity and trust he extended to me at the outset of my doctoral studies.

It is also impossible not to mention all my co-workers and colleagues at Institute of Control and Industrial Electronics, who were always there to help and share their insights.

I am deeply grateful to the Institute of Control and Industrial Electronics at the Warsaw University of Technology for the financial and organizational support provided throughout my research. Without this support, the successful completion of the project would not have been possible.

Thank you all for being part of this journey with me.

Kamil Możdżyński

Niniejszą pracę dedykuję całej mojej Rodzinie

Streszczenie rozprawy doktorskiej

Sieć elektroenergetyczna nieprzerwanie ewoluuje i się rozwija, co rodzi wyzwania w efektywnym zarządzaniu energią elektryczną, szczególnie w obszarze niskiego napięcia. Kluczowym problemem jest integracja rozproszonych odnawialnych źródeł energii (OZE) o małej mocy, których produkcja energii charakteryzuje się losowym profilem, silnie zależnym od warunków atmosferycznych.

Obecnie stosowane transformatory dystrybucyjne, zaprojektowane do pracy przy częstotliwości 50 Hz, działają w sieciach, które nie są przystosowane do efektywnego zarządzania energią pochodzącą z odnawialnych źródeł oraz do jej magazynowania. Dlatego istnieje pilna potrzeba opracowania i wdrożenia nowej klasy urządzeń energoelektronicznych, które umożliwią lokalne zarządzanie energią elektryczną oraz regulację przepływu energii między sieciami o różnych poziomach napięcia i różnych typach – prądu przemiennego (AC) i stałego (DC).

Odpowiedzią na te wyzwania są badania nad technologią transformatorów wspieranych przez urządzenia energoelektroniczne, określanych w literaturze jako transformatory energoelektroniczne lub inteligentne transformatory. Ta zaawansowana technologia umożliwia wprowadzenie wielu dodatkowych usług do sieci dystrybucyjnych, przede wszystkim w kontekście integracji rozproszonych źródeł energii oraz zasobników. W rzeczywistości, urządzenia te pełnią funkcję routera energii elektrycznej, oferując szereg korzyści dla sieci dystrybucyjnej:

- separacja podsieci elektroenergetycznej i dwukierunkowa transmisja energii z główną siecią dystrybucyjną,
- poprawa efektywności zarządzania energią poprzez skrócenie drogi transmisji między producentami a konsumentami,
- zarządzanie bilansem energii w podsieci elektroenergetycznej i dostosowanie profilu odbioru i dostarczania energii elekrycznej do sieci dystrybucyjnej w celu utrzymania najkorzystniejszej taryfy,
- praca w dwóch trybach:
  - tryb formowania napięcia sieci, określany jako praca wyspowa,
  - tryb wspierania danego punktu sieci znacznie oddalonego od głównego źródła.
- zapewnienie wysokiej jakości napięcia i prądu w sieci elektroenergetycznej oraz zarządzanie bilansem energii elektrycznej.

Transformator energoelektroniczny składa się z wielu przekształtników AC/DC i DC/AC połączonych z transformatorem średniej lub wysokiej częstotliwości (10–200 kHz). Mimo licznych korzyści, transformatory energoelektroniczne nie są powszechnie stosowane, głównie z powodu problemów technicznych związanych z zapewnieniem niezawodności konstrukcji oraz skomplikowanym sterowaniem. Dla tradycyjnych transformatorów dystrybucyjnych wymagana długość cyklu życia wynosi kilkadziesiąt lat. Wdrożenie nowej technologii wiąże się również z koniecznością utrzymania standardów zapewniających odpowiednią moc zwarciową do uruchomienia automatyki zabezpieczeniowej.

Urządzenia energoelektroniczne charakteryzują się zwiększoną podatnością na uszkodzenia z powodu stosunkowo niskich parametrów wytrzymałości napięciowej i prądowej. Istnieje wysokie ryzyko, że w trakcie pracy systemu energoelektronicznego dany element może ulec uszkodzeniu, co prowadzi do przerwania funkcjonowania całego systemu. W związku z tym konieczne jest opracowanie systemu zdolnego do pracy w warunkach awaryjnych, który pozwoli na utrzymanie ciągłości przetwarzania energii elektrycznej bez pogorszenia jakości parametrów.

Aby zapewnić zdolność do działania w stanach awaryjnych oraz zwiększyć wydajność prądowo-napięciową, konieczne jest wdrożenie modułowej struktury systemu. To z kolei pociąga za sobą rozproszenie układu sterowania oraz konieczność synchronizacji przełączeń tranzystorów w odrębnych przekształtnikach energoelektronicznych.

Celem niniejszej rozprawy jest identyfikacja i analiza wspomnianych problemów oraz przedstawienie propozycji rozwiązań, które prowadzą do opracowania systemu przetwarzania DC/AC niskiego napięcia w zastosowaniu dla transformatora energoelektronicznego zdolnego do pracy w warunkach awaryjnych. Praca ta prezentuje zagadnienia związane z niezawodnością konstrukcji oraz sterowaniem równolegle połączonych przekształtników czterogałęziowych DC/AC.

Aby osiągnąć wymaganą niezawodność systemu, należało uwzględnić trzy kluczowe aspekty projektowania modułowych systemów energoelektronicznych: topologię, układ sterowania oraz system komunikacji, z uwzględnieniem ich wpływu na bezawaryjność działania.

Niezawodność topologii została osiągnięta dzięki zastosowaniu mechanizmów rekonfiguracji gałęzi modułów przekształtnikowych DC/AC, co przynosi następujące korzyści:

- utrzymanie ciągłości działania systemu w stanach awaryjnych,
- dopasowania wydajności systemu do potrzeb sieci niskiego napięcia,

- zrównoważenia obciążenia wszystkich półprzewodników w module w celu wydłużania cyklu życia całego modułu.

Możliwość rekonfiguracji systemu wymagała zaprojektowania rozproszonego układu regulacji zarządzającego liczbą aktywnych modułów i gałęzi tranzystorowych, jak również scenariuszy załączania i odłączania gałęzi tranzystorowych od sieci prądu przemiennego.

Niezawodność z punktu widzenia układu sterowania dotyczy stabilnej pracy systemu pod wpływem zaburzeń prądów i napięć oraz zmiennej impedancji systemu. Stopień niskiego napięcia transformatora energoelektronicznego jest zdolny do pracy w dwóch trybach:

- tryb formowania napięcia sieci jako główne źródło zasilania sieci niskiego napięcia, w której odbiorniki mają nieznany charakter (priorytetem jest tu utrzymanie nieodkształconego i symetrycznego napięcia nawet pod wpływem nieliniowego i asymetrycznego obciążenia),
- tryb wspomagania sieci dystrybucyjnej w danym punkcie poprzez niezawodne dostarczanie energii i kompensację mocy biernej.

W celu utrzymania stabilności oraz jakości napięć i prądów przedstawiono prosty układ kompensacji zaburzeń pracujący równolegle do regulatora prądu.

Cały system został zintegrowany z wykorzystaniem sieci komunikacyjnej EtherCAT, spełniającej wymagania pracy w czasie rzeczywistym. Interfejs ten umożliwia implementację rozproszonego układu sterowania z zachowaniem synchronizacji pomiędzy modułami. Dodatkowo, system komunikacji został oceniony pod kątem odporności na przerwy w transmisji danych, a zastosowana topologia zapewnia możliwość dalszego działania systemu mimo zakłóceń w łączności.

Komunikacja w systemie ma na celu przekazanie minimalnego zbioru zmiennych procesowych wymienianych między przekształtnikami DC/AC a centralnym sterownikiem. Proponowane rozwiązania zostały zweryfikowane zarówno w modelach symulacyjnych, jak i w eksperymentach.

Słowa kluczowe: Transformator Energoelektroniczny, Odporność na uszkodzenia, Sterowanie rozproszone, Regulacja napięcia i prądu, Rekonfiguracja systemu energoelektronicznego.

Abstract

The power grid is continuously evolving and developing, which poses challenges in the effective management of electrical energy, particularly in the low-voltage domain. A key problem is the integration of small-scale distributed renewable energy sources (RES), whose energy production is characterized by a random profile, strongly dependent on atmospheric conditions.

Currently used distribution transformers, designed for operation at 50 Hz, are implemented in networks that lack the capability for effective management and storage of energy generated from renewable energy sources (RES). This creates an urgent need for the development and deployment of a new class of power electronic devices that can provide localized energy management while also enabling controlled energy transmission between networks operating at different voltage levels and using different current types (AC or DC).

Research on the technology of transformers supported by power electronic devices, referred to in the literature as power electronic transformers or smart transformers, offers a response to these challenges. This advanced technology enables the introduction of many additional services to distribution networks, primarily in the context of integrating distributed energy sources and storage systems. In fact, these devices function as an electrical energy router, offering a range of benefits for the distribution network:

- separation of the power sub-network and bidirectional energy transmission with the main distribution network,
- improved energy management efficiency by shortening the transmission path between producers and consumers,
- management of the energy balance in the power sub-network and adjustment of the electricity consumption and supply profile to the distribution network to maintain the most favorable tariff,
- operation in two modes:
  - network voltage forming mode, referred to as island operation,
  - support mode for a network point located far from the main source.
- ensuring high voltage and current quality in the power grid and managing the electrical energy balance.

A power electronic transformer consists of multiple AC/DC and DC/AC converters connected to a medium or high-frequency transformer (10–200 kHz). Despite numerous

benefits, power electronic transformers are not widely used, mainly due to technical problems related to ensuring the reliability of the design and complex control. For traditional distribution transformers, the required lifespan is several decades. The implementation of new technology also involves the need to maintain standards ensuring adequate short-circuit power for the activation of protective automation.

Power electronic devices are characterized by increased susceptibility to damage due to relatively low voltage and current withstand parameters. There is a high risk that during the operation of a power electronic system, a component may fail, leading to the interruption of the entire system's operation. Therefore, it is necessary to develop a system capable of operating in fault conditions, which will allow for maintaining the continuity of electrical energy processing without degrading the quality of parameters.

To ensure the ability to operate in fault conditions and increase current and voltage efficiency, it is necessary to implement a modular system structure. This, in turn, entails the distribution of the control system and the need for synchronization of transistor switching in separate power electronic converters.

The aim of this dissertation is to identify and analyze the aforementioned problems and present proposed solutions that lead to the development of a low-voltage DC/AC processing system for a power electronic transformer capable of operating in fault conditions. This work presents issues related to the reliability of the design and the control of parallel-connected four-leg DC/AC converters.

To ensure the required system reliability, it was necessary to consider ensuring fault tolerance in three basic aspects of modular power electronic system design: topology, control system, and communication system.

The reliability of the topology was achieved by introducing reconfiguration mechanisms for the DC/AC converter branches, which provides the following benefits:

- maintaining the continuity of system operation in fault conditions,
- matching the system performance to the needs of the low-voltage network,
- balancing the load of all semiconductors in the module to extend the lifespan of the entire module.

The possibility of system reconfiguration required the design of a distributed control system managing the number of active modules and transistor branches, as well as scenarios for connecting and disconnecting transistor branches from the AC network.

Reliability from the perspective of the control system concerns the stable operation of the system under the influence of current and voltage disturbances and variable system impedance. The low-voltage side of the power electronic transformer is capable of operating in two modes:

- network voltage forming mode as the main power source for the low-voltage network, where the loads have an unknown character (the priority here is to maintain an undistorted and symmetrical voltage even under non-linear and asymmetrical loads).
- distribution network support mode at a given point by reliably supplying energy and compensating reactive power.

To maintain stability and the quality of voltages and currents, a simple disturbance compensation system operating in parallel with the current regulator is presented.

The entire system is connected via an EtherCAT communication system that meets real-time constraints. The EtherCAT interface enables the implementation of a distributed control system with synchronization. Additionally, the communication system has been evaluated for its ability to operate in the event of data transmission interruptions, and the selected topology allows for the continued functioning of the system.

The communication in the system aims to transmit a minimal set of process variables exchanged between the DC/AC converters and the central controller. The proposed solutions have been verified both in simulation models and in experiments.

TABLE OF CONTENTS

List of publications

Publications related to the completion of the doctoral dissertation:

1. A. Milczarek, K. Możdżyński, M. Malinowski and S. Styński, „Effective and Simple Control of Grid-Connected Three-Phase Converter Operating at a Strongly Distorted Voltage", IEEE Access, vol. 8, 2020, pp. 12307-12315,

2. M. Malinowski, K. Możdżyński, T. Gajowik, and S. Styński, „Fault tolerant smart transformer in distributed energy systems", Conference on Sustainable Energy Supply and Energy Storage Systems, NEIS 2019,

3. K. Możdżyński, M. Malinowski and S. Styński, „Simple grid current control under strongly distorted grid voltage", IECON 2017 - 43rd Annual Conference of the IEEE Industrial Electronics Society, Beijing, China, 2017, pp. 5380-5385,

4. K. Możdżyński, M. Malinowski, and S. Styński, „Modified Voltage Oriented Control Resistant to Grid Voltage Disturbances", 3rd IEEE Annual Southern Power Electronics Conference 2017, Puerto Varas, Chile.

Other publications:

1. K. Możdżyński, K. Rafał and M. Bobrowska-Rafał, Engineering, „Application of the second order generalized integrator in digital control systems", Archives of Electrical Engineering vol. 63(3), 2014, pp. 423-437,

2. K. Możdżyński, „Simple digital integration algorithm with saturation and drift elimination based Second-Order Generalized Integrator", 2015 9th International Conference on Compatibility and Power Electronics, Costa da Caparica, Portugal, 2015, pp. 312-316,

3. A. Milczarek and K. Możdżyński, „A Unified Data Profile for Microgrid Loads, Power Electronics, and Sustainable Energy Management with IoT", Energies, vol. 17(6), 2024, pp. 1277-1293,

4. K. Mozdzynski, T. Gajowik, M. Malinowski, S. Bayhan and H. Abu-Rub, „Control of grid connected H-bridge quasi-Z source converter with compensation of current distortion at minimized passive components", IEEE 12th International Conference on Compatibility, Power Electronics and Power Engineering, Doha, Qatar, 2018,

5. T. Gajowik, K. Możdżyński, M. Malinowski, H. Abu Rub and K. Ghazi, „SiC Mosfet versus Si IGBT based H-Bridge quasi Z Source converter", 12th IEEE International Conference on Compatibility, Power Electronics and Power Engineering, 2018, Doha, Quatar.

List of projects

Projects related to the doctoral dissertation:

1. "Highly efficient and fault tolerant SiC-based smart transformer in distributed energy systems", Foundation for Polish Science, TEAM TECH/2016-1/5.

Other projects:

1. „Uniwersalne algorytmy regulacji prądu dla energoelektronicznych przekształtników sieciowych AC/DC odporne na zaburzenia własne i zaburzenia napięcia sieci elektroenergetycznej", National Science Centre, UMO-2018/31/B/ST7/00954,

2. „1-MW PV Power RD&D Using SiC based qZS Cascade Multilevel Inverter and Battery Energy Storage", NPRP-EP X-033-2-007,

3. „Opracowanie i walidacja modelu laboratoryjnego robota kosmicznego zawierającego układ silników resistojet, Zadanie:Projekt i budowa układu zasilania silników resistojet w energię elektryczną", PAN, PBS3/A3/22/2015,

4. „Opracowanie i wdrożenie technologii Małych Elektrowni Wiatrowych o mocach 5kW i 10kW", Narodowy Fundusz Ochrony Środowiska i Gospodarki Wodnej, GEKON1/04/213398/22/20.

Abbreviations

3L – Three Level

AC – Alternate Current

ASIC – Application Specific Integrated Circuit

CPT – Conventional Power Transformer

DC – Direct Current

ESC – EtherCAT Slave Controller

FC – Flying Capacitor

HFT – High Frequency Transformer

LV – Low Voltage

MF – Medium Frequency

MFT – Medium Frequency Transformer

MTTF – Mean Time to Failure

MV – Medium Voltage

NPC – Neutral Point Clamped

PCC – Point of Common Coupling

PEBB – Power Electronics Building Block

PET – Power Electronics Transformer

PI – Proportional Integral

PLL – Phase Locked Loop

PR – Proportional Resonant

PWM – Pulse Width Modulation

RMS – Root Mean Square

SiC – Silicon Carbide

SG – Smart Grid

ST – Smart Transformer

SST – Solid-State Transformer

TC – Transistor Clamped

THD – Total Harmonics Distortion

1. Introduction

Currently, the development of the electric power industry mainly seeks to reduce environmental pollution and increase the availability of electricity. To achieve these two objectives, the centralized electric power system is gradually being transformed into a distributed system by increasing local electrical energy microgeneration and storage [1], [2]. This way, the energy transmission path is significantly shortened, reducing energy losses in the transmission network (**Figure 1**). In addition, local distribution networks become independent of only one energy supplier. Microgeneration may involve the acquisition of energy from renewable sources, its storage, and subsequent recovery, exemplified by energy derived from rail vehicle braking processes [3], [4]. The transformation of the energy system is particularly noticeable in the growth of domestic photovoltaic installations [5]. Household energy can completely cover local load needs, while the surplus should be stored or given back to the grid. In a situation where the energy must be injected into the grid, the voltage may increase. As a result of exceeding the normative voltage threshold, photovoltaic installations must be disconnected to protect equipment on the grid. This phenomenon hampers the development and profitability of photovoltaic installations [6].
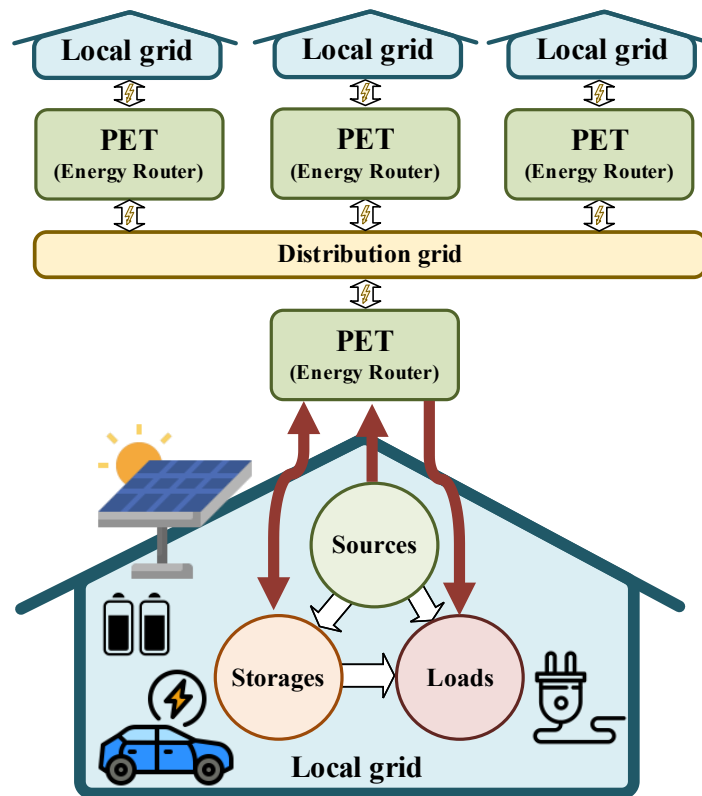

Figure 1. Power electronics transformer role in distribution grids.

Increased energy availability is associated with reduced dependence on the power system. Domestic installations are striving for energy self-sufficiency [7]. However, developing and implementing a new class of power electronic devices is necessary to achieve this. These devices must ensure the integrity of all types of equipment in the local installation by properly managing energy distribution between sources, storage, and loads [8].

Local energy management increases energy availability because it is no longer dependent on the condition of the grid and the main transformer. Developing the power distribution network towards microgrids for enhanced electricity management efficiency requires the implementation of power electronic devices that can [9]:

- manage local energy flows effectively [10],
- process energy bidirectionally across network interfaces [11],
- generate voltage for a specific microgid, thereby enabling grid-forming mode [12], [13],
- offer supplementary services related to the advantageous utilization of electric vehicle charging and energy storage profiles for grid support called Vehicle-to-Grid (V2G) [14],
- maintaining a high quality of voltage and current with reactive power compensation (grid-supporting mode) [15], [16],

The conditions listed above can only be met by power electronics converters. The combination of solid-state technology with a digital control unit and a medium-frequency transformer provides the ability to actively control current and voltage on both sides of the converter. The resulting technology is a Power Electronic Transformer (PET) [17]. It is also referred to in the literature as Solid-State Transformer (SST) and Smart Transformer (ST) [18].

Advancements in semiconductor technology enable higher switching frequencies, increased blocking voltages, and higher conduction currents. Additionally, modern microcontroller units offer greater computing power, making it possible to implement complex multi-threaded control algorithms, multi-channel synchronized measurements, and efficient distribution of control signals.

The combination of a high-performance embedded control unit with high-frequency switched semiconductors enhances control capabilities while reducing the size of passive components. However, power electronic converters have a complex architecture with many vulnerable elements, requiring a high degree of reliability. When replacing Conventional Power

Transformers (CPT) with Power Electronics Transformers, it is essential to maintain the same level of reliability.

Achieving this requires integrating additional mechanisms to enhance converter reliability at every design stage, including the power module, control unit, and communication system. A well-designed converter system should anticipate potential failures and incorporate reliability mechanisms that ensure continuous operation, even in post-fault conditions.

1.1. Energy distribution system development

The integration of PET into the power grid represents a technological revolution, offering significant benefits for efficient energy management. Traditional power systems primarily enable unidirectional energy transmission over long distances, leading to substantial power losses along transmission lines (**Figure 2**). In addition, power losses are increased by the lack of reactive power compensation. Any transformer or line damage interrupts energy delivery.
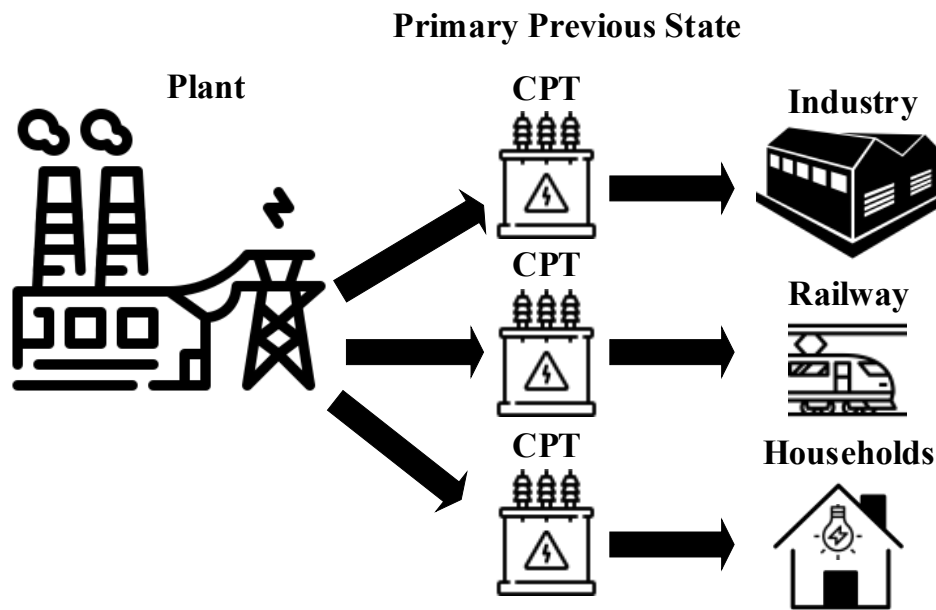
Primary Previous State

Figure 2. Previous power system state.

The current power system increasingly incorporates distributed renewable energy sources, including energy storage systems. Additionally, some energy is recovered from industrial processes (**Figure 3**). However, the distribution system remains largely unmanageable, as most devices lack communication capabilities for effective energy management.
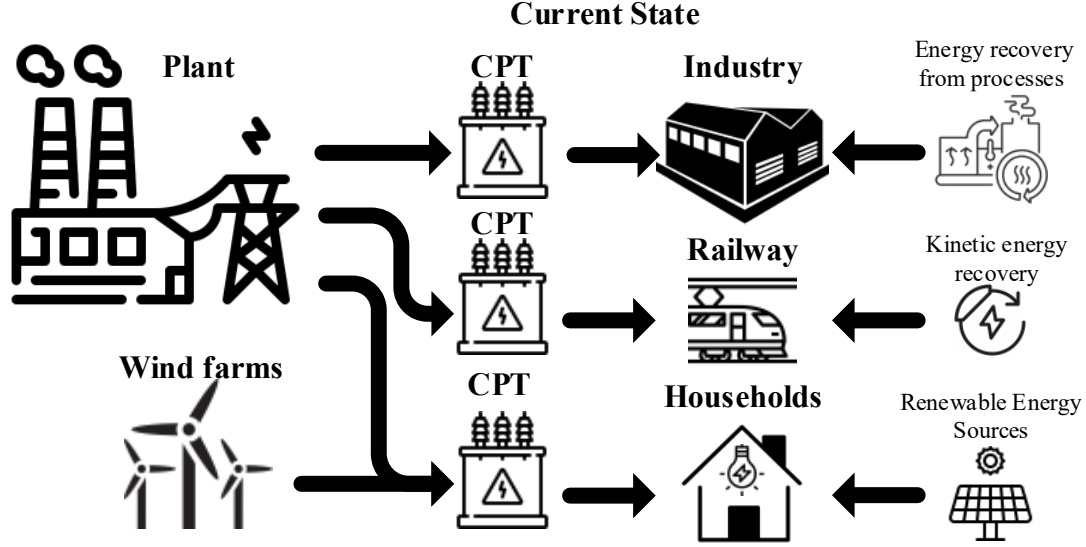
Figure 3. The current state of electrical energy distribution grid.

In the near future (**Figure 4**), power electronic systems will be gradually implemented to support CPT. Due to its high reliability and efficiency at close to nominal power, CPT continues to provide more significant benefits. Power electronics modules can extend the CPT's functionality to include load management, disturbance, and reactive power compensation capabilities. The mentioned solution is called Hybrid Transformer [19]. In this way, the energy distribution grid becomes an active distribution grid.

The replacement of CPT by PET will enable complete management of energy distribution at the expense of increased complexity. It will also be possible to multiport coupling MV and LV grids. In addition, it will be possible to connect DC grid. The future goal is multidirectional power flow to optimize energy utilization [20]. Large central generators won't be necessary for energy trading.

The average lifecycle of a power transformer is 40 years [1]. Therefore, the PET must show similar reliability due to its critical role in the distribution grids. Semiconductor devices are sensitive to overvoltage's, overcurrent's, and thermal cycling. A particular challenge is to balance the load of all semiconductors in order to maximize the system life cycle. Damage detection mechanisms and scenarios for maintaining system operation should also be developed. The **Table 1** summarizes the advantages and disadvantages of successive stages of transformer-based energy conversion development.
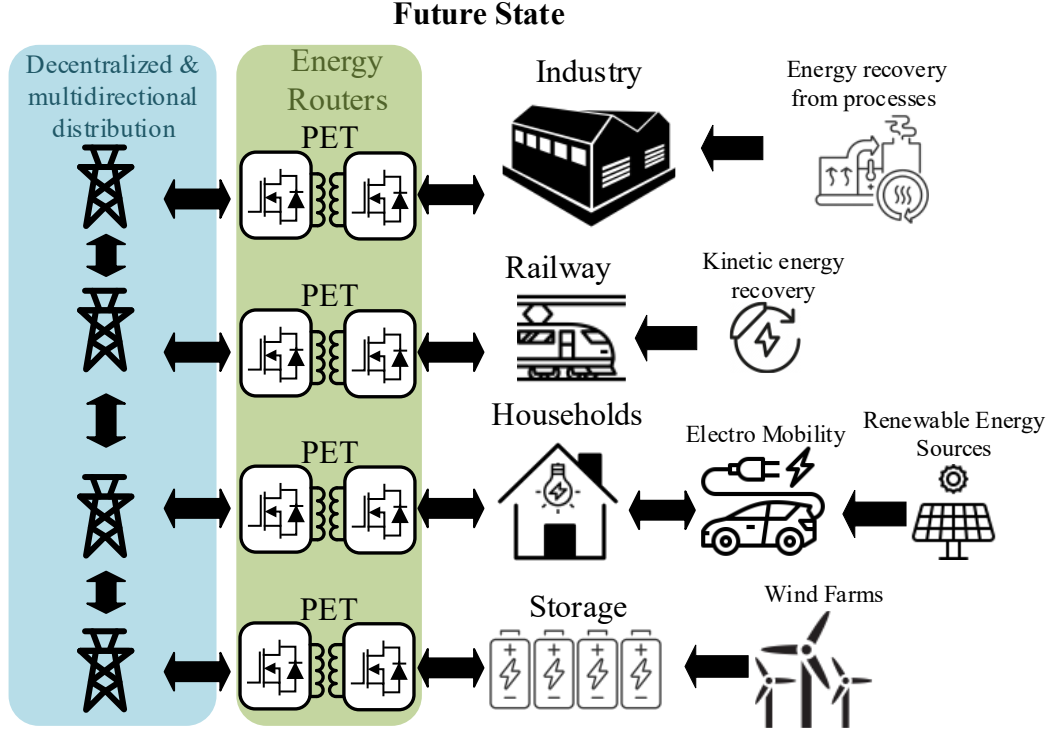
Figure 4. Example of future state of electrical energy distribution grid.

Table 1. Summary of transformer technology development stages.

State	PREVIOUS	CURRENT	NEAR FUTURE	FUTURE
Technology	Distribution Transformer	Distribution Transformer	Hybrid Transformer	Power Electronics Transformer
Advantages	• simple • robust • high short circuit current	• simple • robust • monitored • high short circuit current	• digital control • disturbance compensation • high short circuit current • monitored	• multidirectional • digital control • disturbance compensation • managed RES • monitored
Drawbacks	• unmonitored	• unmanaged RES • single MV/LV port	• unmanaged RES • complex	• complex • limited overload

1.2. Power Electronics Transformer structure

The PET system comprises multiple power electronics modules equipped with medium- or high-frequency transformers (MFT or HFT). The higher the voltage frequency at the transformer terminals, the smaller the transformer size that can be achieved for a given power level. The PET architecture is typically categorized into three main types based on the number of conversion stages: single-stage, dual-stage, and three-stage topologies [2]. The single-stage topology is designed to perform voltage transformation directly using power electronic

converters in combination with MFT or HFT (**Figure 5a**). The two-stage topology introduces a low-voltage (LV) DC intermediate grid (**Figure 5b**), while the three-stage topology incorporates both medium-voltage (MV) and low-voltage (LV) DC intermediate grids (**Figure 5c**). The flexible architecture, featuring multiple voltage conversion stages and a compact insulation transformer, enables PET systems to be applied in a wide range of fields, including aerospace, maritime, railway, and space applications.
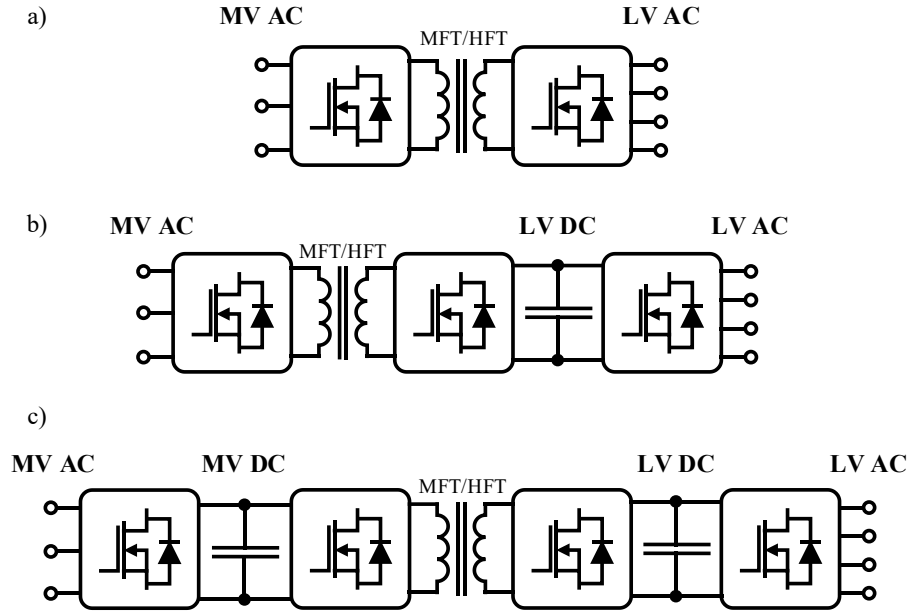

Figure 5. Power Electronics Transformer topologies: a) single-stage, b) two-stage, and c) three-stage.

The voltage and current capacity of semiconductors compared to system power ratings require a modular structure. From the MV side, modules are connected in series to multiply voltage capacity, and from the LV side, modules are connected in parallel to increase current capacity. An example of MV and LV phase coupling is shown in **Figure 6**. The transformer's galvanic isolation stage guarantees that the inputs and outputs from different modules can be flexibly combined. Indirect AC/DC conversion stages implement additional DC grids and full MV and LV AC grids decoupling. The three-stage topology of PET divides the system into three main energy conversion stages:

- MV AC/DC stage,
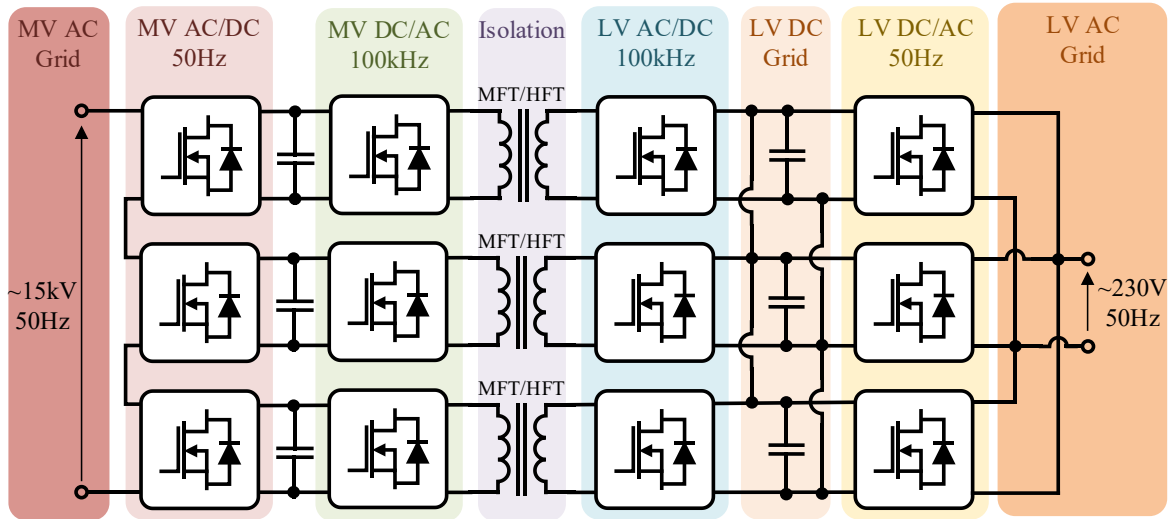- isolation MV DC to LV DC stage,
- LV DC/AC stage.

Figure 6. The modular structure of PET.

1.3. Power Electronics Transformer requirements and features

PETs offer numerous advantages for both MV and LV grids. Their advanced control capabilities enable the provision of various ancillary services to the distribution network [3]. These benefits are summarized in **Table 2** , categorized into services specific to MV and LV grids, as well as common advantages shared by both.

On the MV side, PETs contribute primarily to enhancing power quality and phase balancing through dynamic reactive power management—features that are highly valuable to distribution system operators. For LV grids, PETs provide a key advantage by enabling operation in two distinct modes: grid-supporting and grid-forming. These modes unlock functionalities that are not achievable with CPTs, such as local voltage and frequency regulation, support for weak grids, and seamless integration of distributed energy resources.

Table 2. Benefits from PET application in MV and LV distribution grids.

MV	MV and LV	LV
▪ load symmetrization ▪ reactive power support ▪ power factor correction ▪ separate control of active and reactive power	▪ controllability ▪ advanced protection ▪ redundancy ▪ fault-tolerance ▪ distortion decoupling ▪ energy monitoring ▪ communication ▪ energy storage management ▪ DC grids inclusion and transfer of RES and energy storage to the DC grid	GRID-FORMING MODE ▪ voltage amplitude and frequency modification ▪ load identification ▪ overload control GRID-SUPPORTING MODE ▪ possibility of phase recovery, ▪ managing RES generation by changing the grid voltage frequency ▪ soft load reduction ▪ load symmetrization

The main challenge in PET deployment is providing a similar reliability level to CPT. **Table 3** compares crucial evaluation factors for comparing CPT and PET technologies. The PET can offer additional services while improving energy quality and processing efficiency. However, many unresolved problems arise from power electronic converters' hardware and control design. The complexity level increases costs related to the system's production and maintenance.

Table 3. Transformer technologies factors comparison.

Factor	CPT	PET
Efficiency of conversion	High if the load is close to nominal power	Managed by module activation/deactivation
Quality of voltage	It depends on the load character and primary side voltage	Depends on the control algorithm
Reliability of operation	High	High with redundant design and post-fault operation algorithms
Controllability of voltage and current	Stepped by tap changers	High with ancillary services
Complexity of construction	Low	High
Scalability of power	No	Depends on the number of parallel/series connected power converters

1.4. Low voltage stage of Power Electronics Transformer

Depending on the operating mode, the LV stage of PET can operate as a voltage or current source. PET output current depends on connected devices in the grid forming mode operation as a voltage source. As a result, the current shape and power direction are unpredictable in each grid line. The implemented control method must meet this challenge. A converter system typically operates as a soft voltage source, making it susceptible to current distortions that negatively affect the voltage waveform. Ensuring voltage quality remains a challenge, as no existing solution fully satisfies all control criteria, despite extensive research in the literature [21], [22].

In grid-supporting mode, the low-voltage stage operates as a current source. The key challenges include maintaining stable operation under distorted voltage conditions and fluctuating impedance. Additionally, the amount of energy exchanged with the grid in each phase must be dynamically adjusted to reflect the current state of the distribution grid.

The LV DC/AC conversion stage of PET can be doubled and also act as an energy router in LV grids (**Figure 7**). Energy router, is an advanced device used in smart grids to manage the flow of electricity between different sources, consumers and energy storage systems. Its functions and advantages can be described as follows: energy balancing, multi-source management, power quality management. As a result, all the benefits associated with the two possible modes of operation can be obtained.
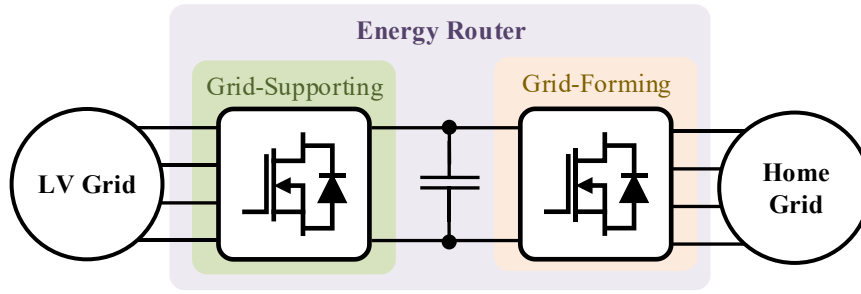

Figure 7. Power electronics-based energy routers in LV grid example.

Regardless of the operating mode, the LV stage of the PET must exhibit a high degree of reliability, defined as resistance to voltage and current overloads. Additionally, since it is impossible to completely eliminate the possibility of internal faults within the system, its design must ensure the capability to maintain continuous operation. This entails incorporating various additional hardware and software components that can isolate the detected fault and redirect the energy through an alternative pathway.

The challenges associated with controlling a single converter are compounded by those related to their parallel operation. To date, literature has primarily focused on the stable operation of a single converter within a grid. However, when multiple converters are connected in parallel, the issue of maintaining stable operation among them becomes a significant concern [23].

1.5. Reliability of modular Power Electronics Transformer

The actual implementation of the PET technology will only occur when its reliability is equal to that of a CPT. So, the system life cycle will be counted as tens of years, and service actions will not be frequent and expensive. A PET is a complex device with many semiconductor devices, wires, contacts, distributed software, and external communication. More components bring more risk for system failure. Hence, there is a need to develop a strategy to maintain system operability after component failure. In PET, three reliable design

domains can be distinguished: converter topology, control strategy, and communication. From a topology point of view, limited parameters of semiconductors, inductors, and capacitors necessitate using a modular system. Series connection increases voltage capacity, while parallel connection enhances current performance.

In the selection process of converter topologies, determining the optimal number of voltage levels is particularly important. The appropriate choice allows for achieving a significant voltage margin for the employed semiconductors and for reducing the dimensions and parameters of passive components in the output stage. Furthermore, multilevel converter branch can operate in fault-tolerant modes, where the failure of a single semiconductor only results in a reduction of the number of generated output voltage levels, rather than causing a complete shutdown of the converter.

Therefore, modularity ensures that a failure of a single element does not lead to system shutdown. The modular design also allows for the replacement of damaged modules without interrupting the overall operation of the system. The conditions that must be met to achieve reliability through modularity are as follows:

- multiple parallel modules for current reserve and redundancy,
- systems of switches for fault isolation and system reconfiguration,
- additional sensors and algorithms are needed to monitor the state of semiconductors,
- hot plug capability for power module and communication,
- communication with physical fault detection capability and data consistency diagnosis.

Meeting these conditions necessitates additional equipment, increasing implementation costs and demanding the development of complex control algorithms. More equipment does not necessarily mean improving reliability because each element has a given degree of unreliability. Single failure may exclude the entire set of parts from the operation. PET technology covers almost all issues related to grid-connected power electronic converter technology.

In the real-time control algorithm domain, the LV stage of PET is another set of risks. The control system is subjected to current and voltage distortion depending on the operating mode adopted. If the spectrum of the disturbance is outside the spectrum of the controller, there is a severe risk of losing the grid-connected converter system's stability. There is a need to develop a control algorithm that maintains stability over the full range of disturbances that can occur in the current and voltage waveforms, such as:

- voltage and current harmonics,
- short circuits,
- voltage and current asymmetry,
- variable impedance.

The last domain to consider for reliability is network communications. Due to the system's modularity, the communication integrates and synchronizes the entire system's operation. The reliability of the communication relies on the correctness of the data and the delivery route. Data correctness can be controlled through checksum mechanisms, while connection fault tolerance can be realized through additional data transfer paths. In addition, the communication system must allow the most accurate and reliable synchronization. In summary, the communication system binds the whole system together and must maintain data exchange even in incidence conditions:

- data line interruptions,
- electromagnetic disturbances,
- data distortion,
- system reconfiguration.

The complexity of the modular PET requires the implementation of power electronics digital control with real-time communication solutions. Due to the wide range of fields, the following section presents the limited scope of issues the author addresses.

1.6. Formulation of the Thesis

The aforementioned issues are of significant importance for the practical realization of PET in power systems. Currently, PET technology is in the scientific research and prototyping phases. While the literature offers individual solutions to many power electronics challenges, a clear need exists for the integration of these solutions into a comprehensive system. Thus, the following thesis can be formulated: **"The use of multiple parallel-connected DC/AC converters with a distributed control algorithm allows reliable and fault tolerant operation of the low voltage stage of Power Electronics Transformer in grid forming and grid supporting modes."**

In the author's opinion, the following parts of the thesis are his main contributions:

- Reliable multi-parallel design of PET LV stage able to reconfiguration DC/AC converter and grid connection for:
  - component failure,

31

- avoiding current overload,
- load balancing.
- Distributed control algorithm that provides:
  - voltage harmonics compensation in grid forming mode,
  - current harmonics compensation in grid-supporting mode,
  - DC/AC converter branch over switching between grid lines for matching PET system performance to grid load needs and balancing system load,
  - adaptation of the number of active DC/AC modules to load conditions for system conversion efficiency.
- Real-time communication adaptation for control of multi parallel-connected DC/AC converters with minimal necessary data profile.

The author of the dissertation analyzes fundamental issues related to the reliability and parallel operation of converter systems that connect low-voltage DC and low-voltage AC grids. The first topic addressed is the analysis of reliability mechanisms through redundancy. Subsequently, the discussion shifts to topics related to distributed control. For multi-parallel converters, real-time control and synchronization are critical. Therefore, the design and implementation of distributed control using the EtherCAT interface are presented.

1.7. Summary of challenges and scope of the dissertation

The previous sections have outlined numerous benefits of implementing PET in LV distribution grids. However, the feasibility of a PET LV subsystem primarily depends on addressing the challenges associated with DC/AC power converters operating in an input-parallel, output-parallel (IPOP) configuration.

Key issues affecting both DC and AC grids have been identified and analyzed, with a primary focus on developing a fault-tolerant topology, control strategy, and communication system. The parallel operation of DC/AC converters introduces additional complexities that must be resolved to ensure stable system performance.

Given the broad scope of challenges, it is essential to clearly define the extent of the author's contributions. This section will further explore the implementation challenges of the PET LV stage and specify the aspects addressed in this thesis.

A modular design adds another dimension to power electronics system development. While single-module control presents its own challenges, multi-module configurations introduce interoperability concerns. Modularity complicates the management of both input and

output circuits, requiring precise coordination among multiple units. Additionally, certain control functions must be delegated to an external system management module to ensure seamless operation.

The following issues are the focus of the dissertation as the author's work:

- fault-tolerant modular topology and system configuration management:
    - selection of the number of active parallel DC/AC converters for system capacity management,
    - DC/AC branch to grid line switching to match system performance to grid demand and to maintain system operation continuity in the event of a failure,
    - load balancing of DC/AC branches using re-connection between single- or three-phase operation of converter to maximize module life cycle.
- fault-tolerant distributed control under distorted grid voltage and current conditions:
    - voltage quality is maintained in the grid-forming mode under the influence of non-linear load current,
    - maintaining stable current control under distorted grid voltage conditions.
- DC/AC converter communication profile for real-time distributed control:
    - setting a minimal converter process data set,
    - simulation model and hardware selection and configuration with experimental verification of the system.

The following issues have been raised to comprehensively explain the topic, not being the author's discovery, but have been shortly analyzed and adapted to the proposed solution:

- modules synchronization using EtherCAT communication interface to prevent circulating current [24],
- DC capacitor voltage balancing in a common DC grid [25], [26],
- common stability of the DC/AC converter connected to the AC grid [27],
- interactive stability among parallel-connected DC/AC converters [27] .

Due to the complexity of the system, the following facts should be noted:

1. Power routing capability assumes a varying load on the converters, resulting in differences in modulation that may cause circulating currents, which reduces system efficiency.

2. Minimizing circulating currents forces the synchronization of PWM signals with a zero phase shift, eliminating the operation of modules in interleave mode.

3. A multilevel topology enhances the voltage margin for semiconductors. However, it also requires the use of additional DC capacitor voltage balancing algorithms and increases the number of elements.

4. The modular system gives fault-tolerance capability and increases system capacity but requires distributed control with reliable real-time communication. In addition to the intrinsic stability issues, there are problems with the stability between modules. Also, unequal parameters of module components introduce control stability issues.

5. Post-fault operation capability may not always turn out to be profitable. The possibility of reducing voltage levels after semiconductor failure in a parallel connected multi-level converter increases the circulating currents.

This dissertation presents a detailed analysis of the aforementioned issues and proposes an optimal, comprehensive solution for the fault-tolerant low-voltage stage of PET system design. By addressing these critical aspects, the research significantly contributes to the advancement of PET technology, paving the way for more reliable and resilient electrical distribution systems in the future. The findings underscore the potential for PET systems to enhance energy distribution efficiency while maintaining operational integrity, even under adverse conditions. The author's contributions offer a valuable foundation for future work aimed at fully integrating PET solutions into modern grid infrastructure.

2. Reliability of low voltage stage of Power Electronics Transformer

Reliability is defined as an item's ability to perform the required function under stated conditions for a certain period, often measured by the probability of survival and failure rate [28]. In the power electronics domain, reliability means ensuring the high availability of power sources. Stressors such as temperature cycles, vibration, humidity, overcurrent, and overvoltage are the leading causes of failure in power electronic devices. Reliability tests of power converter components show that semiconductors (diodes and transistors) and electrolytic capacitors are the most vulnerable to failure [29], [30]. Many strategies related to design for reliability (DFR) were presented in the literature to prevent component failure. DFR methods are mainly based on the principle of avoiding damage. However, assuming failure occurs, only the fault-tolerant design ensures the system's continuous operation. In power electronic converters, appropriate metrics can be used to assess reliability, such as failure rate, mean time between failures, mean time to repair, and availability [31].

This chapter focuses on the reliability analysis of LV DC/AC energy conversion through a fault-tolerant design strategy. The objective is to identify an approach that ensures continuity of operation by determining the most favorable DC/AC converter topology to meet the following requirements:

- fault-tolerant operation,
- adaptability of the system configuration to the required load.

2.1. Fault-tolerant DC/AC conversion system

Power electronic devices comprise power conversion channels as a combination of diodes, transistors, capacitors, and inductors with control and monitor equipment. In general, the DC grid is connected to the four lines of the AC grid through a combination of transistors called a transistor branch with an output filter (**Figure 8**). The DC/AC branch can be realized in several topologies depending on the number of voltage levels and connection with the DC Link. Damage to any branch element may interrupt energy conversion in this path because all components form a series system in the transistor branch reliability model (**Figure 9**). The supply of a three-phase grid with a neutral line is complex due to line-to-line coupling. Thus, all four energy conversion paths must always be operational during the transformer operation. Failure of even one component of a DC/AC converter affects the quality of current and voltage regulation of the entire module.

The failure rate λ is simply the number of failures over time [32]. It is a statistical value measured by observing the device and evaluating its performance. Based on previous observations, it is possible to determine the probability of how long the device maintains the assumed operating parameters under the given conditions. The failure rate of the entire device can be decomposed into component failure rates. This factor allows identify the weakest link.
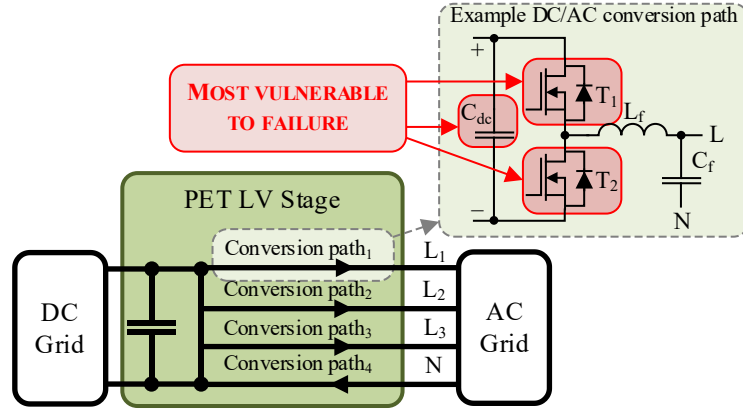

Figure 8. Energy conversion paths between LV DC and LV AC grids.

The DC/AC conversion path reliability model comprises series component failure rates $\lambda_{DC/AC}$ (**Figure 9**). The failure rate first depends on the technological complexity of the devices. The conversion path consists of essential components with corresponding failure rates, such as a DC capacitor λ_{Cdc}, semiconductors λ_{S1}, λ_{S2}, an AC filter λ_{filt}, and measurements devices λ_{meas}.
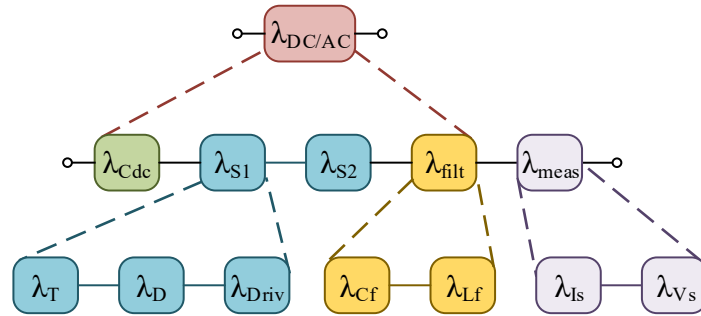
Figure 9. Reliability model for DC/AC conversion path.

Extracting the branch reliability model, each element consists of another set of components with its failure rates. The switching device failure rate results from the following failure rates: transistor λ_T, diode λ_D, and driver λ_{Driv}. The subsequent failure rates can contribute to the reliability of a line filter: capacitor λ_{Cf}, inductor λ_{Lf}, and measurement devices: current sensor λ_{Is}, and voltage sensor λ_{Vs}. Going more into design details of the chain of the reliability

model and adding more elements worsens the reliability of the subsystem. A detailed theory of reliability calculation for converters is described in [33].

The following formula is used to determine the Mean Time To Failure (MTTF) for one DC/AC conversion path depending on voltage levels:

$$\text{MTTF}_{DC/AC\ Branch} = \frac{1}{\lambda_{Cdc}+l(\lambda_{S1}+\lambda_{S2})+\lambda_{filt}+\lambda_{meas}} = \frac{1}{\lambda_{Cdc}+2l(\lambda_T+\lambda_D+\lambda_{Driv})+\lambda_{Cf}+\lambda_{Lf}+\lambda_{Is}+\lambda_{Vs}} \qquad (2.1)$$

where: l - number of voltage levels.

The multiplication of energy conversion paths for each grid line allows the system to maintain operational continuity in the event of a single-path failure (**Figure 10**). Each path consists of a combination of semiconductor and reactive components. By duplicating these components and applying appropriate parallel or series configurations, the system can continue processing energy even in the presence of a component failure. To ensure this strategy works effectively, it is also necessary to implement mechanisms for isolating the damaged components.

Increasing the number of conversion branches transforms the reliability model of the system into a parallel configuration (**Figure 11**). , in which the overall reliability improves with redundancy. In this architecture, the failure of a single branch does not compromise the operation of the entire system, as the remaining branches can continue to operate independently.

As a result, the total number of components—particularly semiconductor devices and passive elements is multiplied by n, where n is the number of DC/AC conversion paths. While this increases the system's complexity and component count, it significantly enhances fault tolerance and operational continuity.
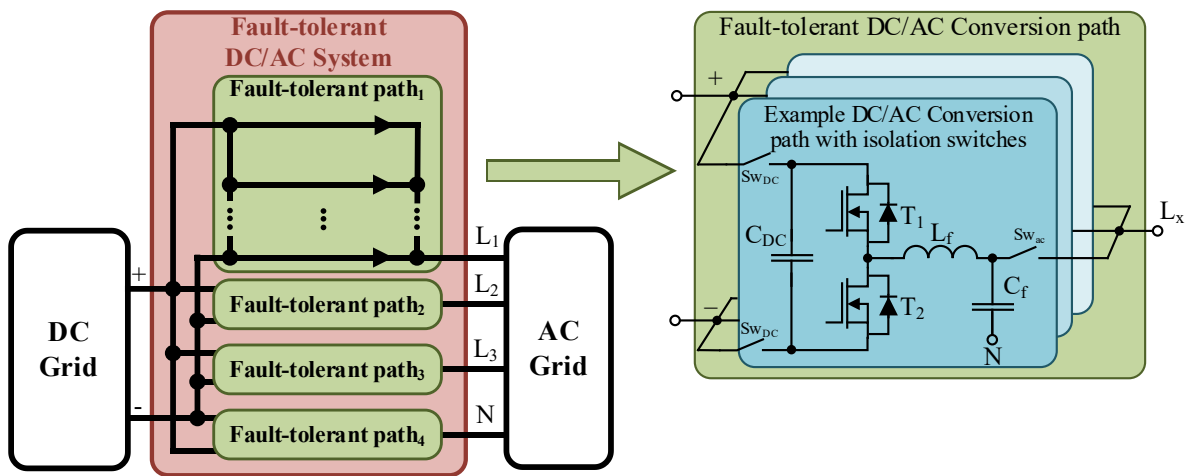

Figure 10. Fault-tolerant DC/AC conversion system.

Figure 11. Reliability model for parallel DC/AC conversion system with separated DC capacitor.

The total system reliability is increased in a parallel DC/AC with a branch configuration with separate DC link:

$$\text{MTTF}_{Parallel\ DC/AC\ Branches} = \frac{n}{\lambda_{Cdc}+1(\lambda_{S1}+\lambda_{S2})+\lambda_{filt}+\lambda_{meas}} \qquad (2.2)$$

For example, typical DC/AC module branches share DC capacitors. Damage to a DC link capacitor C_{DC} eliminates the whole module. It should be noted at this point that the fewer common elements in the system, the higher the reliability. In addition, all branches operate with separate grid lines that are coupled to each other. In this case, the DC/AC converter's reliability model can be considered a serial (**Figure 12**). The equation describing the MTTF of a four-branch DC/AC converter is as follows:

$$\text{MTTF}_{DC/AC\ 4\ branch\ converter} = \frac{1}{\lambda_{Cdc}+4\left(2l(\lambda_T+\lambda_D+\lambda_{Driv})+\lambda_{Cf}+\lambda_{Lf}+\lambda_i+\lambda_u\right)} \qquad (2.3)$$

To summarise the reliability considerations for DC/AC converters, the conversion path should be designed with the minimum possible number of components to reduce potential points of failure. If additional parallel branches are introduced to enhance fault tolerance, they should share as few common elements as possible in order to limit the risk of simultaneous failure propagation.

From a reliability standpoint, the most advantageous configuration is a parallel arrangement of four-branch, two-level converters, which offers a balanced trade-off between redundancy and complexity.

Although the general design principle is to minimise the number of components, it is also worth considering multilevel converter topologies. In selected fault scenarios—such as the failure of individual switching transistors—multilevel architectures can maintain output voltage modulation by reducing the number of active voltage levels. This feature adds an additional layer of operational resilience, which may be critical in applications requiring high availability.
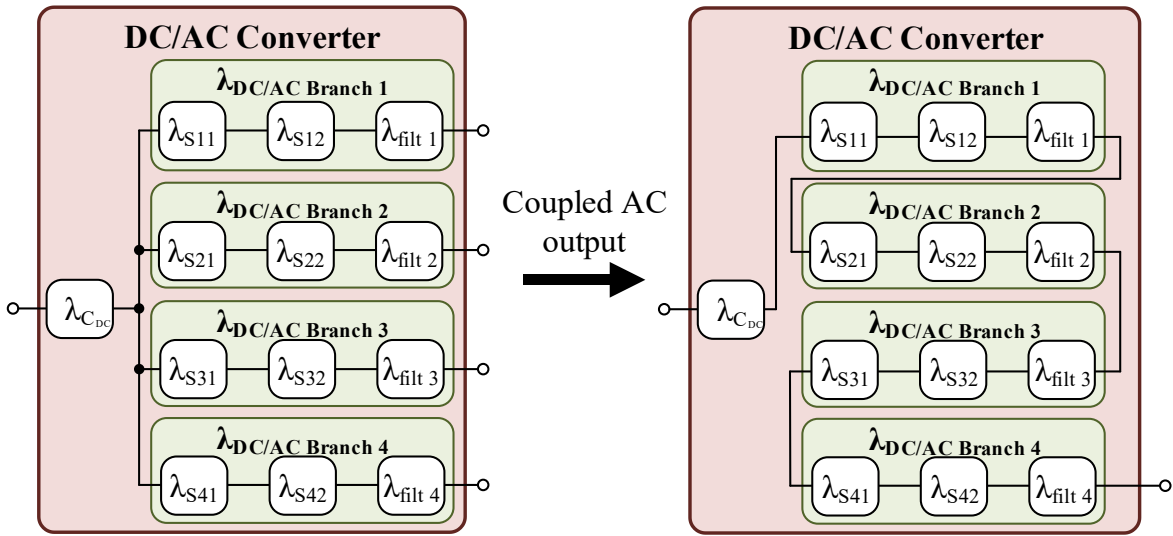
Figure 12. Reliability model of 4-branch DC/AC converter connected to AC grid.

2.2. Fault-tolerant DC/AC converter design

The fault-tolerant design applies additional equipment and requires an extended control algorithm. Redundant elements are connected in parallel or series [31]. This way, a broken conversion path can be unplugged without stopping the entire system. The design of the power electronic module, including parallel redundant elements, may consider additional elements on four levels: component, branch, module, and system (**Figure 13**). The component level multiplies a single part with the necessary equipment. The branch level multiplies elements pursuing a common objective (transistors with filter). A module is a set of branches. The system is a set of modules. When selecting the level at which redundant design will be implemented, the following factors should be taken into account:

- How many additional components need to be added?
- How many additional signals need to be fed in?
- How complex will the algorithm be, and whether it can be implemented?
- Whether replacing a faulty component will be possible without stopping the system?
- Whether redundant components can also be used in regular system operation?

Component	Branch	Module	System
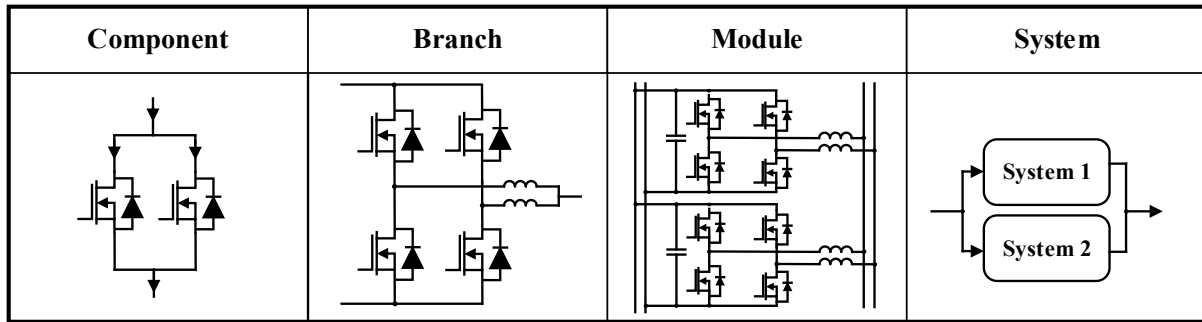
Figure 13. Redundant design at different levels: component, branch, module, and system.

At each level, the number of elements is duplicated, which entails an adequate duplication of measurement and control signals. Replacement of faulty components without stopping system operation is only possible at the module level. Modules are also the fundamental element containing all energy conversion functionalities. Hence, the optimal choice is redundancy in power electronics converter systems at a module level.

2.2.1. Availability of the low voltage stage of the Power Electronics Transformer

An essential part of system reliability is system availability under the broadest possible operational conditions. The LV stage of PET has a limited current capacity due to semiconductor device parameters. An asymmetric and unpredictable load characterizes the LV grid. Currently, uncoordinated distributed energy sources are also negatively affecting the quality of voltage on the grid. The semiconductors are unevenly loaded if the system cannot reconfigure with a continuous unbalanced load. Hence, particular component's life cycles vary. As a result, the module's life cycle is equal to the shortest of the branch life cycle. Other adverse phenomena are overloads and line short circuits. The PET must deliver or receive the required current amount to the grid. This case requires the system's ability to adapt to the actual load, i.e., switch the appropriate number of branches to a more loaded phase. By adding a switch between the output filter and the grid to each branch output filter, the system's adaptability to the current needs of the grid can be achieved (**Figure 14**). Additional switches for grid line selection do not significantly increase the number of equipment and control signals. It should also be noted that the DC/AC branch is the primary actuator from the system management point of view because it has current-forming and voltage-forming capabilities.
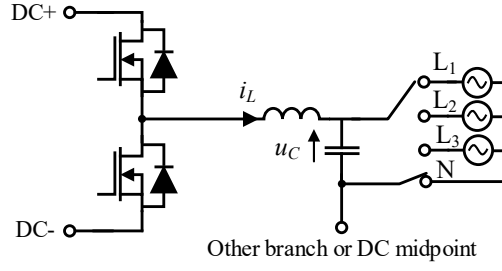
Figure 14. DC/AC converter branch with switch for grid line selection.

Reliability is also considered the device's usability in the system's broadest possible range of cases. Another important aspect is the usability of the PET in the case of grid-forming operation mode. An unbalanced load makes uneven operation of transistors branches if they are rigidly connected to a grid line. The ability to reconfigure the connections makes it possible to balance the load on the DC/AC branches (**Figure 15**). Load symmetrization in power electronics devices is very important in order to maximise the life cycle, and a single-phase LV module connected to more loaded grid line may be more beneficial to the grid than a three-phase connection.
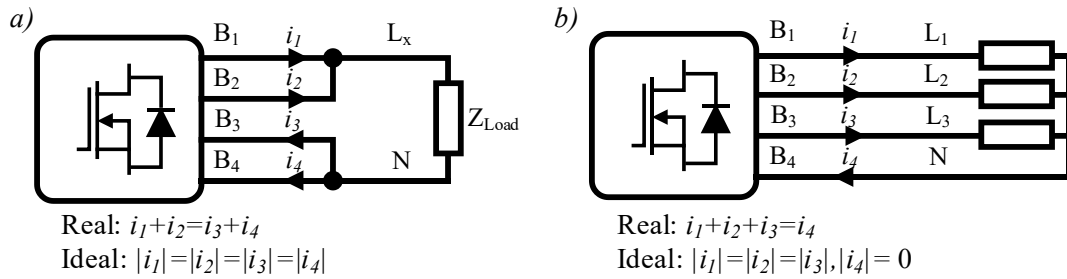
Figure 15. Comparison of: a) single-phase and b) three-phase connected four-branch DC/AC converters.

To date, the literature has not adequately addressed the design of a DC/AC grid coupling power electronic system that can maintain operation following the failure of a system component and adapt effectively to the current conditions of the AC grid. This gap in research highlights the need for innovative designs that prioritize system resilience and flexibility. As power systems progressively incorporate renewable energy sources and energy storage solutions, the capability to withstand component failures without interrupting service becomes increasingly critical. Further investigation is essential to develop methodologies and frameworks that enable such systems to dynamically adjust their operation in real time, ensuring stability and reliability in varying grid conditions. This underscores the importance of

advancing our understanding of fault-tolerant designs and adaptive control strategies in modern power electronic systems.

2.3. Overview of fault-tolerant strategies in power electronics devices

Electronic components can experience three primary types of permanent damage: short circuits, open circuits, and deterioration of component parameters. The impact of these failures on a DC/AC branch, module, or system varies depending on the converter topology. For instance, a short circuit in a transistor within a branch can disable the entire branch, necessitating its disconnection from the phase. Additionally, parameter deterioration may compromise the stability of system control.

To establish a fault-tolerant design, several steps should be considered. First, an assessment of how the aforementioned types of damage affect system operation should be conducted. If any of these failures impede the correct functioning of other components, a monitoring mechanism and failure assessment process should be implemented. Next, the damaged component or subsystem must be isolated, and, if necessary, the system should be reconfigured promptly for continued operation. Finally, the system should remain operational until technical service can be performed following the component fault.

Detection methods for open switch faults and fault-tolerant control strategies for power electronic systems are well-documented in the literature, offering valuable insights into developing more resilient systems [34].

In summary, the redundant design proves the best reliability improvements; however, it requires surplus elements, signals, and extended control algorithms that finally increase costs and system complexity (**Figure 16**). The system's total power is appropriately divided between the DC/AC converters connected in parallel. The control system must be split into local units (module controller) and one global unit (system controller) due to the potential local faults that must be removed from the system with the module and the limitation of the number of signals to be transmitted. The module controller realizes primary control algorithms for monitoring the status and managing the actuators. In contrast, the system control realizes that the secondary control algorithm determines the number of actuators to match the system configuration to the current load requirements.

Redundancy means adding spare elements to a standard design that are waiting for a failure to occur. Many solutions have been presented in the literature with redundant features that do not participate in regular operation and do not increase the current or voltage

performance of the system. For LV grid-connected converters with uneven branch load, it will be more beneficial to use redundant elements in regular operation to balance the load, ultimately extending the entire module's life cycle.
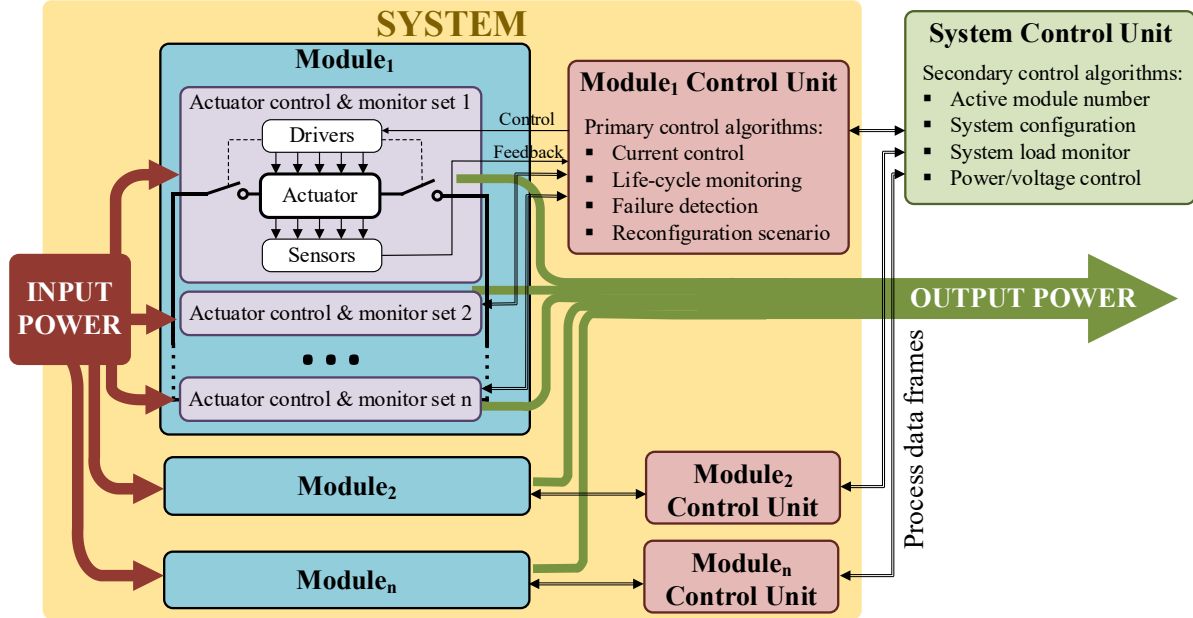
Figure 16. Distributed control block diagram of a power electronics system.

2.3.1. Reliability assessment with fault-tolerant power converter systems

A commonly used method for assessing the ability of a system to operate in post-fault states is the Markov chain [35]. The chain begins with a state of total health system and ends with a state of complete system shutdown (**Figure 17**). A system capable of operating in failure states is characterized by additional states with reduced system performance between the total health and stopped states (**Figure 18**). In power electronics, other states depend on topology and redundant elements. Maintaining continuity of operation after a component failure, particularly when the number of redundant components is limited, can result in a degradation of current or voltage performance. Implementing parallel connections among devices allows for servicing without requiring a complete system shutdown.
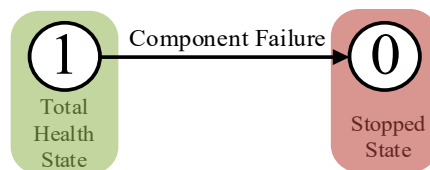
Figure 17. No fault-tolerant system.
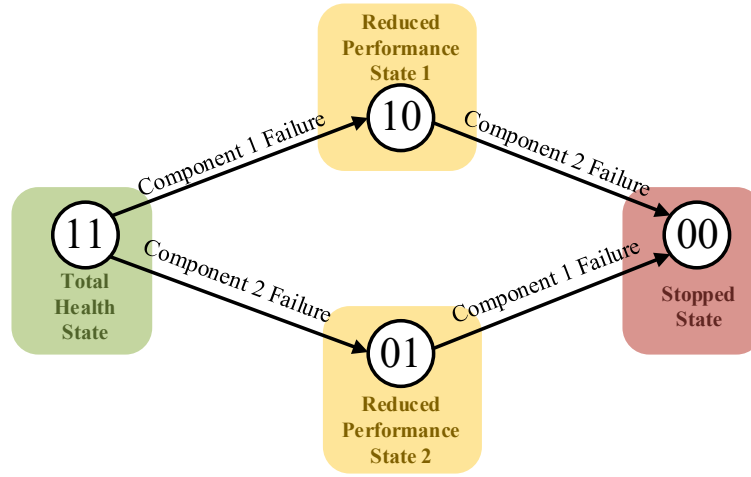
Figure 18. Example Markov chain for the fault-tolerant system.

This approach not only improves system reliability but also minimizes downtime, ensuring the uninterrupted operation of critical functions. Implementing effective monitoring and diagnostic tools is essential for promptly detecting failures and enabling rapid response, thereby maintaining optimal performance even during periods of reduced capacity. By prioritizing redundancy and serviceability in the design phase, systems can achieve a more effective balance between reliability and operational efficiency.

When analyzing the reliability of a four-branch DC/AC converter using a Markov model, it becomes evident that the failure of any single component does not necessarily render the entire module inoperative. However, the interconnection of grid lines means that the continued operation of a faulty module can adversely affect voltage shaping and current flow throughout the system. According to Kirchhoff's law, the sum of the currents in all branches of the module must equal zero, indicating that imbalances can lead to further complications.

The grid load can take various forms, including three-phase configurations with or without a neutral line, single-phase loads, and phase-to-phase connections (**Figure 19**). A fully functional module is essential to power all types of loads effectively. Furthermore, the design allows for the flexibility to switch branches between different phases of the grid by incorporating additional switches.

Given this architecture, it is crucial to assume that any damage to the converter module will require its deactivation to maintain overall system stability and performance. During operations, a structured approach to identifying faults and implementing corrective measures should be employed, ensuring minimal disruption. By prioritizing reliability and adaptability within the converter design, the system can better manage the complexities associated with various load types and potential component failures.
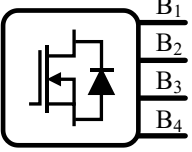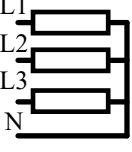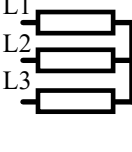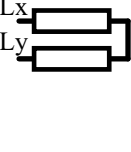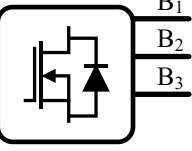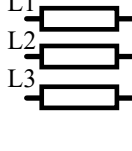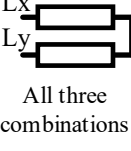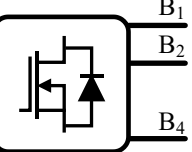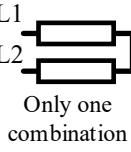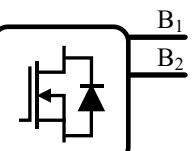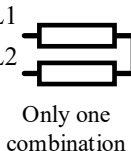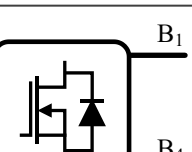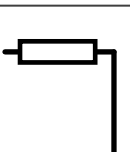
Module Condition	3-phase + Neutral	3-phase	Inter-phase	Single-phase
Fully Operational	B₁ B₂ B₃ B₄ — L1 L2 L3 N	L1 L2 L3	All three combinations Lx Ly	All three combinations
B₄ Fault	B₁ B₂ B₃ — ✗	L1 L2 L3	Lx Ly — All three combinations	✗
B₃ Fault	B₁ B₂ B₄ — ✗	✗	L1 L2 — Only one combination	Two combinations
B₃ & B₄ Fault	B₁ B₂ — ✗	✗	L1 L2 — Only one combination	✗
B₂ & B₃ Fault	B₁ B₄ — ✗	✗	✗	Only one combination

Figure 19. Examples of grid-connected DC/AC module performance under various branch fault conditions.

2.3.2. Redundant power electronics circuit design analysis

Redundancy can be applied to different levels of converter design. The first level is the single electronics component (e.g., transistor, diode, or capacitor). **Figure 20** shows the analysis of the influence of short-circuit and open-circuit failure of the semiconductor on two series or parallel connected devices. Short-circuit in parallel connections and open circuits in series connections eliminate the entire circuit from operation. Markov model evaluates circuit operability under a specific device state. To eliminate the negative influence of given failure on the rest of the circuit, it is necessary to use additional insulating connectors. Then the

unfavourable damage condition is removed from the Markov model. Using redundancy at the chosen level introduces other issues because it requires an extra semiconductor condition observer.

Moreover, the control circuit must be fast enough to respond appropriately to a failure. Consider the module's many semiconductors; each would have to be doubled. This approach significantly increases cost and design effort. Conversely, increasing the component number worsens reliability. And the most reliable part is the one that does not exist.
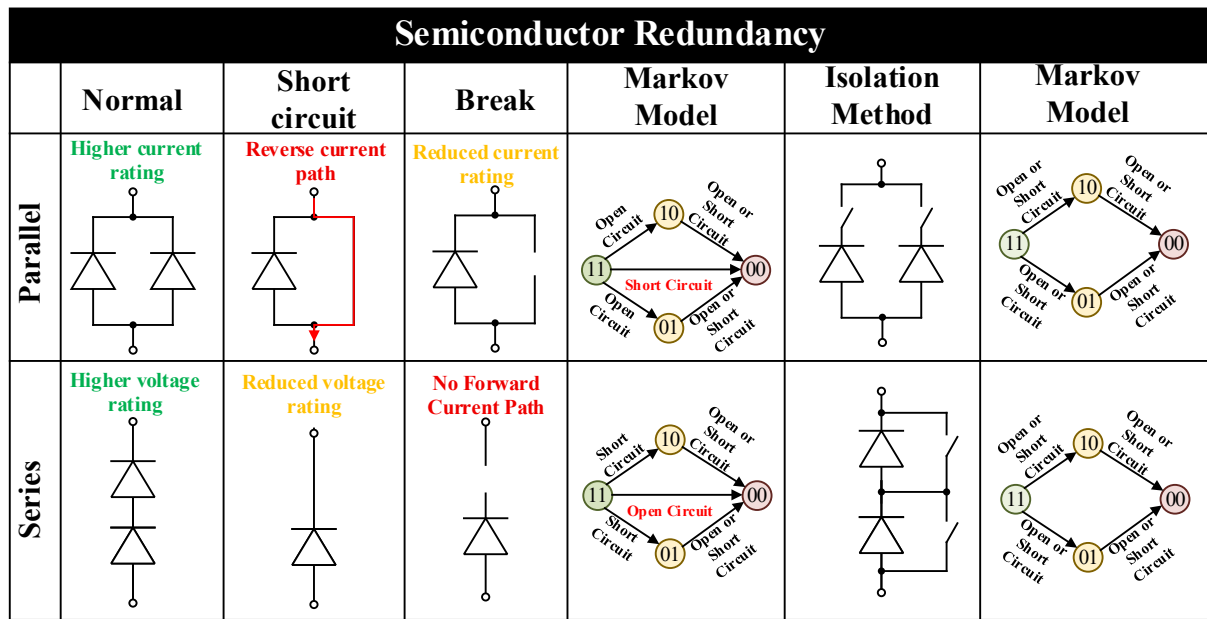

Figure 20. Semiconductor redundancy.

The second level includes elements combined to realize one task (e.g., transistor branch with output filter). Damage to a component decreases the capabilities or completely turns off the entire system. Furthermore, damage to a branch can result in the blocking of the module and other module branches. Failure to maintain this condition leads to unstable behavior of the system. To prevent system blocking, the damaged branch must be isolated. Redundancy at the branch level also duplicates the number of elements and thus measurement and control signals, while it reduces the number of factors separating the branch from the system (**Figure 21**). Adding additional switches to the branch, reconfiguring the connection with the AC grid, and increasing the system's flexibility is possible.

The third level comprises a power electronics module, i.e., a set of transistor branches with a DC intermediate circuit. **Figure 21** shows the impact of possible damage on a branch or module's operation and cases in which type of isolation is necessary. The ability to work in

post-fault states assumes that the system will maintain the operational capacity at reduced parameters until the service. An important aspect is the possibility of replacing a faulty element or a set of parts without stopping the work of the whole system. The module gives such a possibility as a set of elements managed by an internal control unit with external communication and protective casing. Redundancy at the module level is the most advantageous way to increase system reliability regarding hardware resources and control algorithms. However, it creates challenges for the implementation of distributed control algorithms. The fourth stage covers the entire system, i.e., a set of modules, and is not considered in this work.
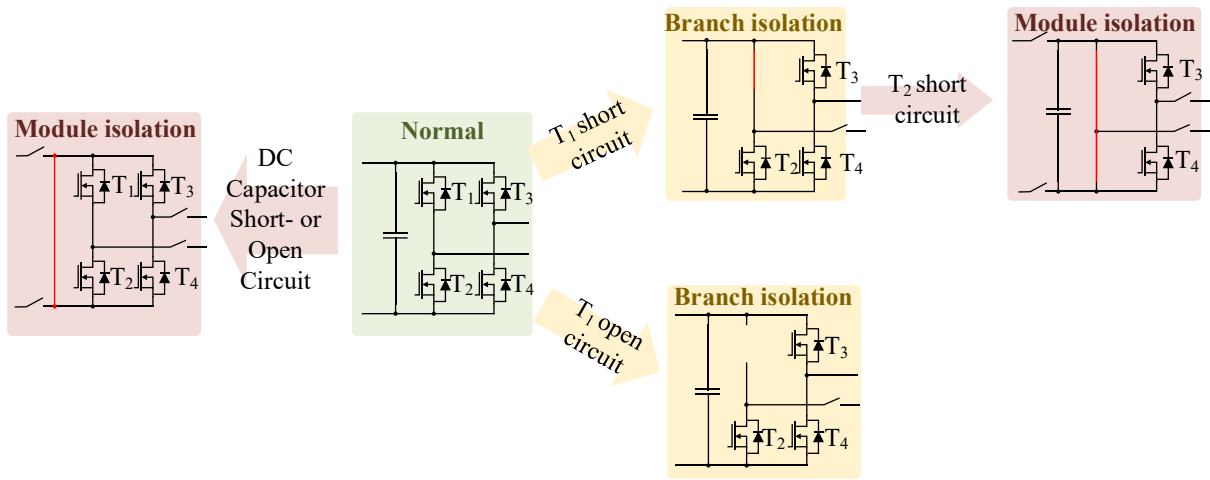

Figure 21. Impact of transistor short or open circuit to DC/AC branch and module isolation.

After compiling how redundant elements can be used in selecting a design, there are many factors to consider based on which design strategy will be chosen. **Table 4** summarizes the characteristics comparing redundancy levels.

In summary, implementing redundancy at the component level effectively doubles the number of elements within the module and introduces additional health monitoring features. This increase in components also translates to a greater number of signals to manage. The control unit has a strictly limited capacity for handling measurement and control signals, which must be carefully considered.

Redundancy at the branch level necessitates the addition of at least one reconfigurable branch to take over in the event of a failure. However, it is important to note that a transistor branch cannot be replaced without temporarily halting module operation. The converter module itself serves as a critical unit that connects the DC grid to all lines of the AC grid. It houses both a control unit and a communication system that integrates the modules with the entire system framework.

Ultimately, the module is designed to be a replaceable unit that can be exchanged without shutting down other elements of the system, thereby enhancing overall operational reliability and minimizing downtime during maintenance or upgrades.

Table 4. Comparison of redundancy on different power electronics converter design levels.

Characteristic	Component	Branch	Module	System
Reconfigurability	No	Yes	Yes	Yes
Service access during operation	No	No	Yes	Yes
Common elements in the system	No	DC link capacitors	DC and AC lines, communication interface	DC and AC lines
Component failure consequences	Operation disabled	Operation disabled or reduced performance	Operation enabled after branch isolation	Operation enabled with lowered parameters

2.3.3. Fault-tolerant DC/AC converter branch topology analysis

The analysis in the previous section demonstrates that two-level converter topologies are unable to operate under component failure conditions without the inclusion of redundant elements. In contrast, multilevel converter topologies gain particular relevance in this context due to their increased number of switching elements, which provide enhanced structural flexibility.

As shown in **Figure 22** and **Figure 23**, some failures allow the branch to continue operation with reduced parameters. Multilevel topology provides less voltage stress to semiconductors and reduced AC filter parameters, which offers the ability to maintain continuous operation after transistor failure. Three well-known converter topologies, Neutral Point Clamped (NPC), Flying Capacitor (FC), and Transistor Clamped (TC), also called T-Type provide various options for operation under transistor short-circuit or open-circuit fault [36]. These characteristics enable partial reconfiguration of the system, allowing it to continue operating even in the presence of certain faults under specific conditions. Analyzing the subsequent damage in three-level topologies, the following conclusions are drawn:

- In the NPC topology, the break of transistor T_1/T_2 disables the generation of $0.5v_{DC}$, and the break of transistor T_3/T_4 disables the generation of $-0.5v_{DC}$. In this situation, the branch is completely inoperative and must be disconnected. When T_2 or T_3 is short-

circuited, transistors T_1 and T_4 are capable to maintain two-level voltage modulation. A short-circuited transistor T_1 or T_4 can still allow voltage modulation, provided that the remaining semiconductor devices are rated for higher voltage classes.

- In the FCC topology, the break or short-circuit in any transistor results in a loss of voltage equalization capability on the FCC capacitor. As a result, the entire branch is disabled,

- In a T-type topology, only short circuit failure of transistors T_1 and T_4 prevent full voltage modulation due to the exclusion $\pm 0.5 v_{DC}$ levels, respectively. Damage to transistors T_2 and T_3 changes the T-type topology to a two-level topology.
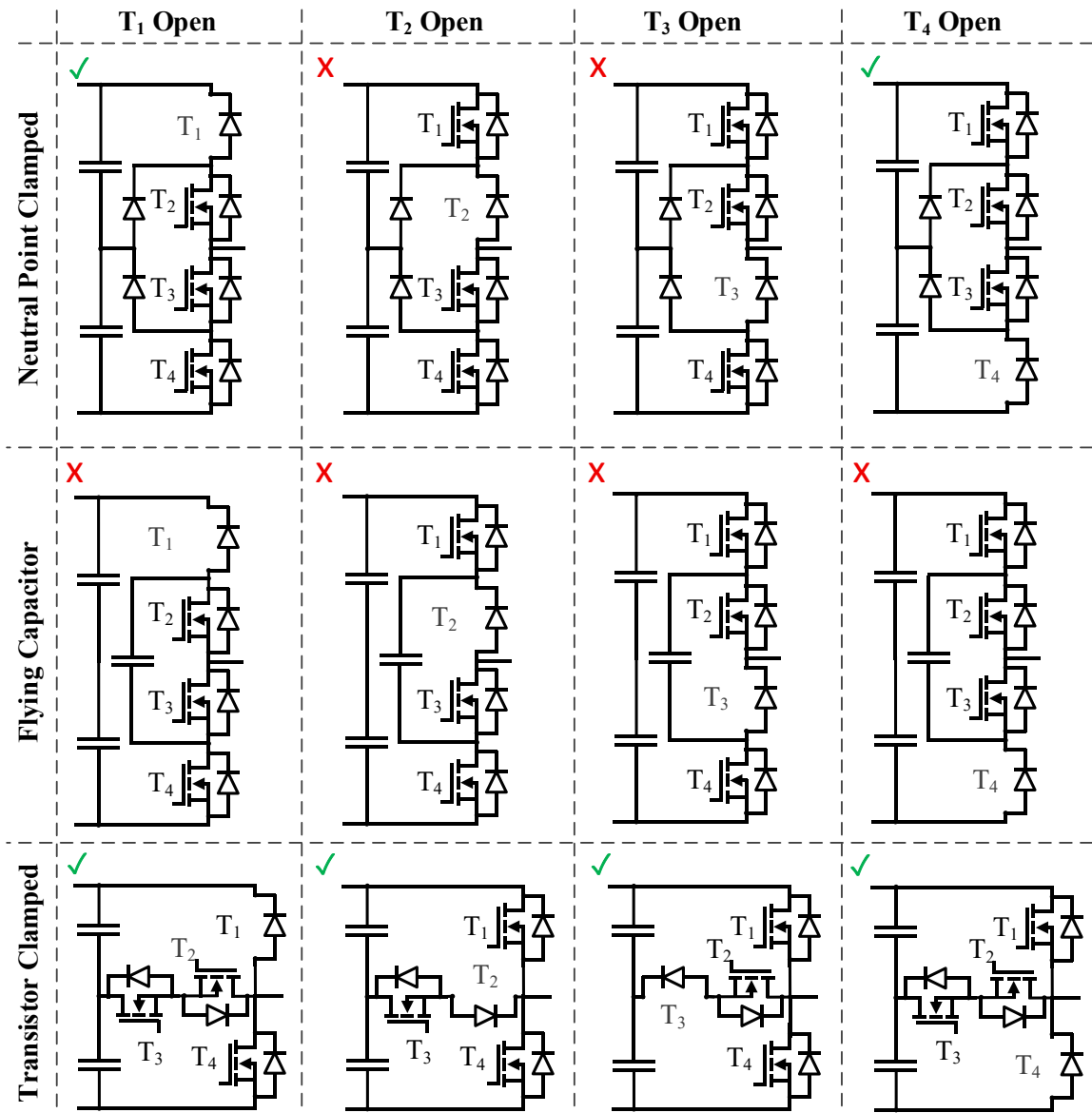

Figure 22. Summary of semiconductor open circuit failure influence on the three-level transistor branch.
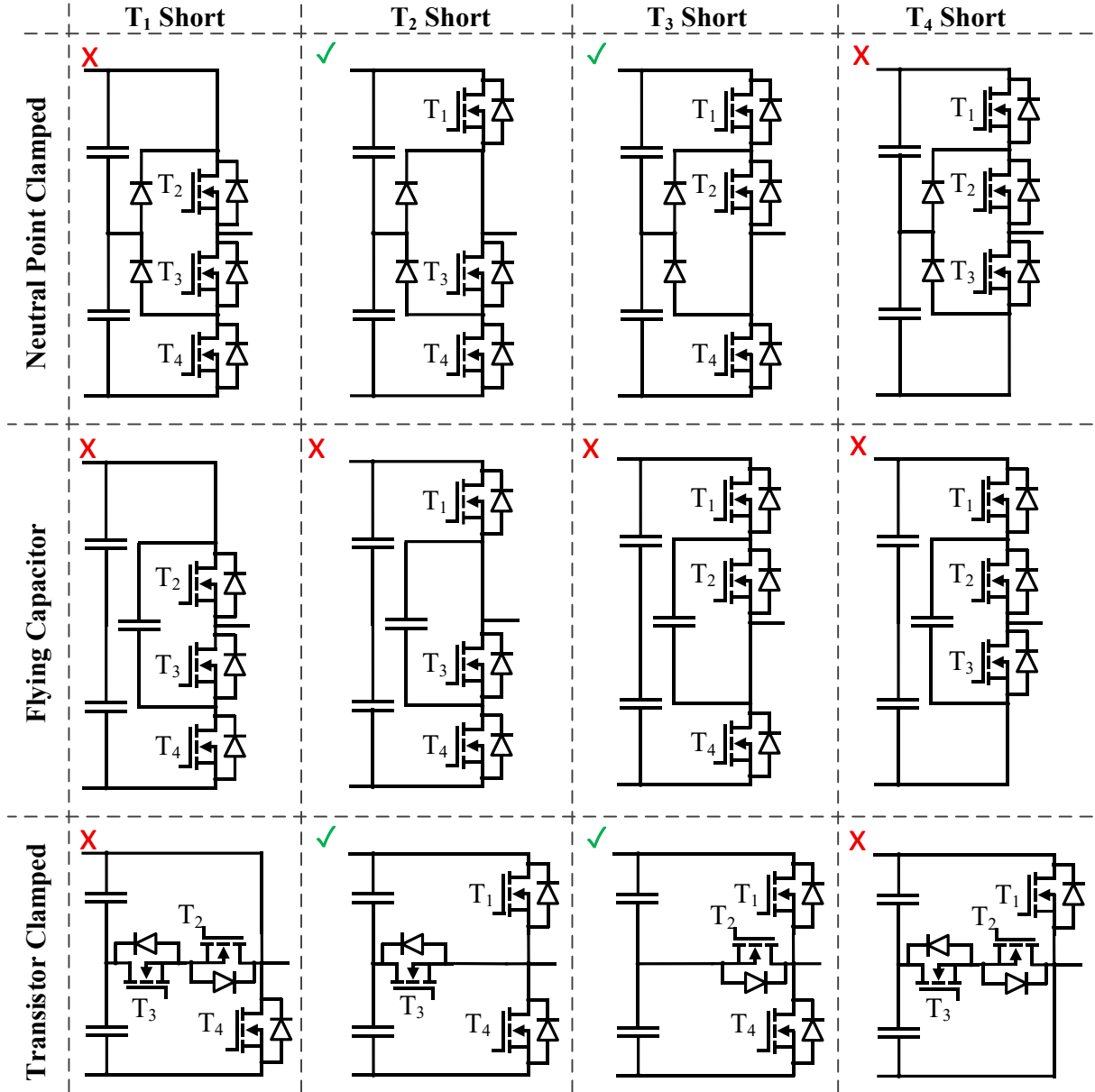
Figure 23. Summary of semiconductor short circuit failure influence on the three-level branch.

A summary of the performance capabilities of three-level topologies under the influence of transistor short circuits and open circuits is presented in **Table 5**. The T-Type topology addresses the greatest number of scenarios and demonstrates higher processing efficiency compared to the other topologies. In the event of a transistor failure, the number of voltage levels reduces from three to two.

In summary, the T-type topology exhibits the broadest range of performance under fault conditions. Following a fault, the operation necessitates a reduction in voltage levels, and further analysis is required to assess its application in parallel operations.

Table 5. Post-fault operation capability for 3L-NPC, 3L-FC, and 3L-TC (T-type).

Post-fault operation in	NPC	FC	T-Type
T_1 or T_4 open-circuit	YES	NO	YES
T_2 or T_3 open-circuit	NO	NO	YES
T_1 or T_4 short-circuit	NO	NO	NO
T_2 or T_3 short-circuit	YES	NO	YES

2.3.4. Analysis of the operation of parallel connected DC/AC branches with different number of voltage levels.

The ability to reduce voltage levels to maintain the continuity of the three-level branches from the previous section proves disadvantageous when applied to a system with parallel connected DC/AC branches. The combination of branches with different numbers of voltage levels leads to an increase in current ripple where the number of levels has been reduced. And there are circulating currents resulting from differences in the output voltage of the branches. **Figure 24** shows an example diagram of the parallel connection of branches with different voltage levels. For the same output voltage vector, two components of currents will appear in both branches: common i_{com} and differential i_{diff}. Diferential current results from the difference in voltage v_{diff} that will occur at any given time between the DC/AC branches outputs.
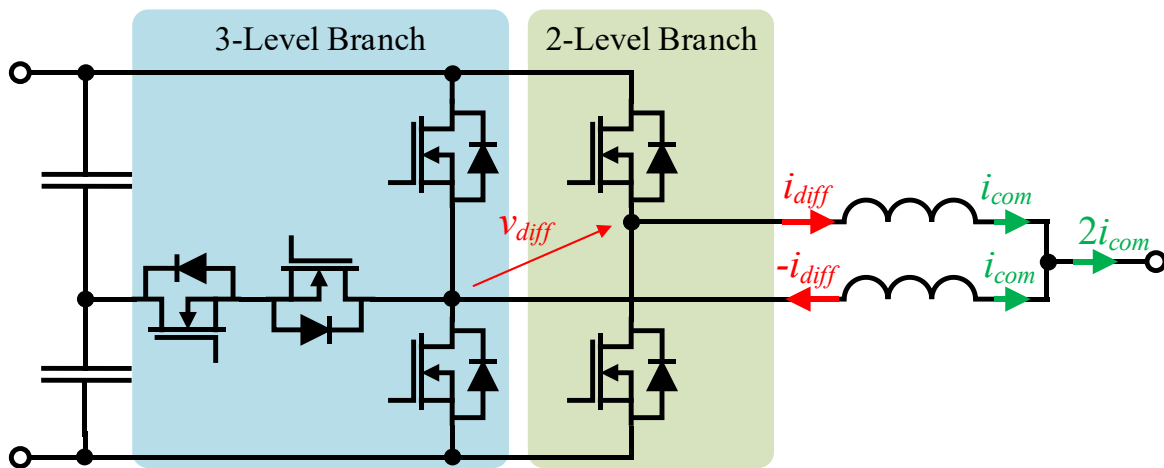

Figure 24. Parallel connection of two- and three-level DC/AC transistors branches.

Examples of current waveforms of parallel connected DC/AC branches with different level numbers are shown in **Figure 25**. It can be seen that the closer to the zero value the greater the value of the circulating currents. This means that operation of the system in this configuration should be avoided.
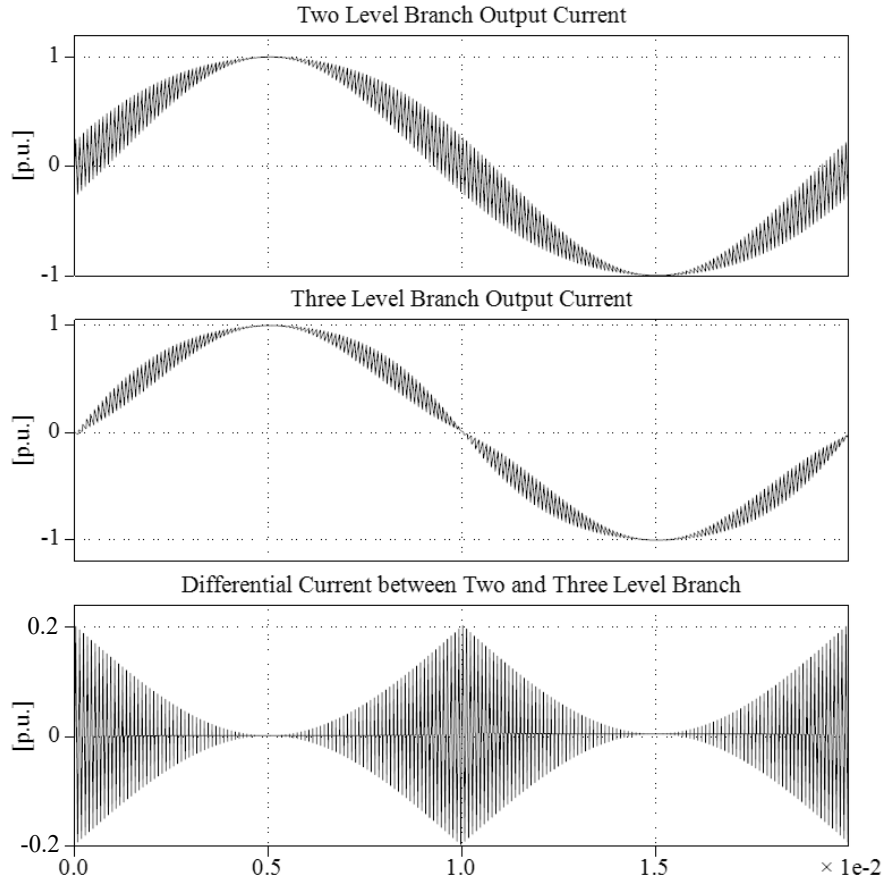

Figure 25. Current waveforms in parallel connected DC/AC branches with different voltage levels.

Circulating currents further stress transistors and reduce the efficiency of the circuit. Hence, in the event of failure of a three-level branch element, it should be turned off and replaced. If there was a case where system performance was required and there were no backup DC/AC branches then the whole system would have to go from a three-level operation to a two-level operation. Analysing and investigating the feasibility of parallel connected mains converters with different voltage levels is not the main purpose of this dissertation. This issue has been described more extensively in the literature [37].

2.4. Fault-tolerant low voltage stage of Power Electronics Transformer

The LV side of the PET couples two lines of the DC grid to four lines of the AC grid. One transistor branch couples one AC line to two DC lines. If one element in the branch fails, energy conversion is deteriorated or interrupted. The ability to operate in post-fault necessitates additional DC/AC energy conversion paths for each AC grid line. Another DC/AC module included in parallel increases reliability by multiplying transistor branches. **Figure 26** presents a graph with the representation of modular LV stage architecture.
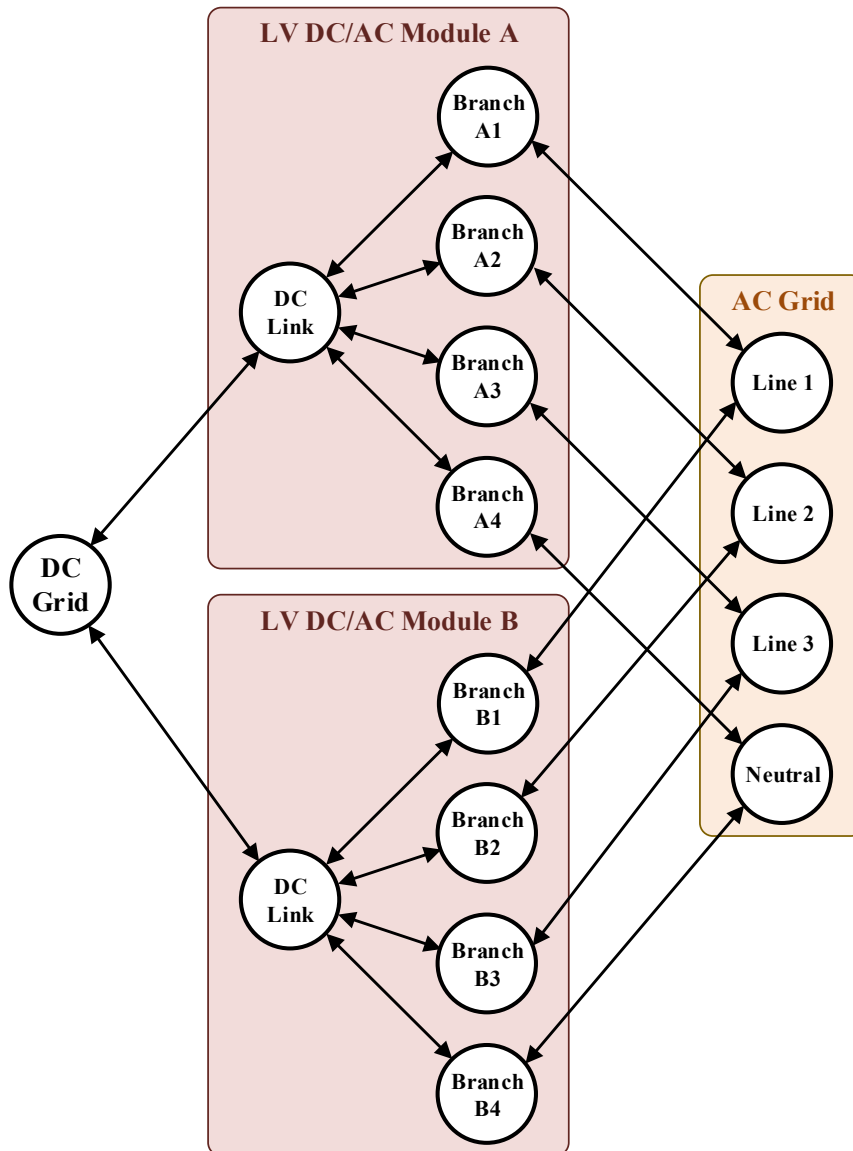

Figure 26. Graph representation of DC and AC grid connection through LV stage modules.

Additional system configurations can be realized if each branch is capable of switching between grid lines. It is also important to note that the load on the LV grid lines is often

unbalanced. As a result, the permanent connection of branches can lead to uneven system operation, which may cause discrepancies in the wear and tear of module components. For instance, one grid line may experience significantly higher loads than the others.

Reconfiguring the branch connection to the AC grid can enhance system performance in this power conversion path while simultaneously balancing the load across the branches within the module. An illustrative graph representing the reconfigured module for single-phase operation is shown in **Figure 27**.
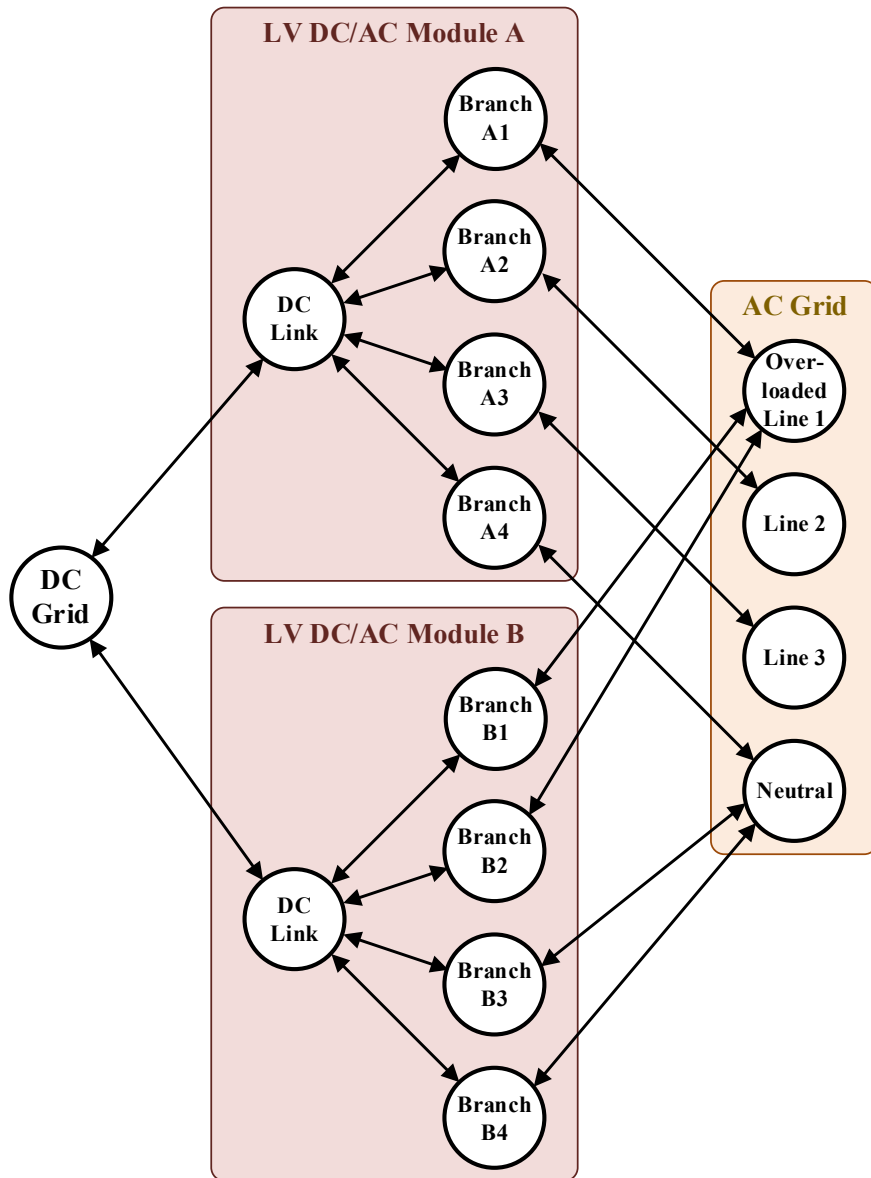

Figure 27. The graph representation for line overload case.

By considering the Markov model for reconfigurable systems, it can be deduced that reliability enhancement is based on increasing the flexibility of the system to match the number

of attached branches to the grid lines based on the state of the system and the LV grid. As a result, the converter module only needs to be extended with additional switches between phases, which does not significantly increase the design and control complexity.

2.5. Proposed topology of low voltage stage of Power Electronics Transformer

The primary goal of this dissertation is to present a system topology to enable the continuous operation of the LV stage of the PET system after a component failure. Summarizing the fault-tolerant design analysis from the previous sections, a set of facts can be identified as follows:

- the multiplication of parallel connected DC/AC conversion paths ensures the system fault tolerance,
- increasing energy processing paths can be implemented at four levels: component, branch, module, or system, but only the module is the replaceable unit during system operation,
- additional switches are necessary to exclude short-circuit failure in multi-parallel processing paths,
- fault-tolerant design requires additional monitoring equipment and extended control algorithms,
- single-component failure reduces branch operability, and parallel operation of different voltage levels increases circulating current,
- increasing the number of elements does not necessarily improve overall reliability,
- adding additional switches to each branch to enable grid line switching improves the DC/AC converter's capability to:
  - adjust the system capacity to meet the demands of the distribution grid load,
  - balance the load and life cycle of the DC/AC branches,
  - provide isolation and reconfiguration without significantly increasing the number of signal lines,
  - switch branches between phases, allowing system parameters to be tailored to grid needs and contributing to branch load balancing.

Based on the analysis from the previous sections, a decision was made to connect the T-type four-branch modules in parallel. The T-type topology is regarded as the most efficient of the three-level converter topologies in terms of overall performance. With the inclusion of additional transistors, current flow can be more effectively controlled in this topology, resulting

in reduced switching losses and lower thermal loads. Furthermore, the T-type configuration promotes a more balanced load across individual semiconductor components, which also enhances the efficiency and prolongs the lifespan of the system [38].

In order to balance the DC circuit voltages of the DC/AC modules and minimize circulating currents between them, the DC midpoints of all modules were interconnected (**Figure 28**). The output filter employs an LC topology, and a static switch array between the filter and the AC grid facilitates the branch connection to the grid lines (**Figure 29**). All switches are implemented using two MOSFET transistors arranged oppositely. It is important to note that connecting the branch to the neutral line results in a short circuit across both terminals of the LC filter capacitor designated for that branch, as further detailed in the following sections.
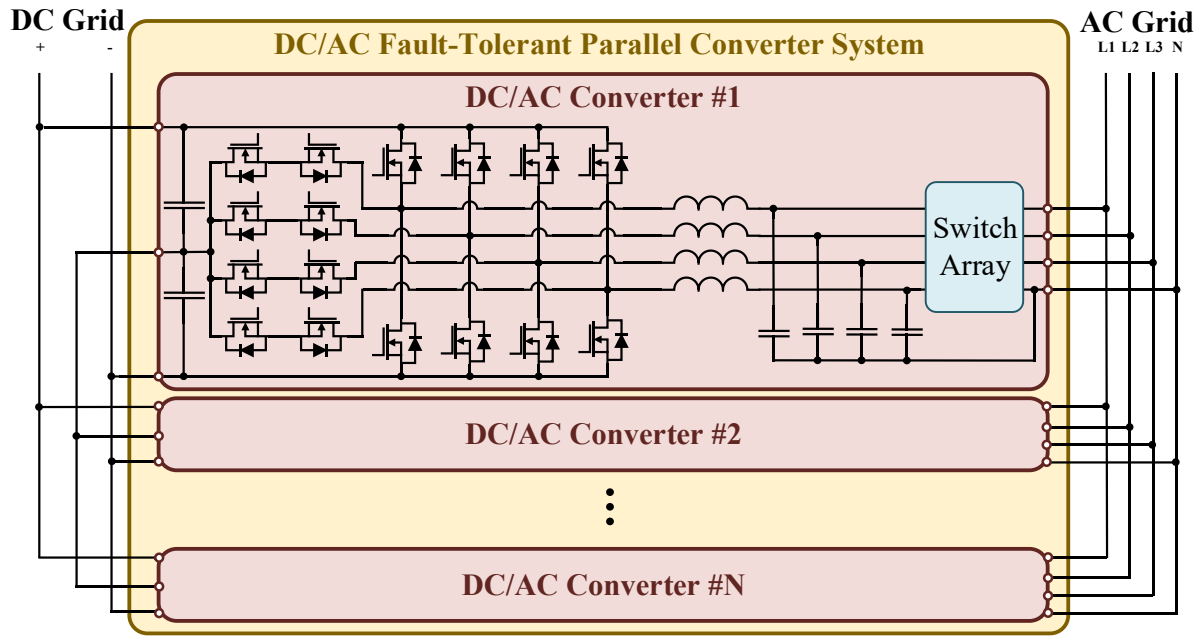

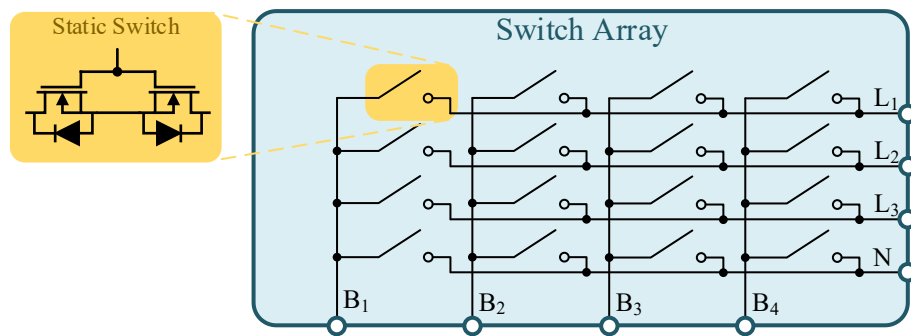**Figure 28.** Proposed parallel DC/AC converter topology.

Figure 29. Branch to line static switches array.

56

The proposed topology meets the assumptions regarding the modular structure of the system. Multiple parallel DC/AC power conversion paths are provided. Using an additional array of high-speed bidirectional solid-state switch enables reconfiguration of the branch connection to any line of the AC grid [39]. This system structure, in turn, presents several challenges that require resolution, including:

- **Distributed Control**:
  - the control strategy is segmented across multiple digital control units, each with constrained computational resources,
  - highly reliable real-time communication is essential for effective coordination among these units,
  - synchronization of data and PWM signals is crucial for optimal performance,
  - a comprehensive set of process variables must be defined to enable accurate monitoring and control within the distributed system.

- **Management of Active Branches and Modules**:
  - continuous load monitoring is necessary to adapt to dynamic operating conditions,
  - dynamic branch switching between grid lines is implemented to optimize efficiency and maintain load balance across transistor branches.

- **Electrical Circuit Characteristics**:
  - mitigation of internal circulating currents,
  - ensuring current and voltage stability despite variations in grid filter parameters,
  - prevention of overvoltages and overcurrents during module connection and reconfiguration to the grid,
  - maintaining DC capacitor voltage balance.

2.6. Output AC filter

Connection of the four-branch DC/AC module to a four-wire LV grid with reconfigurable connections requires appropriate LC filter topology. Each branch must maintain identical connection capability with three phases and a neutral line. This functionality is provided by an LC filter in which the capacitors are connected in a star, and the star point is connected directly to the neutral line. On the module side, each branch has its inductor. The capacitors can be connected to the grid via separate switches for each phase on the grid side. The capacitor's star point is connected to the neutral line and maintains the corresponding phase voltage on the

capacitors. Three generic operation modes are distinguished: three-phase, single-phase, and phase-to-phase:

- in the three-phase mode, the capacitor from the branch connected to the neutral point is inactive because both terminals are connected to the neutral line (**Figure 30**),
- only two capacitors are active in the single-phase mode because the other two have both terminals connected to the neutral line (**Figure 31**),
- in the inter-phase mode, two parallel capacitors are connected between the neutral line and the first active phase, and the following two parallel capacitors are connected between the neutral line and the second operational phase (**Figure 32**).
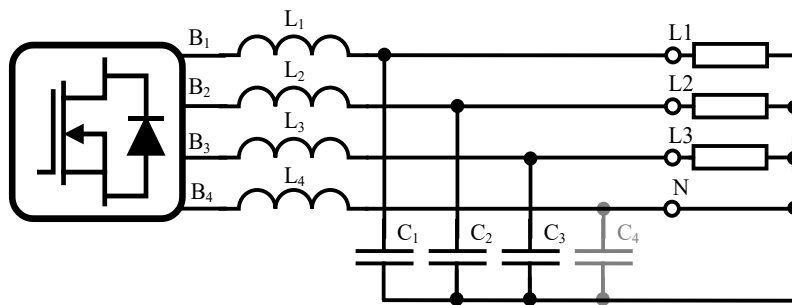

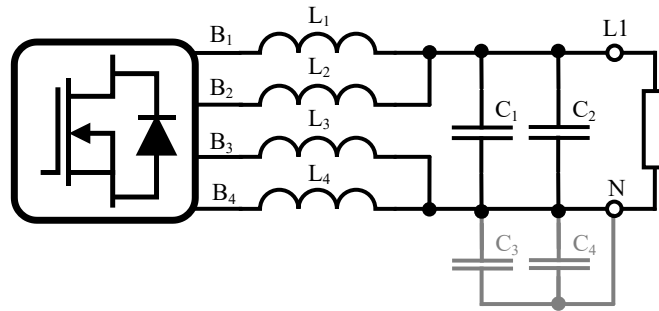
Figure 30. LC filter in a three-phase configuration.

Figure 31. LC filter in a single-phase configuration.
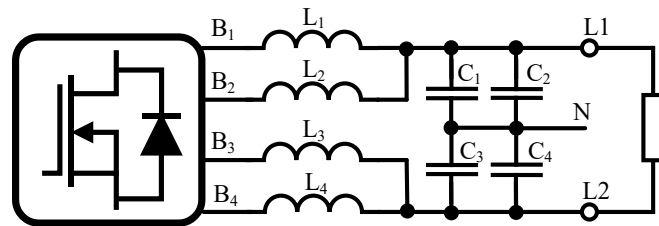

Figure 32. LC filter in inter-phase configuration.

2.7. Analysis of the effects occurring in parallel connected DC/AC converters

The parallel connection of DC/AC converters alters the internal structure of the system, leading to significant changes in circuit configuration and the resulting output impedance. This subsection examines how such reconfiguration impacts two critical issues: circulating currents, which increase stress on system components, and LC resonance, which can compromise the stability of the control system.

2.7.1. Circulating currents in parallel connected DC/AC converter with common DC

Increasing the number of energy conversion paths by connecting multiple DC/AC branches in parallel introduces additional phenomena that can negatively impact the system's efficiency and operational stability. The most significant of these are circulating currents and variable output impedance.

Circulating currents are internal current components that flow through transistor branches without reaching the load—their paths are closed within the system itself. As the magnitude of circulating currents increases, overall system efficiency declines. These currents also place additional stress on semiconductor components and can lead to control instability by introducing voltage and current harmonics [40].

Circulating currents can be classified based on their origin into the following categories:

At first, circulating currents result from the formation of AC voltage through PWM modulation with LC filters (**Figure 33**). The current path is closed in an LC filter between two branches within the converter. The circulating current between two branches connected to selected grid line and neutral point, $i_{Lx \to N \, PWM,}$ and between two branches connected to different grid phases, $i_{Lx \to Ly \, PWM,}$ are inherent in DC/AC converters, and their magnitude depends on inductance L_x and capacitance C_x values in the AC output filter and DC voltage v_{DC}. The value of the circulating currents is variable during the period of the base component, where the voltage on the capacitor is formed:

$$i_{Lx \to N \, PWM}(t) = \frac{1}{2L} \int_0^{D_x T_{PWM}} (v_{DC} - v_{Cx}(t)) \, dt \qquad (2.4)$$

$$i_{Lx \to Ly \, PWM}(t) = \frac{1}{2L} \int_0^{D_{xy} T_{PWM}} \left(v_{DC} - \left(v_{Cx}(t) - v_{Cy}(t) \right) \right) dt \qquad (2.5)$$

$$v_{Cx}(t) = \frac{1}{C_x} \int_0^{D_x T_{PWM}} \left(i_{Lx \to N \, PWM} + 2 i_{Lx \to Ly \, PWM} + i_{C \, Base} - i_{Load} \right) dt \qquad (2.6)$$

where: x – selected grid line {1,2,3}, y – other selected grid line, and: $x{\neq}y$, Lx – grid line, N – neutral point of grid lines, D_x – duty of PWM signal in selected line, D_{xy} – duty of PWM signal between two selected lines, $i_{C\,Base}$ – capacitor current associated with the fundamental harmonic, i_{Load} – load current.
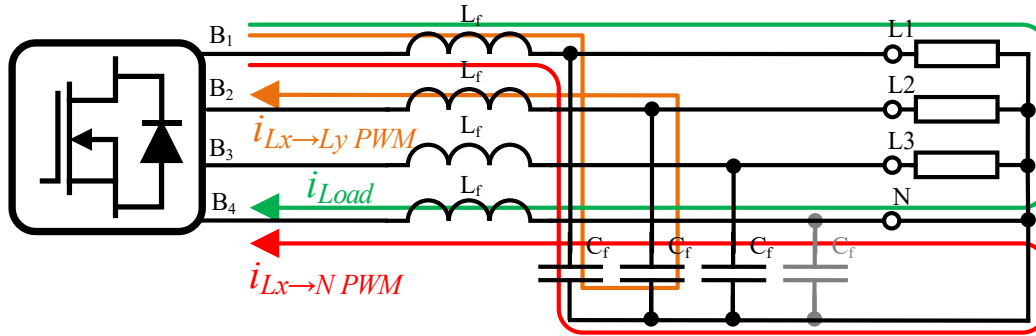

Figure 33. Internal circulating currents in DC/AC converter.

Due to the parallel connection of multiple converter branches to a shared LC filter, the effective capacitance of the system changes dynamically depending on the number of active branches and their respective control states. As a result, the magnitude of circulating currents which arise from inter-branch modulation differences and voltage mismatches can also vary. These circulating currents not only reduce overall system efficiency but may also introduce additional thermal stress on power components, requiring careful design of control strategies and mainly filter capacitance parameter to minimize their impact:

$$C = nC_B \tag{2.7}$$

where: C – resultant capacitance, n – number of branches, C_B – capacitance of branch LC filter.

Secondly, the circulating current between branches connected to common grid phase $i_{PWM\,IB,}$ arises from improper synchronization of the parallel-connected DC/AC branches, which are controlled by a PWM signal with varying duty cycles, phase shifts, dead times, voltage level v_{DC}, and components parameters drift (**Figure 34**):

$$i_{PWM\,IB}(t) = \frac{1}{L_{f1}+L_{f2}} \int_0^{(D_1-D_2)T_{PWM}} (v_{DC})\, dt \tag{2.8}$$

where: D_1, D_2 – PWM signal duty for the transistor in the first and second branch respectively, T_{PWM} – period of PWM signal.
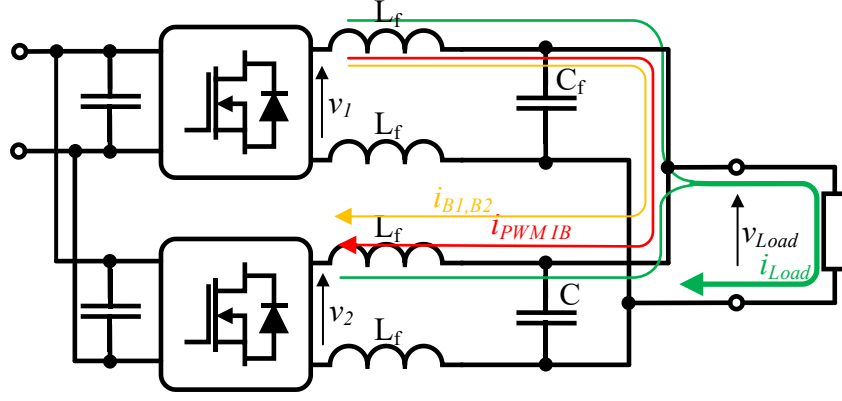
Figure 34. External circulating current in parallel DC/AC converters.

These currents can be eliminated if the PWM signals controlling the branches in each cycle are in the same phase and duty. In addition, the number of levels and the value of the DC voltage will be the same. If the listed conditions are not met, the circulating current is limited by the impedance of the two inductances L_{f1} and L_{f2} connected in series between the branches. To prevent circulating currents between DC/AC modules, the control system must provide synchronized PWM signals, balanced DC voltage, and an equal voltage vector.

The third type of circulating currents, $i_{B1,B2,}$ results from the difference in the output voltages v_1, v_2 of the converters with different amplitudes A_1, A_2 and different phase shifts θ_1, θ_2:

$$i_{B1,B2}(t) = \frac{1}{2L} \int_0^{T_{Base}} \big(v_1(t) - v_2(t)\big)\, dt \qquad (2.9)$$

where the branch output voltages are defined by the equations:

$$v_1(t) = A_1 \sin(\omega_{Base} t + \theta_1) \qquad (2.10)$$

$$v_2(t) = A_2 \sin(\omega_{Base} t + \theta_2) \qquad (2.11)$$

In summary, parallel connection can increase circulating currents in the system due to:

- variability of LC filter parameters,
- asynchronous PWM modulation: deadtime, phase shift, and frequency differences,
- asynchronous reference signals are used for base frequency ω_{Base} signals, where amplitude, and phase shift differences may occur.

All parallel-connected branches should have synchronized PWM signals and the same current reference signal to minimize the value of circulating currents. Since the modules have

separate control units, with PWM synchronization and equal inductances, the current regulators should produce the same output voltage signal. Which, consequently, should produce the same duty.

2.7.2. Stability in parallel connected DC/AC converters with variable filter impedance

The DC/AC converters' control system must ensure the operation's stability for the selected LC filter impedance. If the number of modules is multiplied, another problem arises due to the variable impedance of the output filter. In addition, as the number of parallel connected branches changes, additional paths for current are created. Therefore, the problem of maintaining the stability of a single module is extended to a system of multiple parallel-connected branches this configuration is the Multiple Input Single Output (MISO) system (**Figure 35**). This issue has been addressed mainly in the literature for LCL filter circuits without a common DC circuit [41].
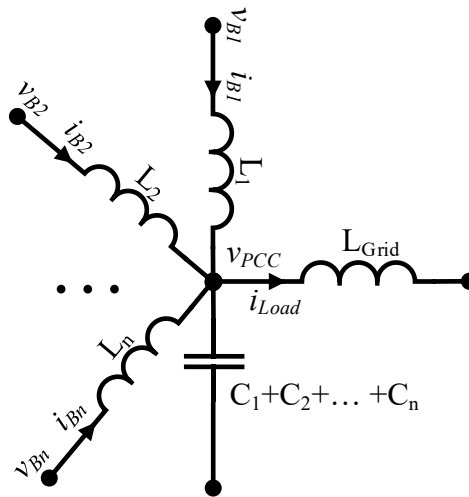

Figure 35. Equivalent circuit of the combined branch output filters and grid.

The solution presented in the thesis assumes parallel operation of the DC/AC modules with the following conditions:

- common DC without galvanic isolation,
- the control systems of the modules are synchronized via a Real-Time communication interface,
- the control system is distributed between a central controller and the controllers of the DC/AC modules.

Thus, the risks affecting the value of circulating currents are:

- unequal LC filter impedance values between branches and PCC,
- PWM synchronization inaccuracy,
- jitter - random time fluctuations of the PWM signal.

Controlling parallel-connected DC/AC branches with different AC filter inductors L_f requires a compromise between balancing the branch load and minimizing the circulating currents. The closer the AC filter inductance values are to each other, the easier this compromise is to achieve. The system of equations for branch current i_B flow the circuit in the **Figure 35** is as follows:

$$\frac{di_{B1}}{dt} = \left(\frac{1}{L_1} + \frac{1}{L_1+L_2} + \cdots \frac{1}{L_1+L_n}\right) v_{B1} - \frac{1}{L_1+L_2} v_{B2} - \cdots - \frac{1}{L_1+L_n} v_{Bn} - \frac{1}{L_1} v_{PCC} \qquad (2.12)$$

$$\frac{di_{B2}}{dt} = -\frac{1}{L_1+L_2} v_{B1} + \left(\frac{1}{L_2} + \frac{1}{L_1+L_2} + \cdots \frac{1}{L_2+L_n}\right) v_{B2} - \cdots - \frac{1}{L_2+L_n} v_{Bn} - \frac{1}{L_2} v_{PCC} \qquad (2.13)$$

The equation for n branch connected in parallel takes the following form:

$$\frac{di_{Bn}}{dt} = -\frac{1}{L_1+L_n} v_{B1} + \left(\frac{1}{L_2+L_n}\right) v_{B2} - \cdots + \left(\frac{1}{L_n} + \frac{1}{L_1+L_n} + \frac{1}{L_2+L_n} + \cdots + \frac{1}{L_{n-1}+L_n}\right) v_{Bn} - \frac{1}{L_2} v_{PCC} \quad (2.14)$$

Assuming that all reference signals are equal:

$$i_{L1\,ref}(t) = i_{L2\,ref}(t) \qquad (2.15)$$

the final simplified model in the state space is as follows:

$$\begin{bmatrix} \dot{\iota}_{B1} \\ \dot{\iota}_{B2} \\ \vdots \\ \dot{\iota}_{Bn} \end{bmatrix} = \begin{bmatrix} L_{11} & L_{12} & \cdots & L_{1n} \\ L_{21} & L_{22} & \cdots & L_{2n} \\ \vdots & \vdots & \ddots & \vdots \\ L_{n1} & L_{n2} & \cdots & L_{nn} \end{bmatrix} \begin{bmatrix} v_{B1} \\ v_{B2} \\ \vdots \\ v_{Bn} \end{bmatrix} + \begin{bmatrix} -\frac{1}{L_1} \\ -\frac{1}{L_2} \\ \vdots \\ -\frac{1}{L_n} \end{bmatrix} v_{PCC} \qquad (2.16)$$

$$L_{xx} = \frac{1}{L_x} + \frac{1}{L_1+L_2} + \cdots \frac{1}{L_x+L_n} \qquad (2.17)$$

$$L_{xy} = L_{yx} = \frac{1}{L_x+L_y} \qquad (2.18)$$

where: x – row index, y – column index, n – number of branches.

The voltage driven on all branches connected to the same line must be identical to prevent circulating currents. However, even with identical voltage references, practical factors can lead to unequal current sharing among the branches. The primary cause of this imbalance is the difference in filter inductance values between branches, as shown in following equation:

$$
\begin{bmatrix} \dot{\iota}_{B1} \\ \dot{\iota}_{B2} \\ \vdots \\ \dot{\iota}_{Bn} \end{bmatrix} = \begin{bmatrix} \frac{1}{L_1} & 0 & \cdots & 0 \\ 0 & \frac{1}{L_2} & \cdots & 0 \\ \vdots & \vdots & \ddots & \vdots \\ 0 & 0 & \cdots & \left(\frac{1}{L_n}\right) \end{bmatrix} \begin{bmatrix} v_B \\ v_B \\ \vdots \\ v_B \end{bmatrix} + \begin{bmatrix} -\frac{1}{L_1} \\ -\frac{1}{L_2} \\ \vdots \\ -\frac{1}{L_n} \end{bmatrix} v_{PCC}
\qquad (2.19)
$$

In addition to minimizing circulating currents, it is essential to ensure the stability of the current control loop. The circuit shown in **Figure 35** represents multiple current sources connected through individual inductors to a shared output capacitor. The effective capacitance of this configuration varies depending on the number of active branches. The relationship between the branch current i_{Bx} and v_{Bx} and the output voltage is described by the following equation:

$$
\frac{i_{Bx}(s)}{v_{Bx}(s)} = \frac{1}{L_x L_g (\sum_1^n C) s^3 + (L_x + L_g) s}
\qquad (2.20)
$$

where: i_x – branch current, n – number of branches, L_x – branch side filter inductor, L_y – filter inductor from other parallel connected branch, L_g – grid side inductor

When multiple branches are connected in parallel, resonance phenomena can occur due to the interaction between branch inductances and the common capacitance. These can be categorized as:

- Common resonance - this occurs when all branches oscillate in unison, as described by:

$$
\omega_{res\ x} = \sqrt{\frac{L_x + L_g}{L_x L_g \sum_1^n C}}
\qquad (2.21)
$$

- Interactive resonance - this type of resonance arises from the interaction between different branches, particularly when their filter parameters differ

$$
\omega_{res\ x,y} = \sqrt{\frac{L_x + L_y}{L_x L_y \sum_1^n C}}
\qquad (2.22)
$$

Based on the interactive resonance equation and the known number of transistor branches attached to the common grid line, the set and resonant frequency range of the LC filter in which the common capacitance changes can be determined (**Figure 36**). This fact needs to be taken into account when selecting regulator settings and an analysis of this issue has been carried out in [23].
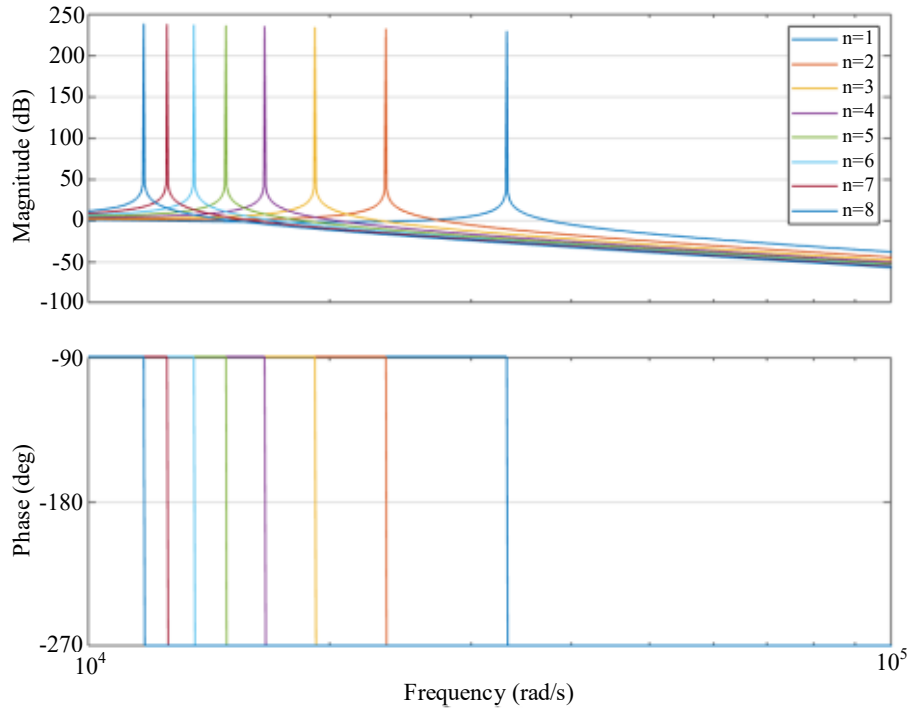

Figure 36. Grid-side AC filter resonance frequency dependency from parallel branch number.

When considering the dependence of the resonant frequency on the number of branches, it can be seen that the largest impedance changes occur when the number of branches is small (**Figure 37**). As the difference increases, the changes become smaller and smaller. Impedance spikes can negatively affect the stability of the control system.

The resonant frequency, which is influenced by the number of branches operating in parallel, varies within a specific range. Notably, smaller changes in resonant frequency indicate that more branches are actively functioning. This implies that the system's stability is maintained as long as the switching frequency exceeds the resonant frequency of individual modules.

In practical terms, when multiple branches are connected in parallel, the overall resonant frequency tends to stabilize due to the distributed nature of the load. As more branches are added to the system, the effects of any individual branch become less pronounced, leading to a

narrower range of frequency variations. This characteristic is critical for ensuring reliable operation, as it allows the system to accommodate fluctuations in load without compromising stability.
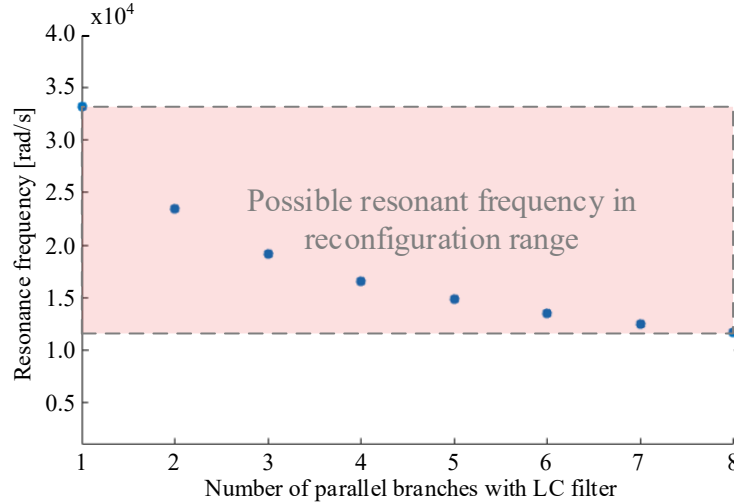

Figure 37. The lower limit of the resonant frequency.

To achieve optimal performance, it is essential that the switching frequency of the control system is consistently higher than the resonant frequency of any single module. Operating above this threshold allows the system to mitigate the risks associated with resonance, such as voltage spikes or oscillations, which can occur if the switching frequency approaches the resonant frequency. By ensuring that the system operates under these conditions, the reliability and efficiency of the DC/AC converter system are significantly enhanced, facilitating its ability to handle dynamic load conditions effectively.

2.8.   Summary of reliability analysis in a parallel converter system

The main research objective of this dissertation is to develop an energy conversion system capable of operating under emergency conditions and resisting the adverse effects of deteriorated grid parameters. Based on the analysis carried out in this chapter, the author draws the following conclusions:

- continuity of energy conversion during fault conditions can be ensured by connecting multiple parallel energy conversion paths, when connecting a four-wire AC grid to a DC grid, more than one transistor branch should be provided for each line of the AC grid;

66

- the LV grid is asymmetrically loaded most of the time, which in turn affects the uneven load on the semiconductor elements leading to their uneven ageing, the DC/AC power conversion system should provide the ability to reconfigure and adjust the number of active branches to balance the ageing of the semiconductor elements;
- parallel connection of multiple transistor branches brings additional control system challenges related to:
  - the variable impedance of the LC line filter,
  - the possibility of circulating currents associated with PWM modulation,
  - the need to develop additional algorithms for zero-impact switching on and off of transistor branches without stopping the system,
  - adjustment of the number of active branches to maximize system efficiency.
- the operation of the system when a component failure is detected should allow the faulty unit to be replaced without stopping the whole system, the replacement unit is a four-branch DC/AC module, after analysis, the design of a DC/AC module with the following characteristics is proposed:
  - four branches with a T-type topology, requiring:
    - sixteen PWM control signals,
    - four AC current measurements,
    - four AC voltage measurements,
    - two DC voltage measurements.
  - each transistor branch can be connected to any line of the grid which requires a switch matrix,
  - each module has one controller with real-time communication with the central unit.
- depending on the operating mode, the degraded parameters of currents and voltages in the AC grid may negatively affect the quality of regulation and the control algorithm should be resistant to the following factors:
  - in grid-forming mode, the distorted current should not deteriorate the quality of the system's output voltage,
  - in grid-supporting mode, the output current should be correctly formed according to the reference value despite the distorted grid voltage at the system connection point.

- none of the multilevel converter topologies offer a clear reliability advantage in the context of multi-parallel configurations. In such systems, a typical fault-handling strategy such as reducing the number of voltage levels in a single faulty branch can lead to an increase in circulating currents between branches, potentially compromising system stability. Although in critical scenarios it is possible to reconfigure the entire system to operate with a reduced number of voltage levels, such a strategy introduces additional complexity and is not considered within the scope of this study.

In summary, the chapter presents key architectural strategies that enable reliable energy conversion under fault conditions and degraded grid parameters. The proposed system emphasizes modularity, fault tolerance, reconfigurability, and operational continuity, while addressing challenges such as asymmetrical load distribution, control coordination in parallel branches. The resulting design forms a solid foundation for the development of a fault-resilient DC/AC conversion system suitable for critical applications.

3. Control strategy for reliable low voltage stage of Power Electronics Transformer

Reliable control for DC/AC power electronic systems must provide stable and accurate current and voltage control over possible grid operating scenarios [42]. The PET LV stage interacts with the grid in two main modes [43]. First is the grid-forming mode, where the PET is the primary voltage source (grid voltage forming unit). In the literature, this mode of application of grid connected converters has been described as either uninterruptible power supply or dynamic voltage restorer [44], [45], [46]. The second mode is the grid-supporting mode, where another distribution transformer or another power supply unit are the primary voltage source, and the PET system generally operates as the current source [47]. The control algorithm must provide a dedicated set of functionalities for both modes, including management of PET's for fitting the hardware configuration to load condition. To recognize the most essential requirements and functionality for the LV stage of PET control system, it is necessary to analyze the main parameters for evaluating converter systems concerning LV grids. **Table 6** shows the set of functions in the main domains required on the control system of the PET LV stage.

Table 6. The grid sets requirements and goals for the PET LV stage's control system.

Domain	Grid-forming mode	Grid-supporting mode
Voltage/Current Quality	Maintain pure sinusoidal and balanced voltage under distorted and unbalanced load current [48]	Stable current regulation under distorted grid voltage.
Grid Safety	Ability to force a large short circuit current by switching on subsequent modules or limit short-circuit power by reducing voltage.	An additional source of energy for the grid relieves the primary source.
Energy Management	Energy management is achieved through interaction with smart devices (loads, storage systems, and distributed energy sources)	Energy management by interaction with the main distribution transformer.
System Reliability	Uninterrupted energy supply and post-fault operation capability after fault isolation.	Maintain appropriate grid voltage parameters and reconstruct or support one of the phases in the event of a fault in the primary transformer [46].
System Efficiency	Maximize the system's efficiency by adjusting the number of operating branches or modules to the load power.	

Additional considerations in the design of the control system include the topology and the connection type with both DC and AC grids. The proposed design for the PET LV stage consists of parallel-connected modules featuring switchable four-T-type branches along with a

common DC link. The challenges associated with controlling a single module are compounded when operating multiple modules connected in parallel. While the advantages of a modular structure are significant, they are offset by the complexities that need to be addressed to ensure that parallel operations are cost-effective. **Table 7** summarizes the benefits and challenges that must be addressed in the proposed design outlined in the previous chapter.

Table 7. Summary of benefits and issues for the control system posed by PET's proposed LV system topology stage.

Feature	Benefit	Issue	Requirements and objectives
Common DC Link	One grid without galvanic separation	Circulating Currents [40]	Circulating currents result from the lack of synchronization of the PWM signals and the difference in voltage vectors for branches operating on the same phase. The synchronization of PWM signals is done in hardware using a communication chip. To minimize the circulating currents, the branches in a common phase should have the same voltage vector, assuming that the inductances in the output filter are equal.
Multilevel Converter	Better voltage quality with a smaller grid-side filter volume	Series DC capacitor voltage balancing [49]	Multilevel topologies with series-connected capacitors in a DC circuit are prone to uneven charging and discharging. A different control system is necessary to balance the capacitor voltages.
Over-switching branches between grid lines	Increase system reliability and flexibility	Reconfiguration without stopping the system while maintaining operational stability [50]	Branch switching is intended to increase system reliability and provide a higher power supply to the phase with increased load, which balances the branches in the converter modules. In addition, the branch's current control must be independent or decoupled from the others.
Multiple modules and control units	System scaling and fault-tolerance	Distributed control algorithm [51]	The primary internal control system is extended to many converters, which must interact with the rest of the modules and be managed externally. The control system is then distributed, and the data transmission time must be considered.
Parallel Connection	Internally balanced load sharing and multiple conversion paths	Common and interactive stability [27]	A variable number of branches and AC filters connected to a common point causes impedance variations, negatively influencing stability.

As can be seen from the **Table 7**, providing certain benefits brings problems that the control system should deal with. The last set of requirements relates to standard evaluation factors for control systems: control accuracy, dynamics, ease of tuning, and low computational resource consumption.

The listed set of conditions and problems guides the design of the control method for the PET LV stage. Many of the issues mentioned have been addressed in the literature. However,

no comprehensive solution for a modular parallel DC/AC system with distributed control and reconfiguration ability has been presented. The following sections describe the control system configuration depending on the mode of operation and type of module-to-grid connections. Firstly, control methods are given for the system in ordinary states of operation in grid-supporting and grid-forming modes, considering the typical current and voltage deformations in the LV grid. Then, in the following sections, the methods are considered where the system reconfigures itself adequately to maintain system performance.

3.1. Grid-connected converter with output LC filter modeling

A typical DC/AC grid-connected converter control system includes two state variables: inductor current i_{Lf} and filter capacitor voltage v_{Cf}. In turn, the DC/AC grid-connected converter can operate in two modes depending on the appearance of the external voltage source [52]. For both modes (grid-forming and grid-supporting), it is necessary to analyze the converter model with LC filter and grid separately to select the optimal control method.

3.1.1. The grid-connected converter with the external voltage source

Grid-connected converter operate as a current source if there is another primary voltage source in the grid. **Figure 38** shows a simplified circuit with two voltage sources, DC/AC converter v_I and grid voltage v_g, connected through LC filter and grid impedance Z_g. In this mode, the converter is capable to:

- support the primary voltage source,
- receipt energy surplus.
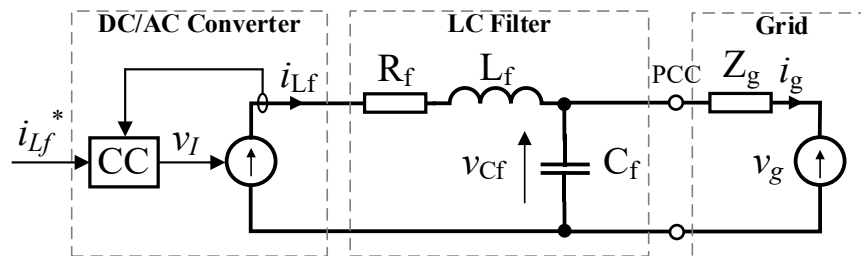
Figure 38. The grid-connected converter circuit with an external voltage source.

The set of equations describing the DC/AC converter model from **Figure 38** is as follows. Equation for the current in the inductor of the LC filter:

$$i_{Lf} = sC_f v_{Cf} + (v_{Cf} - v_g)\frac{1}{Z_g} \qquad (3.1)$$

Voltage equation on the converter side:

$$v_I = (sL_f + R_f)i_{Lf} + v_{Cf} \qquad (3.2)$$

Voltage equation on the grid side:

$$v_g = Z_g i_g + v_{Cf} \qquad (3.3)$$

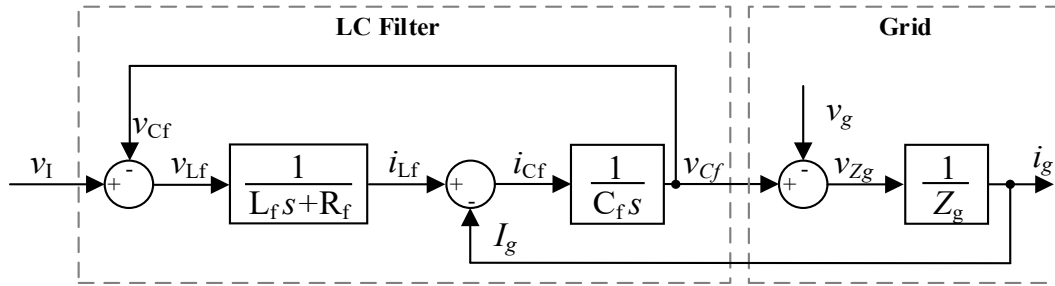The equation-based model is shown in **Figure 39**.

Figure 39. The current source model of the grid-connected converter with an LC filter.

3.1.2. Grid-connected converter as primary voltage source

A DC/AC converter in grid-forming mode controls the output voltage on the filter capacitor (**Figure 40**). The output current is load-dependent. In this case, a typical control system consists of a cascaded voltage controller, which sets the reference value i_{Lf}^* for the current controller. The current controller sets the converter's output voltage v_I.
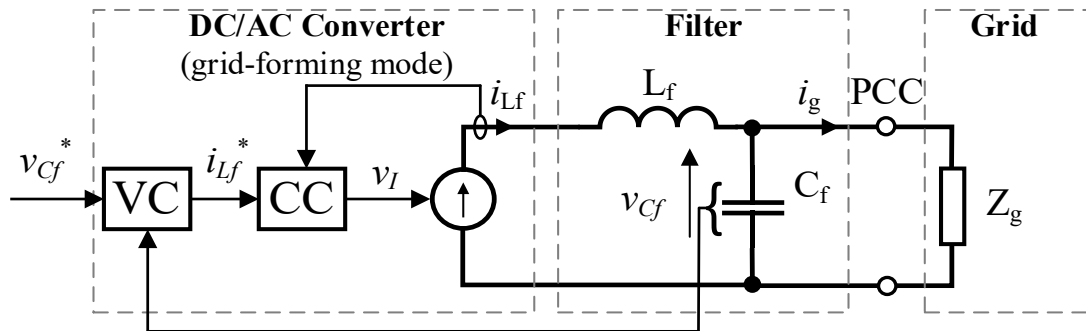
Figure 40. DC/AC converter converter as primary grid voltage source.

An equivalent model of the LC filter in grid-forming mode is shown in **Figure 41**. The converter's output voltage and load current are the main forces.
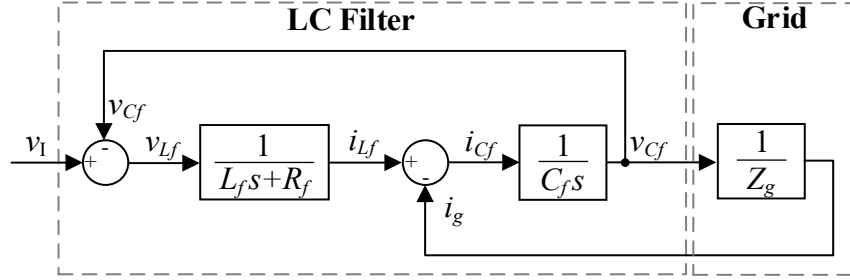
Figure 41. Grid-forming mode block diagram.

The equations of the LC filter model are as follows. Equation for the current in the inductor of the LC filter:

$$i_{Lf}(s) = \frac{1}{L_f s + R_f}\left(v_I - v_{Cf}\right) \tag{3.4}$$

Voltage across the LC filter capacitor:

$$v_{Cf}(s) = \frac{1}{C_f s}\left(i_{Lf} - i_{Load}\right) \tag{3.5}$$

The transfer function describing the relationship between the capacitor voltage and the converter output voltage:

$$\frac{v_{Cf}(s)}{v_I(s)} = \frac{1}{C_f L_f s^2 + C_f R_f s + 1} \tag{3.6}$$

3.2. Closed-loop control of DC/AC converter with output LC filter

The control system is a critical part of grid-connected DC/AC converters. In this case, the leading state variables are the inductor current i_{Lf} and the capacitor voltage u_{Cf} of the LC filter. The main control tasks to be performed are:

- maintaining current and voltage values as close to the reference value as possible,
- maintaining the stability of the system under the influence of external disturbances,
- avoiding resonance excitation in the LC filter.

73

The primary challenge in designing a control system for grid-connected converters lies in selecting an appropriate controller type and addressing its inherent limitations. Most existing literature focuses on linear control strategies, particularly combinations of Proportional-Integral (PI) and Proportional-Resonant (PR) controllers. These controllers are favored for their good dynamic response, accuracy, ease of implementation, and simple tuning procedures.

An important advantage of PR controllers is their ability to be applied independently to each converter branch, allowing phase decoupling and enhancing modularity in control. However, a major drawback is their narrow bandwidth, typically limited to a single harmonic, which restricts their effectiveness in compensating for broader frequency disturbances. Additionally, PR controllers can suffer from instability if the output circuit parameters such as impedance undergo significant variation.

Addressing these limitations is essential to ensure robust and reliable performance in a wide range of grid conditions

3.2.1. Closed-loop control of DC/AC converter in grid-supporting mode.

In grid-supporting mode, the primary controlled variable is the output current of the converter. A closed-loop control system is implemented using a PR controller, which is tuned to operate at the fundamental grid frequency $\omega_I = 2\pi \cdot 50$ rad/s. The PR controller enables accurate tracking of sinusoidal current references without steady-state error, making it suitable for applications requiring high power quality. The control structure is shown in **Figure 42**.
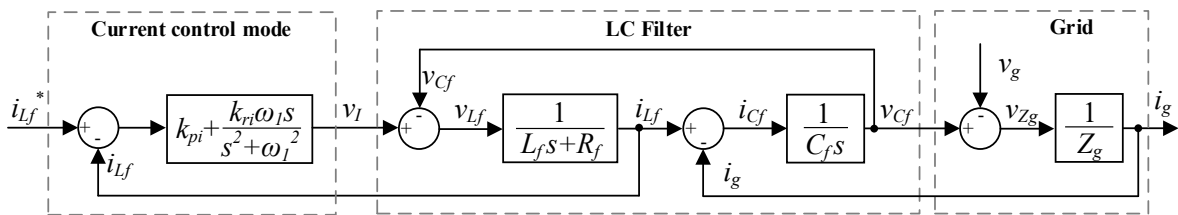
Figure 42. The control scheme of the grid-connected converter in grid-supporting mode

In this model, it is necessary to analyze the influence of the grid voltage v_g on the grid current i_g, as shown in **Figure 43**. The performance of the PR controller is primarily determined by the tuning of its resonant component, particularly the selected resonant frequency. This is evident in the controller's frequency response, which shows optimal damping at the fundamental grid frequency. However, in the frequency range between the fundamental and the

resonant peak, the attenuation degrades noticeably. As a result, if higher-order harmonics are present in the grid voltage, they may propagate to the current, leading to waveform distortion.

Solutions proposed in the literature to address the problem of grid voltage harmonics typically involve augmenting the control structure by adding multiple resonant components, as illustrated in **Figure 44**. Each of these components is specifically tuned to target selected harmonic frequencies—such as the 3rd, 5th, or 7th harmonics—to improve the controller's ability to suppress current distortion caused by harmonic content in the grid voltage [53], [54]. This multi-resonant approach enhances the harmonic rejection capability of the PR controller but also increases the complexity of tuning and may impact system stability if not properly designed.
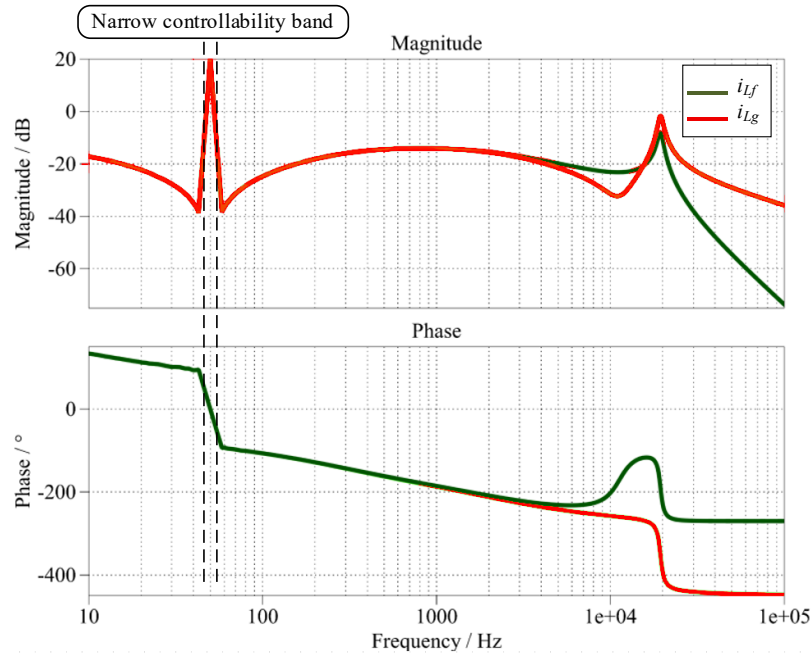
Figure 43. Bode characteristics for current control using PR controller in grid-supporting mode.
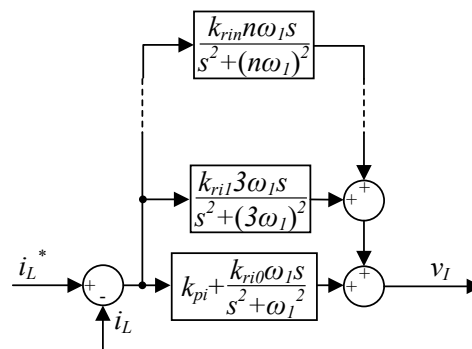
Figure 44. Multi-resonant current controller block diagram.

By duplicating the resonant components of the current controller, only specific harmonics can be suppressed, and there remains a risk to control stability if there is a harmonic present in the line voltage that has not been accounted for by the resonant elements. **Figure 45** shows the frequency characteristics and how the distorted voltage affects the controlled current depending on the selection of the current feedback signal on the converter side i_{Lf} and the grid side i_{Lg}. Since it is not possible to determine the grid voltage, tuning the resonant elements is pointless because the resonant parts would have to be able to adapt to the occurring harmonics.

The limitations of linear controllers have been partially mitigated by duplicating them and assigning each a specific bandwidth centered around selected harmonic frequencies. However, this approach significantly increases computational complexity and provides only selective harmonic compensation, remaining ineffective for harmonics outside the predefined frequency set.
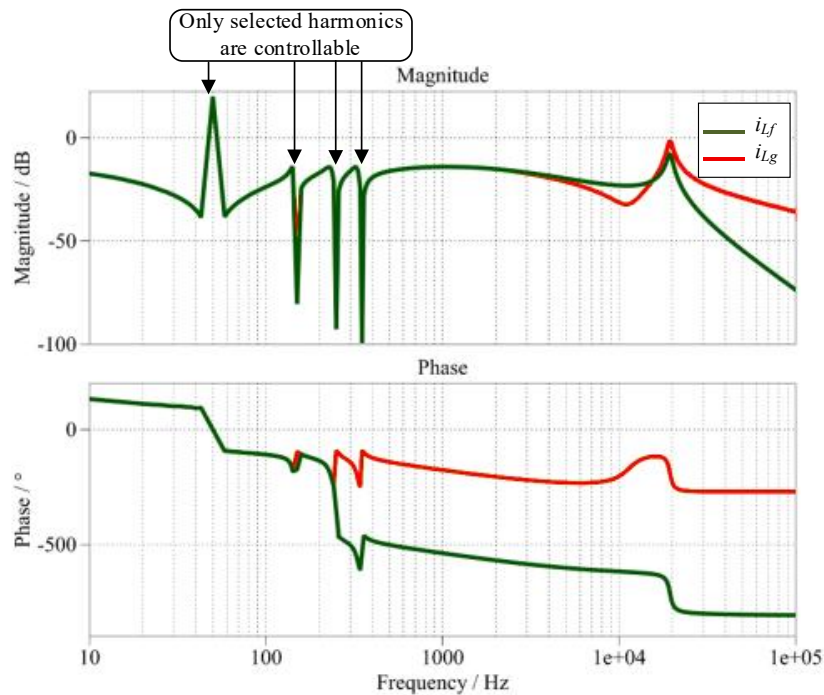
Figure 45. Bode characteristics of the multi-resonant current controller.

3.2.2. Analysis of current harmonic compensation in grid-supporting mode

In grid-supporting mode, the PET LV stage must maintain a set current value regardless of the voltage shape at the connection point. A distorted voltage forces currents with frequencies outside the bandwidth of linear regulators. Consequently, this leads to a loss of stability in the converter system. A simplified single-phase circuit of PET LV stage connection to the grid with

an external voltage source is shown in **Figure 46**. The inductances on both lines connecting the output of the PET to the capacitor reflect the actual configuration of the transistor branch connection to the grid.
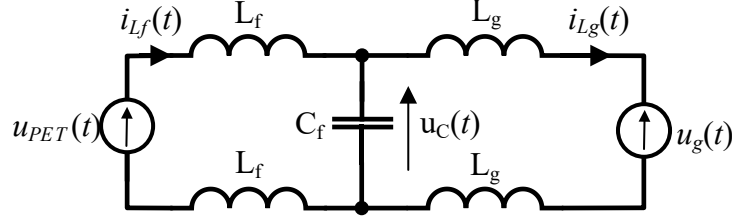

Figure 46. Simplified connection of PET to grid with an external voltage source.

By applying the principle of superposition, the circuit shown in **Figure 46** can be decomposed into two separate equivalent circuits. The first represents the system behavior at the fundamental frequency (**Figure 47**), while the second models the response to the entire spectrum of higher-order harmonics (**Figure 48**).
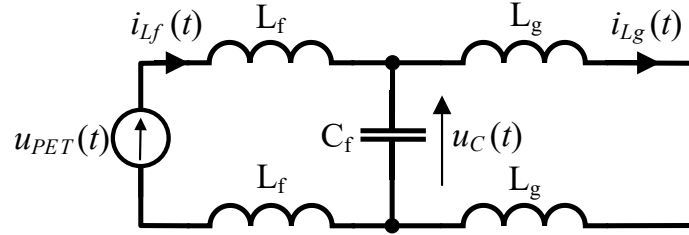
Figure 47. Superposition circuit for fundamental harmonic.
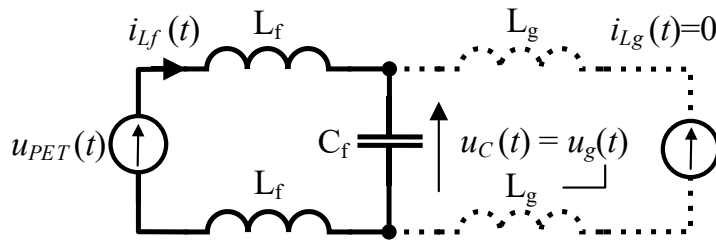
Figure 48. Superposition circuit for external voltage source compensation.

The main objective of this decomposition is to ensure that the voltage across the filter capacitor $u_c(t)$ closely follows the grid voltage $u_g(t)$, effectively balancing out the higher-order harmonics present in the external voltage source. When this condition is satisfied, no harmonic

current flows between the filter capacitor and the grid, which significantly improves the quality of the injected current.

Under this condition, the current controller is only responsible for generating the appropriate voltage drop across the filter inductance in order to enforce the desired reference current. This simplification reduces the controller's burden in compensating for distortions, allowing for more precise and stable current regulation.

The proposed control strategy for current harmonics compensation is shown in **Figure 49**. A proportional resonant controller with limited bandwidth tracks the single harmonic reference current i_{ref}. The capacitor voltage v_{Cf}, is feedforwarded, gained by K_{comp}, and then added to the PR controller output.
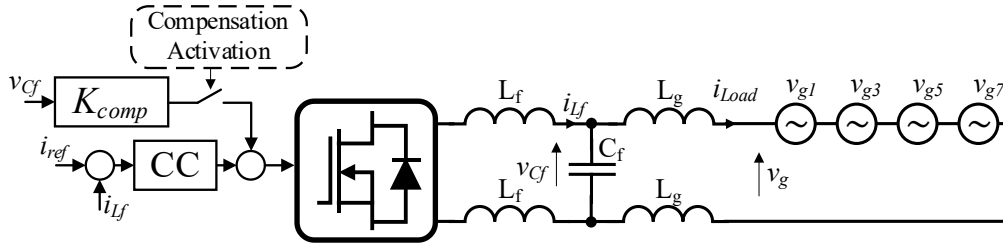
Figure 49. Proposed control strategy with current harmonics compensation.

An additional control component is a voltage controller with only proportional gain, which directly transfers all distortions and disturbances to the output voltage of the converter branch. Although this means that any disturbance will be reflected in the output voltage, it offers benefits in terms of harmonic suppression. However, it also introduces the risk of voltage degradation if noise or non-physical (fictitious) components appear in the reference signal or measurement.

The simplified simulation results from the **Figure 49** circuit diagram are shown in **Figure 50**. Waveforms are divided into two parts. First, it shows the current controlled only by the PR controller. The resulting grid current waveform i_{Lg} is strongly distorted because the current controller cannot balance higher-order harmonics. The second part adds AC filter capacitor voltage v_{Cf} to the PR output, and the grid current is close to pure sinusoidal as confirmed by the FFT charts.

The introduction of a current disturbance compensation component favorably influences the frequency response of the i_{Lf} and i_g currents against the v_g voltage in the range from zero to the resonance frequency. Significant attenuation of higher-order harmonics can be seen (**Figure 51**).
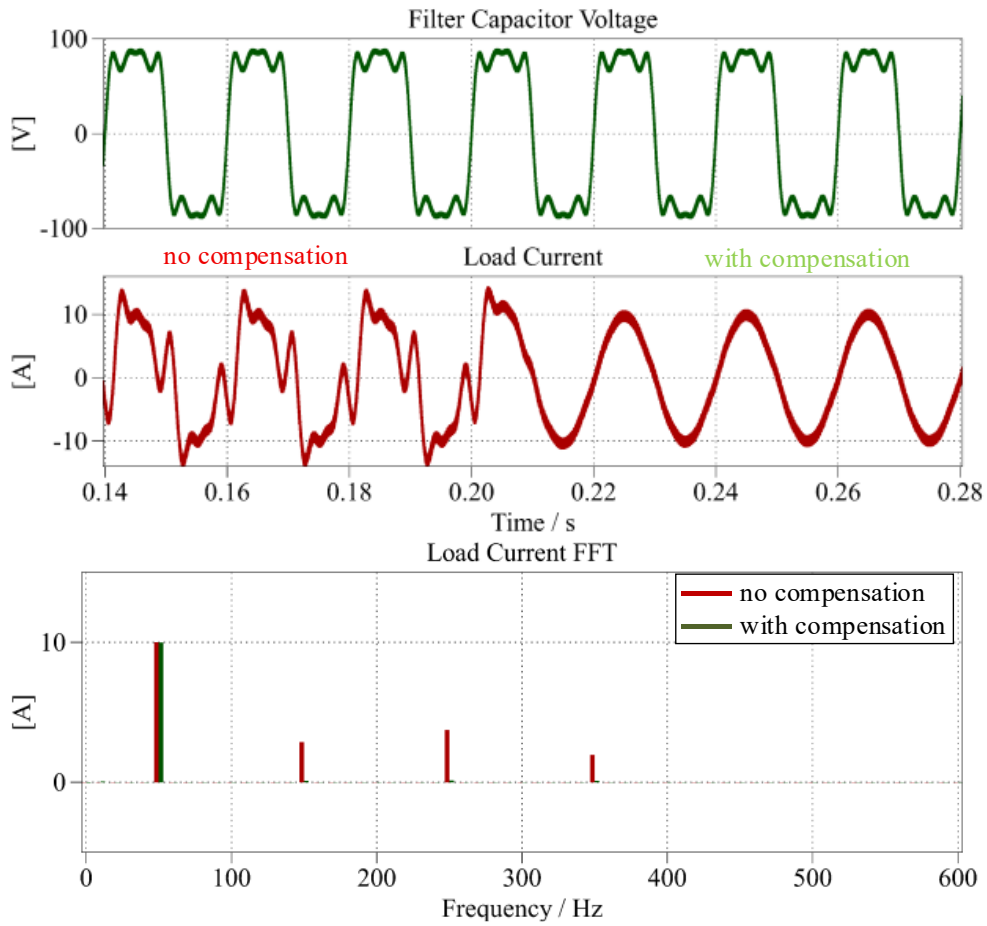
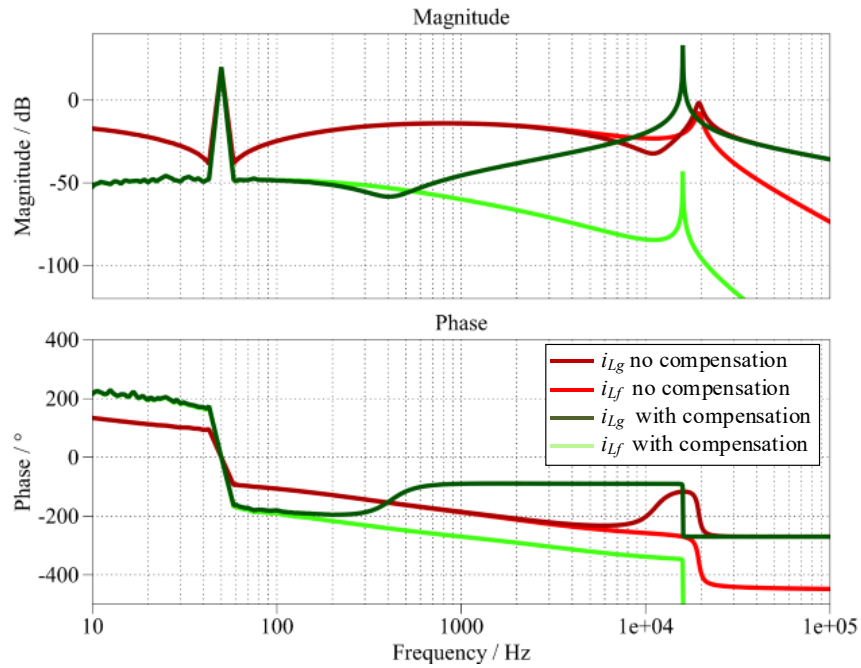**Figure 50.** Simulation result of current harmonics compensation activation.

Figure 51. Bode characteristics of the grid voltage v_g influence on the filter inductor and grid currents with and without a compension in grid-supporting mode.

It is also noticeable that the system's resonant frequency is reduced by moving the resonant frequency away from the PWM modulation frequency, improving active resonance suppression.

Adding a compensation component extends the control system, giving the expected effect of decoupling the current harmonics from the influence of the distorted voltage. The added component acts as a proportional voltage controller on the grid filter capacitor, operating between grid frequency and base frequency.

3.2.3. Analysis of voltage harmonic compensation in grid-forming mode

The basic assumption for the control system for a four-branch DC/AC converter is that the branch can be controlled independently due to load asymmetry. The branch's output current controller is tuned to the fundamental grid harmonic. As a result, the control system analysis can be simplified to a single-phase circuit. A proposal to solve multiplied controllers is to use an additional voltage harmonics compensator that is included parallel to the current controller.

In a typical grid-connected DC/AC converter with an LC filter in the grid-forming mode, the equivalent circuit has two sources (**Figure 52**). Voltage as the primary source (PET LV stage) and the current source representing the sum of load in the grid. To maintain the quality of the supply voltage, the source voltage $v_i(t)$ should keep the THD of the voltage $v_C(t)$ as low as possible under the influence of the distorted current $i_{load}(t)$.

To analyze the dynamic behavior of the converter model with an LC filter, the following set of equations is used to describe the system shown in **Figure 52**. These equations capture the relationships between voltages and currents within the filter and the converter, forming the basis for control system design and frequency-domain analysis.
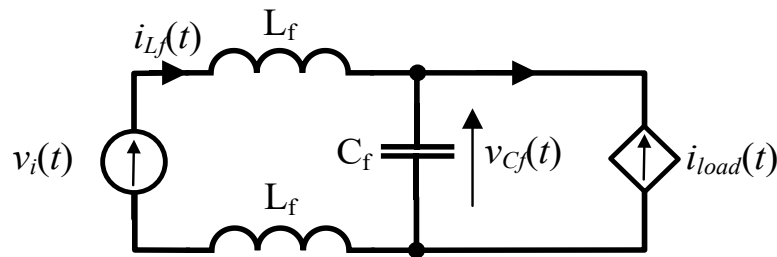

Figure 52. A single-phase LC filter circuit with a fundamental harmonic voltage source.

Voltage equation from the converter side:

$$v_i(t) = 2L_f \frac{di_{L_f}(t)}{dt} + v_{C_f}(t) \qquad (3.7)$$

State equation for the filter inductor:

$$\frac{di_{L_f}(t)}{dt} = \frac{1}{2L_f} v_{C_f}(t) - \frac{1}{2L_f} v_i(t) \qquad (3.8)$$

Equation of currents of a common node:

$$i_L(t) = C \frac{dv_C(t)}{dt} + i_{load}(t) \qquad (3.9)$$

State equation for the capacitor voltage:

$$\frac{dv_C(t)}{dt} = \frac{1}{C} i_L(t) - \frac{1}{C} i_{load}(t) \qquad (3.10)$$

The final form of the state equation system is as follows:

$$\begin{bmatrix} \frac{di_L(t)}{dt} \\ \frac{dv_C(t)}{dt} \end{bmatrix} = \begin{bmatrix} 0 & \frac{1}{2L} \\ \frac{1}{C} & 0 \end{bmatrix} \begin{bmatrix} i_L(t) \\ v_C(t) \end{bmatrix} + \begin{bmatrix} -\frac{1}{2L} & 0 \\ 0 & -\frac{1}{C} \end{bmatrix} \begin{bmatrix} v_i(t) \\ i_{load}(t) \end{bmatrix} \qquad (3.11)$$

Since a linear controller typically has limited bandwidth, an additional control loop is required to operate in the higher harmonic frequency range (**Figure 53**). The primary objective of this auxiliary controller is to suppress the higher-order harmonics of the voltage $v_{Cf}(t)$, ideally driving them to zero.
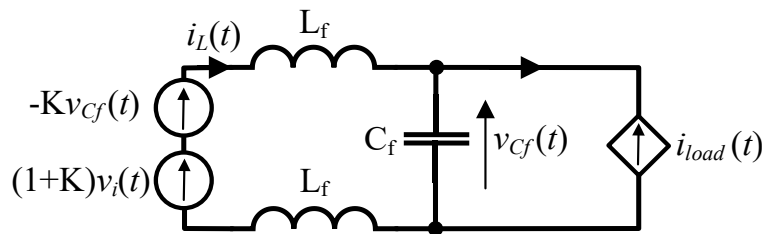
Figure 53. Single phase LC filter circuit with capacitor voltage harmonics compensation.

The proportional controller is one of the simplest and most effective solutions for this purpose, as it can operate across the entire frequency spectrum. When the setpoint for the higher

harmonics is zero, the harmonic compensation control law based on a proportional controller simplifies to $-Kv_{Cf}(t)$.

To analyze the behavior and characteristics of the proposed harmonic compensation system, the following set of equations has been formulated.

Voltage equation from converter side:

$$v_i(t) + K(v_i(t) - v_{C_f}(t)) = 2L_f \frac{di_L(t)}{dt} + v_{C_f}(t) \tag{3.12}$$

After transformation, the equation for the current through the LC filter inductor i_{Lf} was obtained:

$$\frac{di_{L_f}(t)}{dt} = \frac{1+K}{2L_f} v_{C_f}(t) - \frac{1+K}{2L_f} v_i(t) \tag{3.13}$$

Current equation for the node connecting the converter to the load:

$$i_{L_f}(t) = C_f \frac{dv_{C_f}(t)}{dt} + i_{load}(t) \tag{3.14}$$

As a result, the expression for the the capacitor voltage, was obtained:

$$\frac{dv_{C_f}(t)}{dt} = \frac{1}{C_f} i_{L_f}(t) - \frac{1}{C_f} i_{load}(t) \tag{3.15}$$

As a result, the model in the state space takes the following form:

$$\begin{bmatrix} \frac{di_{L_f}(t)}{dt} \\ \frac{dv_{C_f}(t)}{dt} \end{bmatrix} = \begin{bmatrix} 0 & \frac{1+K}{2L_f} \\ \frac{1}{C_f} & 0 \end{bmatrix} \begin{bmatrix} i_{L_f}(t) \\ v_{C_f}(t) \end{bmatrix} + \begin{bmatrix} -\frac{1+K}{2L_f} & 0 \\ 0 & -\frac{1}{C_f} \end{bmatrix} \begin{bmatrix} v_i(t) \\ i_{load}(t) \end{bmatrix} \tag{3.16}$$

The frequency analysis depicted in **Figure 54** compares the response of the capacitor voltage v_{Cf} to the supply voltage and the line output current. After applying an amplified negative feed-forward to the capacitor voltage, the resonant frequency is shifted to higher frequencies. As a result, the effect of the output current is more significantly attenuated in the frequency range between zero and the resonant frequency.

An example of a voltage harmonics compensation system is illustrated in **Figure 56**. A schematic of the circuit under test is presented in **Figure 55**, with its parameters detailed in

Table 8. In the initial segment of the waveform, the flattening of the voltage peaks across the capacitor is clearly evident. The load current i_{Load} displays a pulsed waveform that exhibits reduced amplitude and increased width. Subsequently, the amplification of the compensation system is gradually increased, leading to a restoration of the voltage to its ideal shape. Both the time waveforms and bode graphs demonstrate a marked improvement in voltage quality at the capacitor.
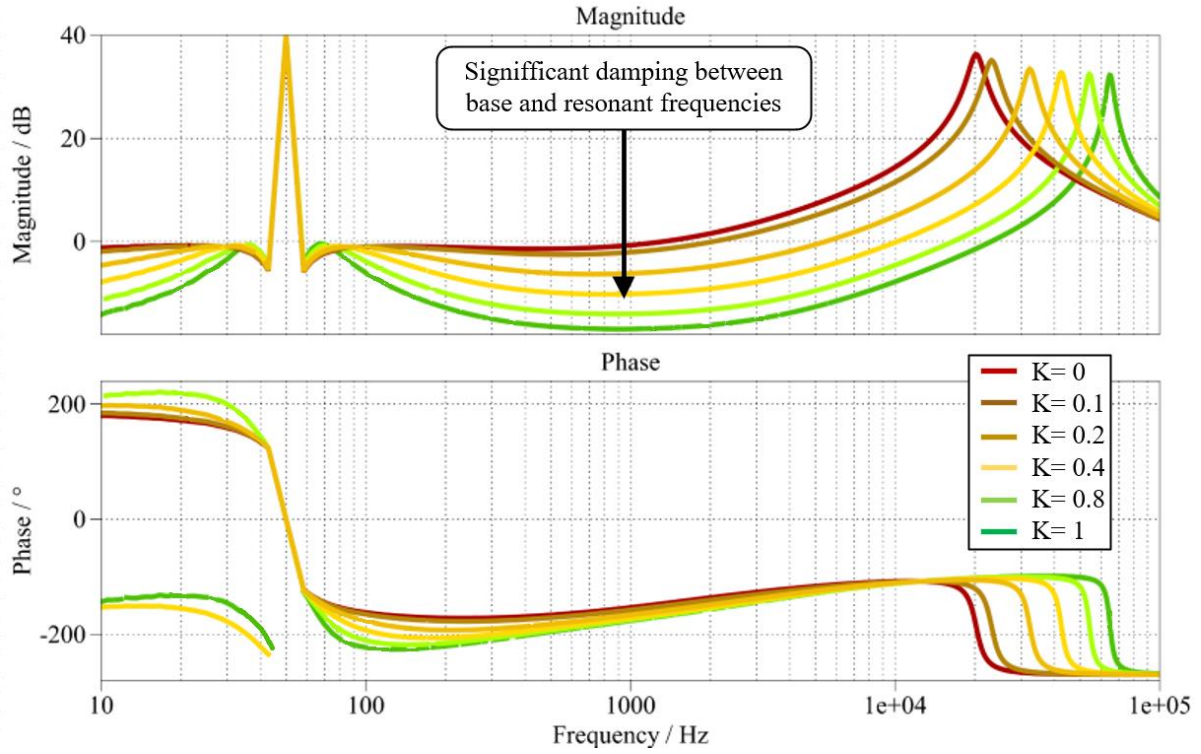

Figure 54. Bode characteristics of the grid current i_{Lg} influence on the filter capacitor voltage v_{Cf} with compension in grid-forming mode.
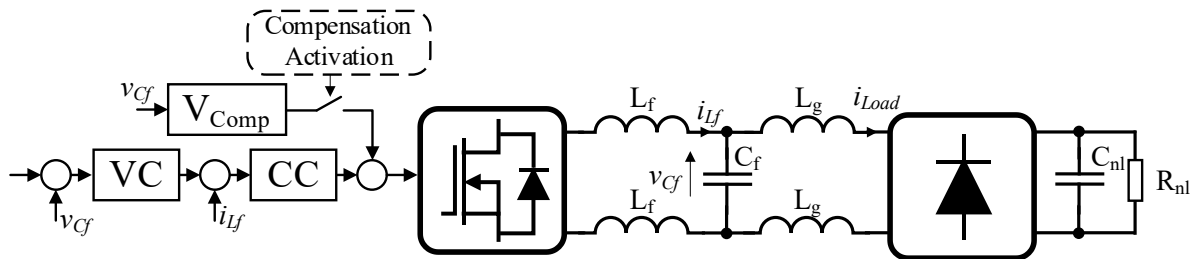
Figure 55. Grid-forming mode with non-linear load.
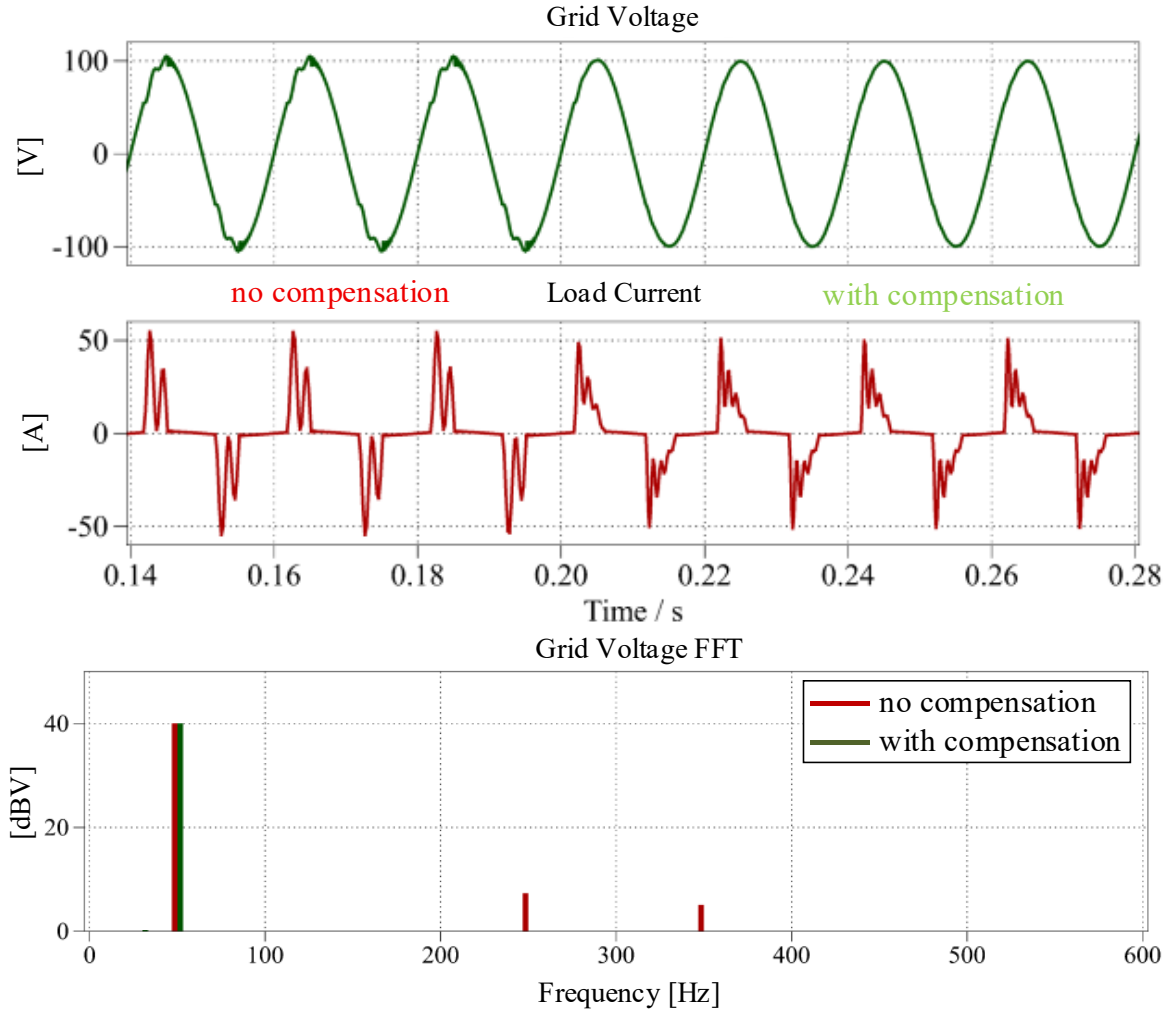
Figure 56. Voltage harmonics compensation example for non-linear load.

Table 8. System model parameters.

Parameter	Symbols	Value	Unit
Grid filter inductance	L_f	200	uH
Grid filter capacitance	C_f	680	nF
Filter capacitor voltage	v_{Cf}	70	V_{RMS}
Non-linear load resistance	R_{nl}	10	Ω
Non-linear load capacitance	C_{nl}	1	mF

The preliminary results suggest that the proposed method provides a promising and effective approach to mitigating voltage distortion at the point of common coupling (PCC), particularly in the presence of nonlinear current loads. The implemented compensation strategy leads to a noticeable improvement in the quality of the voltage waveform, thereby validating its effectiveness within the controller's designated operating bandwidth.

However, one important limitation must be addressed. Since the voltage across the filter capacitor is directly transferred to the converter's output, any high-frequency disturbances,

noise, or measurement inaccuracies in this signal will also appear in the output voltage. This can degrade overall power quality, especially when the capacitor voltage contains unfiltered components.

Therefore, the effectiveness of the proposed method strongly depends on the accuracy of the voltage measurement and the suppression of electrical noise. Ensuring high-quality sensing and, where necessary, applying appropriate low-pass filtering are essential for maintaining the integrity and performance of the voltage compensation strategy.

3.3. Control strategy for the grid-forming mode of operation of the Power Electronic Transformer's Low-Voltage stage

Based on the analysis of reliability and grid-forming operation in the previous chapters, where the main objectives are to be able to operate after a fault and to maintain high voltage quality, the control system must meet the following criteria:

1. the possibility of distributed and scalable implementation,
2. uncoupled current regulation in grid lines due to load asymmetries,
3. the ability to supply energy to the grid and receive energy from it,
4. load balancing of the semiconductor components in the DC/AC module,
5. ensure the ability to disconnect faulty modules without stopping the system,
6. dynamic reconfiguration of the DC/AC branch connections to the grid:
    a. switching on further branches to increase capacity in a given grid line,
    b. insulation of damaged branches,
7. ability to operate in various configurations of the DC/AC module branch connection to the grid lines:
    a. three-phase mode,
    b. single-phase mode,
    c. inter-phase mode,
8. compensation of voltage harmonics under the influence of the deformed current,
9. small amount of data exchange between the DC/AC modules and the central controller.

The proposed control system meeting the above criteria is presented in **Figure 57**. The control algorithm is divided between a master module and multiple sub-modules. In the system controller, a voltage control loop is implemented based on proportional-resonant controllers. A voltage three-phase reference signal $v_{L1}{}^*$, $v_{L2}{}^*$, $v_{L3}{}^*$ is generated using a *dq-ABC* transformation using phase angle θ and voltage amplitude $|v_C|^*$. Phase angle θ is obtained from the integrated

frequency signal ω_1. The voltage feedback v_{C1}, v_{C2}, v_{C3} signals are collected from all the slave modules but only one is used for a given phase. The others are backup signals to secure the algorithm's operation in case of communication or module failure. The line current reference signals $i_{L1}{}^*$, $i_{L2}{}^*$, $i_{L3}{}^*$, determined by the voltage controllers, is transmitted to all slave modules. The resultant value of the grid currents i_{L1}, i_{L2}, i_{L3}, are equal to the product of the reference current and the number of active branches connected to the grid line $i_{Lx} \approx n_x \cdot i_{Lx}{}^*$, where x is grid line.
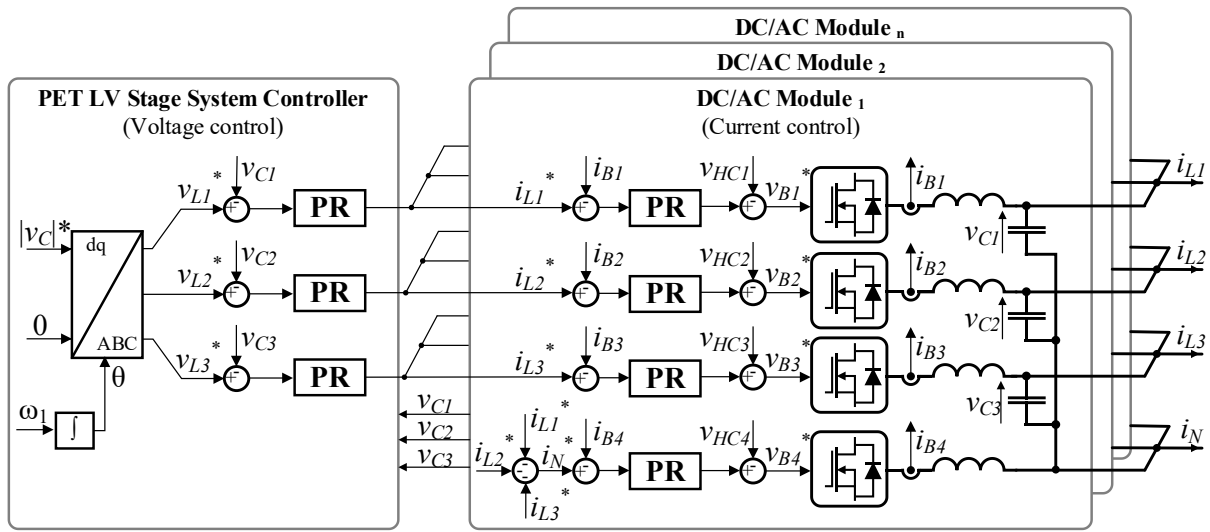
Figure 57. Control strategy block diagram for normal grid-forming mode.

The DC/AC modules contain identical current control algorithms based on PR controllers and a voltage harmonics compensation system. Each branch has a dedicated current controller. The feedback signals i_{B1}, i_{B2}, i_{B3}, i_{B4}, is the current flowing through the output filter inductance L_f. The current reference signals $i_{L1}{}^*$, $i_{L2}{}^*$, $i_{L3}{}^*$, $i_N{}^*$, depend on the grid line to which the branch is connected. For branches connected to grid lines *L1*, *L2* or *L3*, currents are determined from the voltage controllers, while for the neutral line, the reference current $i_N{}^*$ value is the negative sum of all phase currents $i_{L1}{}^*$, $i_{L2}{}^*$, $i_{L3}{}^*$.

A very narrow control bandwidth characterizes the PR controller. As a result of the current harmonics, the voltage quality will decrease because the control bandwidth does not cover the higher-order harmonics. Therefore, a positive feedback signal v_{HC1}, v_{HC2}, v_{HC3}, v_{HC4} are added to the output signals of the current controllers (**Figure 58**). Signals: v_{HC1}, v_{HC2}, v_{HC3} result from the difference between the reference voltage $v_{L1}{}^*$, $v_{L2}{}^*$, $v_{L3}{}^*$, and the filter capacitor voltage. Each DC/AC module locally determines the value of the reference voltage as it occurs

in the master module. Then the difference is determined which, after amplification by the K_{HC} coefficient, is summed by the output of the current regulator and fed to the PWM modulator.
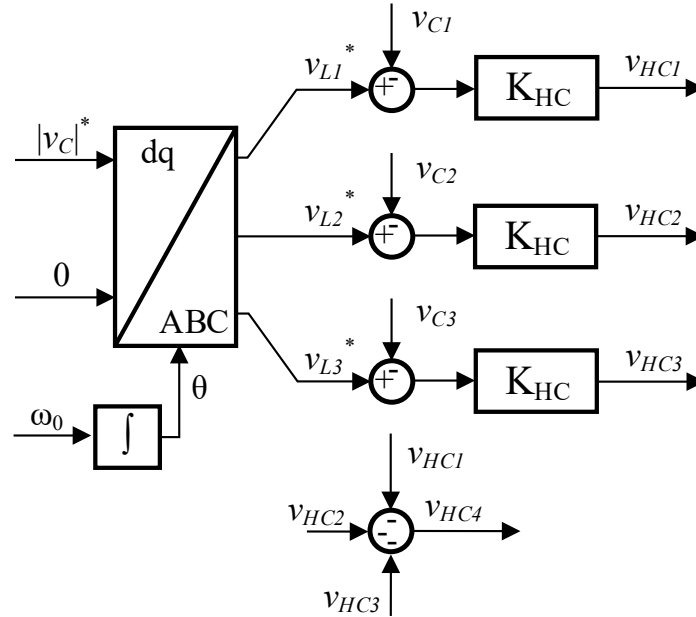

Figure 58. Voltage harmonics compensation component.

Since control is distributed between the central controller and individual DC/AC converter controllers, a communication interface is required to manage data exchange within the system. Based on the developed control algorithm, a set of control variables has been defined those transmitted from the master (central controller) to the slave modules, and the corresponding feedback values sent from the slave modules back to the master.

The complete set of process variables is presented in **Table 9**, representing the minimum required reference signals and feedback values necessary for implementing the distributed control system. Minimizing the number of transmitted variables is critical to ensure fast and reliable data exchange, especially when using a real-time communication protocol.

Table 9. List of variables exchanged between the central controller and DC/AC modules in grid-forming mode.

Direction	Symbols	Unit	Description
Central to Module	$i_{L1}{}^{*}, i_{L2}{}^{*}, i_{L3}{}^{*}$	A	Line current references
	$\lvert v_{Cf} \rvert^{*}$	V	Reference voltage amplitude
	θ	rad	Phase angle
	ω	rad/s	Frequency
Module to Central	v_{C1}, v_{C2}, v_{C3}	V	Filter capacitors voltages

3.4. Control strategy for the grid-supporting mode of operation of the Power Electronic Transformer's Low-Voltage stage

In grid support mode, the control system of the DC/AC converter has the task of regulating the branch output currents i_{B1}, i_{B2}, i_{B3}, and i_{B4} (**Figure 59**). The central controller determines the reference values of the amplitude of the active $|i_{P1}|^*$, $|i_{P2}|^*$, $|i_{P3}|^*$, and reactive $|i_{Q1}|^*$, $|i_{Q2}|^*$, $|i_{Q3}|^*$ components of the current [55]. The estimation of the current reference values $i_{L1}{}^*$, $i_{L2}{}^*$, $i_{L3}{}^*$, and $i_N{}^*$ is carried out in the controller of the DC/AC converter. The system must synchronize the grid voltage phase angle θ; hence, the central controller implements a Phase Locked Loop (PLL) algorithm [56]. The grid voltage signals measured on filter capacitors v_{C1}, v_{C2}, and v_{C3} for the PLL circuit are taken from all active DC/AC converters. A current disturbance compensator signal is added to the current regulators v_{HC1}, v_{HC2}, v_{HC3}, and v_{HC4} output.
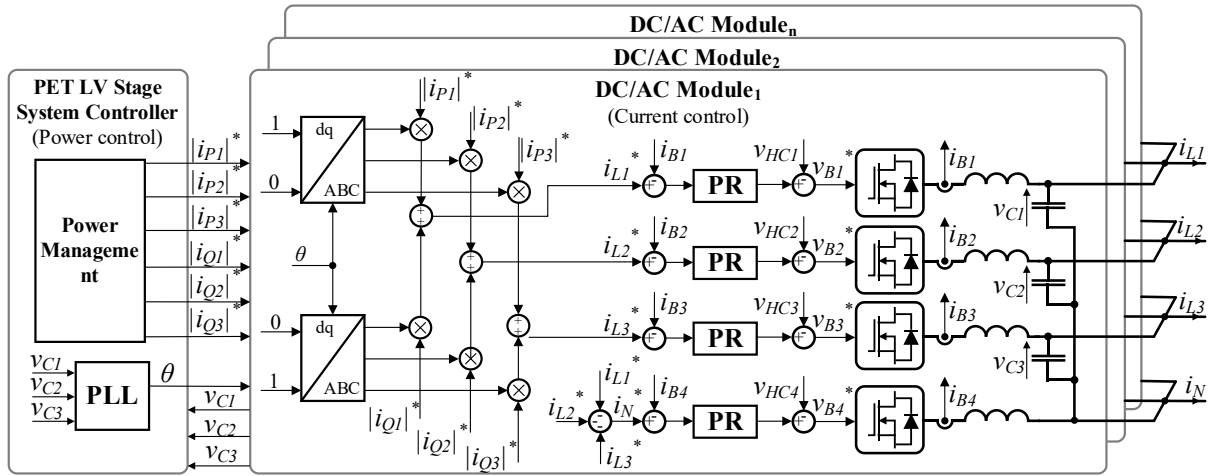
Figure 59. Three-phase grid-connected mode control strategy.

The set of process variables exchanged between the central controller and the individual DC/AC module controllers is presented in

Table 10. The reference values generated by the central controller such as current setpoints or operational modes are broadcasted identically to all DC/AC modules, ensuring synchronized and coordinated operation across the system.

However, each DC/AC module also performs its own local measurement of the grid voltage, which introduces a level of redundancy in voltage sensing. While this redundancy may

appear unnecessary, it enhances the system's robustness by allowing each module to independently verify grid conditions and maintain operation even in the event of partial communication loss or sensor failure. Additionally, locally acquired voltage measurements can be used for fault detection, synchronization, or advanced control functions at the module level.

Table 10. Set of variables exchanged between the central controller and the controllers of DC/AC converters in grid-supporting mode.

Direction	Symbols	Unit	Description
Master to slaves (common for all)	$|i_{P1}|^*, |i_{P2}|^*, |i_{P3}|^*$	A	Active Power Reference
	$|i_{Q1}|^*, |i_{Q2}|^*, |i_{Q3}|^*$	A	Reactive Power Reference
	θ	Rad	Phase angle
	ω_0	Rad/s	Frequency
Slave to Master	v_{C1}, v_{C2}, v_{C3}	V	Phase voltages

3.5. Design procedure for parallel connected DC/AC modules with LC filter

The proposed topology and control system requires the selection of key parameters that determine the correct operation of the entire system:

- switching frequency f_{PWM},
- AC output voltage v_{PCC}, and output power maximum $P_{out\ max}$,
- grid filter inductance L_f and capacitance C_f,
- voltage controller gains: proportional – K_{PV}, resonant – K_{RV}
- current controller gains: proportional – K_{PI}, resonant – K_{RI}

The transistor branch should be switched by a PWM signal with the highest possible frequency resulting from available semiconductor technologies. In addition, the number of voltage levels should be as high as possible and results from the complexity of the module design and the capabilities of the control system. The above-mentioned aspects make it possible to extract two basic assumptions: switching frequency, which is 100kHz, and the number of levels equal to three according to T-Type topology. Due to experimental verification, the grid voltage was assumed to be 70V$_{RMS}$. The choice of this voltage level is related to the specific requirements of the entire PET model design. On the primary side, the voltage was 230 V$_{RMS}$, while on the secondary side it was 70 V$_{RMS}$. Another important factor to consider is the variable configuration of the system, where one or more transistor branches with LC filters may be attached to a single grid line. Varying the number of branches changes the capacitance of the LC filter (**Figure 60**).
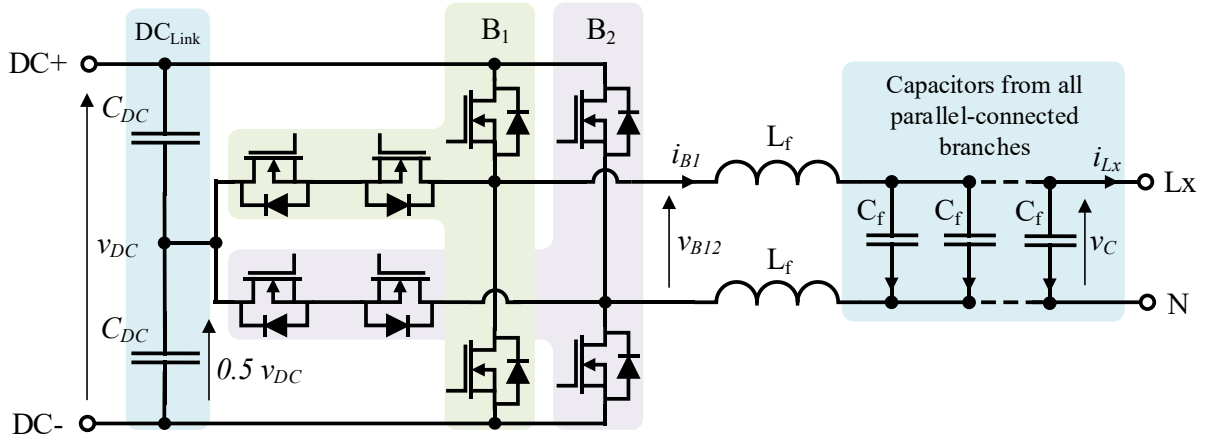
Figure 60. Two branches operating on selected grid line with variable capacitance.

3.5.1. LC Filter design

The method of selecting LC filter prameters is widely analyzed in the literature [57]. The selection of filter inductance L_f depends on the assumed level of current ripple Δi_L and the value of DC voltage v_{DC} divided into the number of levels m and switching frequency f_{PWM}:

$$L_f = \frac{v_{DC}}{(m-1)*8*f_{PWM}*\Delta i_L} = \frac{100V}{(3-1)8*100kHz*0.3A} \approx 208uH \qquad (3.17)$$

The value of the filter capacitance C_f is selected based on the assumption that the resonant $f_{LC\,res}$ frequency of the LC filter should be at least half the PWM switching frequency and at least ten times higher than the grid frequency.

$$0.5f_{PWM} \geq f_{LC\,res} \geq 10*50\text{Hz} \qquad (3.18)$$

It is important to note that the value of capacitance is variable and depends on the number of parallel-connected branches. However, to satisfy the condition, the resonant frequency must be calculated assuming that the number of branches is equal to one. Since, according to **Figure 36** for one branch is the highest frequency value. In the proposed topology, there are two series filter inductances between the branches and the capacitor.

$$f_{LC\,res} = \frac{1}{2\pi\sqrt{\sum L * \sum C}} = \frac{1}{2\pi\sqrt{(2L_f)\sum_1^{2n} C_f}} \qquad (3.19)$$

Ultimately, given the selected PWM frequency, the assumed resonant frequency, and the calculated inductance, the capacitance value can be determined as follows:

90

$$C_f = \frac{\left(\frac{10}{2*\pi*f_{PWM}}\right)^2}{2*L_f} \approx 633 nF \qquad (3.20)$$

The assumed and calculated values based on the presented formulas are summarized in the **Table 11**. The selected real-world values differ from the calculated ones due to the availability of standard component series and have been rounded to the nearest available values within that series.

3.5.2. Voltage and current controller design

The proposed solution uses two cascaded PR controller for voltage and current tuned to the fundamental harmonic $\omega_1 = 2\pi 50$ rad/s. Proportional gain of current controller K_{PI} affects the dynamics of the system. We can estimate it using the following formula, which takes into account inductor attenuation and fundamental frequency with assuming ctritical attenuation:

$$K_{PI} = \frac{\zeta}{\omega_1 L_f} = 5.57 \qquad (3.21)$$

where: $\zeta = 1/\sqrt{2}$ is critical attenuation.

The resonance gain K_{RI} according to [58] where the Naslin Polynomial method is proposed K_{RI} is calculated from the DC voltage v_{DC}, the filter inductance L_f and the assumed critical attenuation ζ:

$$K_{RI} = \frac{\omega_1^2 L_f \left[(2\zeta+1)^2 - 1\right]}{2 v_{DC}} = 94 \qquad (3.22)$$

The voltage controller generates a current reference for the current controller creating outer control loop. The interaction between these controllers can affect the stability of the whole system. To ensure stability the gains of voltage controller: K_{PV}, K_{RV} should be less than K_{PI}, K_{RI} respectively, to prevent the voltage controller from dominating the system dynamics. Voltage reference is constant, and the controller is mainly intended to respond to load spikes. According to the recommendations developed in [59] voltage controller gains are based on the identification of the system time constant and damping:

$$K_{PV} = \frac{1}{\left| G_{sys}(s)\right|_{s=j\omega_{outer}}} = 0.0045 \qquad (3.23)$$

$$K_{RV} = K_{PV} \frac{\omega_{outer}^2 - \omega_1^2}{\omega_{outer}} \cdot \tan\left(\forall \left|G_{sys}(s)\right|_{s=j\omega_{outer}} + 180 - M_{def}\right) = 0.0012 \qquad (3.24)$$

where: M_{def} – defined phase margin, $G_{sys}(s)$ – system transfer function, ω_{outer} – outer loop frequency.

The outer control loop (voltage controller) operates more slowly and provides the reference for the inner loop (current loop). Its bandwidth, referred to as the outer loop frequency ω_{outer}, is significantly lower (typically 5 to 10 times lower) than that of the inner loop to avoid interfering with the stability and dynamic response of the current control.

Table 11. Summary of design parameters of proposed system.

Component	Description	Symbol	Value	Unit
Grid	Frequency	f_g	50.0	Hz
	Line to neutral voltage peak	V_p	100	V
	Inductance	L_g	100	uH
	Resistance	R_g	0.03	Ω
Module	Number of modules	n_m	4	-
	Number of branches in module	n_{mb}	4	-
Branch	DC voltage	v_{DC}	250	V
	Voltage levels	m	3	-
	Switching frequency	f_{PWM}	100	kHz
LC Filter	Ripple current	ΔI_{Lf}	0.3	A
	Inductance	L_f	200	uH
	Resistance	R_f	0.05	Ω
	Capacitance	C_f	680	nF
	Resonance frequency	$f_{LC\,res}$	13,65	kHz
Current Controller	Proportional gain	K_{PI}	5.57	-
	Resonant gain	K_{RI}	94	-
Voltage Controller	Proportional gain	K_{PV}	0.0045	-
	Resonant gain	K_{RV}	0.0012	-

A system is considered stable if all poles of its closed-loop transfer function lie in the left half of the complex plane, as illustrated in **Figure 61**. This condition ensures that all system responses decay over time, avoiding sustained oscillations or instability.

When the filter capacitance Cf is small, the poles are located well within the left half-plane, indicating a strong stability margin. However, as the resultant filter capacitance increases (e.g., to an effective value of $8Cf$ due to parallel branches), the poles begin to shift closer to the imaginary axis. This movement reduces the damping of the system and narrows the stability margin, increasing the risk of oscillatory behavior or even instability.

Additionally, a larger capacitance leads to a lower resonant frequency of the LC filter, which can interfere with the controller's bandwidth and dynamic performance. This effect is

particularly critical in scenarios where the feedback loop operates at high speed, as the faster response may unintentionally excite resonant modes near the new, lower resonance frequency.

Thus, careful consideration must be given to the design of both the LC filter parameters and the control loop dynamics to maintain stable operation across varying system configurations.
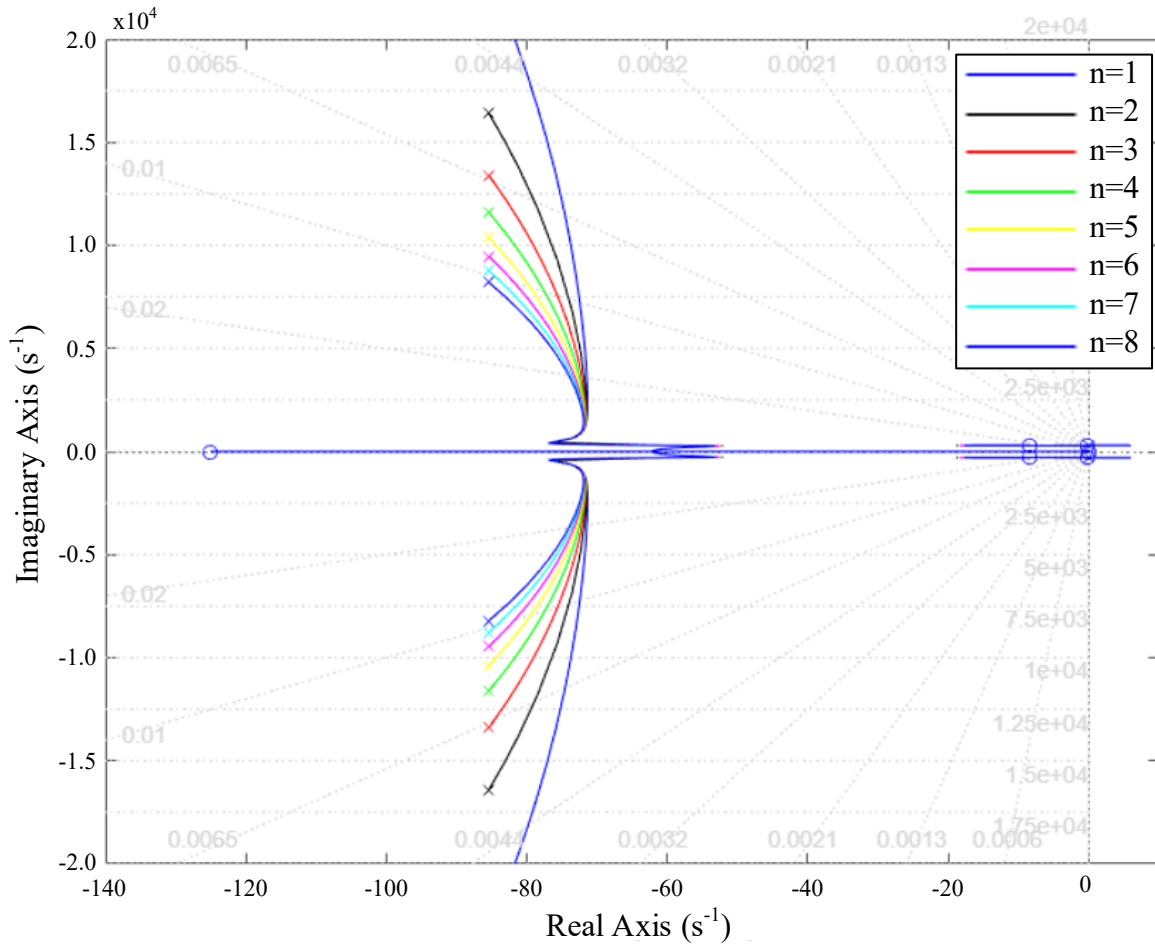
Figure 61. Stability analysis of cascaded PR controllers with LC filter depending on number of parallel connected branches.

3.6.   Reconfiguration of the parallel DC/AC converter system

One of the main functions of a modular DC/AC system is to ensure uninterrupted operation under various conditions, such as:

- a fault occurring in one of the modules,
- replacement of a module nearing the end of its life cycle,
- system reconfiguration to adapt performance to grid requirements.

In all of these cases, the system is reconfigured without shutting down. The key component responsible for this flexibility is the transistor branch. To maintain overall system stability during branch reconfiguration, the process must follow a defined sequence. Specifically, certain rules must be observed during branch-switching operations. These rules are based on the need to maintain continuous choke current and stable capacitor voltage.

When connecting a branch to the AC grid, the capacitor voltage must be synchronized to prevent uncontrolled current surges. Conversely, when disconnecting a branch, the inductor current must be zero to avoid voltage spikes.

To enable stable reconfiguration via branch switching, the control system must implement a dedicated switching scenario. This process involves two main stages: first, the branch is safely disconnected; then, after being connected to another grid line, it is reactivated. Therefore, designing a correct and reliable branch-switching procedure is essential.

3.6.1. Procedure for connecting a branch to the AC grid phase

When connecting a branch to the grid phase, it is crucial to synchronize the voltage on the output filter capacitor v_{Cf} with the v_{PCC} voltage to prevent current surges from the AC grid or other branches. Once the branch is connected to the selected grid line, the initial current $i_B = 0$, and must equalise with the reference current i_L^* for the grid line. This means that the switching operation consists of two steps:

- synchronisation of the voltage on the filter capacitor v_{Cf} with the PCC voltage v_{PCC},
- synchronisation of the branch current i_B with the global reference i_L^* of the branch.

In the first phase, closed-loop voltage control can equalize voltage across the filter capacitors C_f. However, a current controller with zero initial current must be activated in the next phase. The voltage controller only determines the current setpoint for regular branch operation and cannot be used in synchronization. An additional voltage controller in the module's local controller is necessary, and it only operates during synchronization (**Figure 62**).
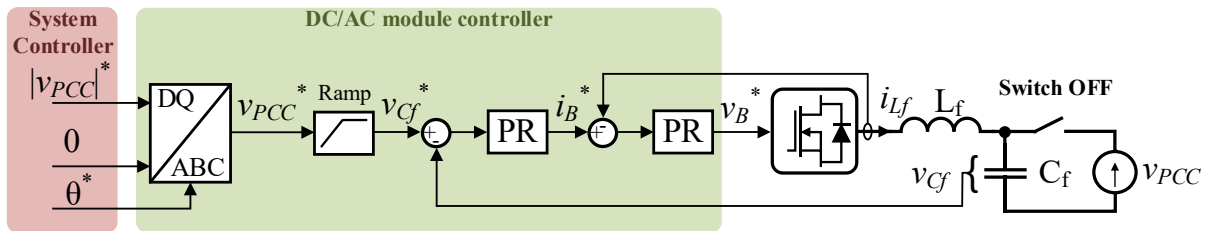
Figure 62. Internal voltage control strategy for filter capacitor voltage synchronization.

When the branch is connected, the reference value of the current regulator is switched to the value from the central controller. A current controller is involved in both steps, whose output value is always appropriately prepared so that no voltage or current surges occur (**Figure 63**).

Figure 63. DC/AC module current balancing strategy during startup.

The first part of **Figure 65** presents the results of the proposed strategy for synchronizing and connecting converter branches to the AC grid phase. The top section of the figure compares the grid voltage with the voltages measured at the filter capacitors. The third waveform illustrates the states of the grid contactors, indicating the sequential connection of four converter branches to the grid lines (three phases and a neutral). The fourth waveform presents the voltage and current ramp signals, along with the activation signal from the central controller used to initiate the module.

The last two waveforms show a comparison between the actual branch current and the reference current provided by the central controller. The entire figure is divided into columns, each representing a distinct operating state of the system.

In the first stage, an overload condition is demonstrated, prompting the central controller to connect an additional DC/AC module. In the second stage, voltage synchronization is performed across the filter capacitors. Once synchronization is complete, the branches are connected to the AC grid, and the current reference is switched from the internal regulator to the external voltage controller.

In the final stage, the branch currents gradually converge to the reference value set by the central controller, completing the transition to normal operation.

3.6.2. Module connection and disconnection cycle algorithm

The algorithm for module or branch connection management within the network necessitates the development of an appropriate state machine. This section introduces the branch management cycle and presents preliminary simulation results.

The branch disconnection case must respect the zero current i_{Lf} condition when disconnecting the grid switch. Hence, the current reference i^*_{global} value must be progressively zeroed locally in the module. When the AC grid is disconnected, there may still be voltage on the filter capacitors v_{Cf}. The filter capacitor voltage v_{Cf} should also be zeroed. This will facilitate the re-synchronisation of the voltage and the stored energy will be returned to the DC grid. Branch disconnection also consists of two steps and is a reversal of the scenario in the previous section. The control system is the same but the ramp direction is reversed from one to zero. The DC/AC module operation life cycle state diagram is shown in **Figure 64**.

1: Module Inactive
$v_{DC} = 0$
$v_{Cf} = 0$
$i_{Lf} = 0$

Run Cmd

2: Capacitor Voltage Sync
$v_{DC} = v_{DC\,grid}$
$v_{Cf} \rightarrow v_{PCC}$
$i_{Lf} = 0$

$v_{Cf} = v_{PCC}$

3: Current Sync
$v_{DC} = v_{DC\,grid}$
$v_{Cf} = v_{PCC}$
$i_{Lf} \rightarrow i^*_{global}$

$i_{Lf} = i^*_{global}$

6: Capacitor Discharge
$v_{DC} = v_{DC\,grid}$
$v_{Cf} \rightarrow 0$
$i_{Lf} = 0$

$v_{Cf} = 0$

$i_{Lf} = 0$

5: Current Zeroing
$v_{DC} = v_{DC\,grid}$
$v_{Cf} = v_{PCC}$
$i_{Lf} \rightarrow 0$

Stop Cmd

4: Normal Operation
$v_{DC} = v_{DC\,grid}$
$v_{Cf} = v_{PCC}$
$i_{Lf} = i^*_{global}$
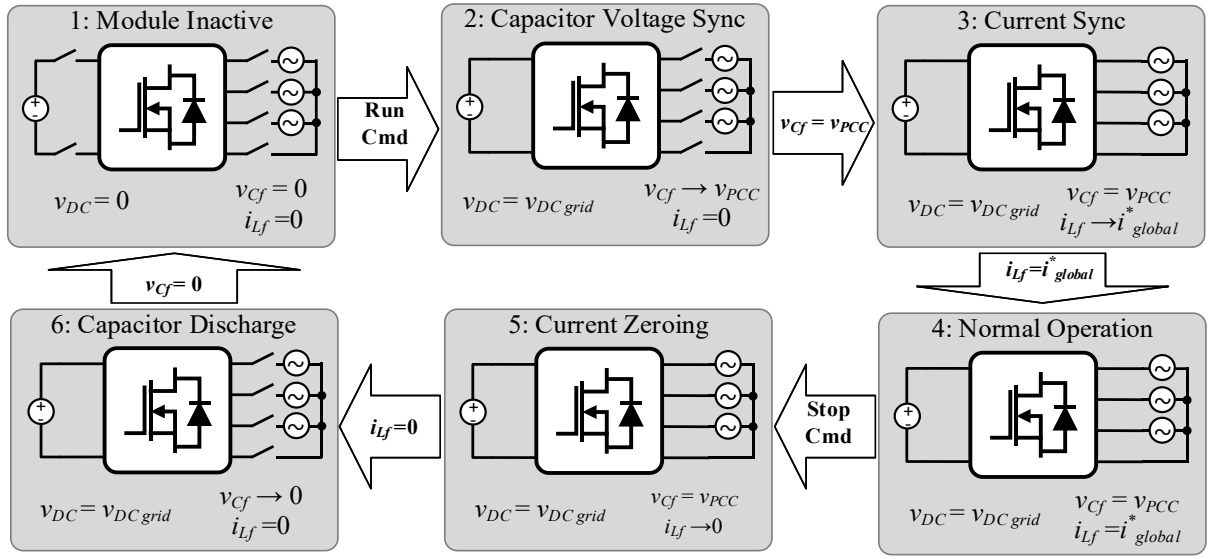
Figure 64. DC/AC module operation life cycle state machine.

Ultimately, six distinct operational states are identified, and the preliminary simulation results of the developed algorithm are presented in the **Figure 65**. The preliminary results indicate that the algorithm is functioning correctly, as the switching operations do not produce overvoltages during disconnection or current surges during connection. It is also important to note the current reference value i^*_{Lx}. When an additional module is connected, the current value temporarily drops below the acceptable limit, indicating the system's dynamic response to changes in configuration.

This proposed scenario is consistent across all operational modes of the system, including both grid-forming and grid-supporting modes, as well as all configurations of the DC/AC modules (three-phase, single-phase, and inter-phase). The system's ability to adjust dynamically in response to load changes primarily depends on the speed at which the load value is determined and the responsiveness of the control system during module switching. The threat

of system overload from sudden load spikes necessitates a rapid response to maintain stability and prevent damage.

Preliminary simulation results indicate that the minimum system response time to a stable load change is approximately 60 milliseconds. This total response time includes several critical steps: (1) assessing whether the measured current values fall within the thresholds that require system reconfiguration, (2) synchronizing the voltage across the output capacitors, and (3) synchronizing the reference current after switch connection. Each of these operations is completed within one grid voltage period (20 ms), ensuring a timely and coordinated system response.
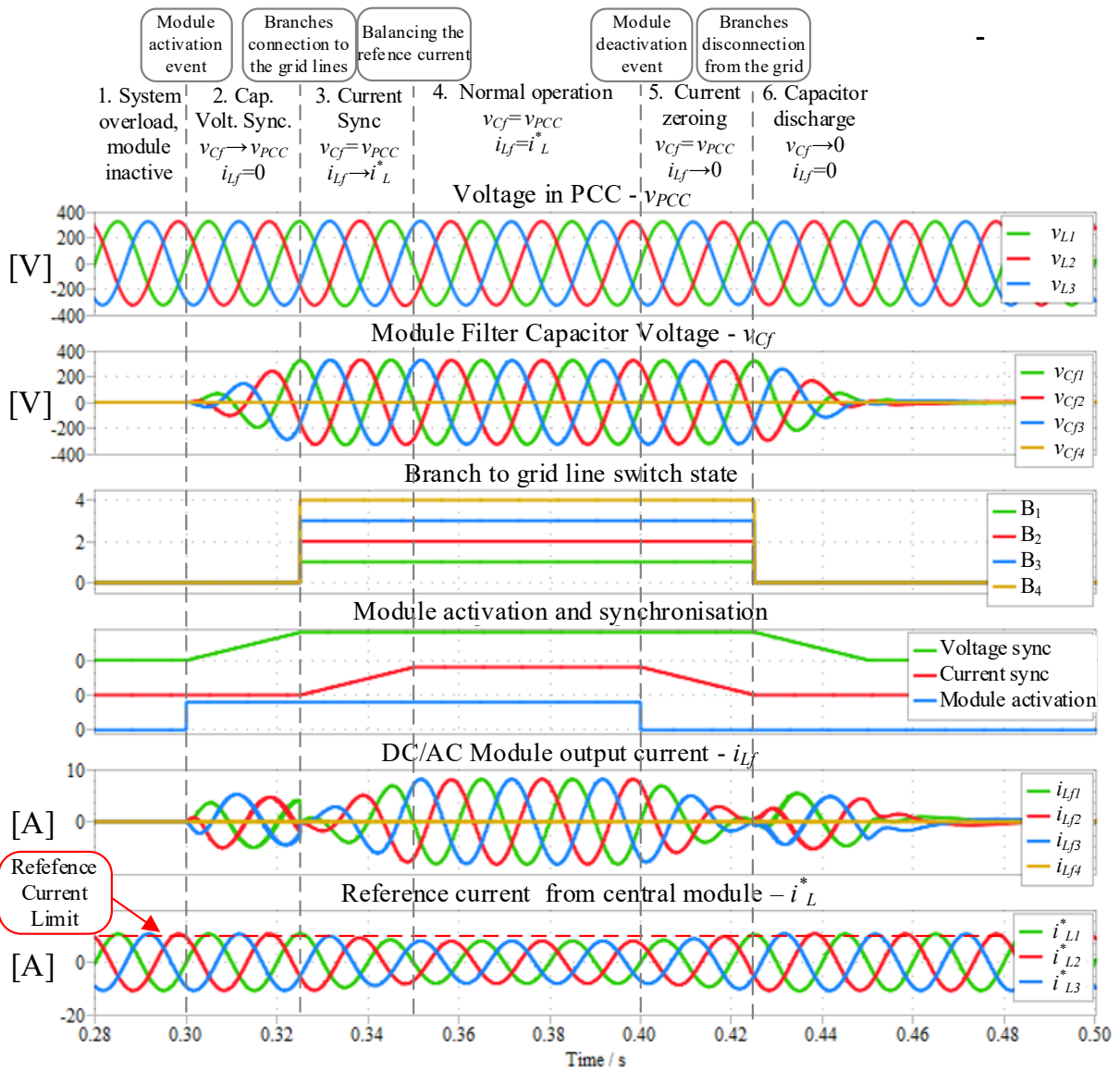
Figure 65. Connection and disconnection DC/AC module to grid line in the three phase connection mode.

However, it is important to note that this analysis did not account for fluctuations in load or explore methods of determining module switching beyond single-step changes. The results presented are primarily aimed at demonstrating effective and stable system reconfiguration.

Another critical factor in the performance of the system is the timing for activating the grid switch contactor. A fundamental requirement is that the voltage difference between the capacitor voltage v_{Cf} and v_{PCC} must be zero prior to connection. Failure to meet this condition may expose the system to potential overcurrent conditions that can arise from misalignment between the grid voltage and the capacitor voltage.

To ensure proper synchronization, the first element implemented is a ramp block that gradually raises the reference value to its target level. Once the reference signal reaches the target value, a verification check is performed to assess the difference between the capacitor voltage and the PCC voltage. This verification is averaged over a time window equivalent to the voltage base period, allowing for a more stable and reliable synchronization process. This careful consideration of timing and voltage alignment minimizes the risk of overcurrent conditions and enhances the overall reliability of the system during operation.

This section presents detailed information about the algorithm and demonstrates that connecting or disconnecting the module from the network does not lead to short circuits or power surges. Moreover, the analysis verifies the safety and reliability of the switching procedures, ensuring seamless operation without risking damage to the network or connected components. The dynamics of the switching operations depend on the speed and accuracy of voltage and current synchronization. The focus was not on minimizing switching times but rather on proving the correct functioning of the algorithm. The comprehensive experimental validation of the proposed algorithm is thoroughly documented in the chapter dedicated to all experimental results.

3.7. Reconfiguration of the DC/AC module

The proposed system topology allows branch switching between AC grid lines. The branch is also the primary actuator performing DC/AC conversion. In contrast, the four-branch DC/AC module is the unit that couples all four AC grid lines to the DC grid. Therefore, it is necessary to analyze the configuration of the module's connections to the grid to determine proper modes and operating conditions other than the standard three-phase one.

A typical complete control chain of a converter branch includes cascaded voltage control on the capacitor and current control on the inductor of the low-pass output filter (**Figure 66**).
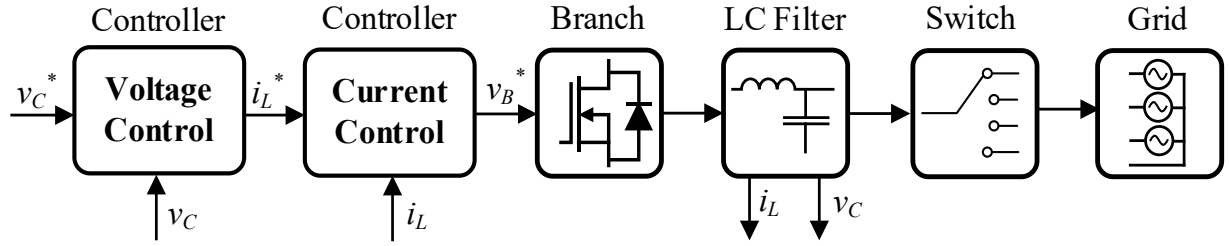
Figure 66. Block diagram of a single controllable unit of DC/AC converter system.

Due to the parallel connection of several branches to a given line, the regulated voltage will be shared. Consequently, all branches will have the same reference current value. A reference signal consistent with the phase or neutral line is given depending on the grid line to which the branch is connected (**Figure 67**). The neutral line current $i_N{}^*$ is the negative sum of lines $i_{L1}{}^*$, $i_{L2}{}^*$, and $i_{L3}{}^*$ reference currents.
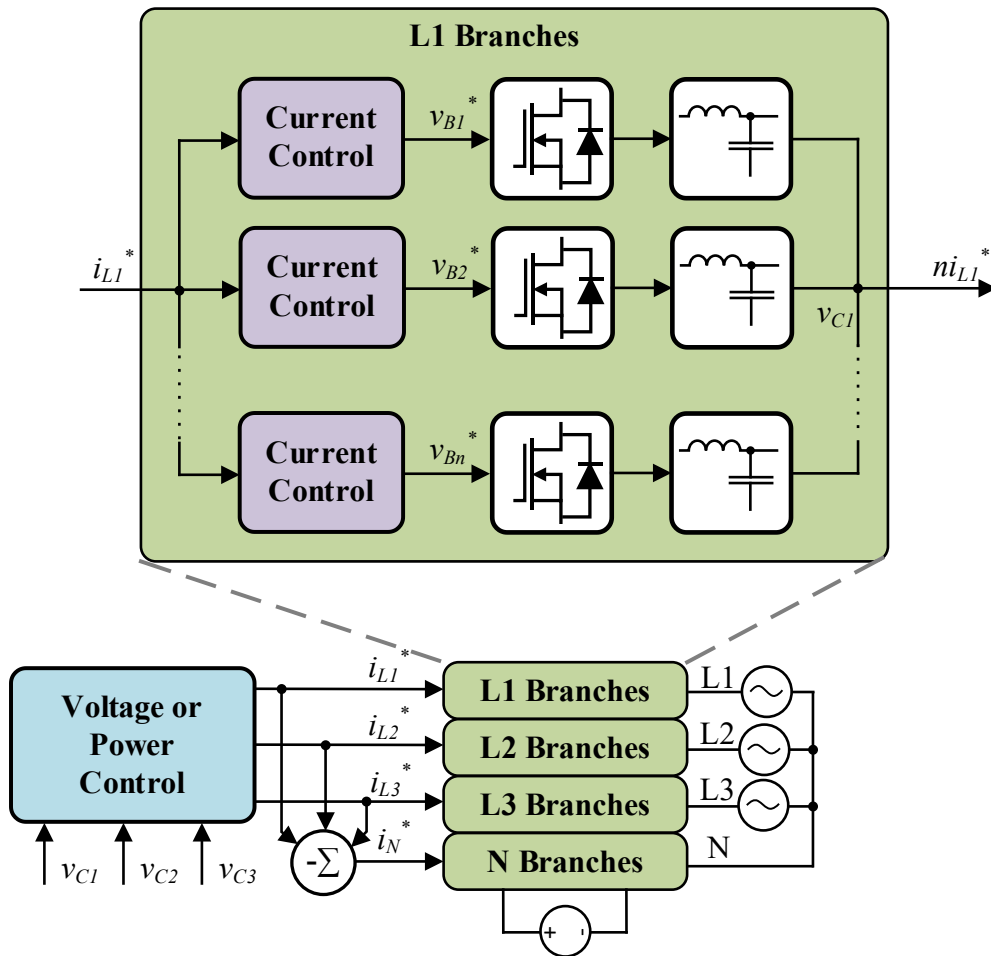
Figure 67. Parallel DC/AC conversion system control diagram.

The proposed solution enables scalable integration of multiple branches between DC and AC grids. A key advantage of this approach is that only a single voltage controller is needed, as the voltage at the PCC is shared across all branches connected to the same phase. However, to maintain precise control and stability, each branch is equipped with its own dedicated current controller.

This modular configuration significantly enhances the flexibility and expandability of the system, allowing for efficient management of multiple connections while maintaining high levels of reliability and performance.

Given the potential variety of load types and connection schemes within the grid, the power source must be appropriately adapted to meet the required demand. The following section outlines the possible load connection configurations, illustrating how the system can be tailored to support diverse operating scenarios:

- three-phase with a neutral line,
- three-phase without a neutral line,
- single-phase,
- inter-phase with neutral line,
- inter-phase without a neutral line.

A summary of the possible connection combinations for the four-branch module is presented in **Table 12**. Notably, in single-phase and inter-phase operating modes, the load is evenly distributed across all module branches. This balanced distribution is highly beneficial, as it ensures uniform stress on the components, contributing to longer operational life, enhanced system reliability, and lower maintenance costs. By avoiding overloading of individual branches, the system also improves overall efficiency and supports more stable grid operation.
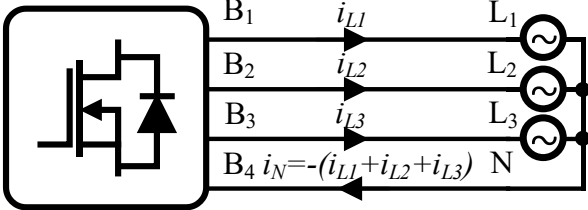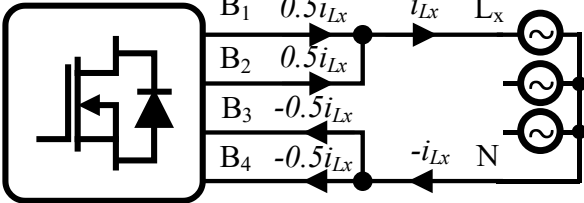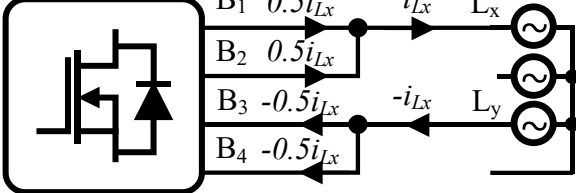
However, the introduction of these additional operating modes necessitates the development of dedicated control algorithms. These are required to handle the more complex switching logic and regulation demands associated with dynamic operating conditions. The following section presents a comprehensive overview of these advanced control strategies and their implementation, demonstrating how they increase the flexibility, resilience, and functionality of the power conversion system.

3.7.1. Single-phase operation mode of the DC/AC module

The single-phase connection mode of a four-branch module involves assigning two branches to one phase conductor and the remaining two to the neutral line (**Figure 68**). This

configuration is compatible with both grid-forming and grid-connected modes of operation. However, to ensure voltage symmetry across the system, it is essential that at least one module operates in a fully three-phase grid-forming mode. This three-phase module acts as a voltage reference, maintaining balanced conditions in the grid.

Table 12. DC/AC Module operation modes.

Connection Mode	Description
Three-phase connection mode B_1 i_{L1} L_1 B_2 i_{L2} L_2 B_3 i_{L3} L_3 B_4 $i_N=-(i_{L1}+i_{L2}+i_{L3})$ N	Each branch operates on a separate grid line. To ensure stable system operation, at least one module must operate in three-phase grid-forming mode. This configuration enables support for all types of load connections. The corresponding control strategy is described in detail in the previous section.
Single-phase connection mode B_1 $0.5i_{Lx}$ i_{Lx} L_x B_2 $0.5i_{Lx}$ B_3 $-0.5i_{Lx}$ B_4 $-0.5i_{Lx}$ $-i_{Lx}$ N	Two branches are connected to one phase, while the other two are connected to the neutral line. This configuration can be utilized when one phase experiences a significantly higher load than the other two. An indicator of a dominant phase is the presence of a neutral line current with an RMS value close to or exceeding that of the less-loaded phases.
Inter-phase connection mode B_1 $0.5i_{Lx}$ i_{Lx} L_x B_2 $0.5i_{Lx}$ B_3 $-0.5i_{Lx}$ $-i_{Lx}$ L_y B_4 $-0.5i_{Lx}$	Two branches are connected to one phase, while two branches are connected to the other phase. An indicator for operating in this mode is the presence of a current in one phase that is opposite in direction to the current in the other phase.

To preserve current symmetry and prevent load imbalance, the RMS current values in all branches of the single-phase module must remain equal. This is achieved by assigning identical reference current values to the controllers of the branches connected to the phase conductor, while the controllers of the branches connected to the neutral conductor receive the same reference current with an inverted polarity. This approach ensures that the module's internal current distribution remains balanced and neutral current is properly handled.

A critical aspect of this mode is the behavior of the neutral current. Any increase in load on the phase wire results in a proportional rise in current flowing through the neutral conductor. Therefore, the current reference for the single-phase module must be dynamically adjusted

based on the actual neutral current. To accomplish this, the control system's supervisory algorithm must measure the current in the neutral line, compute the required current reference accordingly, and update the control signals for the module operating in single-phase mode.
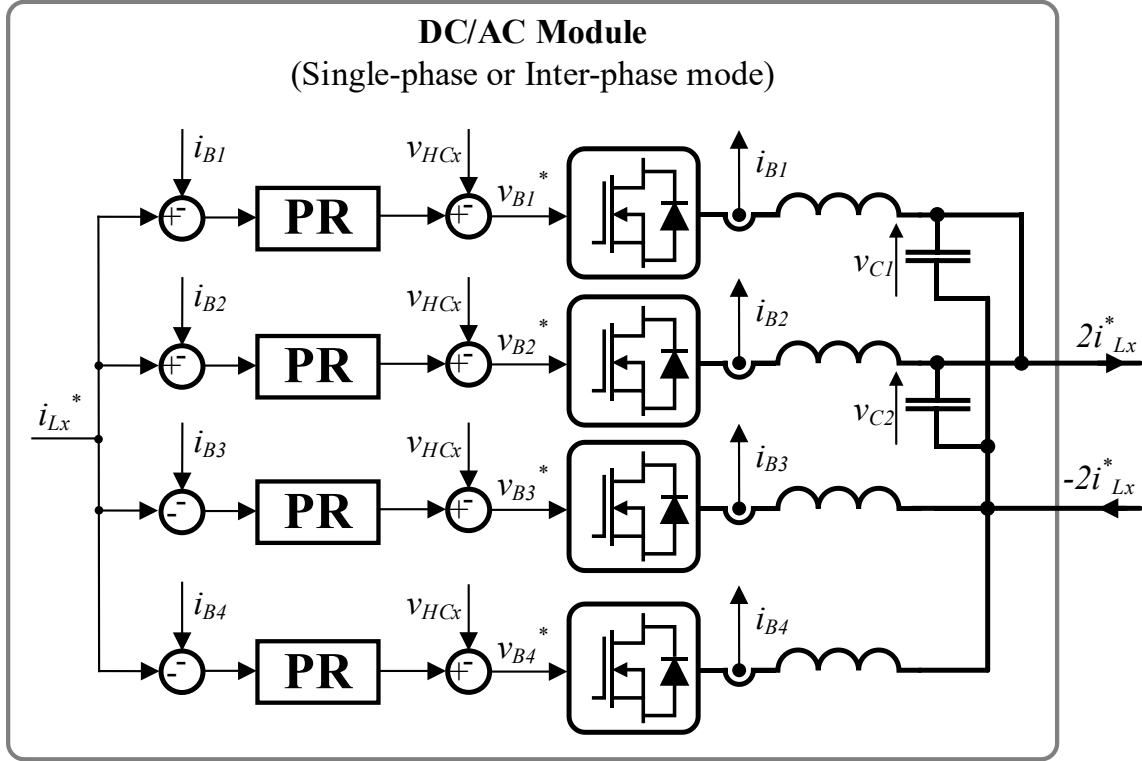
Figure 68. Control strategy block diagram for single-phase mode.

This control strategy ensures proper current sharing, minimizes the risk of overloading the neutral path, and maintains the overall balance and performance of the modular system, regardless of asymmetrical load conditions.

The preliminary simulation result of the control system for single-phase mode is shown in **Figure 70**. Module 1 operates in the normal mode and supplies a symmetrical load. The second module operates in single-phase mode and supplies a single-phase load (**Figure 69**). Switching to single-phase mode doubles the current capacity for one phase at the expense of disconnecting the other two phases.

In the case of inter-phase operation of one of the modules, the waveform shapes will be analogous to those observed in single-phase mode. The currents in the paired branches will be also equal in magnitude but opposite in direction.

The proposed control strategy enables seamless transitions between different operating modes of the DC/AC modules. The underlying control structure remains unchanged; the

transition is achieved by simply switching the branch to the designated grid line and providing the appropriate reference signal or its inverted counterpart, depending on the desired mode of operation.
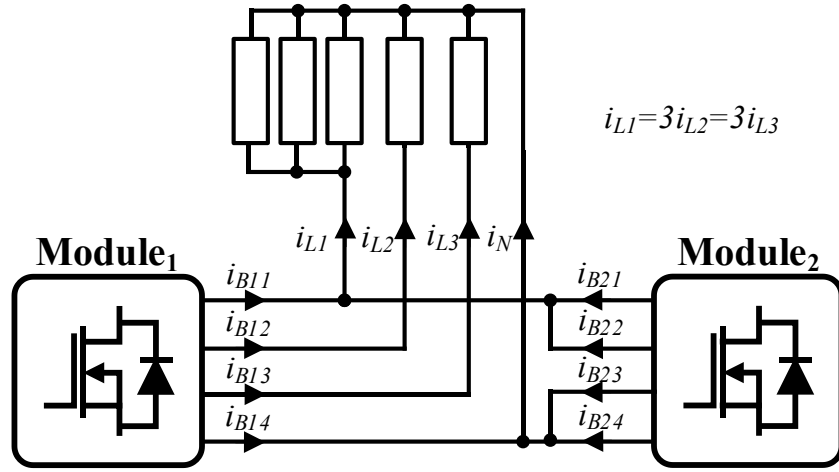
Figure 69. Single-phase operation mode example.
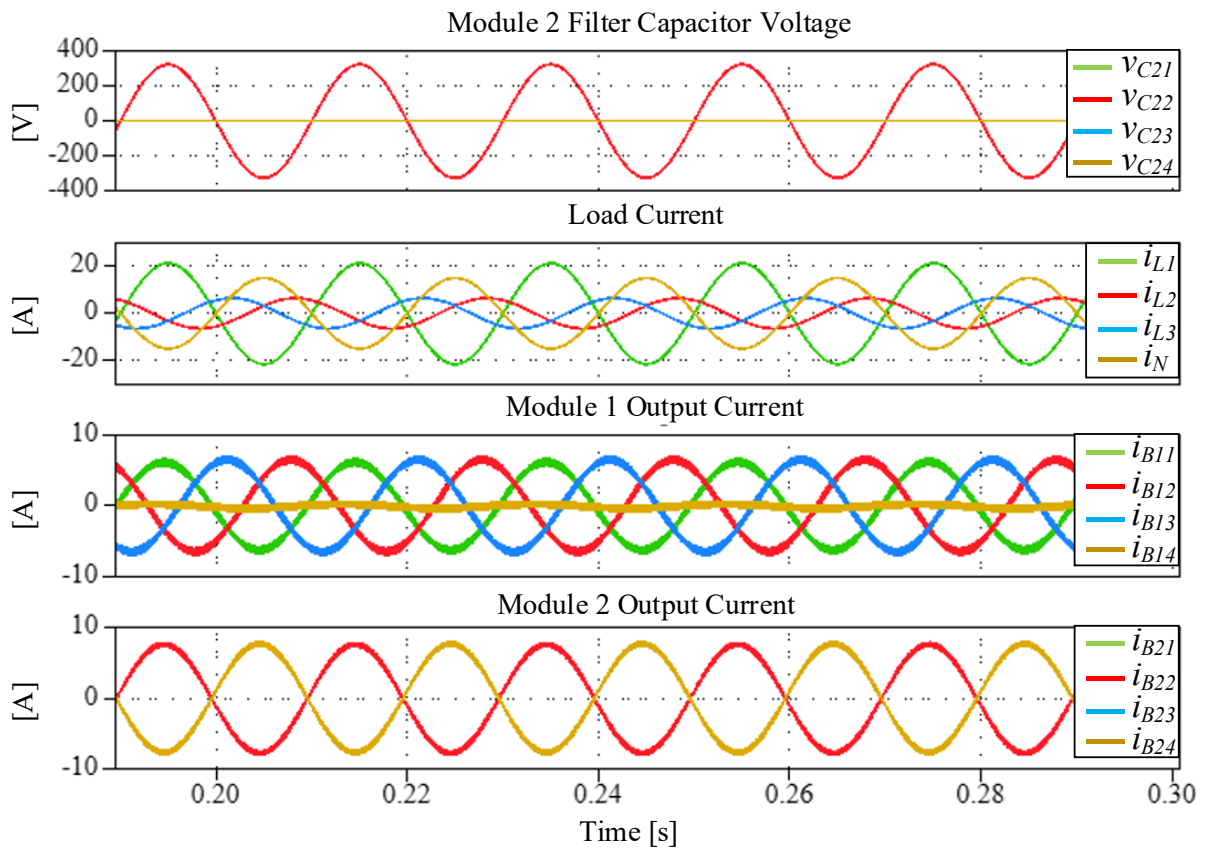
Figure 70. Preliminary simulation results of single-phase mode of DC/AC module.

3.7.2. Reconfiguration scenario for switching DC/AC module branches between AC grid lines

Dynamic switching of branches requires safe disconnection, which involves reducing the output current to zero and turning off the transistors. The simplest scenario involves connecting module branches that were previously inactive. However, dynamic reconfiguration must also occur during normal operation, particularly when all modules are active and grid conditions change in real time.

The primary goal of reconfiguration is to maintain uninterrupted system operation, although performance may temporarily degrade during the switching process until stable control is re-established in the new configuration.

To ensure a smooth transition, branches should be switched from the least loaded phase, as the disconnection momentarily shifts the current burden to the remaining active branches. From a hardware perspective, the inductor must be disconnected at zero current, while the capacitor should be connected only when its voltage closely matches the voltage of the target phase. This prevents unwanted inrush currents or voltage spikes.

From the control standpoint, current reference signals must be updated in real-time to reflect the new connection. An example of this reconfiguration process is shown in **Figure 71** while **Figure 72** presents a detailed illustration of the DC/AC module switching modes relative to the grid.
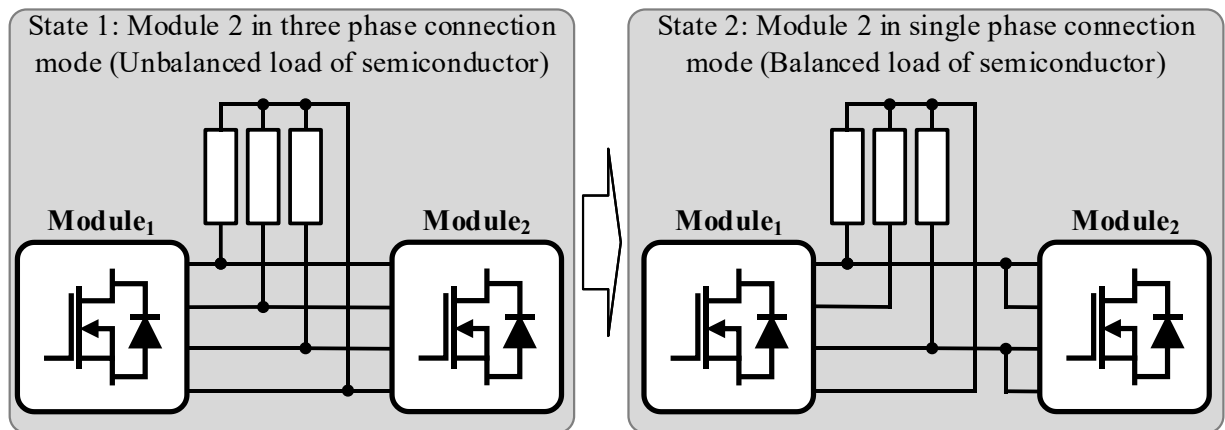
Figure 71. Example of system states during connection mode change.
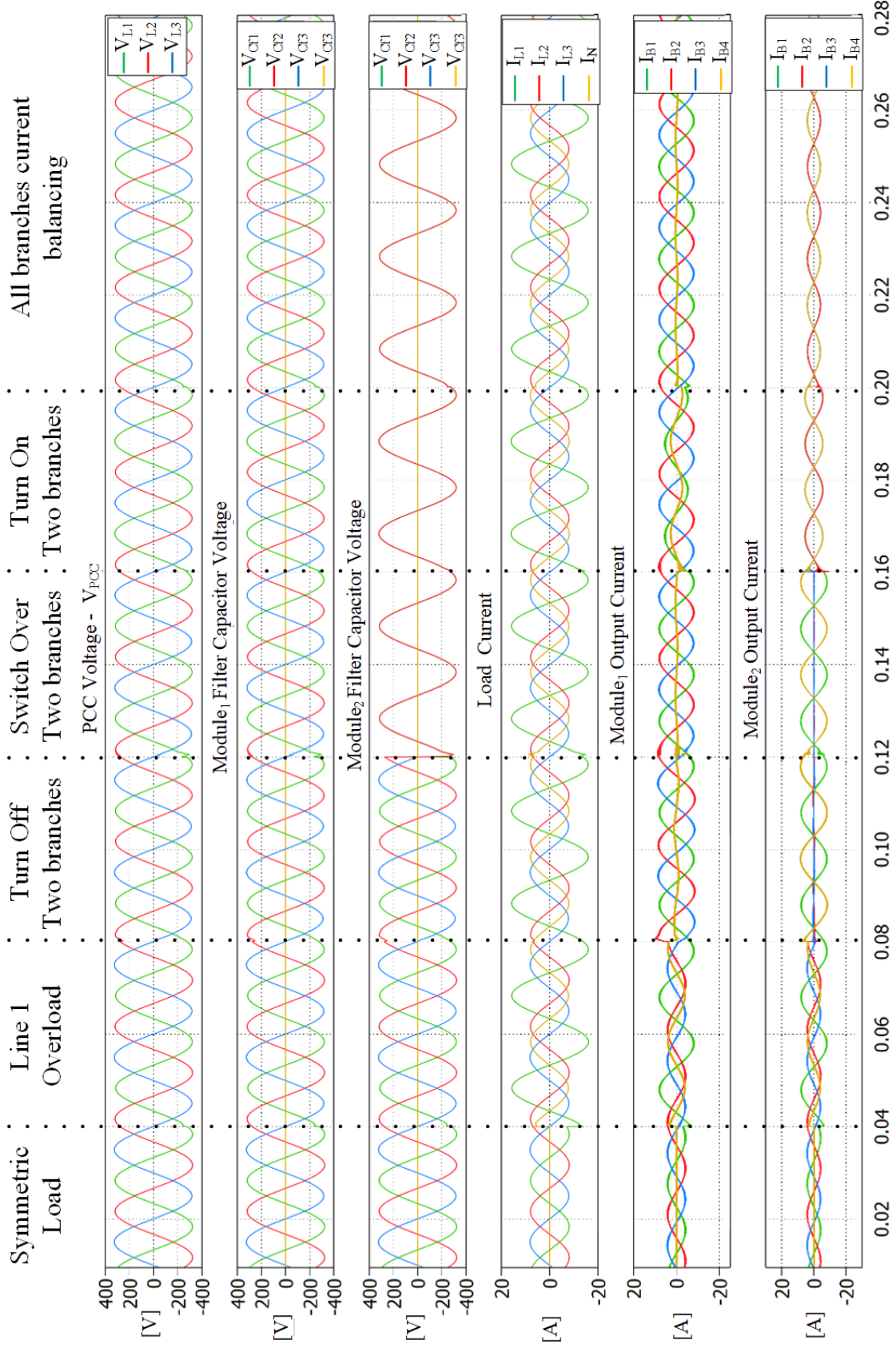
Figure 72. Three-phase connection mode to single-phase connection mode switchover preliminary simulation results.

The decision to connect or disconnect a DC/AC module is based on three primary factors, each critical to ensuring optimal performance and reliability of the system:

1. **Operating parameters of the transistor**: This includes the maximum conduction current $i_{D,max}$ and the thermal loss power during continuous operation, calculated as $i_{D,avg}$ $\cdot R_{DS,on}$. These parameters indicate the limits of the transistor's performance and its capacity to dissipate heat without overheating, thus influencing the safe operating conditions for the module.

2. **Current processing parameters**: This aspect involves the characteristics of the current being handled by the system, specifically the peak current i_{peak} and the average current i_{avg}. Understanding these parameters is crucial because they determine the load that each module needs to manage and whether it falls within the allowable limits set by the operating parameters of the transistors.

3. **Number of active branches per grid line**: Denoted as n_b, this factor significantly impacts the system's ability to handle current overloads. As the number of active branches increases, the tolerance for current overload $i_{ovrld,}$ proportionately increases.

The overload current can be calculated by dividing the total system load current by the number of branches:

$$i_{ovrld} = \frac{i_{load}}{n_b} - i_{D,max} \tag{3.25}$$

The number of active branches should be increased if the following condition is met:

$$\frac{i_{load}}{n_b} > i_{D,max} \text{ and } n_b \in Z \cap [1, n_{max}] \tag{3.25}$$

The conditions for determining whether to activate additional branches are based on the resultant average $i_{ovrld,\,avg}$ and peak $i_{ovrld,\,peak}$ overload current being greater than zero:

$$i_{ovrld,peak} > 0 \cap i_{ovrld,avg} > 0 \tag{3.26}$$

This condition applies to both peak and average overload currents, indicating that if either measurement exceeds zero, it signals a need for additional support from more branches.

To quantify the number of additional branches needed, the following formula is used:

$$n_{add} = \left\lceil \frac{i_{ovrld}}{i_{D,max}} \right\rceil \tag{3.27}$$

The occurrence of an overload can be classified as either temporary or continuous. A temporary overload may not necessitate the activation of additional branches since it may resolve itself without significant impact on system performance. In contrast, a continuous overload indicates a persistent issue that requires immediate attention and the addition of extra branches to distribute the load effectively.

Ultimately, the decision to activate additional branches hinges on a careful consideration of the time window during which the overload condition persists. By analyzing this time frame, operators can make informed decisions about when to engage additional modules, ensuring both system reliability and efficiency in response to varying load demands

The simple moving average (SMA) in the context of AC load current monitoring, the SMA is particularly useful for estimating the average value of the current waveform over a defined window of time, while suppressing high-frequency noise and switching ripple introduced by power electronic converters.

The SMA of a discrete-time signal $x[n]$, representing the instantaneous current samples, calculated over the last N points, is given by:

$$\text{MA}[n] = \frac{1}{N}\sum_{k=0}^{N-1} x[n-k] \tag{3.28}$$

The peak hold detection algorithm was implemented to determine the maximum value based on the following equation:

$$I_{peak}[n] = \max\{|x[n-k]| \, 0 \leq k < N\} \tag{3.29}$$

3.8. Adaptive modules management for efficiency and reliability improvement

System reliability is also understood as system availability in the broadest possible range of environmental conditions. The three-phase LV grid is usually asymmetrically loaded. Typical converter modules are rigidly connected to the grid, and their efficiency and capacity are not ideally matched to load. For example, **Figure 73** shows that the system capacity must be adjusted to the grid line with the highest load for modules rigidly connected in three-phase mode. The number n of active DC/AC modules depends on the phase with the highest load. The number of active modules in this case will be equal to the phase load i_{Lx} of the grid divided

by the nominal branch current i_{BN}. The remaining branches work with a lower load and different efficiency points, leading to unbalanced wear of elements in the DC/AC module.
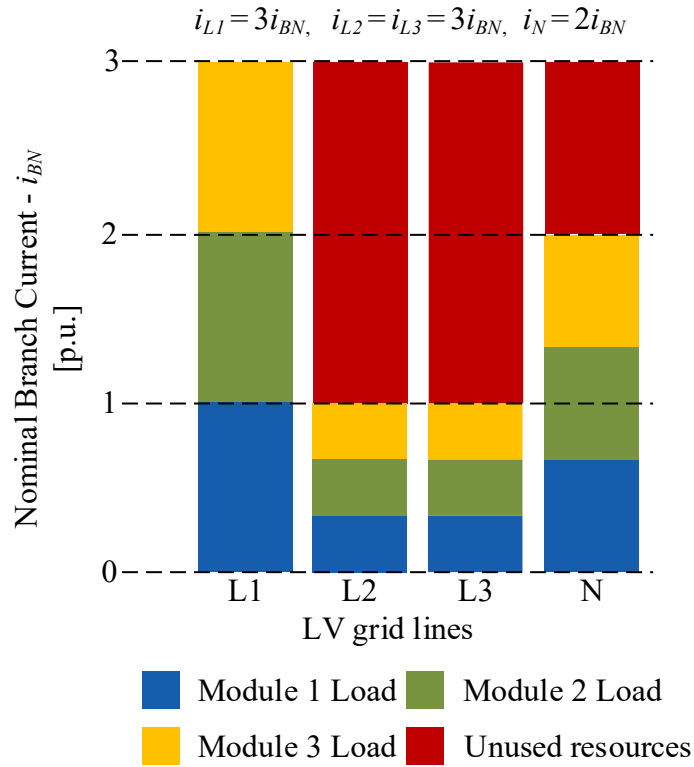
Figure 73. Example of mismatch between module mode and grid load.

One of the main requirements posed for power electronic systems is to maximize energy conversion efficiency and increase the life cycle of the equipment. Power electronic converters achieve the highest efficiency values for a limited power range. Due to the dynamic module switching and branch-to-line switching capability, it is possible to reconfigure the system to match the performance to the grid conditions and maximize power conversion efficiency. For the previous example of three modules, it will be much more efficient to connect only two modules where only one operates in three-phase mode and the other in single-phase mode, what is shown in **Figure 74**. Branch switching to change the operating mode of a module also reduces thermal stress and balances the load for all semiconductor components, extending the resultant module life cycle.

$$i_{L1} = 3i_{BN}, \quad i_{L2} = i_{L3} = 3i_{BN}, \quad i_N = 2i_{BN}$$
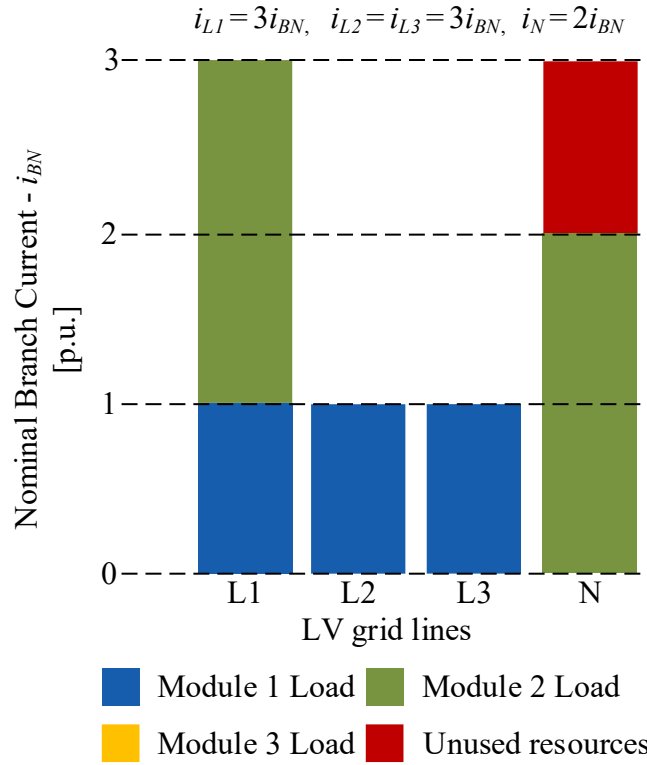
Figure 74. Example of matching the module operation mode to the grid load.

This section describes an analysis of adaptive parallel DC/AC grid-connected converters system reconfiguration to match system performance for grid requirements while maintaining the highest possible efficiency. The analysis is for selected cases and may not cover the full range of potential scenarios. Online optimization and adaptation to the fluctuating grid power realize the proposed adaptive module to grid connection control.

3.8.1. Efficiency model for a single branch of DC/AC power electronics converter

The smallest manageable execution unit in the system is a transistor branch with a line filter. As the branch can be switched between phases, the resulting system efficiency is analyzed based on a branch efficiency model and not based on a module, as in studies reported in the literature. The efficiency of a converter branch can be defined as follows:

$$\eta = \frac{P_{OUT}}{P_{IN}} = \frac{P_{IN} - P_{loss}}{P_{IN}} \tag{3.30}$$

where: η is the efficiency of the converter branch. P_{IN} and P_{OUT} are the input and output power of the converter branch, respectively. P_{loss} represents the power losses of the converter branch, including power losses of the semiconductors and AC filter.

The efficiency of a branch can be calculated using its power loss model to obtain an example efficiency curve [60] (**Figure 75**).
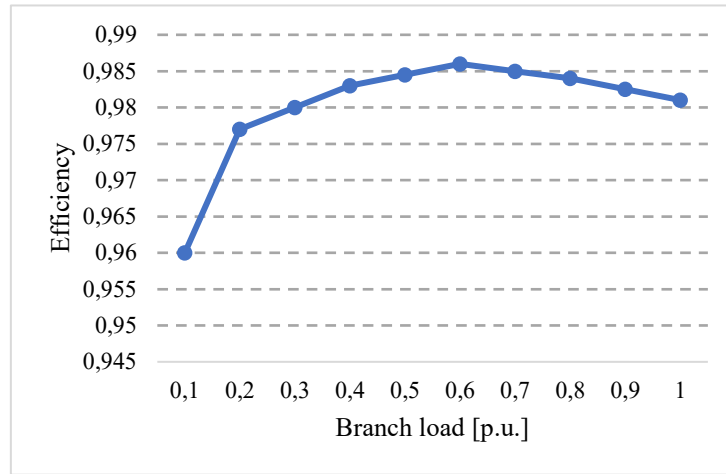
Figure 75. Example of DC/AC branch efficiency characteristics.

Figure 75 illustrates that system efficiency is relatively low under light load conditions but gradually increases as the load power rises, reaching a peak at the optimal operating point. Beyond this point, further increases in load power result in a decline in efficiency due to elevated switching and conduction losses.

This behavior highlights the importance of intelligent power allocation, particularly through the selection of an appropriate number of active, parallel-connected DC/AC branches. By dynamically adjusting the number of operational branches based on the load demand, the system can maintain operation near its maximum efficiency point, thereby improving overall energy performance and reducing unnecessary thermal stress on components.

3.8.2. Efficiency of parallel DC/AC power electronics converter branches

The resultant efficiency of a system of parallel connected branches η_{Total} depends on the number of branches and the load. The figure shows an equivalent circuit diagram showing parallel voltage sources connected to a common load.
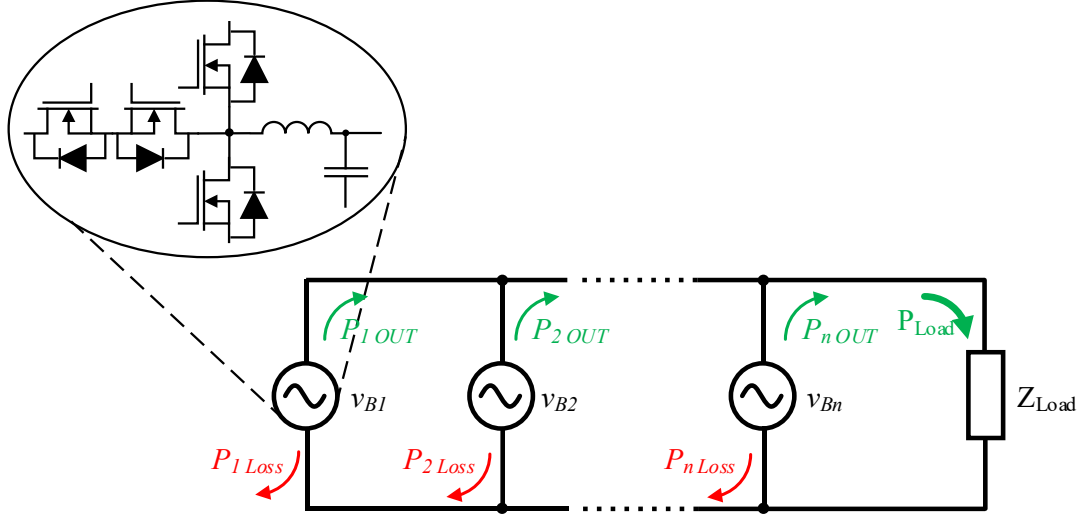
Figure 76. Parallel voltage sources as transistors branch model.

The total operation efficiency of a parallel system with the same *n* converters branches is as follows:

$$\eta_{Total} = \frac{P_{OUT\,Total}}{P_{IN\,Total}} = \frac{\sum_{i=1}^{n} P_{OUT,i}}{\sum_{i=1}^{n} P_{IN,i}} = \frac{P_{Load}}{P_{Load} + \sum_{i=1}^{n} P_{Loss,i}} \qquad (3.31)$$

For the system under consideration, it can be assumed that the sources operate with equal load and are made of the same components:

$$\eta_{Total} = \frac{P_{OUT\,Total}}{P_{IN\,Total}} \qquad (3.32)$$

In turn, the input power range is limited by the branch power rating:

$$0 \leq P_{IN} \leq P_N \qquad (3.33)$$

For the proposed topology and a control system that assumes equal branch loading, efficiency optimization is achieved by selecting the number of active branches in a given grid line:

$$n_{opt} \approx \frac{P_{OUT\,total}}{P_{opt}} \qquad (3.34)$$

Where n_{opt} is the optimal total number of branches rounded upwards, P_{opt} is the power operating point with maximum efficiency. An example graph of the relationship between the

number of branches and the load power in a given phase is shown in **Figure 77**. Subsequent ranges should overlap due to the need to use hysteresis when the load balances on the border of both ranges to avoid continuous branch switching.
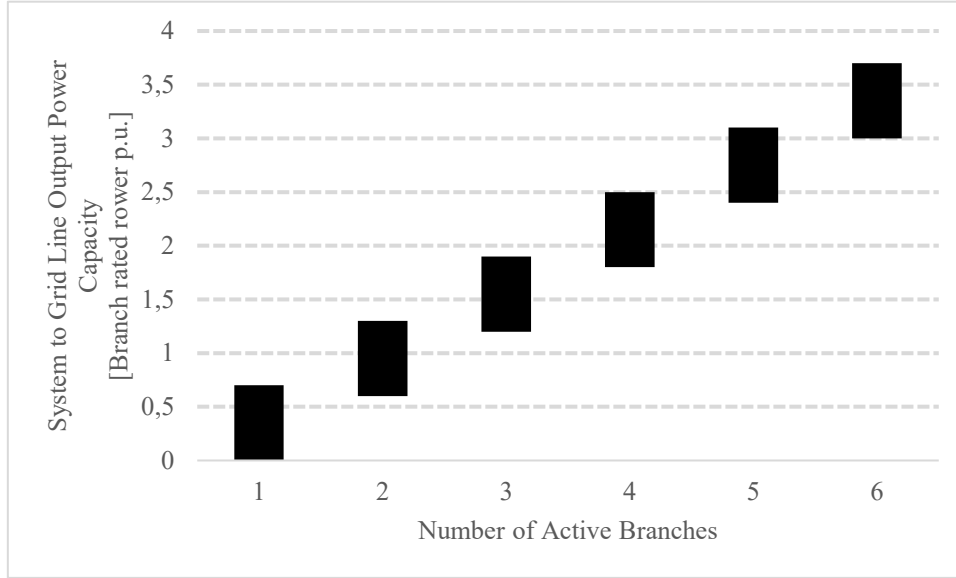
Figure 77. Load power ranges depending on the number of branches in an AC line.

In summary, the selection of the number of branches per grid line is primarily guided by an evaluation of the load demand and the identification of the optimal operating point for branch efficiency, while also incorporating sufficient reserve capacity to accommodate dynamic load variations. In the proposed topology, each DC/AC module consists of four branches, with the flexibility to switch individual branches between different grid lines.

Once the required number of branches is established, the next step involves determining the appropriate number of active modules and defining their connection modes to the grid lines. This decision is critical for achieving both high efficiency and reliable operation of the overall system.

3.8.3. Selection of the optimum number of active DC/AC modules and connection mode

Switching the branches between grid phases enables the DC/AC module to operate in three distinct modes: three-phase, single-phase, and inter-phase. Each of these modes offers varying load capacities, allowing for flexibility in application based on the specific requirements of the electrical system.

In particular, both the phase and inter-phase modes achieve excellent load balancing and thermal cycling among all semiconductors within the module. This is crucial for extending the lifespan and reliability of the components, as it ensures that no single semiconductor experiences excessive stress due to uneven current distribution.

A fundamental principle across all operational modes is that the sum of the branch currents within the DC/AC module must equal zero. This condition ensures that the system remains stable and that energy conservation principles are upheld.

- **Three-Phase Connection Mode**: This mode is designed to accommodate three-phase and two-phase loads that are equipped with a neutral line. It provides balanced power delivery, which is particularly beneficial for industrial applications where three-phase machinery is common.

- **Single-Phase Mode**: This configuration is tailored for single-phase loads, offering a straightforward connection that maximizes efficiency for household or light commercial applications.

- **Inter-Phase Mode**: This mode is suited for inter-phase loads that do not require a neutral line. It allows for efficient operation in systems that utilize inter-phase connections, often seen in specific industrial applications.

By enabling these flexible operational modes, the DC/AC module can seamlessly adapt to different load conditions, ensuring optimal performance and efficiency across various applications.

An example scenario of adaptive operation is illustrated in **Figure 78**, with corresponding simulation results shown in **Figure 79**. In the initial phase, a single power module is activated to supply a three-phase load. Once voltage and current waveforms reach steady-state conditions, an additional three-phase load is connected, resulting in system overload. This necessitates the activation of a second power module operating in three-phase mode.

Upon receiving the activation signal, a synchronization procedure is initiated. This includes aligning the DC-link voltages across the output filter capacitors, followed by grid connection. Subsequently, the reference current is synchronized to ensure seamless power sharing. The simulation shows that the second module operates stably, and the overload condition is mitigated as the load is now distributed across both modules.

In the next step, the three-phase load is disconnected, and after a brief period, the additional module is deactivated.

Following this, a single-phase load is introduced, causing a phase-specific overload condition. To relieve the overload, a second module is again activated this time configured to

operate in single-phase mode. The activation process is similar to the previous case; however, the control signals now instruct the module to connect two branches to the overloaded phase and the remaining two branches to the neutral line. Finally, once the module is fully synchronized with the system, the reference current signal returns to its nominal range, indicating that the overload has been successfully eliminated.

The presented scenario underscores the adaptive capabilities and fault-resilience of the modular converter system, showcasing its ability to dynamically respond to varying load conditions while ensuring operational continuity. By incrementally activating or deactivating modules based on real-time load demand, the system not only mitigates overloads but also optimizes resource allocation across available modules.

This adaptive control strategy significantly contributes to enhancing system reliability, as it prevents prolonged operation under stressed conditions, which are known to accelerate component degradation. Moreover, the selective activation of modules in different operating modes (three-phase or single-phase) allows for targeted load sharing, improving the thermal distribution and extending the lifespan of power electronic components.
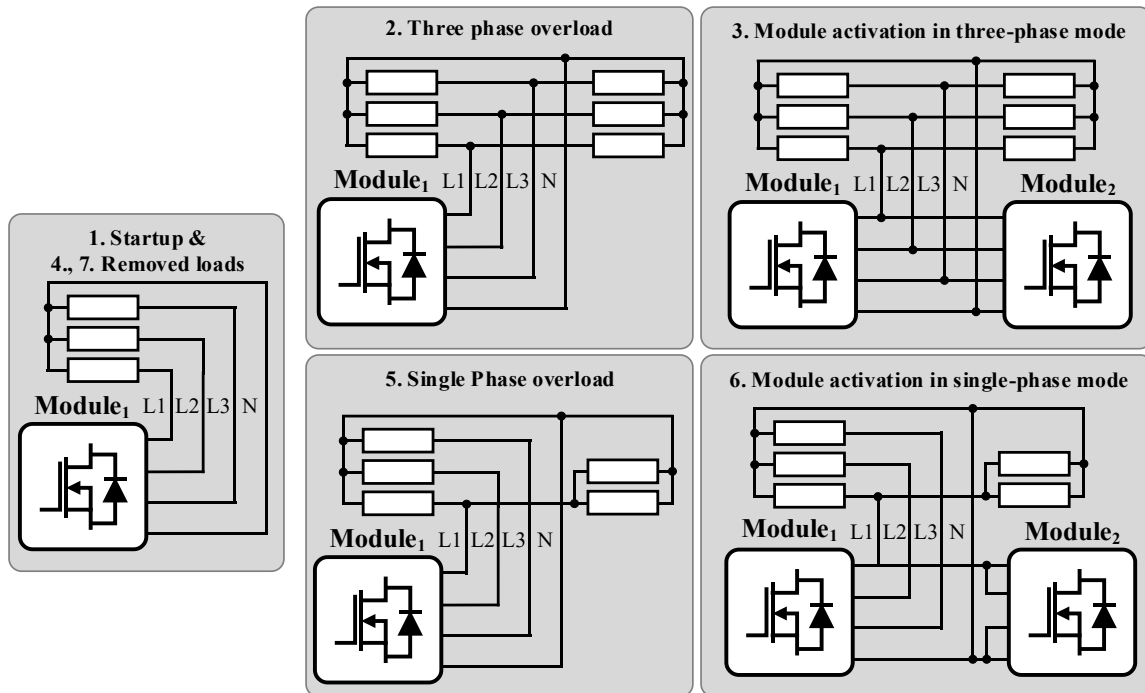
Figure 78. Example scenario for system to load adaptation.
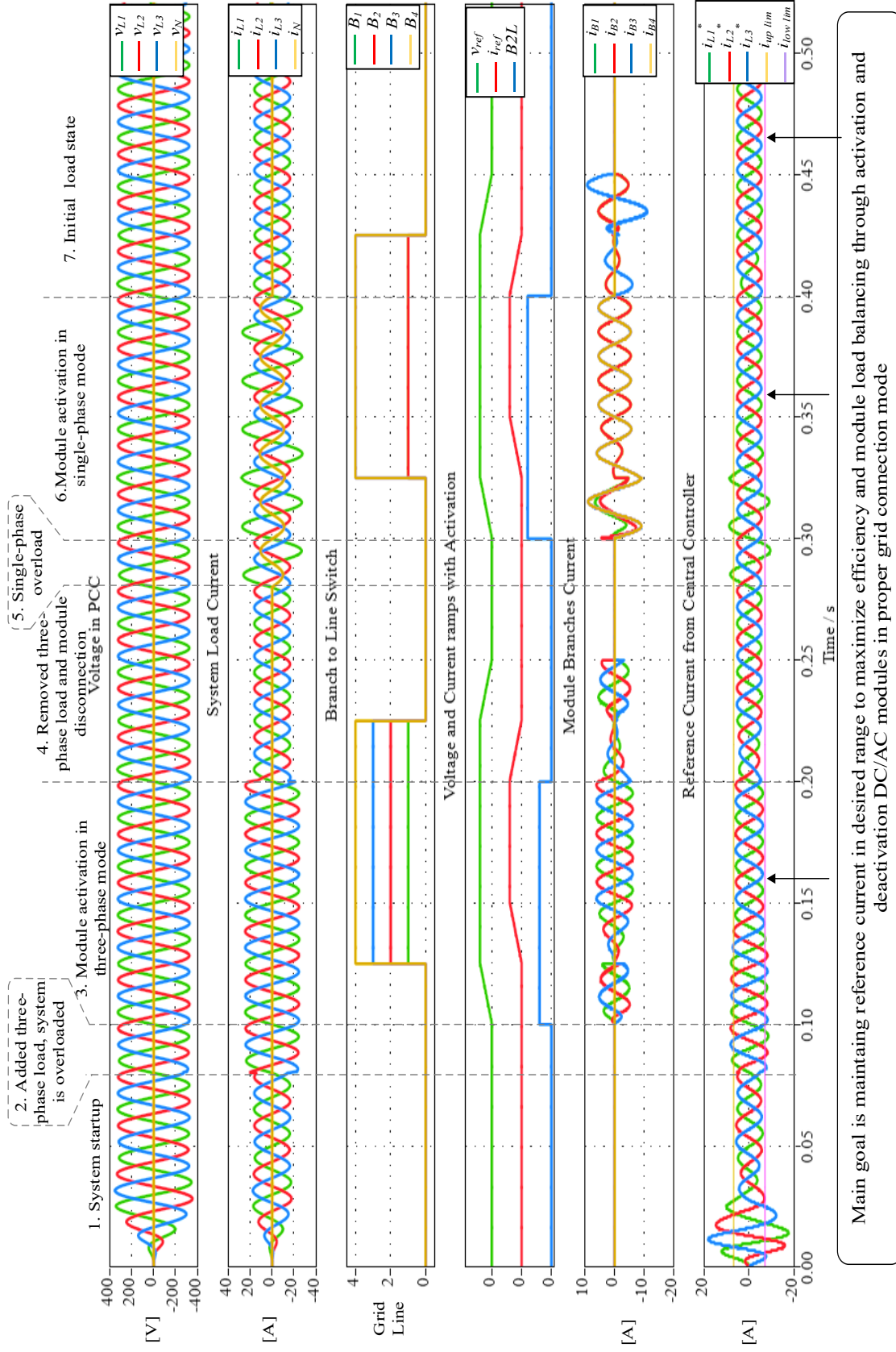
Figure 79. Module and branch switch algorithm simulation results.

3.9. Summary of control strategy

This chapter addresses the challenges involved in implementing distributed control for a modular converter system designed to operate under fault conditions. The author identifies and analyzes several key issues, including:

- **Implementation of a distributed control system**: ensuring efficient communication and coordination among multiple control units within the modular system.

- **Operation under distorted currents and voltages**: managing the impact of non-ideal grid conditions on system performance.

- **Variation of resultant impedance**: understanding how the impedance of the system changes based on the number of branches connected to a given line.

- **Impact of system configuration**: evaluating how different grid connection configurations affect overall system performance and components wear.

- **Control system configuration**: adapting the control system to function effectively in various operational modes of the system and DC/AC modules.

The parallel connection of DC/AC converters, utilizing a common DC circuit and cooperating with a four-wire distribution grid, is essential for providing fault tolerance. This setup necessitates a control system that operates in two primary domains:

- **Continuous control of currents and voltages**: this involves regulating the modular system depending on its operating mode either grid-forming or grid-supporting while maintaining resilience against current and voltage disturbances as well as impedance asymmetries.

- **Management of system connections to the AC grid**: this management considers the fault factors of system components and the load status of the grid to optimize performance.

In relation to continuous current and voltage regulation, the author proposes a solution with the following features:

- **Proportional-resonant controller based method**: this approach includes an additional harmonic compensation component that is effective in both grid-forming and grid-supporting modes (**Figure 80**), This control method is adaptable based on the state of the DC/AC modules and the connection configuration to the grid:
  - system startup where all modules operate in three-phase mode,

- three-phase operation of the DC/AC modules during startup and under steady-state conditions,
- single-phase operation of the DC/AC modules during startup and steady state.

- **Implementation in a distributed control system**: the proposed method is designed for easy integration within a distributed control framework.

- **Scalability**: the system allows for flexible scaling, enabling the addition of more modules as needed.

- **Dedicated current controllers**: each branch features its own current controller, allowing it to operate effectively with any line of the grid (L1, L2, L3, or N).

- **Control system reconfiguration**: the control system can be adjusted depending on the operating mode of the module (three-phase, single-phase, interphase).

- **Increased impedance variation resistance**: the inclusion of a harmonic compensation component enhances the system's resilience to changes in impedance.

- **Switching scenario and synchronization**: the operation of each branch can be synchronized with the corresponding line of the grid.

Within the management domain for the connection of DC/AC modules to LV grid lines, the author proposes additional solutions, including:

- **System reconfiguration after a fault**: an effective strategy for restoring system functionality following a fault incident.

- **Branch selection based on load conditions**: choosing the number of branches to connect to a grid line based on current load conditions to maximize system efficiency and balance the load on the DC/AC module. This approach is informed by optimal branch efficiency.

In summary, this chapter offers a comprehensive analysis of the challenges associated with implementing distributed control in modular converter systems, particularly those required to operate reliably under fault conditions. The author highlights several critical issues, including the complexities of developing a robust distributed control architecture, the detrimental effects of signal distortions, and the impact of fluctuating impedance caused by variations in branch connectivity.

The proposed solutions prioritize continuous regulation of current and voltage levels, adjusted to the system's operational mode: grid-forming or grid-supporting to ensure resilience against disturbances and asymmetries. Additionally, AC grid connections are managed using
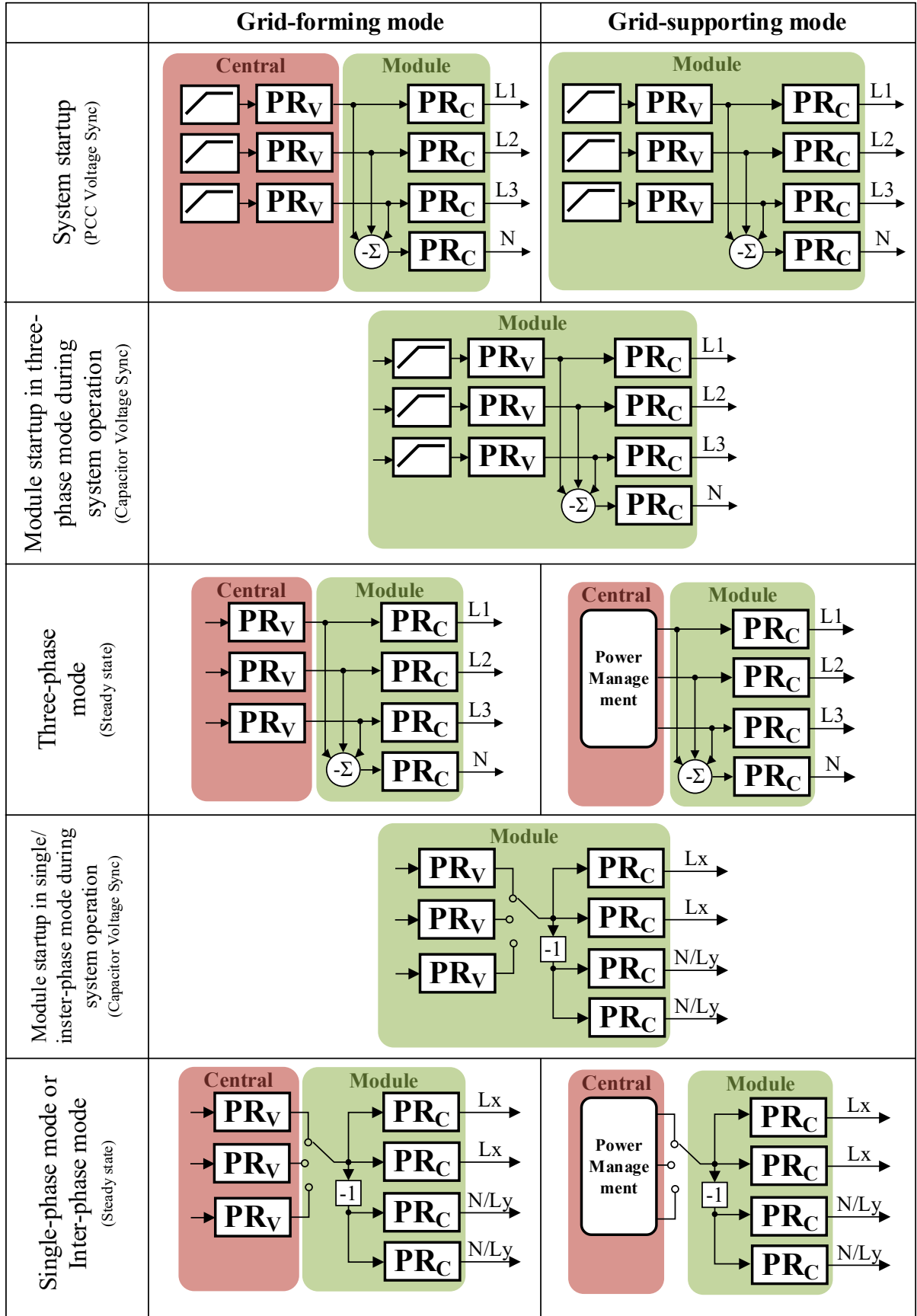
Figure 80. Summary of control system configurations depending on the system operation mode and DC/AC module to grid lines connection modes.

fault-tolerant strategies that enhance overall efficiency by applying real-time adaptive algorithms for load balancing and intelligent branch selection.

A key feature of the proposed control strategy is the deployment of PR controllers with harmonic compensation, which significantly improves system performance during both transient states and steady-state operations. The modular design of the converter system, alongside branch-specific current controllers, allows for flexible adaptation to varying grid conditions, enhancing the overall scalability and operational versatility of the architecture.

Additionally, the chapter emphasizes the importance of reconfigurable control based on the specific operational mode of the DC/AC modules, whether functioning in three-phase or single-phase modes. This adaptability is crucial for maintaining both efficient energy conversion and robust fault management, enabling swift and reliable system responses to external disturbances.

In conclusion, the control solutions presented in this chapter effectively fulfill the reliability and performance criteria outlined in earlier sections of the thesis. The proposed distributed control system markedly improves the LV stage of PET system's resilience under adverse operating conditions, including voltage distortions and fault scenarios. The subsequent chapter will focus on the real-time implementation of this control framework within a communication interface, addressing the practical realization of the theoretical models introduced herein.

4. Real-time communication in the Power Electronics Transformer

Due to the plug-and-play concept of a modular power conversion system, where each converter module has its control unit, it is necessary to ensure data exchange and synchronization to maintain stable operation and correct management of the entire system. If a closed control loop is distributed among several control units, then the communication rate must be equal to the calculation frequency of the loop. It is also necessary to ensure phase synchronization of PWM signals and synchronization of process data transfer. It is also necessary to consider the risk of losing data transmission through link interruption. For this reason, the transmission channel should be multiplied through redundancy. Hence, the communication interface is critical in designing and controlling a modular electrical energy conversion system.

The development of microcontrollers in recent times has led to increased clock frequencies and the manufacture of chips with more than one processor. As a result, it has become feasible to implement modular power converter technologies. A hierarchical power electronics building block (PEBB) control model based on the following levels has been proposed in the literature [61], [62]:

- power switch controller,
- topology or circuit controller,
- application controller,
- system controller.

The solution described in this dissertation fits precisely into this model. The power switch controller level refers to the current control loop and semiconductor condition monitoring. The topology or circuit controller level refers to switching modules and branches. The application level refers to managing the number of active modules and branches. The system level refers to the entire PET system, including all MV and LV voltage conversion stages. The above hierarchical model, implemented on separate control units, requires extracting process variables. Process variables denote a set of control and feedback signals.

Due to data transmission speed limits, the communication interface is a dictating factor in implementing the control strategy. The minimum cycle time was the communication time required by the controller to collect and update the data memories of all sensors and actuators [63]. External data exchange significantly extends the control cycle and must meet real-time restrictions. In addition, the communication system must provide synchronization, low latency,

reliability, and hot-plug capability. The literature mainly describes implementing distributed modular series-connected multilevel converter control systems, including synchronization [24]. A comparative review of industrial communication interfaces that meet real-time requirements was also performed [63], [64], [65], [66]. In most cases, EtherCAT is chosen, which meets all the requirements.

The proposed LV stage of PET topology and control method presented in the previous chapter requires appropriate adaptation of the communication system. This chapter focuses on the problems and offers solutions for a communication system connecting parallel DC/AC converter modules to a central control system. The considerations are divided into two main parts: analyzing and selecting a standard communication interface and selecting and implementing a process data set based on the proposed control system from the previous chapter.

4.1.   Overview of the requirements for the communication system

A prerequisite for the implementation of a modular system structure is the use of reliable communication that meets real-time requirements. Furthermore, the parallel connection of branches from separate modules with a common DC link requires phase synchronization of the PWM signals. The abovementioned requirements also conclude that lack of communication and synchronization leads to loss of module control and unstable system operation. Hence, the communication system must include appropriate mechanisms to maintain communication continuity. To distinguish all the requirements for the communication system for a modular DC/AC converter system, it is necessary to look at the design from folowing points of view:

- current and voltage control loops must provide samples with reference and feedback values at a frequency close to the PWM signal period,
- differences in the frequencies of the oscillators clocking the module control systems lead to a gradual loss of synchronization; hence, a synchronizing pulse must be cyclically supplied,
- the topology of the communication system must maintain continuity of data transfer when module operation is interrupted due to module failure or replacement; the communication system must include mechanisms to check the network status,
- the communication system must be robust to disturbances and include mechanisms to assess the correctness of the transmitted data,

- due to the scaling requirements of modular systems, the communication layout should not impose restrictions on the network size,
- the communication layout should be an accepted, standardized, evolving industry standard.

Once the communication interface has been selected based on the requirements listed above, it is necessary to define the process variables to be exchanged between master and slave control units. Due to bandwidth constraints, network size, and real-time restrictions, this set must contain as little data as possible. The communication interface is the boundary separating the control system; hence, it only has reference and feedback values.

This chapter provides a comprehensive analysis and implementation of the communication subsystem within the LV stage of the modular PET system. In the subsequent sections, the use of EtherCAT will be explored, an industrial standard for real-time communication, as primary interface for data exchange.

Furthermore, the chapter will delve into the selection of critical process variables that are essential for the effective operation of the distributed control system. This architecture features a single central controller managing multiple identical DC/AC power converters, emphasizing the importance of synchronized communication and control.

4.2. Comparison of communication standards for power electronics applications

Power electronic system emits electromagnetic disturbances that are harmful to itself. Therefore, the communication interface should primarily be immune to electromagnetic interference. For this reason, communication at the physical layer should be based on the Ethernet standard. Performance analysis and comparisons of Ethernet-based communication interfaces have been widely reported in the literature. Performance analysis and estimation of minimum and maximum parameters were performed in [67]. Implementation examples in modular power electronic systems were presented in [68]. The findings in publications and market reports indicated that the EtherCAT interface meets the broadest requirements, although other interfaces are still being developed and have comparable performance (**Table 13**). EtherCAT shows advantages in key aspects such as low latency and high performance, topology flexibility, high bandwidth and large number of supported devices, high reliability and self-diagnosis. EtherCAT technology is not expensive to implement and many tools are offered to facilitate the implementation of the control along with the network configuration. EtherCAT

also allows communication to be maintained in cases where the physical connection is interrupted through the ability to add redundant paths.

By leveraging EtherCAT's capabilities, we aim to achieve high-speed communication and real-time performance, which are crucial for the precise coordination of the power converters. The chosen process variables will be analyzed in terms of their impact on system performance, reliability, and overall efficiency, ensuring that the communication subsystem operates effectively within the PET framework.

Table 13. Summary of real-time communication interfaces.

	EtherCAT	Ethernet/IP	Powerlink	Profinet IRT	Sercos III
Real-Time	Hard	Soft	Hard	Soft	Hard
Min. cycle-time	12,5 us	-	-	31,25 us	31.25 us
Max. data rate	10 Gb/s	10 Gb/s	10 Gb/s	10 Gb/s	10 Gb/s
Max. devices for min cycle-time	20	-	-	-	7
Latency	1.35 us	3 us	-	3 us	-
Synchronisation Jitter	< 100ns	-	< 100 ns	< 1 us	< 100 ns
Hot plug	YES	-	YES		YES
Topology	Line, Tree, Star, Daisy-chain, Ring	Bus-based, switch-based	-	Line, Star, Tree, Ring	Ring, Line
Diagnosis and Error location	YES	YES	YES	YES	YES
Redundancy	YES	-	-	-	YES
Link detection time	15us	-	-	-	-
Support for decentral control	NO	YES	-	-	-

4.3.   Specific features of EtherCAT for distributed control of power electronics

From the analyses and comparisons performed in the literature, the EtherCAT interface shows the best fit for modular power electronic system applications. EtherCAT is based on the Ethernet interface at the physical layer. Differential communication via wire cable or fiber optics is possible, which results in high immunity to disturbances. EtherCAT features increased performance with a dedicated application specific circui - ASIC developed for slave devices. It implements the following set of functionalities:

The first is on-the-fly frame processing (**Figure 81**), which involves receiving and forwarding a data frame while simultaneously inserting return data from the device. This feature minimizes the delay introduced by subsequent devices in the network. When receiving and

inserting data, a checksum is calculated to confirm the correctness of the data, and the working counter is modified to show the number of devices in the network. The minimum data exchange cycle is 50us. EtherCAT exchanges only one frame per communication cycle and delivers it to all network devices. It is possible to broadcast a single packet to all devices, which minimizes the amount of data. The third functionality is distributed clocks. Based on a synchronously sent frame, the slave circuit corrects and generates a synchronizing pulse with a jitter at the nanosecond level. This function is significant for generating PWM signals and minimizing the circulating currents in parallel modules.

Input Frame State

| Data in | Data out | CRC | CTR |

EtherCAT Slave Controller

| Data in | Data out | CRC | CTR |

Output Frame State
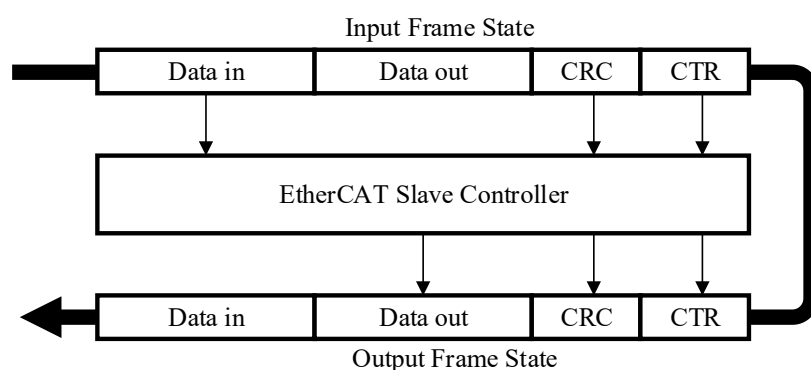
Figure 81. EtherCAT on-the-fly frame processing.

The second key feature of the EtherCAT communication protocol is its advanced loopback function, which plays a critical role in detecting the physical connection status of each port within the network. This capability allows for continuous monitoring of the network integrity so that any disconnection of a device can be swiftly identified. When a device is disconnected, process data is seamlessly forwarded to the next active port in the communication chain, ensuring that data flow is not interrupted.

This intelligent handling of disconnections significantly enhances the flexibility of network topology, enabling configurations that can adapt to changing operational conditions without requiring a complete system shutdown. As a result, EtherCAT supports a wide range of network setups, making it ideal for applications demanding high scalability and modularity.

Moreover, the incorporation of additional EtherCAT junction devices, as illustrated in **Figure 82**, further augments communication reliability. These junction devices facilitate advanced network configurations, allowing multiple branches of devices to connect to a single network. They enhance the robustness of the system by providing alternative communication paths in case of a link failure.

Importantly, the loopback function also supports hot-plug and hot-unplug operations. This means that devices can be added or removed from the network while it is active, without disrupting ongoing communication or requiring manual reconfiguration. This capability is particularly beneficial in dynamic environments where equipment may need to be frequently modified or upgraded, such as in industrial automation systems or advanced medical imaging technologies.

In summary, the loopback function not only contributes to maintaining communication integrity but also empowers users with the flexibility to design and modify their EtherCAT networks in real time. This flexibility, combined with the inherent reliability of the EtherCAT protocol, positions it as a powerful solution for a multitude of applications requiring efficient and resilient communication infrastructures.

The set mentioned above of functionalities determined the choice of the EtherCAT interface for communication in the described LV stage of the PET system. Moreover, the EtherCAT interface is still being improved. It reaches higher and higher communication speeds (currently up to 10Gb).
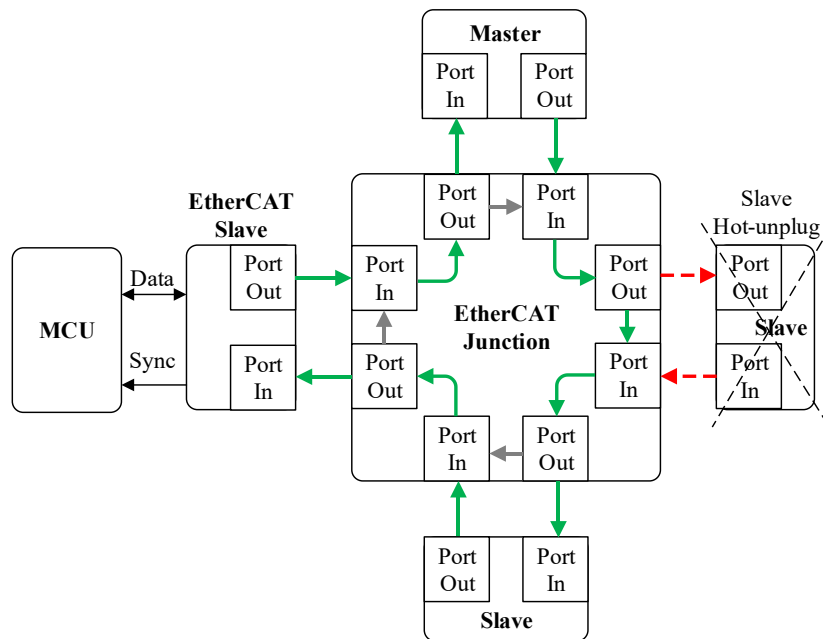
Figure 82. EtherCAT auto-forwarding feature.

4.4. Hardware configuration for distributed control

One of the main criteria for selecting a communication interface is the industry standard and the availability of hardware solutions on the market. The selection of hardware to integrate

a communication system based on an EtherCAT interface requires the choice of four main components:

- EtherCAT master – Beckhoff Industrial PC 6015,
- EtherCAT slave controller – ET1100 modified Ethernet-based frame processing unit,
- microcontroller unit – TMS320F28379D dual core, capable of external PWM synchronization and high-speed external communication,
- EtherCAT Junction for hot-plug purposes.

For experimental verification of the proposed solutions, one central controller and four module controllers connected by the EtherCAT network were used (**Figure 83**). From the data transmission point of view, data is sent from the central controller and sequentially transmitted from the first control board to the last. However, this configuration prevents the operation of hot plugging and unplugging modules.
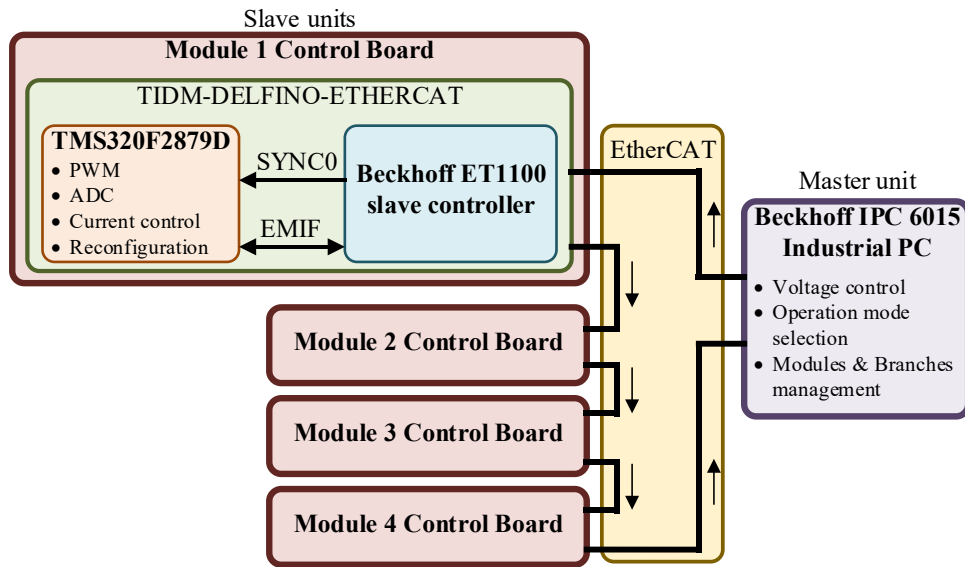
Figure 83. Diagram of EtherCAT integration details into PET LV stage.

Using the auto-forwarding feature and including a hardware chip to change the ring topology into a star topology, data transmission will be maintained as a ring from a data transmission point of view. Thus, an EtherCAT junction box was added to the network devices set mentioned above (**Figure 84**). As a result, it is possible to disconnect and connect modules without physically interrupting the data transmission chain. This is particularly important for maintaining system operation after a fault has occurred and for service replacements.
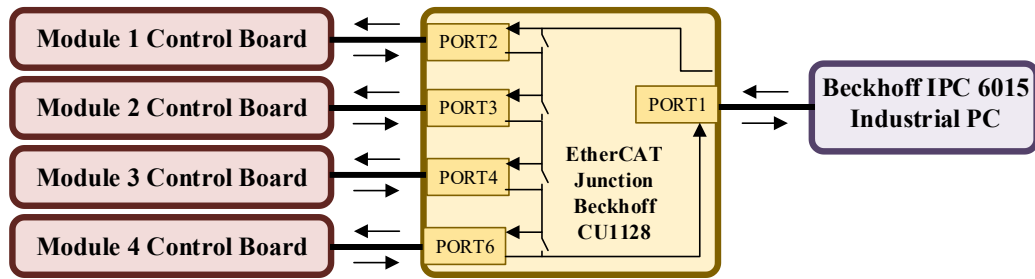
Figure 84. EtherCAT network with hot-plug capability.

4.4.1. Central controller

The central controller is the interface between the system management application and operator and the modules controllers and performs the following main tasks:

- calculates voltage control loops,
- supervision of communication and synchronisation of slaves,
- communication status checking for the sub-modules,
- data processing and analysis of results,
- communication with the operator,
- adaptation of the number of active DC/AC modules,
- reconfiguration of the system in case of a device fault or adaptation power capability to load,
- providing security and access control.

The central controller in a distributed control system acts as the overriding manager of the entire system, taking care of the efficient and safe operation of the slaves. Its tasks include communication supervision, synchronisation, data analysis, alarm management and integration with superordinate systems. Thanks to central control, the distributed control system becomes more consistent, reliable and efficient, which is crucial in industrial applications where real-time, synchronisation and safety are a priority.

4.4.2. Module controller

Dedicated EtherCAT slave controller ET1100 ASICs are used on the slave side. These devices contain the functionality described in the previous section and several communication interfaces for exchanging process data with the microcontroller. The ET1100 includes a set of registers that are accessible to the microcontroller (**Figure 85**). The EtherCAT slave communication stack is implemented in the microcontroller firmware and occupies a relatively

large amount of resources. Hence, it is necessary to use a multi-core microcontroller to execute the communication and control algorithms within a strict time limit. A TMS320F28379D microcontroller from Texas Instruments was selected as the control unit for the module.
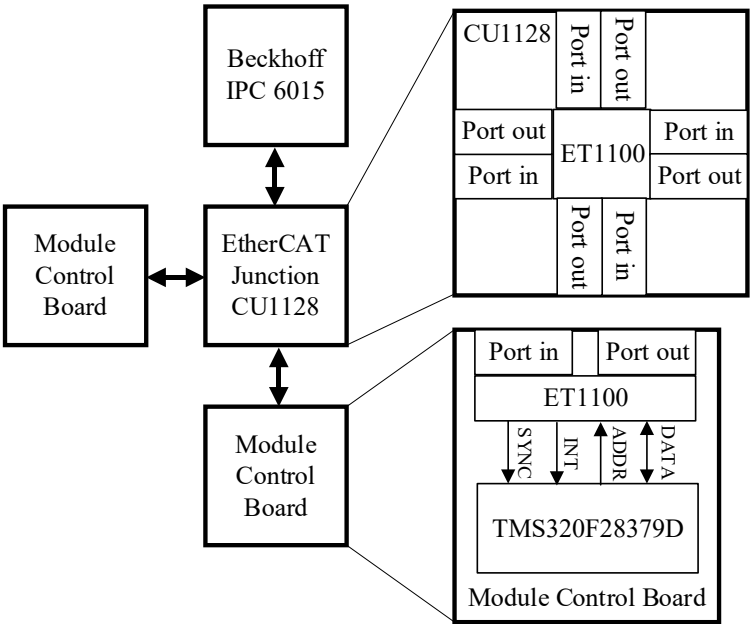
Figure 85. EtherCAT reliable topology block diagram.

4.5.   Distributed control architecture and communication data selection

The primary function of the communication interface is the transmission of process data. In application to real-time systems, the data frame is fixed, and its size is as small as possible. The control algorithm determines the process data list (**Figure 86**). The process data set in the EtherCAT interface is divided into three main groups: input data, output data, and parameters. Input data is variables that reference the control system or commands. Output variables include feedback values and device status information. Input and output variables are exchanged in each frame during regular system operation. Parametric variables are used to configure the module before regular operation begins. These variables can include all process constants, such as controller gains.

To determine the list of variables, the control algorithm should be separated into a central control unit part and a local control unit part. The central control unit part should determine common reference values for all local controllers. This division must also consider the minimum frequency of the control loop calculation. Only the power electronic modules are

129

equipped with sensors. Placing the control loop outside the local controller requires the feedback values to be placed in the data frame.
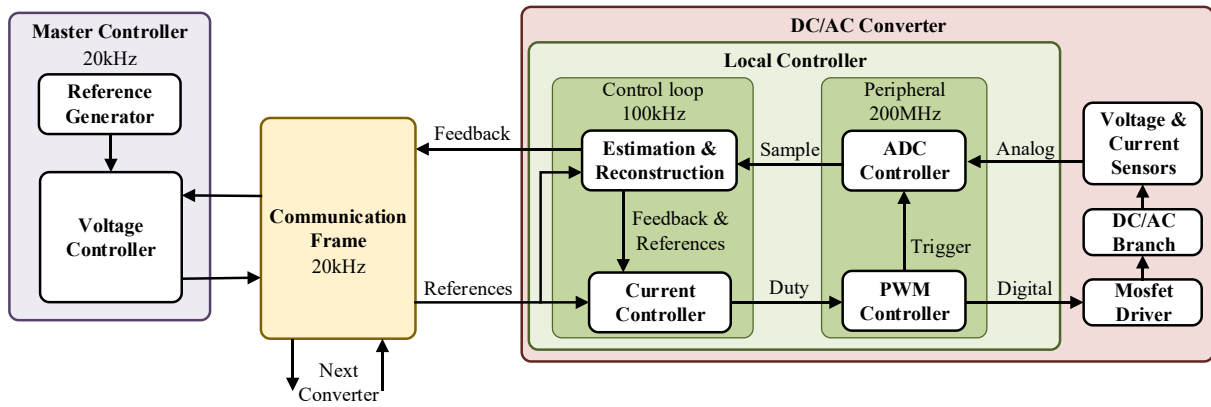
Figure 86. Distributed control system diagram.

The selection of process variables cyclically exchanged between modules and central units must be made according to strict criteria. The variables' value range and bit size must be as small as possible. This is related to the limitations of the speed and number of devices for the assumed cycle time of the data exchange. The list of variables must include all key variables (measurements and references) between the control loops implemented in the central and module controllers (**Figure 87**).

Based on the criteria above, the facts related to the implementation of the control system must also be listed:

- the master module manages the number of modules and branches attached to the network and to which branch is to be attached from here:
  - each branch must have information on whether it is to be switched on or not - 1 bit (reference),
  - each branch must have information to which of the four network lines it is to be attached - 2 bit (reference).

The proposed control system distributes the current control loops to the slave modules, while the voltage control loop is implemented in the master module. Hence:

- the voltage controller calculates reference values for currents; therefore, the master module sends 3-phase current values to all slave modules (reference),
- the reference value for the neutral branch is calculated based on the module's zero-sum condition of the AC currents.

Voltage measurement is carried out by all slave modules, but is not carried out by the master module; hence:

- the mains voltage measurement from each slave module is transmitted back to the central controller as feedback,

- the duplication of voltage measurements provides redundancy in the voltage measurement signal.

The central control unit manages both the frequency and phase angle of the system. In contrast, proportional-resonant controller algorithms are implemented within the slave modules, utilizing the frequency signal as a key parameter. Additionally, seamless synchronization is achieved by precisely supplying the phase angle value to all modules, ensuring coordinated operation across the system.
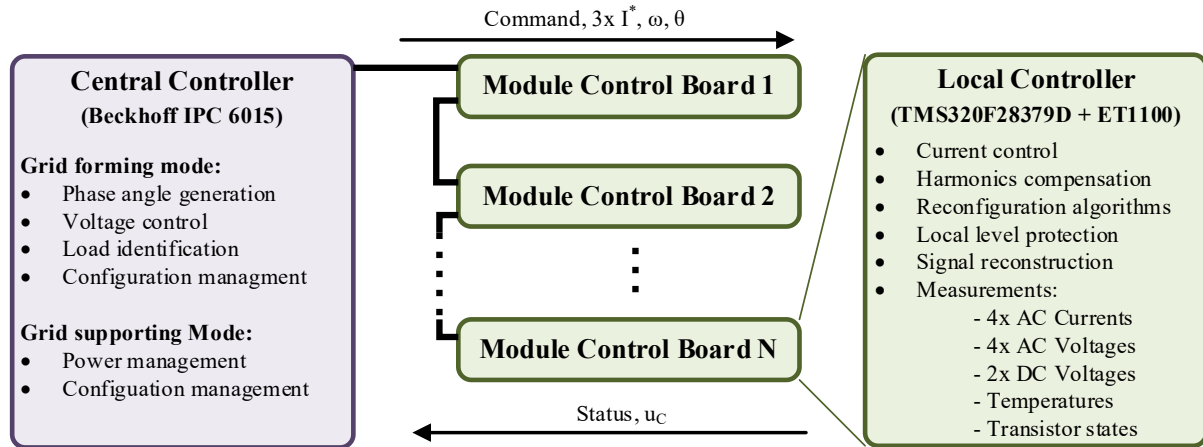
Figure 87. Central and local control tasks and data exchange.

The proposed algorithm operates on the premise that the current reference values are established by the central controller, irrespective of the operational mode. However, in grid-connected mode, it is essential for the central controller to receive voltage feedback. Additionally, a harmonic compensation algorithm implemented in the local controllers necessitates a voltage reference signal, which can be reconstructed from the phase angle. The final distribution of control algorithms with process data summed up in **Table 14** is shown in **Figure 88**. In addition to the variables utilized in the control loop, status variables that provide information about the state of the transistor branches and a command that specifies the operating mode of the DC/AC module are also transmitted.

Table 14. Summary of Process data exchanged between central and local controllers.

Type	Symbol	Name	Description
	Cmd	Command	The command is a set of bit fields intended to force a module to start, stop, or change its branch-to-line configuration.
Input	$i_{L1}{}^*$, $i_{L2}{}^*$, $i_{L3}{}^*$	Iref	Branch to line current reference
	ω	Frequency	Frequency of the fundamental harmonic of the network
	θ_{global}	Global phase angle	Global Phase angle of the PCC voltage reference.
Output	Sts	Status	Information about the current status of the module and its components
	v_{Cf1} , v_{Cf2}, v_{Cf3}	Ufdbk	Filter capacitor voltage feedback
Parameter	K_{PI}	Proportional Gain	Proportional gain of the current controller
	K_{RI}	Resonant Gain	Resonant gain of the current controller
	$v_{out}{}^*$	PCC Voltage	Amplitude of output voltage in PCC
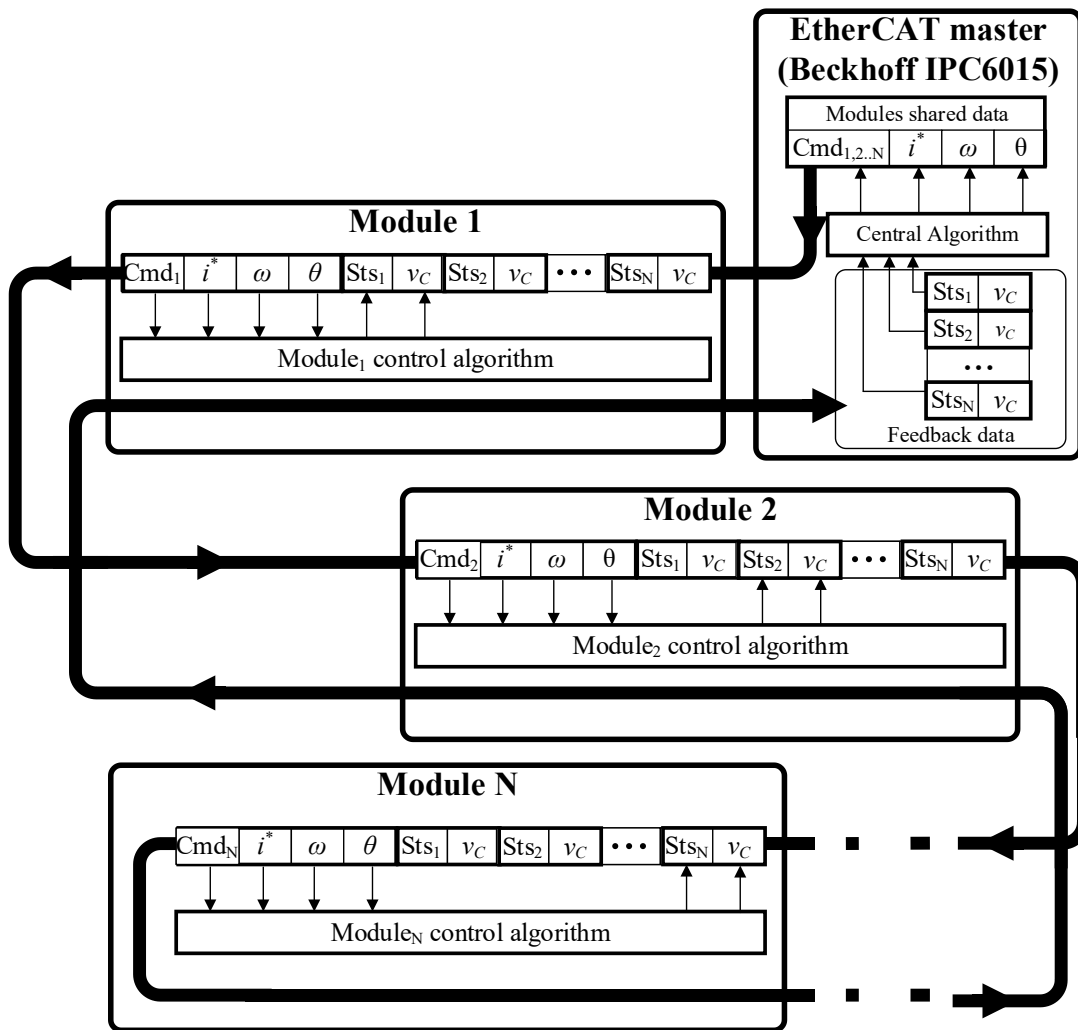
Figure 88. Diagram of the data frame transmitted in the system.

Each local controller contains the same set of variables, and the reference values are shared. The values of reference currents, frequency, phase angle and parameters are common to all slave modules. The individual values for each module are the command and all return values: status and voltage in the PCC.

Based on the set of variables distributed from the central controller, the following values are reproduced locally:

1. The reference value of neutral line current:

$$i_N^* = -i_{L1}^* - i_{L2}^* - i_{L3}^*$$ (4.1)

2. Local phase angle θ_{local} calculated with the period $T_{s\ local}$ of the local control loop (10us) using the global phase angle θ_{global} provided by EtherCAT every 100us and base grid frequency ω_g:

$$\theta_{local} = \theta_{global} + \omega T_{s\ local}$$ (4.2)

3. Instant PCC voltage values v_{L1}^*, v_{L2}^*, v_{L3}^* for voltage and current harmonics compensation using local phase angle θ_{local}:

$$v_{L1}^* = v_{out}^* * \cos(\theta_{local})$$ (4.3)

$$v_{L2}^* = v_{out}^* * \cos(\theta_{local} - \frac{2\pi}{3})$$ (4.4)

$$v_{L3}^* = v_{out}^* * \cos(\theta_{local} + \frac{2\pi}{3})$$ (4.5)

5. Analysis of simulation and experimental results

In order to prove the benefits and effectiveness of the developed system of parallel connected four-branch DC/AC converters with branch-switching capability between AC phases, the research included a simulation model and experimental validation.

5.1. Research methodology

Simulation tools and a specially designed modular converter system were used to obtain the test results. Computer simulations were conducted using PLECS software from Plexim, which allows for precise modeling of the dynamic behavior of power electronic systems. Additionally, the control system was implemented in C and C++. The developed code, incorporating the proposed control methods, was utilized in both the simulation and the experimental test bench. The structure of the simulation model is shown in Appendix 7.1

Laboratory experiments were performed on a dedicated test bench equipped with specially designed four-branch converters in a T-type topology (**Figure 89**). The distributed control system was implemented on four TMS320F28379D microcontrollers with ESC Beckchoff ET1100 ASIC and a Beckhoff IPC6015 industrial computer. The TwinCAT environment with extensions was used to implement the control, compile the code and manage the system. The Code Composer Studio environment was used to develop and compile software for the microcontrollers. Also debug features enbles to debug all four targets at the same time via USB communication bus using USB Hub. On the AC network side, a programmable network simulator and additional loads were used. On the DC side, a programmable DC power supply was used. Details of the implementation of the experimental position are presented in Appendix 7.2

Due to the large number of transistor branches and the limited physical accessibility of internal circuits within the converter modules, measurement data were acquired using the TwinCAT Scope environment. This tool enables real-time monitoring, collection, and recording of system signals by extracting data directly from EtherCAT communication frames, without the need for additional measurement hardware.

Critical status variables such as the currents and voltages across the LC filter components are transmitted over the EtherCAT network and logged for further analysis. This approach ensures high temporal resolution, synchronization across modules, and minimal signal interference.

A summary of the key system parameters used during the measurement process is provided in the **Table 15**.

Table 15 Summary of system parameters.

Parameter	Symbols	Value	Unit
Grid filter inductance	L_f	200	uH
Grid filter capacitance	C_f	680	nF
Maximum branch current	i_{Bmax}	10	A
PCC voltage	v_{PCC}	70	V_{RMS}
PWM frequency	f_{PWM}	100	kHz
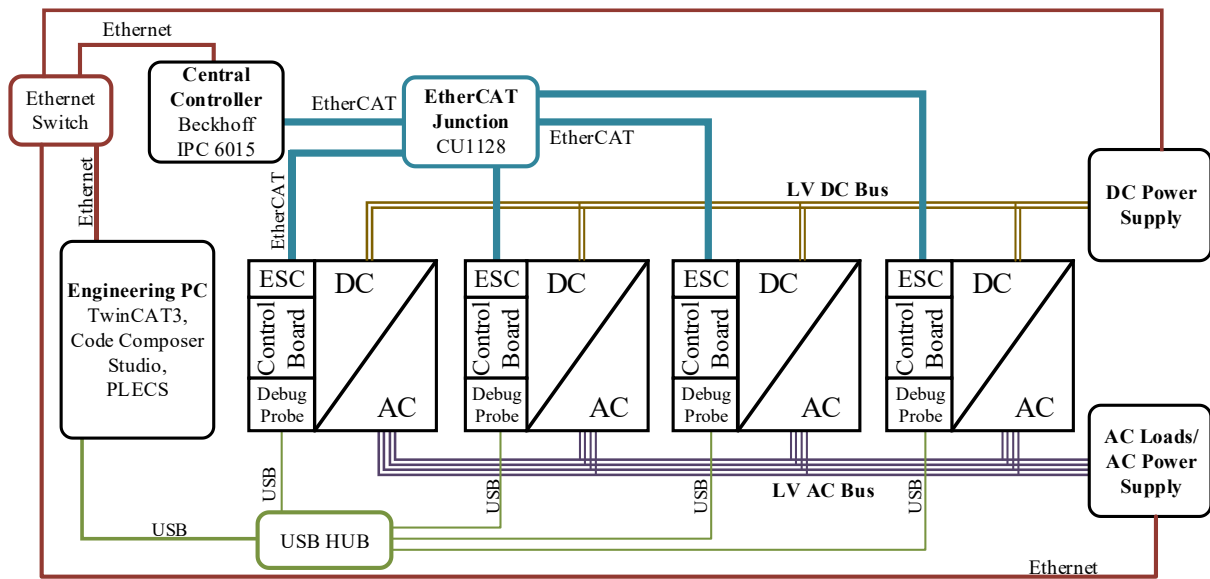
Figure 89. Laboratory setup diagram.

5.2. Aim and scope of research

Due to the complexity of the system and the multitude of AC network operation scenarios, selected test cases were selected to prove stable system operation related to:

- grid-forming and grid-supporting operation,
- activation and deactivation of DC/AC converter modules,
- reconfiguration:
  - resulting from the failure of a particular system component or communication,
  - resulting from matching system performance to load.
- operation with non-linear and asymmetric loads negatively affecting the quality of voltage.

The developed test samples and their analyses do not cover the complex cooperation of the system with the power grid. The tests mainly aim to prove the stable operation of the assumed functionalities in islanding and grid support modes where special attention was paid to:

- maintaining continuity of operation in the event of a fault,
- supply and withdrawal of energy from the grid,
- stable operation of the distributed current and voltage control algorithm,
- synchronisation of PWM signals of parallel connected transistor branches from separate modules.

Based on the above-mentioned scope of research, a series of test scenarios were proposed involving the selection of system configurations and appropriate network and load conditions.

5.3. System startup in grid-forming mode and adapting to load

The first step in system activation is enabling the output voltage. In grid-forming mode, the grid load is initially unknown. To prevent overcurrent in individual branches, all available modules in the system must be activated. Once the current in each network line stabilizes, the system can be reconfigured to balance the load among the DC/AC branches.

All branches follow an identical control structure. The central controller operates in voltage control mode, while individual module controllers function in current control mode. Upon system startup, all modules operate in three-phase mode. Subsequently, if the load is low, some modules are disconnected. If a dominant single-phase load appears in a specific phase, the disconnected modules are reconfigured from three-phase to single-phase mode (**Figure 90**). The relevant system parameters are listed in the **Table 16**.

The final number of active modules depends on the global reference current amplitude. Both the number of active modules and the number of branches are adjusted according to this value. Simulation results (**Figure 91**) and experimental validation (**Figure 92**) show strong consistency.

In the case of a symmetrical three-phase load, the central controller disconnects two modules to improve overall efficiency, while maintaining sufficient reserve capacity for sudden load changes. Thus, the primary objective of maximizing energy conversion efficiency is achieved by dynamically adjusting the number of active modules. For balanced three-phase loads, branches connected to the neutral line remain unloaded.
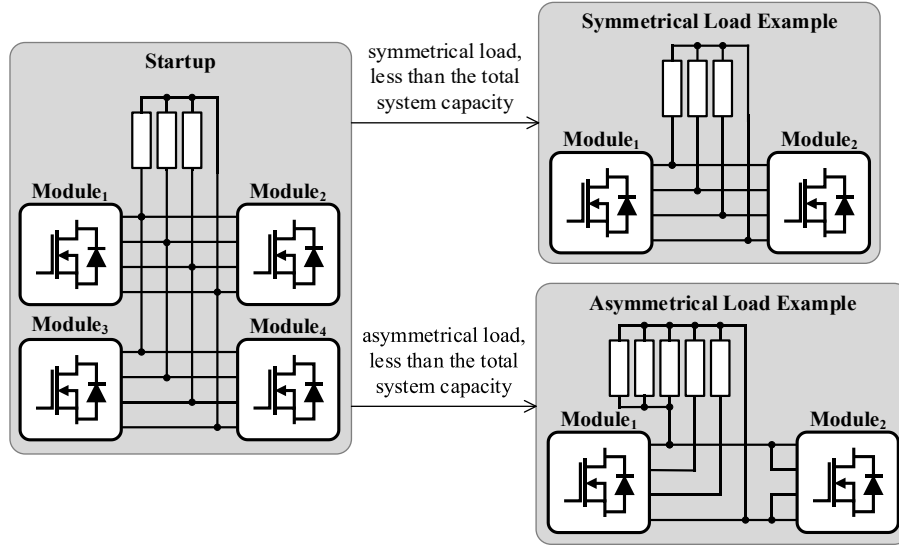
Figure 90. Switching on the system in the grid-forming mode.

Table 16. Startup and system adaptation to load scenario parameters.

State	Parameter	Symbols	Value	Unit
Startup	Number of modules	$n_{DC/AC}$	4	-
	L1 branches	n_{bL1}	4	-
	L2 branches	n_{bL2}	4	-
	L3 branches	n_{bL3}	4	-
	N branches	n_{bN}	4	-
	Symmetric load	R_{L1}, R_{L2}, R_{L3}	6, 6, 6	Ω
	Asymmetric load	R_{L1}, R_{L2}, R_{L3}	4, 12, 12	Ω
After adaptation (symmetric load)	Number of modules	$n_{DC/AC}$	2	-
	L1 branches	n_{bL1}	2	-
	L2 branches	n_{bL2}	2	-
	L3 branches	n_{bL3}	2	-
	N branches	n_{bN}	2	-
After adaptation (asymmetric load)	Number of modules	$n_{DC/AC}$	2	-
	L1 branches	n_{bL1}	3	-
	L2 branches	n_{bL2}	1	-
	L3 branches	n_{bL3}	1	-
	N branches	n_{bN}	3	-

The presented waveforms illustrate the system start-up and the gradual disconnection of modules 2 and 3, indicated by decreasing current and the discharge of capacitor voltage. The currents in modules 1 and 2 increase symmetrically, reaching the optimal values defined by the reference signal and the specified operating range.

It should be noted that the reconfiguration operations proceed smoothly, without overshoots or stability issues. No overvoltages or overcurrents are observed during the transitions, which confirms the correct operation of the proposed method.
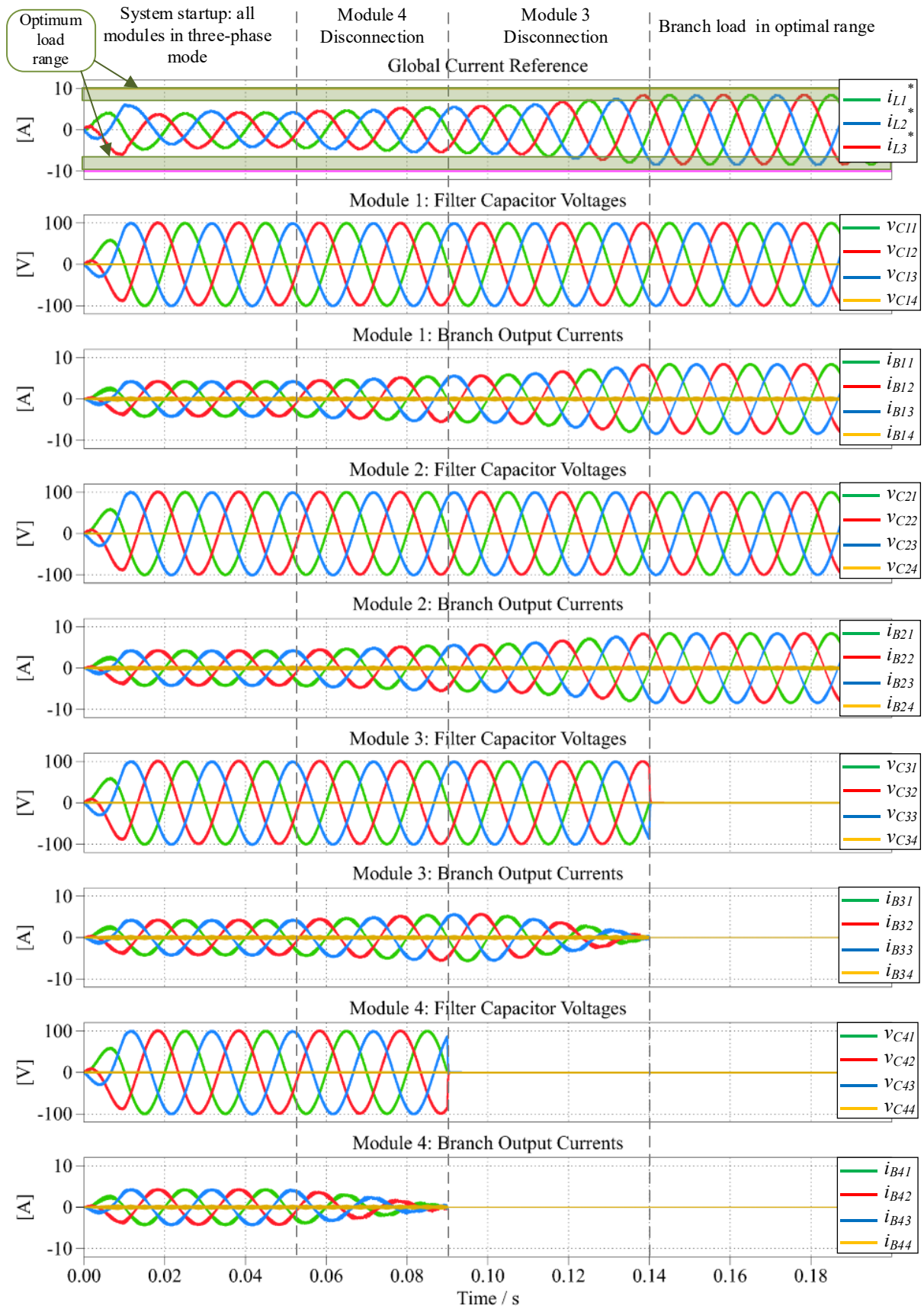
Figure 91. Simulation results of system startup and adaptation to symmetrical load.
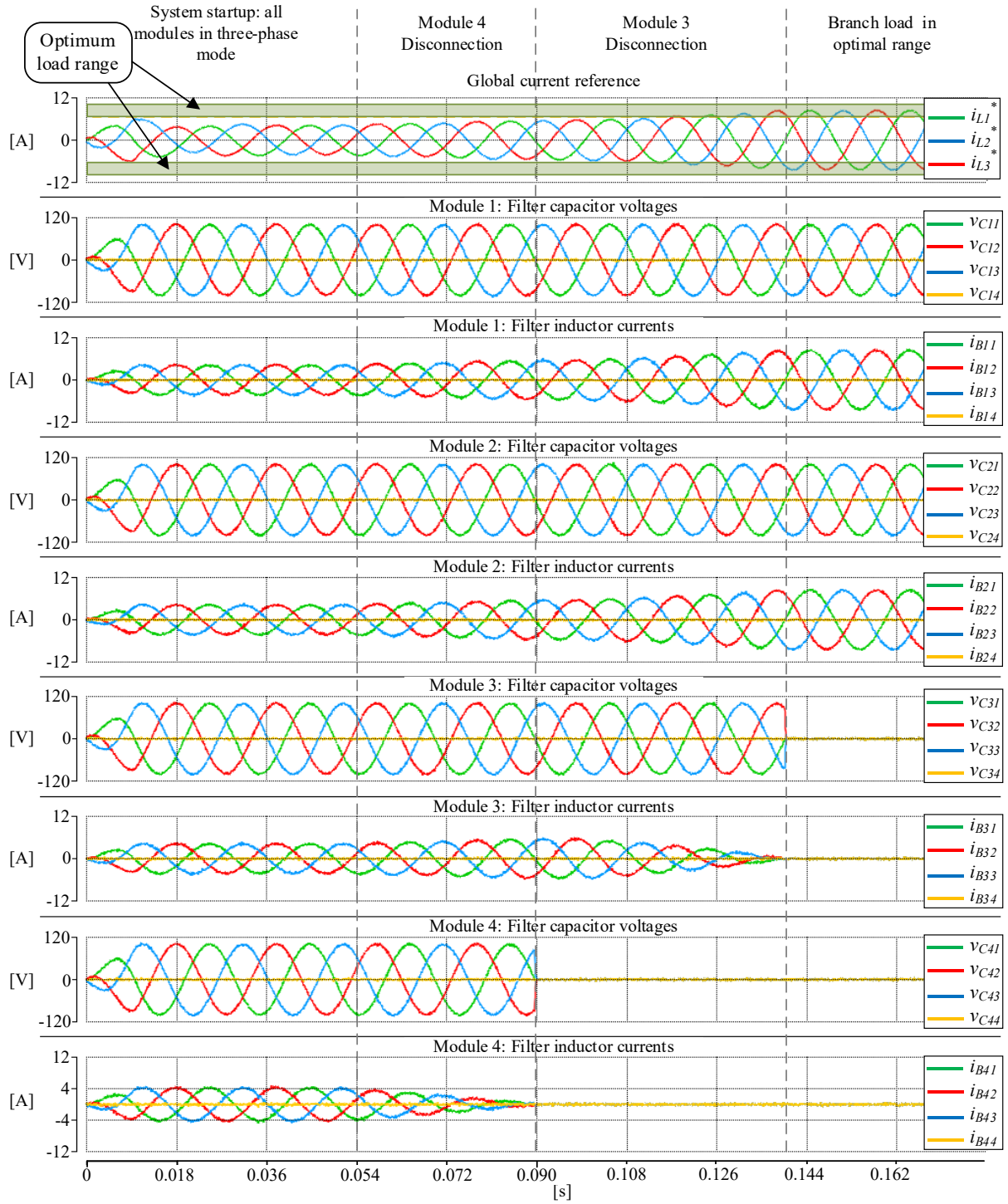
Figure 92. Experimental results of system startup and adaptation to symmetrical load.

When a significant single-phase load is present, the algorithm adjusts both the number of active modules and their connection configuration. In the next variant of the test scenario, all modules are initially activated. Then, module no. 2 is disconnected and reconfigured to single-phase mode, followed by the disconnection of modules 3 and 4. Simulation results (**Figure 93**) are in close agreement with experimental results (**Figure 94**).
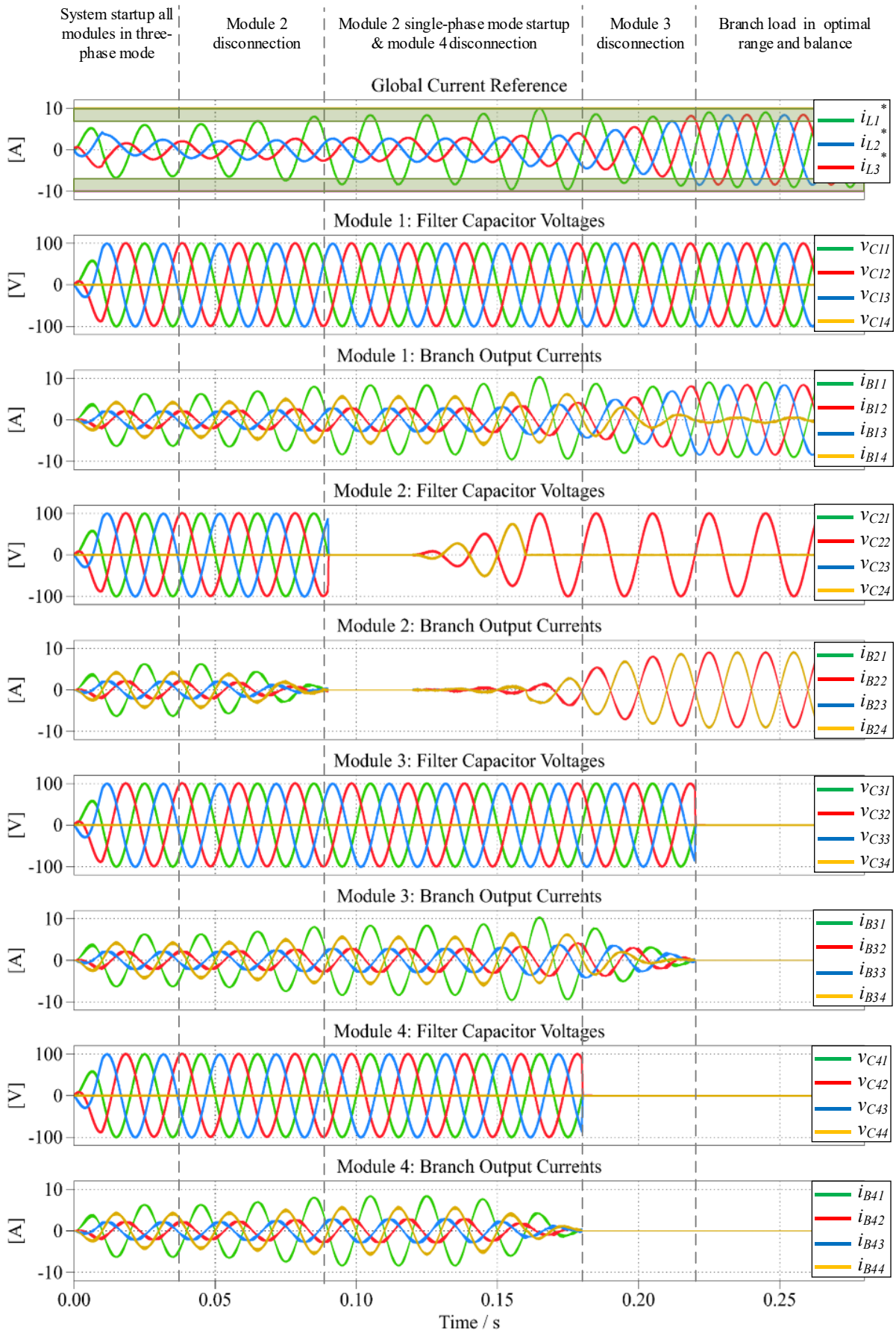
Figure 93. Simulation results of system startup and adaptation to asymmetrical load.
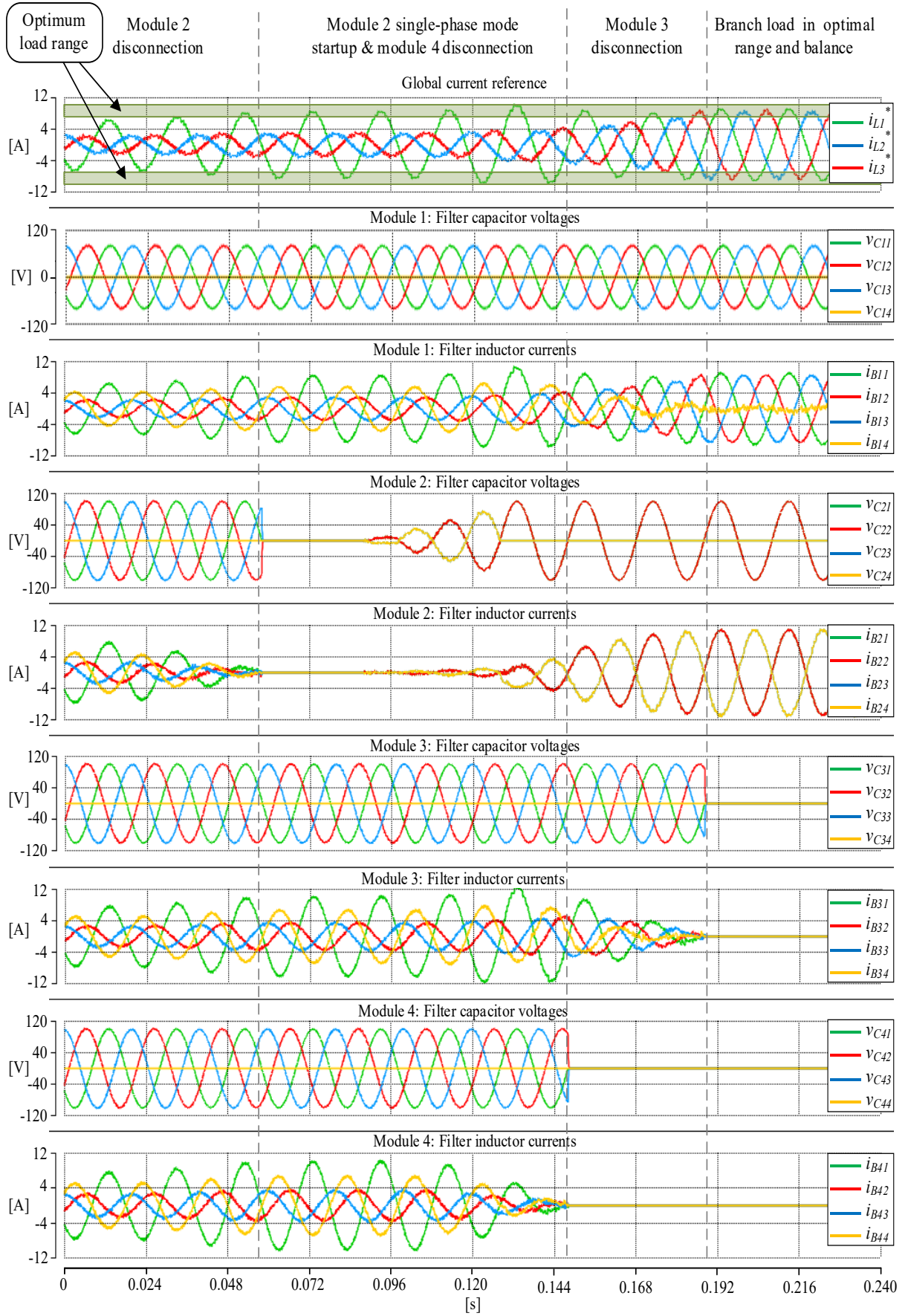
Figure 94. Experimental results of system startup and adaptation to asymmetrical load.

The implemented algorithms for branch selection and the connection/disconnection process function correctly in both three-phase and single-phase configurations. Successful load balancing is evidenced by the equal global reference current observed across all branches at the end of the scenario. Moreover, due to synchronization algorithms for current and voltage during module activation and deactivation, overvoltages, voltage sags, and overcurrents are negligible.

In conclusion, under asymmetric loading conditions, two key objectives are met. First, the load is effectively distributed across active DC/AC branches, with only branches connected to the neutral line of three-phase modules experiencing reduced loading. Second, energy conversion efficiency is maximized by selecting the optimal number of active branches, ensuring operation within their ideal load range.

5.4. System operation in different types of load in the grid-forming mode

The LV grid is characterized by random load variations and the presence of microgeneration sources. In both operating modes: grid-forming and grid-supporting the LV stage of PET system must be capable of independent, bidirectional energy exchange with the grid on each individual line.

To evaluate the performance of the proposed control method in grid-forming mode, a test scenario was designed in which the system is exposed to various load types and additional energy sources (**Figure 95**). Under such conditions, the system is required to maintain a high-quality, symmetrical, and undistorted output voltage across all phases. The key system parameters are summarized in **Table 17**.

The test sequence proceeds as follows:

- State 1: The system is initialized with four active modules.
- State 2: An asymmetric load is applied to a single phase.
- State 3: A nonlinear three-phase load is connected.
- State 4: A current source is introduced into the system.

Throughout this test, no load adaptation is triggered, as the total load remains within the allowable power limit. The goal is to demonstrate that the system maintains stable operation across a broad spectrum of loading conditions, without requiring reconfiguration of modules.

This scenario confirms that the grid-forming control algorithm:

- operates correctly regardless of the load type,
- remains robust in the presence of voltage asymmetries and distortions, and

- effectively manages energy exchange, including drawing excess power from the grid when current sources are active.
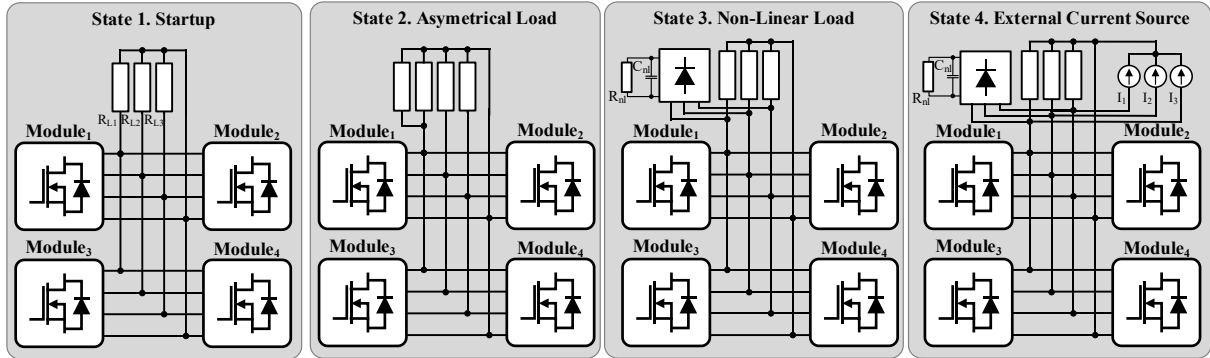
Figure 95. System load sequence states for system operation in grid-forming mode.

Table 17. Startup and system adaptation to load scenario parameters.

State	Parameter	Symbols	Value	Unit
Startup	Number of modules	$n_{DC/AC}$	4	-
	L1 branches	n_{bL1}	4	-
	L2 branches	n_{bL2}	4	-
	L3 branches	n_{bL3}	4	-
	N branches	n_{bN}	4	-
	Symmetric load	R_{L1}, R_{L2}, R_{L3}	6, 6, 6	Ω
Asymetrical load	Asymmetrical load	R_{L1}, R_{L2}, R_{L3}	10, 100, 100	Ω
Non-Linear load	Load capacitance	C_{nl}	100	uF
	Load resistance	R_{nl}	10	Ω
External current source	Injected current	I_1, I_2, I_3	20	A

All modules operate in three-phase mode, and the number of active modules remains undistorted during testing scenario. Both simulation results (**Figure 96**) and experimental measurements (**Figure 97**) validate the correct operation of the control strategy. This is evidenced by the consistently high voltage quality and balanced current sharing among the branches of different DC/AC modules.

In this scenario, particular attention should be paid to the fact that sudden load changes do not lead to any loss of system stability. The shape and quality of the generated grid voltage are consistently maintained, showing no signs of degradation. This demonstrates the robustness of the control algorithm and the converter system's ability to effectively respond to dynamic operating conditions without compromising voltage symmetry or waveform integrity.
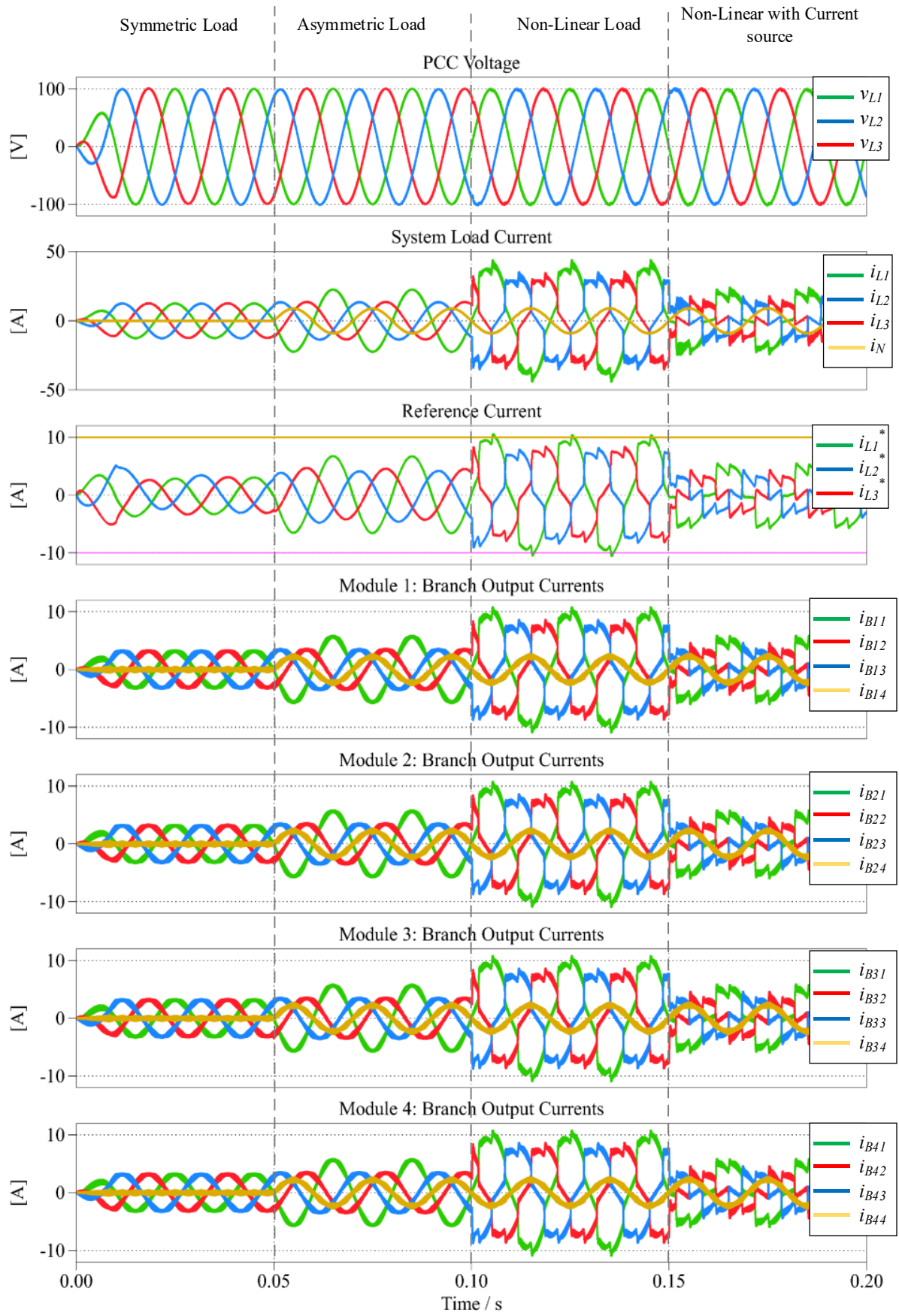
Figure 96. Simulation results for different types of load in the grid-forming mode.
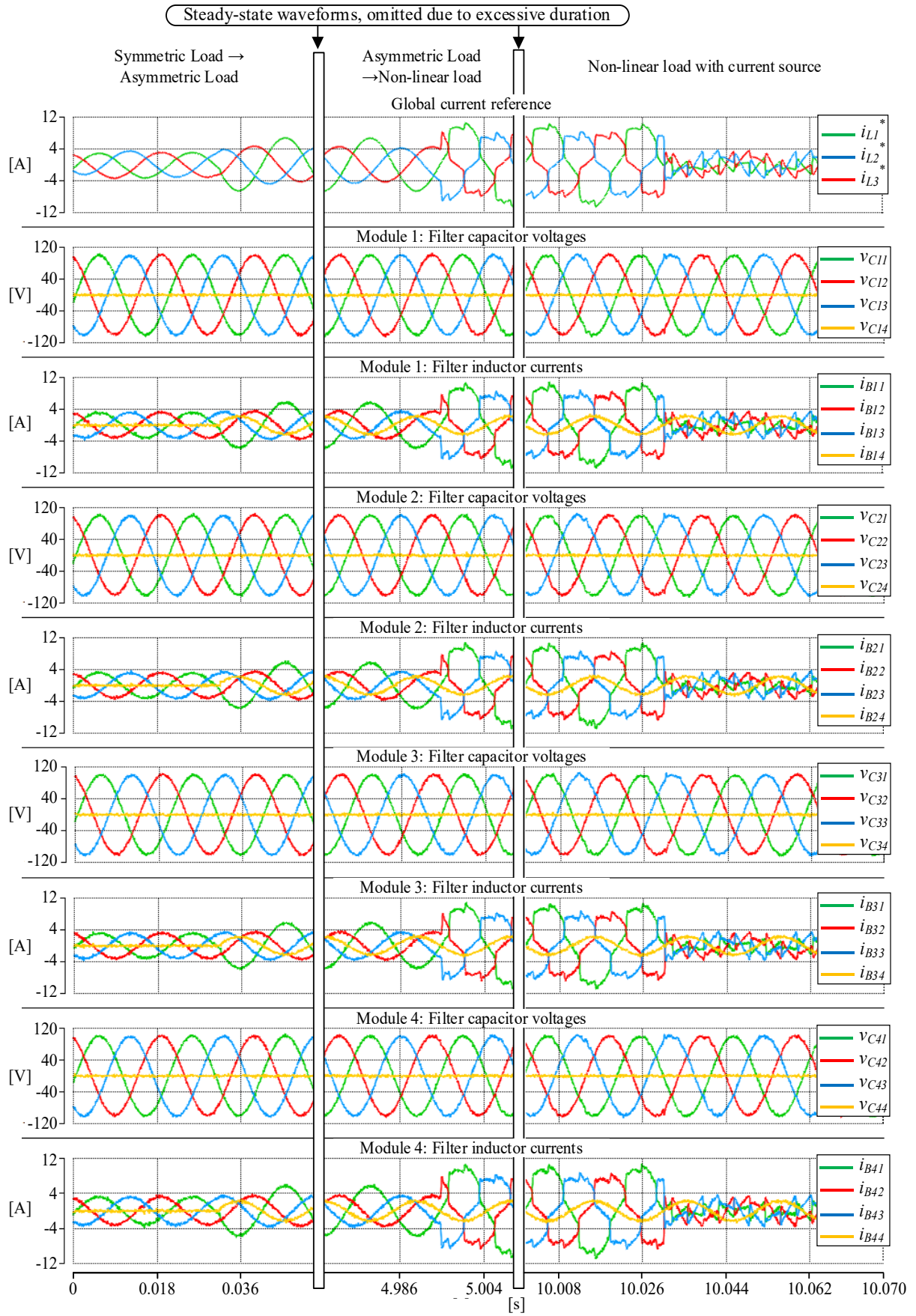
Figure 97. Experimental results for different types of load in the grid-forming mode.

146

5.5. Voltage harmonics compensation in grid-forming mode

Maintaining high voltage quality is critical not only to comply with international standards (e.g., IEC 61000-2-4 for industrial environments) but also to ensure the proper operation and longevity of connected equipment. Devices sensitive to voltage waveform distortion may experience overheating, malfunctions, reduced efficiency, or even premature failure. Therefore, voltage quality becomes especially important in grid-forming systems, which serve as voltage sources for downstream loads.

This scenario is designed to demonstrate the effectiveness of the additional voltage distortion compensation mechanism in grid-forming mode. A strongly nonlinear load is connected to the system (**Figure 98**), resulting in visible voltage distortion at the PCC, as shown in **Figure 99**.
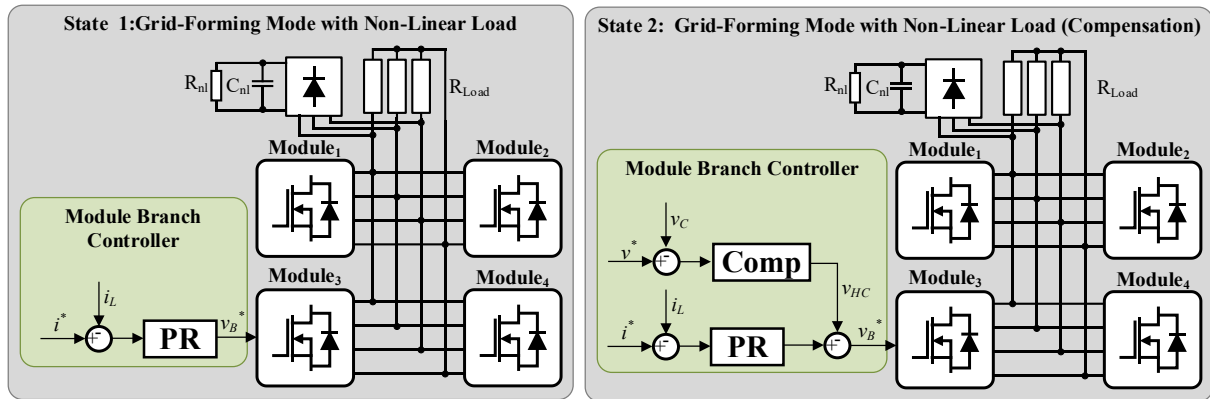
Figure 98. Voltage harmonics compensation influence on distorted system output current in the grid-forming mode.

Table 18. Voltage harmonics compensation scenario parameters.

Parameter	Symbols	Value	Unit
Compensation gaint	K_{HC}	1	-
Non-linear load capacitance	C_{nl}	1	mF
Non-linear resistance	R_{nl}	15	Ω
Load resistance	R_{Load}	100	Ω
PCC voltage	v_{PCC}	70	V_{RMS}
PWM frequency	F_{PWM}	100	kHz

The distorted voltage across the output filter capacitor, caused by the pulsed current drawn by the load, must be compensated by the converter to maintain a stable and high-quality output voltage. Activating the compensation system stabilizes the voltage response and leads

to a significant improvement in output voltage quality. These improvements are clearly visible in both the time-domain waveforms and the FFT analysis diagrams.

Since the proposed harmonic voltage compensation method directly transfers disturbances from the capacitor voltage to the converter's output, the use of high-precision voltage sensors is essential. Any additional noise or measurement inaccuracies can negatively impact the quality of the output voltage. To mitigate this, low-pass filtering is required to suppress high-frequency noise components and ensure signal integrity.

The proposed solution is based on the assumption of a stiff DC-link voltage, a relatively high switching frequency, and low filter inductance. Under these conditions, even strong current distortions have a minimal effect on voltage quality, as the control system is capable of actively maintaining a clean and stable output voltage despite dynamic load variations.
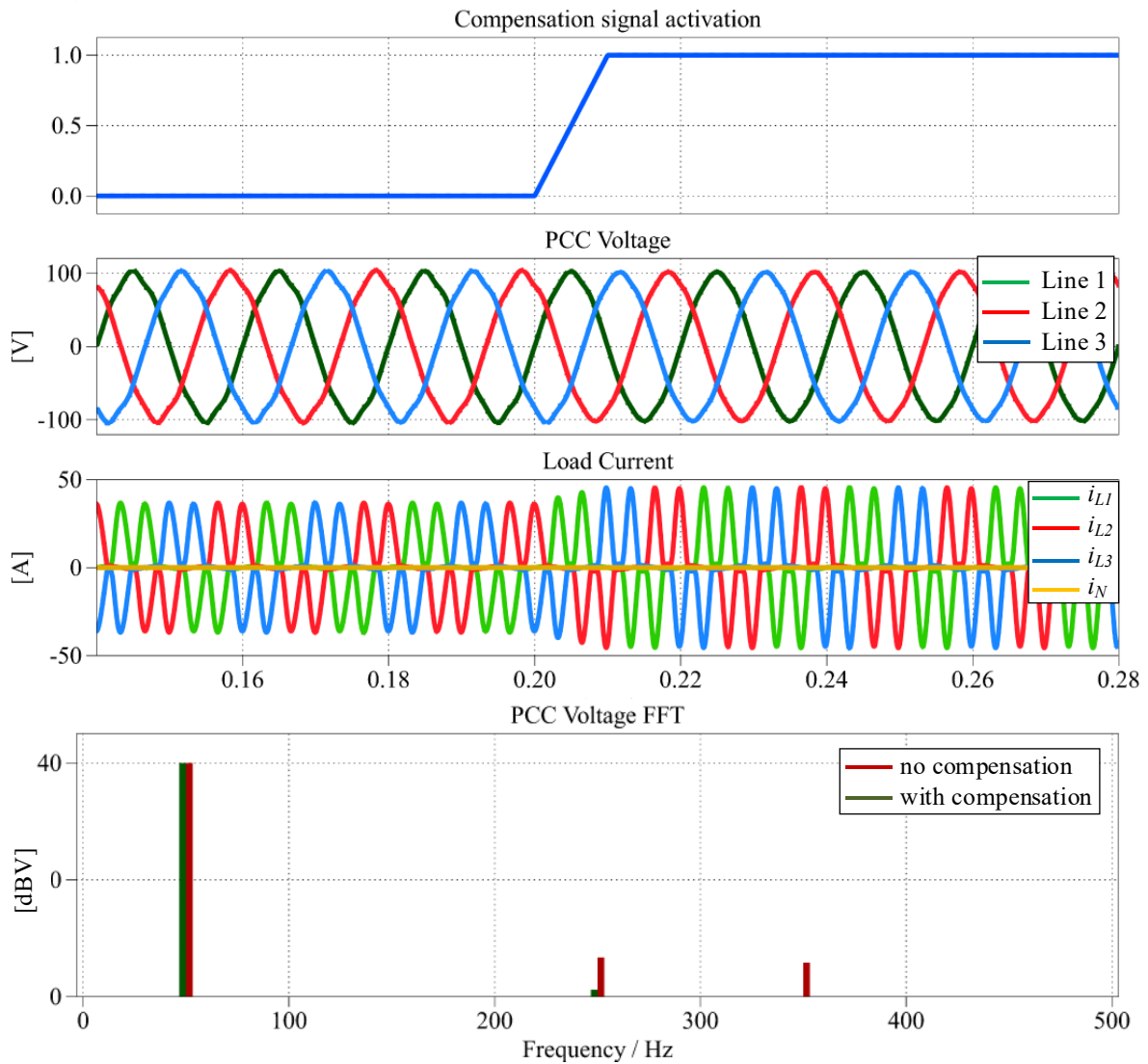
Figure 99. Simulation results of voltage harmonics compensation in grid-forming mode.

5.6.   Current harmonics compensation in the grid-supporting mode

The grid-supporting mode is characterized as a current source and its main task is to supply a given current value, which maintains its parameters regardless of the quality of the grid voltage. The scenario proving the effectiveness of the current disturbance compensation algorithm assumes the connection of a series voltage sources containing the 3rd, 5th and 7th harmonics (**Figure 100**). Initially, the system operates without the current disturbance compensation algorithm enabled. Then the compensation signal gain gradually increases. After reaching the target value, a significant improvement in the current quality can be seen. The effects of the algorithm have been confirmed on simulation (**Figure 101**) and experimental results (**Figure 102**). Parameters for this scenario are listed in the **Table 19**.
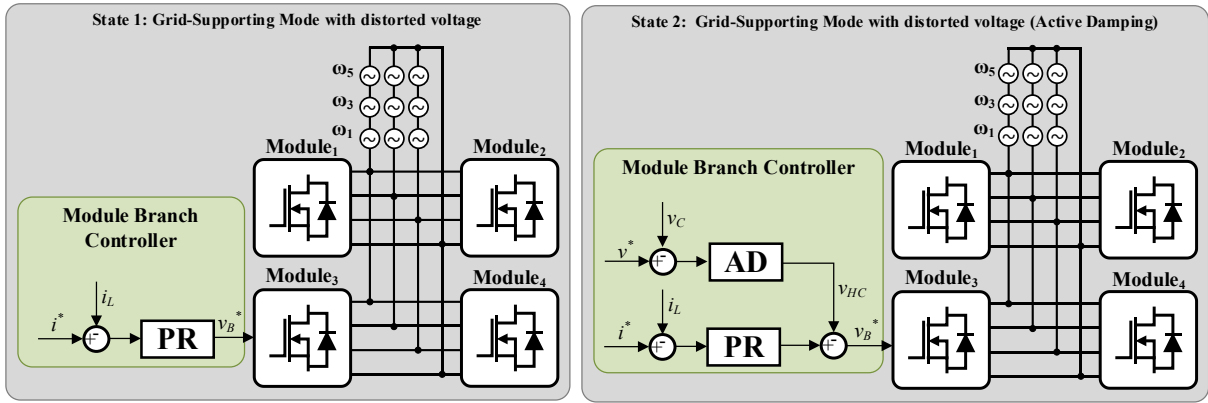
Figure 100. Current harmonics compensation under distorted grid voltage in grid-supporting mode.

The results clearly demonstrate the performance advantages of the proposed compensation method. The system also exhibits a high degree of stability throughout operation. The primary requirement for effective implementation is the accurate measurement of voltage, as any additional disturbances in the voltage signal will be directly transferred to the converter's output.

The proposed method also allows for the injection of selected current harmonics into the grid, provided that the corresponding harmonic component is appropriately filtered from the capacitor voltage signal. In the scenario presented, only the fundamental harmonic is extracted for compensation purposes.

Overall, the test confirms the robustness, accuracy, and adaptability of the control algorithm, making it a reliable and effective solution for improving power quality in distributed energy systems operating in grid-supporting mode.

Table 19. System parameters for current harmonics compensation.

Parameter	Symbols	Value	Unit
Compensation gain	K_{HC}	1	-
Voltage harmonics frequency	$\omega_3, \omega_5, \omega_7$	150, 250, 350	Hz
Voltage harmonics amplitude	A_1, A_5, A_7	20, 15, 10	V
PCC voltage	v_{PCC}	70	V_{RMS}
PWM frequency	F_{PWM}	100	kHz
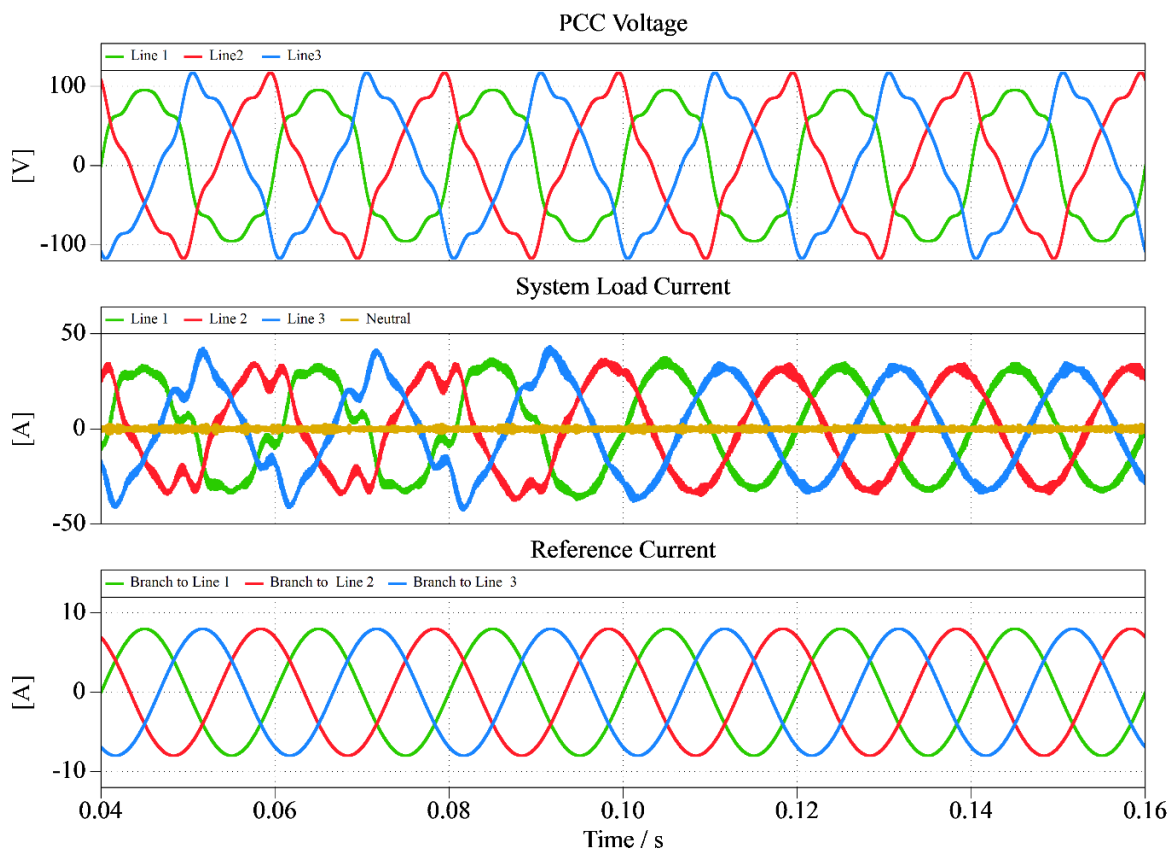
Figure 101. Simulation results of current harmonics compensation under distorted grid voltage.
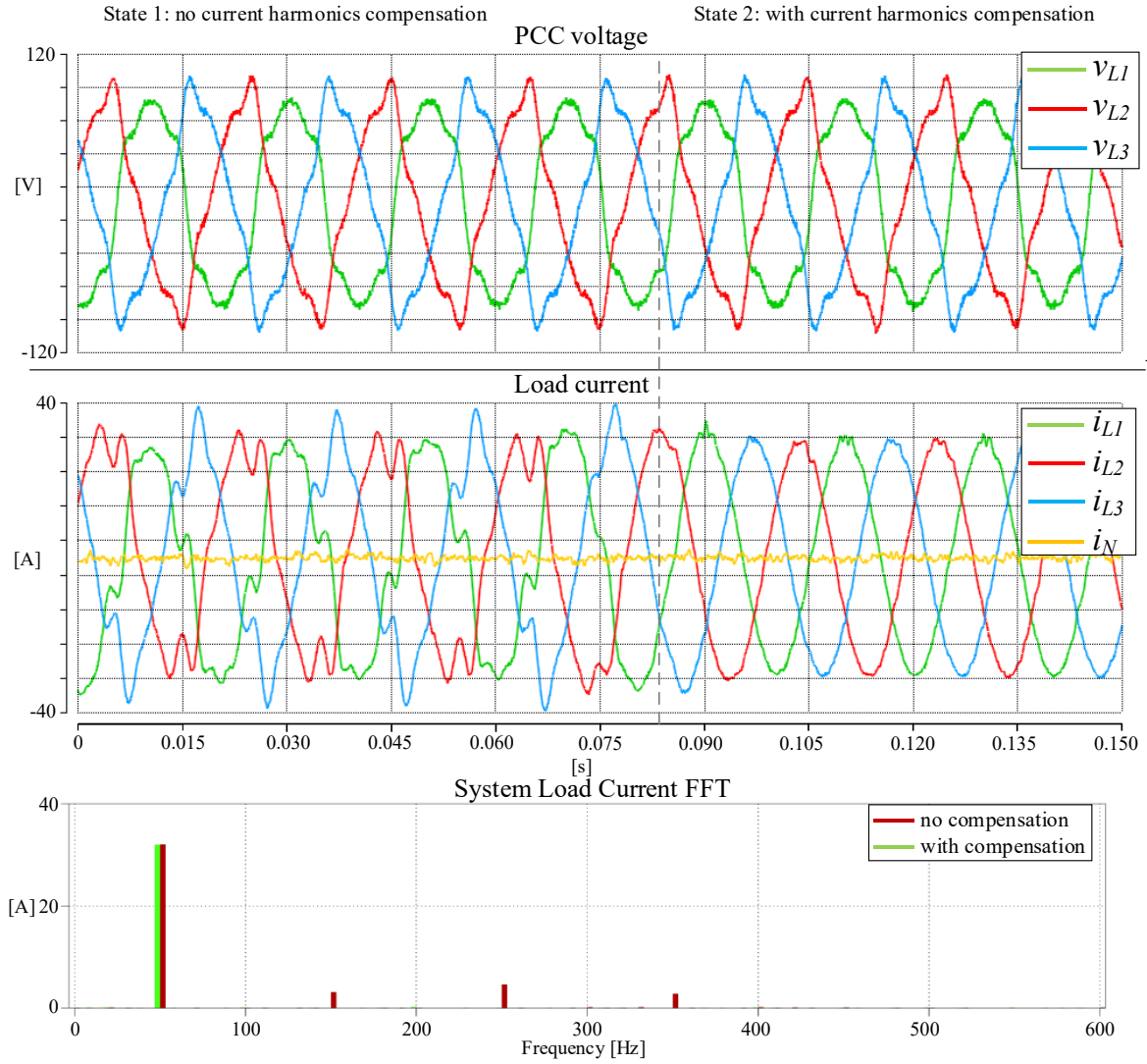
Figure 102. Experimental results of current harmonics compensation under distorted grid voltage in grid-supporting mode.

5.7. Module disconnection after communication loss

A loss of communication between the central controller and a DC/AC module results in the inability to control that module, as it no longer receives current and voltage reference values. Consequently, any module experiencing communication failure must be immediately disconnected from the grid, and a spare module should be activated to take its place.

This communication loss scenario was verified experimentally. Initially, three DC/AC modules were operational when the EtherCAT junction cable was intentionally disconnected (**Figure 103**). Upon detecting the communication fault, the affected module automatically disconnected itself from the network. In response, the central controller activated the next available standby module.

Experimental results (**Figure 104**) show that, following the communication loss, the current and voltage outputs of Module 3 dropped to zero, as no data from the module reached the central controller. Module 3 was promptly disconnected from the grid, causing a temporary increase in branch currents in the remaining modules. Shortly thereafter, Module 4 initiated synchronization with the grid and was activated, effectively restoring system functionality to its state prior to the disconnection.

Importantly, the step change in load did not result in a significant voltage dip, demonstrating the rapid response of the control system. The total recovery time following the communication loss was measured at 130 ms, confirming the effectiveness of the implemented control strategy in handling communication failures.
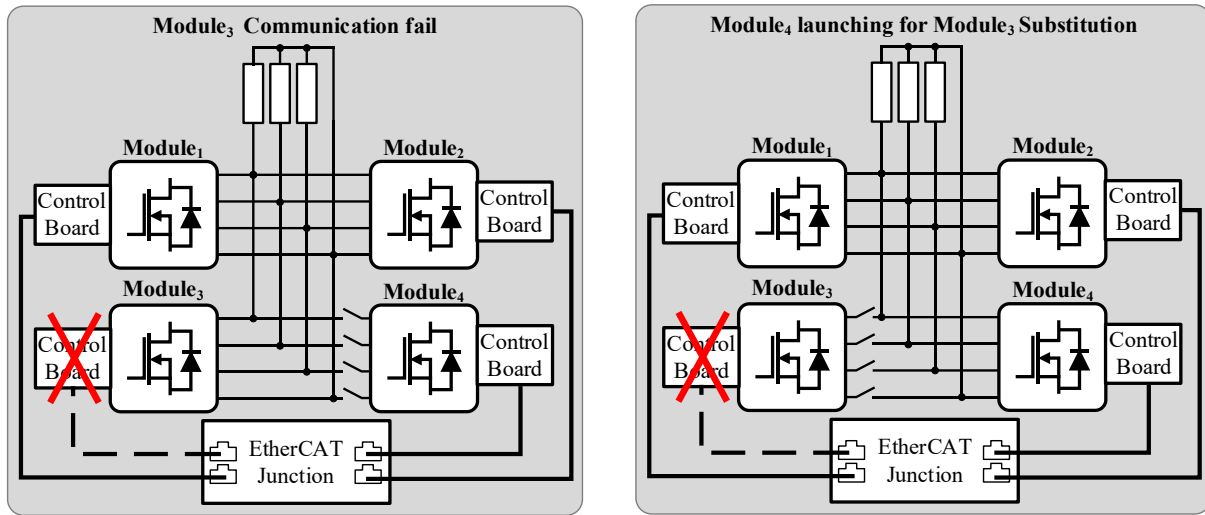
Figure 103. DC/AC module communication loss experiment scenario.

The experimental validation confirms that the proposed control strategy provides reliable system operation even in the event of a communication failure with a DC/AC module. Upon detecting the loss of communication, the system automatically isolates the affected module and initiates the seamless activation of a standby replacement unit. This transition occurs without interrupting the energy conversion process and does not require manual intervention.

The short recovery time, combined with the absence of significant voltage disturbances during the switchover, highlights the robustness and fault-tolerance of the distributed control architecture. These results demonstrate the system's ability to maintain operational continuity under real-time communication failure conditions, validating its suitability for applications requiring high reliability and availability.
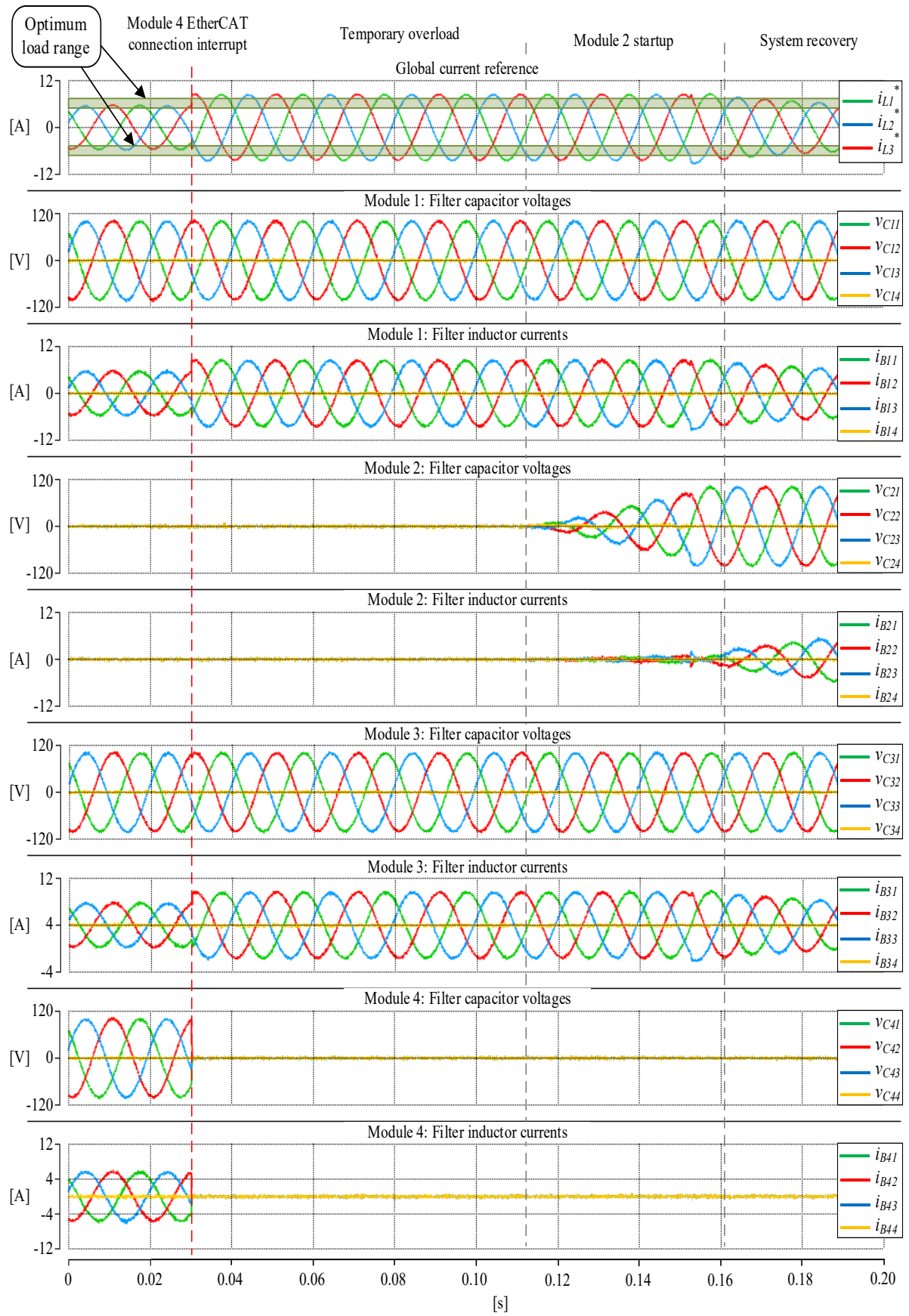
Figure 104. Experimental results of module communication fault with the central controller.

153

5.8. Component failure and post-fault-operation

One of the main assumptions about the system under development concerned the failure of semiconductor components. Despite the occurrence of a fault, the system must maintain continuous operation. The experiment presented in this section assumes a scenario in which one transistor in a branch is short-circuited (**Figure 105**). The gate driver detects the fault and the module is immediately disconnected. The central controller then switches on the spare module to maintain system parameters.
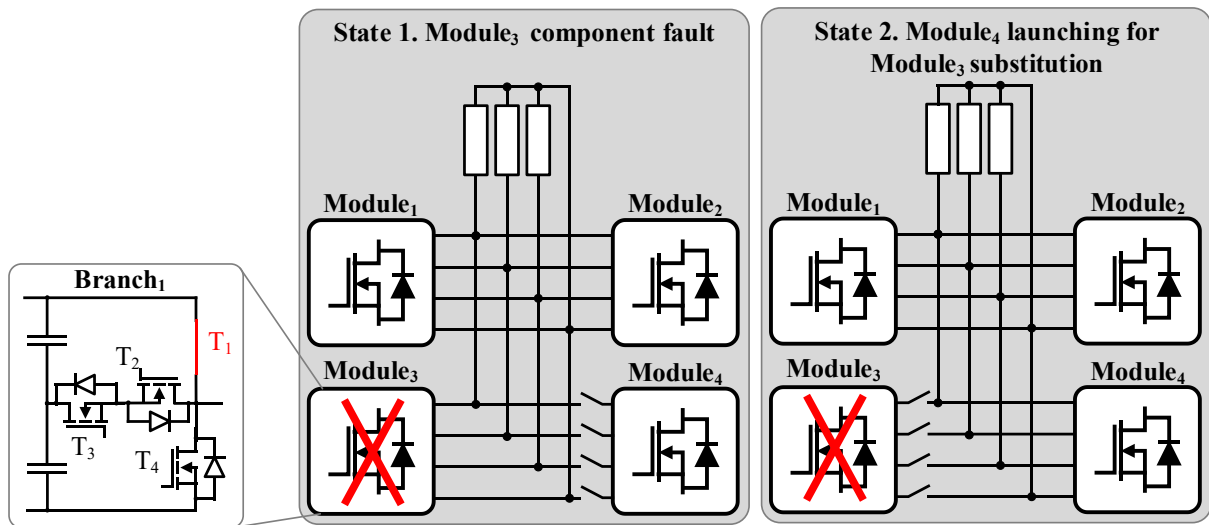
Figure 105. System reconfiguration after transistor short-circuit.

The experimental scenario assumes the operation of three modules in three-phase mode. During normal system operation, a transistor short circuit is forced in one DC/AC module branch. Thanks to the protections in the transistor gate controller, a fault is detected and a signal is sent to the module controller. The control algorithm immediately disconnects the entire module. Then the central system controller receives information about the module disconnection and decides to connect the spare DC/AC module, restoring the previous system efficiency.

The experimental results (**Figure 106**) confirm the correctness of the algorithm and the appropriate response of the entire system to the occurrence of a component failure. The system did not stop working thanks to the greater number of active branches for each network line. It was only overloaded for a certain moment until the next efficient module was switched on. It should also be noted that the impulse disturbance of currents and voltages as a result of a transistor short circuit did not lead to a loss of stability in the control system.
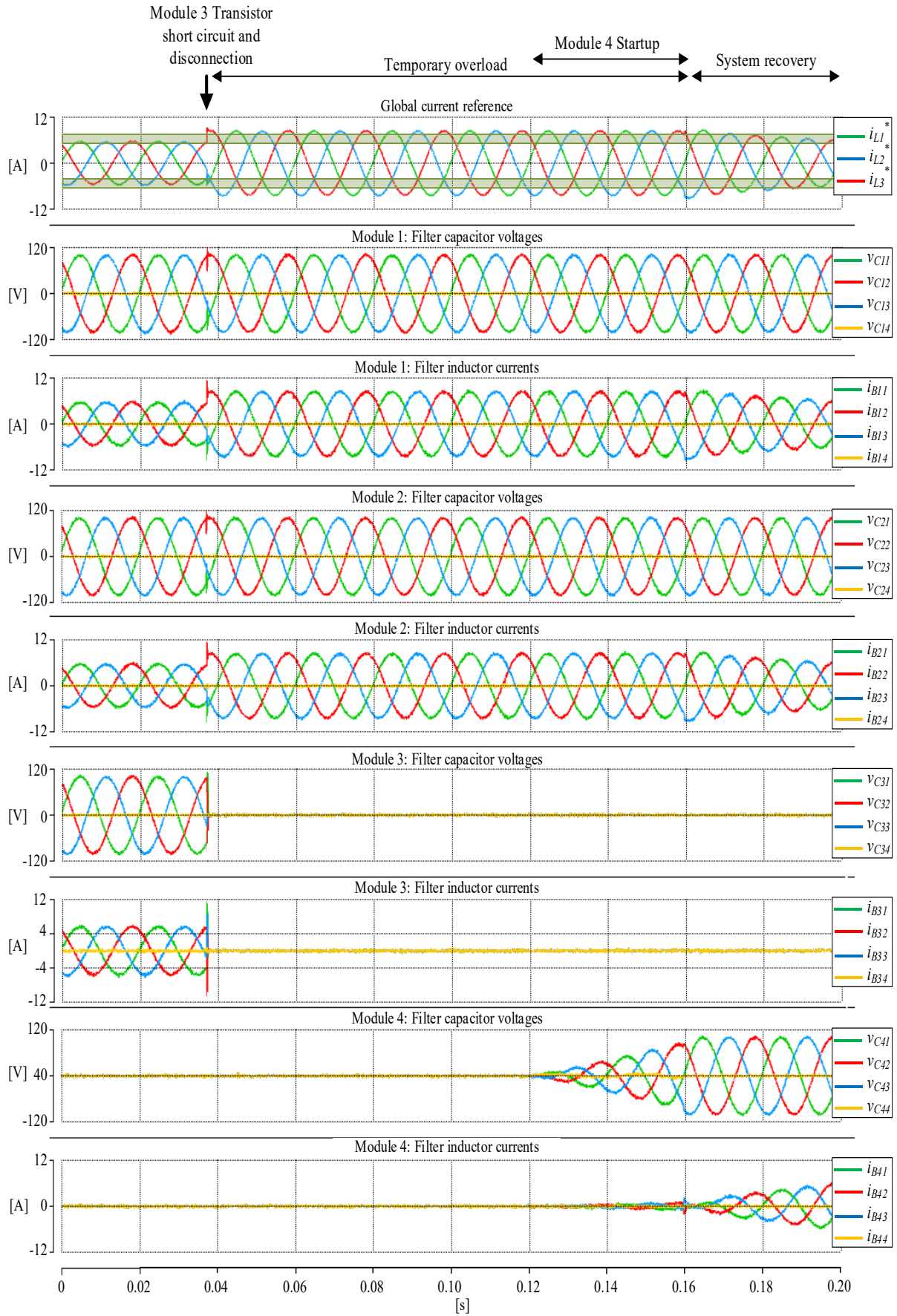
Figure 106. Experimental results of system reconfiguration after transistor short-circuit.

6. Summary

To effectively implement Power Electronics Transformer (PET) technology within the electrical distribution network, ensuring its reliability is essential, particularly in comparison to conventional power transformers (CPT). Given the critical nature of the electrical grid, which necessitates an uninterrupted energy supply, the inherent complexity of power electronics transformer equipment often leads to lower reliability. The failure of a single component in such systems can jeopardize the entire power converter, resulting in potential energy supply interruptions for consumers.

Recognizing this risk, it is crucial to anticipate possible faults and select an appropriate topology for a modular DC/AC converter system that incorporates distributed control and communication. This modular system can autonomously reconfigure to mitigate the impact of faults, ensuring continued operation while accommodating varying load demands. Such a design promotes processing continuity during service actions, allowing for the replacement of converters without requiring a complete system shutdown.

This dissertation successfully addresses these objectives through various proprietary solutions, including:

- **Configuration Development**: A system of parallel-connected four-branch DC/AC converters was developed, accompanied by a real-time EtherCAT communication interface.

- **Distributed Control System**: The dissertation presents a distributed control system operational in two modes: grid-forming, which compensates for voltage distortions caused by non-linear loads, and grid-supporting, which enables stable current regulation under distorted voltage conditions.

- **Branch Switching Capability**: The ability to switch DC/AC converter branches between AC lines was established. This innovation includes a developed switching algorithm that adapts the number of modules and branches according to load requirements, facilitating the isolation of faulty converter paths and their replacement with backup paths. Additionally, this reconfiguration allows the DC/AC converters to operate in three-phase or single-phase modes, promoting balanced load distribution on converter components and extending their operational lifespan.

- **Real-Time Communication**: The implementation of distributed control using the EtherCAT interface allows for a data exchange frequency of up to 20 kHz. The

necessary process variables for the proposed control system are specified, including reference and feedback values tracked by the central controller and the DC/AC converter controllers.

The thesis demonstrates that the developed system of parallel-connected DC/AC converters, when applied to the low-voltage stage of the PET, can operate successfully under post-fault conditions. **The author identifies several key achievements and contributions to the advancement of technology for modular grid-connected converter systems:**

- development of a modular configuration for a grid-forming converter system capable of emergency operation.

- creation of a distributed control method applicable to both grid-forming and grid-supporting modes.

- establishment of compensation methods for:
  - voltage disturbances caused by non-linear currents in grid-forming mode,
  - current disturbances resulting from distorted voltages in grid-supporting mode.

- design of a reconfiguration method for connecting four-branch converters to a four-wire low-voltage power grid, featuring:
  - additional contactors to facilitate branch switching to selected grid lines,
  - a dedicated control algorithm that manages this reconfiguration.

- development of a communication model for the distributed control system of parallel-connected DC/AC converters based on the EtherCAT interface.

Thesis statement: **"The use of multiple parallel-connected DC/AC converters with a distributed control algorithm allows reliable and fault tolerant operation of the low voltage stage of Power Electronics Transformer in grid forming and grid supporting modes"** was proven**.** The findings confirm this assertion, augmented by innovative solutions for the reconfiguration of parallel DC/AC grid connected converter systems.

Despite the advancements made, the complexity of the system analyzed means that not all issues were exhaustively examined. The author plans to continue with future research efforts that will include:

- investigating how the dynamics of the controller are affected by changes in system output impedance due to the switching of branches to specific phases,

- verifying the system's performance under real power grid operating conditions,

- exploring the limitations of the system's scalability regarding operational stability and real-time communication.

- analyzing the system's reconfiguration capabilities in response to highly variable load conditions.

The tests conducted in laboratory settings have not encompassed every conceivable scenario of distribution grid operation but indicate that the integration of PET technology into the distribution grid is feasible in the near future. Improved reliability is achievable owing to the modular structure and its reconfiguration capabilities.

In conclusion, this dissertation not only highlights the potential of PET technology to enhance electrical distribution grids but also lays a solid foundation for its practical implementation. By developing a modular, fault-tolerant DC/AC converter system equipped with advanced distributed control strategies, the research addresses critical challenges faced in traditional transformer systems, such as reliability and operational disruptions. The innovative methods and configurations introduced herein provide a pathway toward more resilient and efficient energy distribution solutions.

Furthermore, the findings emphasize the significance of robust communication protocols and real-time data exchange in ensuring system efficiency and responsiveness. As the energy landscape continues to evolve with increasing demand for sustainable and reliable solutions, the contributions of this research are poised to play a vital role in shaping the future of electrical distribution grids. The ability to operate under fault conditions while maintaining service continuity presents a significant advancement that can influence the design and deployment of next-generation power electronic systems.

Ultimately, the ongoing exploration of the outlined future research directions will not only enhance our understanding of modular converter systems but also foster further innovations in the realm of power electronics, paving the way for a more robust and adaptable electrical grid.

7. Appendix

7.1. Simulation Model

The simulation model was executed in the PLECS environment, while the distributed control system was implemented in C++ using the Visual Studio environment. The control design consisted of two projects compiled into a DLL: a central module controller and a DC/AC converter controller, which was duplicated based on the number of modules (**Figure 107**).

Given the system's complex structure, the model was divided into sub-modules while preserving its overall architecture, consisting of a central module, four DC/AC modules, and a low-voltage grids.
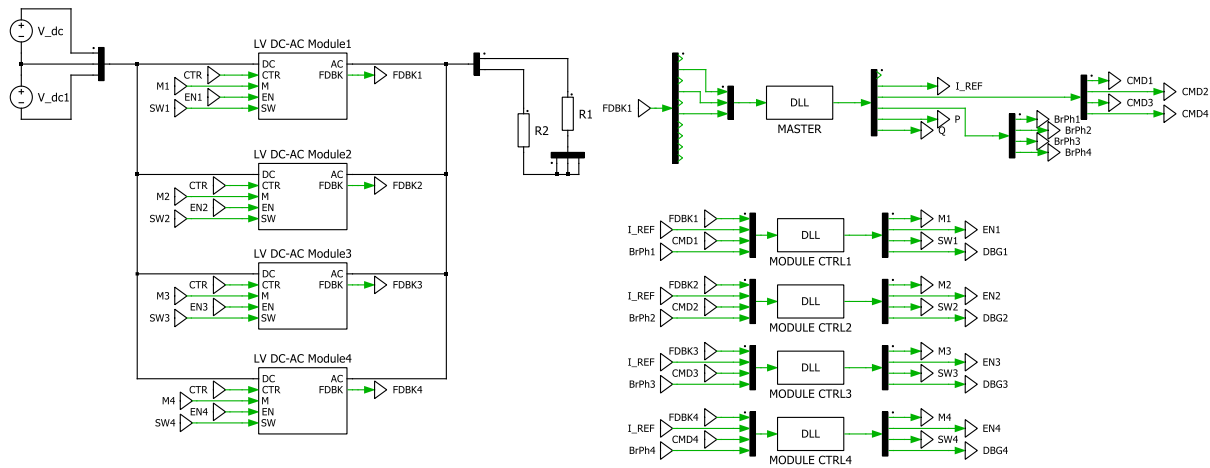
Figure 107. Simulation model diagram of LV stage of PET with four DC/AC converters.

The DC/AC converter sub-module consists of four branches and a matrix of switches between phases of the AC grid (**Figure 108**). Derived from each module are 4 current and 4 voltage signals measured on each branch connected LC filter. The modulation factor, the branch enable signal, and the switch control signal are present as control signals for each branch.

The simulation model includes simplifications related to the communication system between the central control unit and the DC/AC modules. Process variables are extracted and transmitted as "double" data types, as this is the only data type supported for transfer in the PLECS environment.
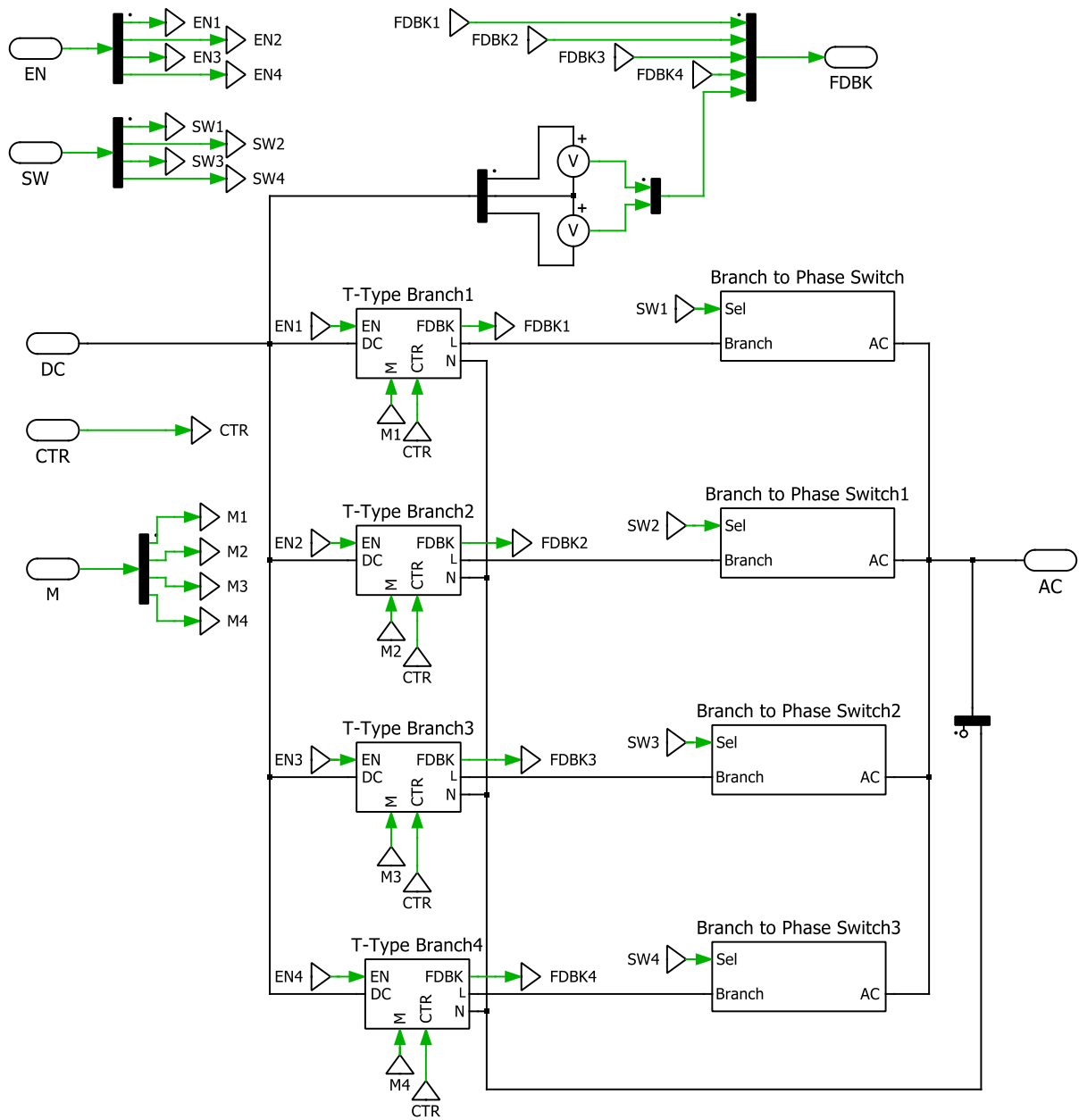
Figure 108. Simulation model diagram of DC/AC four branch converter subsystem.

The branch model consists of a PWM modulator and MOSFET transistors in a three-level T-type topology together with an LC filter (**Figure 109**). Between the branches and switches there is a matrix of switches, enabling the connection of the branch to the selected grid line (**Figure 110**).
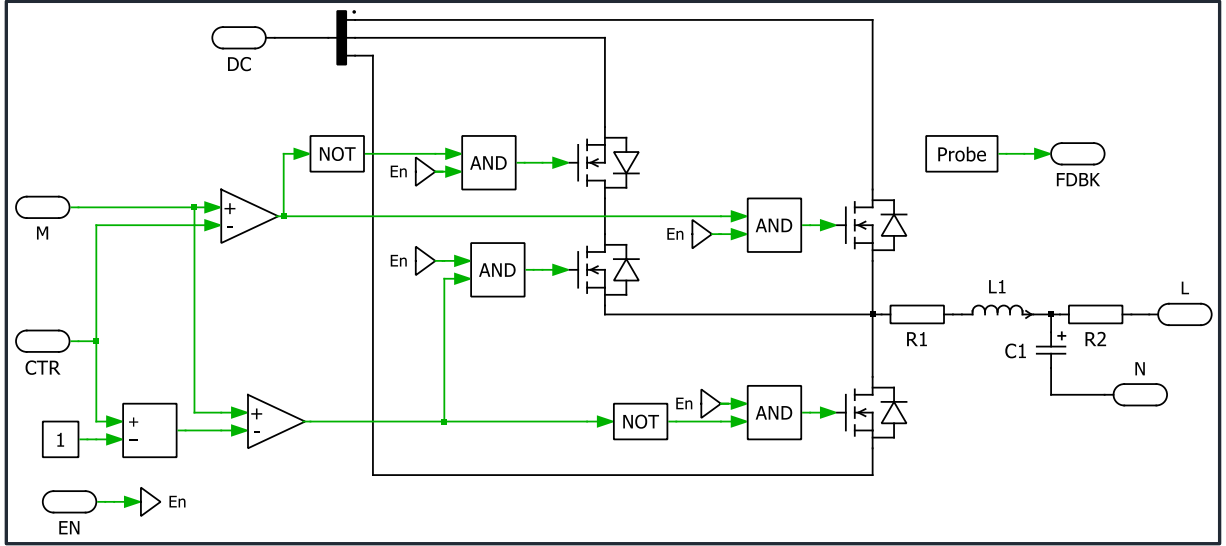
Figure 109. Simulation model diagram of T-Type DC/AC branch with LC filter.
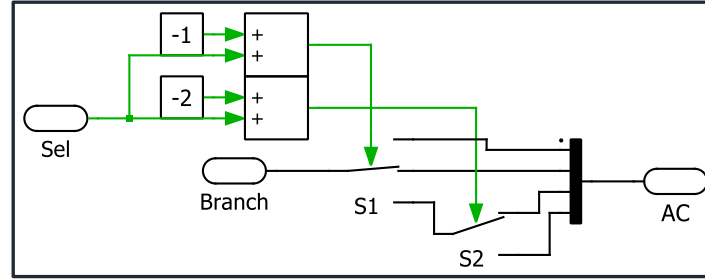
Figure 110. Switch array sub-system diagram.

7.2.   Laboratory setup

A laboratory test bench was constructed to experimentally verify the proposed topology and control system solutions. The experimental setup comprises the following components: four parallel-connected four-branch DC/AC modules, an industrial computer serving as the central control unit (**Figure 111**) , a grid simulator, a DC power supply, power consumers, and a computer for managing the setup and circuit programming.

The following sections provide a detailed description of each component. The solutions presented in this thesis were developed as part of a larger project titled *"Highly Efficient and Fault-Tolerant SiC-Based Smart Transformer in Distributed Energy Systems."* In this project, the LV DC grid voltage was set at 250V, while the LV AC three-phase grid was designed for 120V RMS (line-to-line). As a result, the parameters presented in this thesis are lower than those used in real laboratory tests.
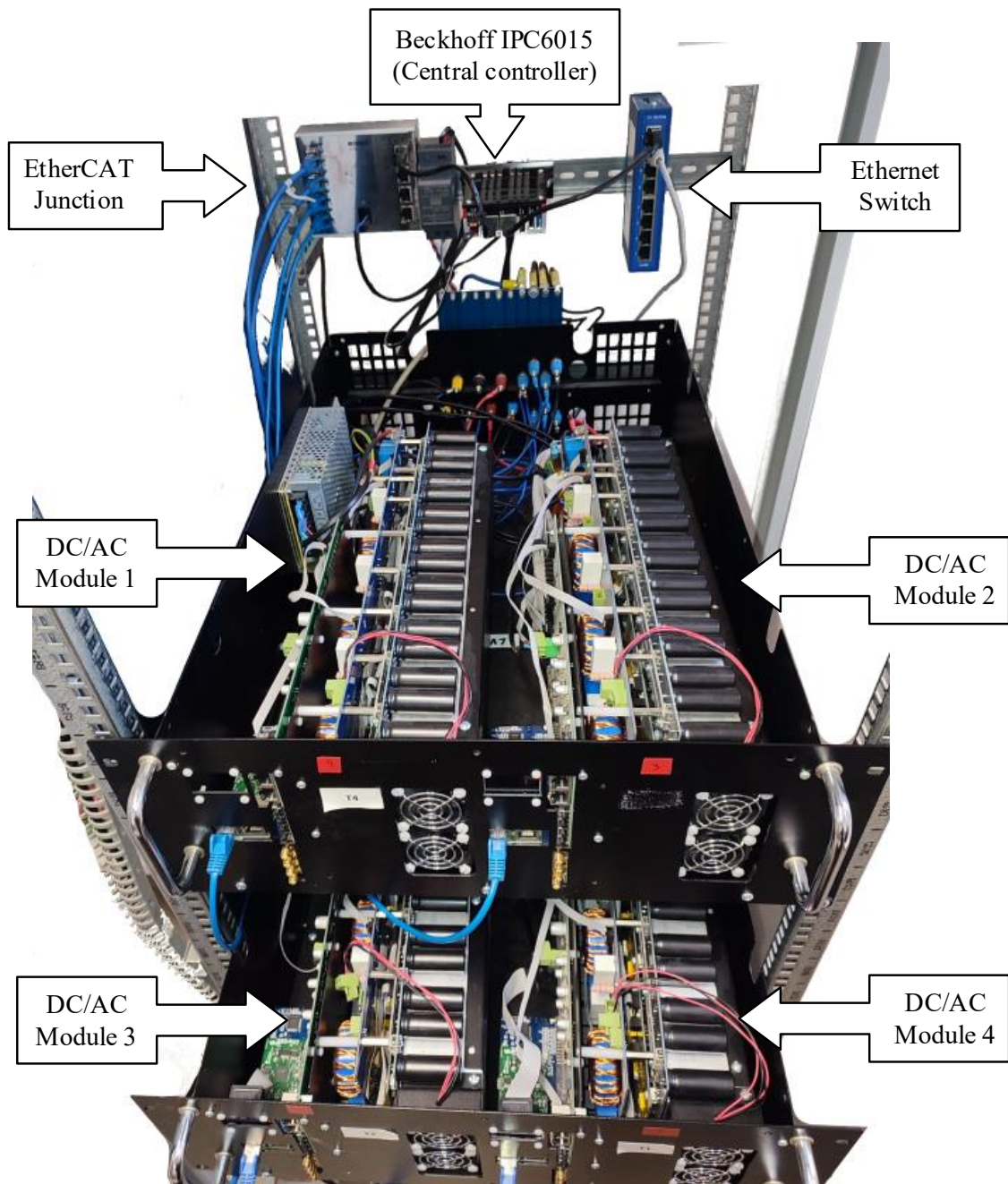
Figure 111. Laboratory setup.

7.2.1. Four branch DC/AC modules

The proposed solutions require a dedicated DC/AC converter design that meets the design assumptions from the analyses and simulations. Each DC/AC module is identical in design and consists of four main components (**Figure 112** and **Figure 113**):

- control board,
- analog signal conditioning board,

- current and voltage measurement board and contactors configuring the connection to the AC grid,
- and power board with a DC Link.
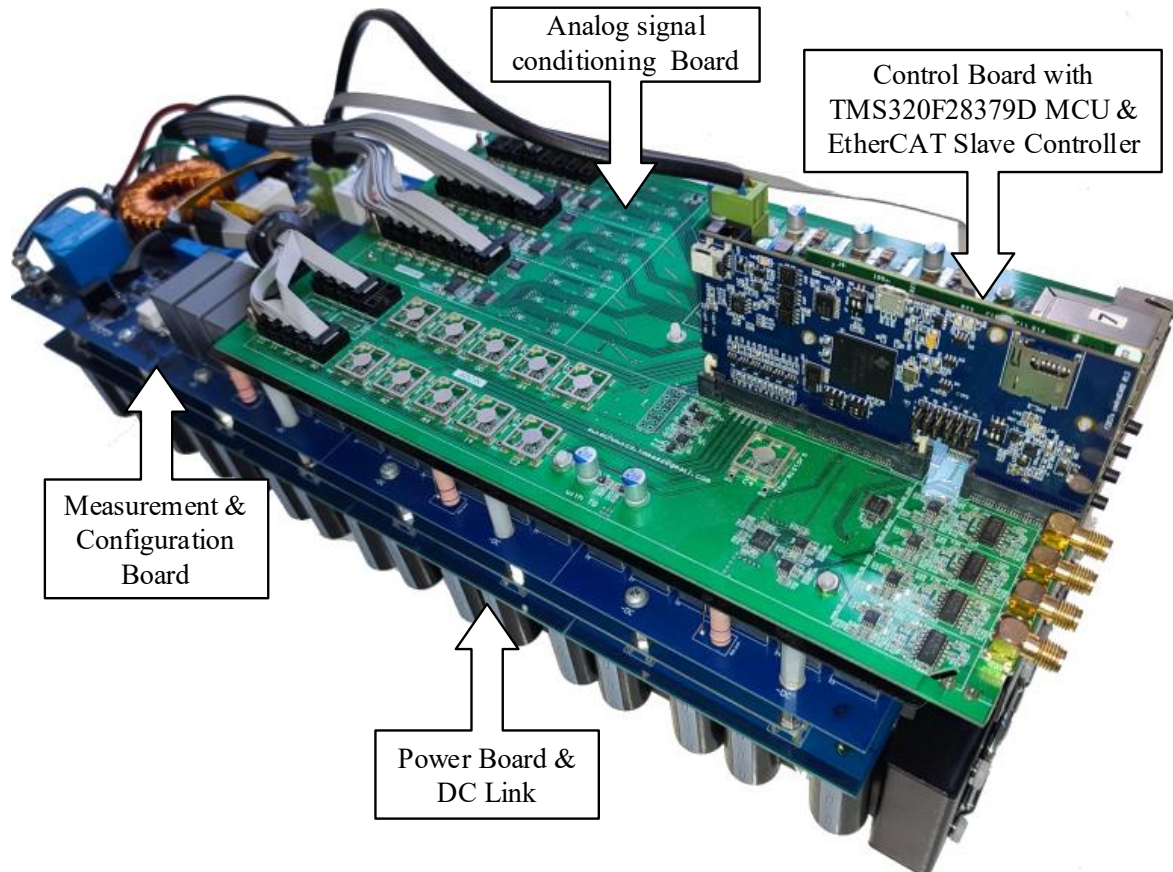
Figure 112. DC/AC power converter module.

7.2.2. Power Board

The power circuit consists of the following components:

- four T-type branches with LC output filters where all capacitors are star-connected. The current is measured at the choke and the voltage at the LC filter capacitor. Behind the LC filters are contactors that switch the filtered branches to the AC mains. Then, after switching contactors, some contactors switch the branch between phases. Due to the test nature of the bench, the number of switches is reduced, only allowing the branch switching scenarios to be tested in single-phase (phase-neutral) or inter-phase (phase-to-phase) mode,
- all branches are connected to a common DC circuit with two electrolytic capacitors connected in series. Connected to the capacitors are two contactors that connect the

module to the DC grid and one contactor that connects the DC midpoints of the modules,

- the gate drivers are equipped with transistor fault detection systems.
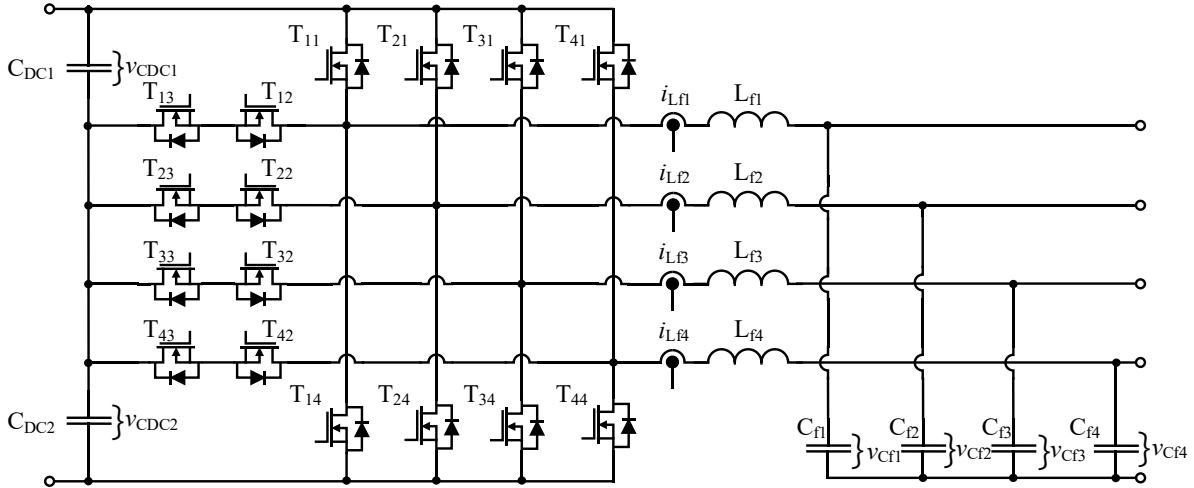
Figure 113. Power board schematic

7.2.3. Control board of DC/AC module

The centerpiece of the DC/AC module control board is the TMS320F28379D microcontroller from Texas Instruments, located on the Control Card evaluation kit (**Figure 114**). An extension with an ET1100 ASIC implementing the EtherCAT Slave physical layer is included.

Following microcontroller resources are used (**Figure 115**):

- currents and voltages are measured using a 10 channels SAR ADC with differential signals,
- 8 complementary PWM channels are used to control the 16 transistors,
- 17 digital outputs for switch control,
- 16 digital inputs for driver fault detection.
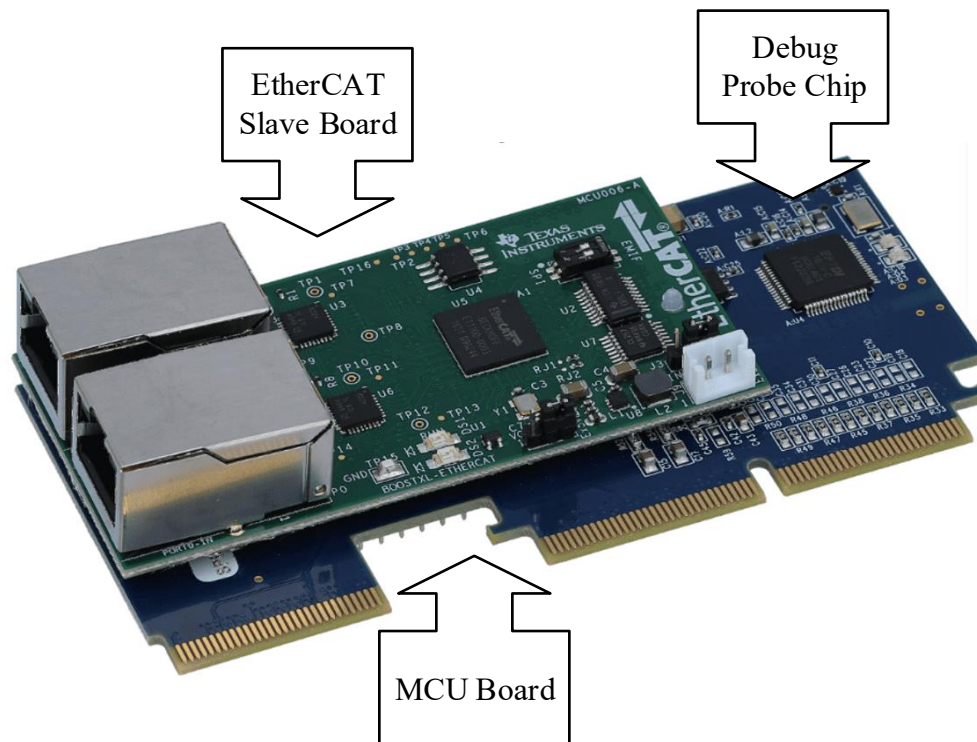
Figure 114. TMDSECATCNCD379D EtherCAT Slave and C2000 Delfino MCU control CARD Kit.
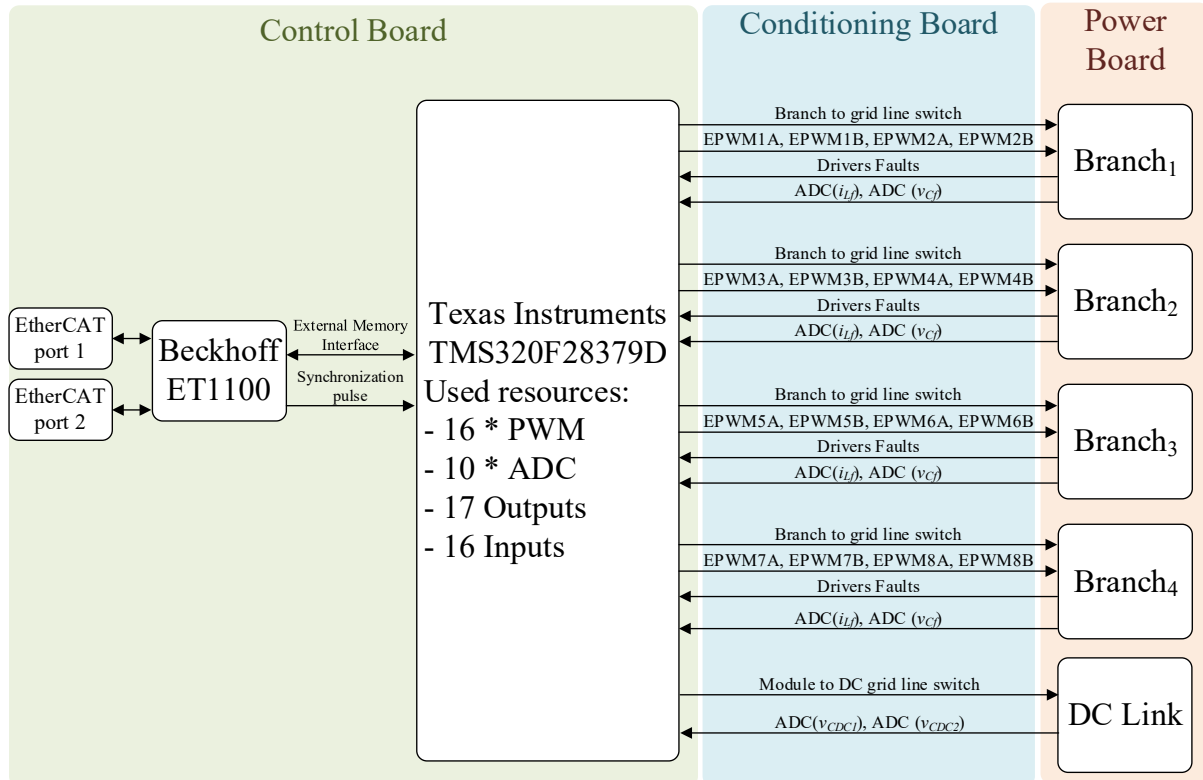
Figure 115. Control board signal diagram.

7.2.4. Central control unit for distributed control

As the central controller, a Beckhoff IPC6015 industrial computer (**Figure 116**) was used to control applications with the EtherCAT grid due to its efficiency, reliability, and scalability. The IPC6015 is equipped with 4 Intel Atom cores operating at a frequency of 1.6GHz, which provides adequate computing power to control the EtherCAT grid. EtherCAT is a high-speed industrial grid that enables effective real-time data transfer, crucial in many industrial applications. A dedicated TwinCAT 3 environment for Beckhoff was used to configure the grid and program the central controller. TwinCAT 3 is based on Windows and provides an easy user interface and development tools that facilitate the development of industrial applications.

Figure 116. Beckhoff Industrial PC 6015.

References

[1] N. B. Arias, S. Hashemi, P. B. Andersen, C. Træholt and R. Romero, "Distribution System Services Provided by Electric Vehicles: Recent Status, Challenges, and Future Prospects," *IEEE Transactions on Intelligent Transportation Systems,* vol. 20, no. 12, pp. 4277-4296, December 2019.

[2] Y. Liu, L. Wu and J. Li, "Peer-to-peer (P2P) electricity trading in distribution systems of the future," *The Electricity Journal,* no. 32, pp. 2-6, 2019.

[3] S. Karytsas, I. Vardopoulos and E. Theodoropoulou, "Factors Affecting Sustainable Market Acceptance of Residential Microgeneration Technologies. A Two Time Period Comparative Analysis," *Energies,* vol. 12, no. 17, 2019.

[4] M. Sandelic, S. Peyghami, A. Sangwongwanich and F. Blaabjerg, "Reliability aspects in microgrid design and planning: Status and power electronics-induced challenges," *Renewable and Sustainable Energy Reviews,* vol. 159, no. 112127, May 2022.

[5] F. Czepło and P. Borowski, "Innovation Solution in Photovoltaic Sector," *Energies,* vol. 17, no. 1, p. 265, 2024.

[6] N. Shabbir, L. Kutt, V. Astapov, O. Husev, R. Ahmadiahangar, F. Wen and K. Kull , "Congestion control strategies for increased renewable penetration of photovoltaic in LV distribution networks," *Energy Reports,* vol. 8, no. 16, pp. 217-223, December 2022.

[7] M. A. Judge, A. Khan, A. Manzoor and H. A. Khattak, "Overview of smart grid implementation: Frameworks, impact, performance and challenges," *Journal of Energy Storage,* vol. 49, May 2022.

[8] J. E. Huber and J. W. Kolar, "Applicability of Solid-State Transformers in Today's and Future Distribution Grids," *IEEE Transactions on Smart Grid ,* vol. 10, no. 1, pp. 317-326, 10 August 2017.

[9] M. Kolenc, I. Papič and B. Blažič, "Minimization of Losses in Smart Grids Using Coordinated," *Energies,* vol. 5, no. 10, pp. 3768-3787, 2012.

[10] C. Feng, F. Wen, S. You, Z. Li, F. Shahnia and M. Shahidehpour, "Coalitional Game-Based Transactive Energy Management in Local Energy Communities," *IEEE Transactions on Power Systems,* vol. 35, no. 3, pp. 1729 - 1740, 4 May 2020.

[11] Y. Kabalci, "A survey on smart metering and smart grid communication," *Renewable and Sustainable Energy Reviews,* vol. 57, pp. 302-318, May 2016.

[12] R. Rosso, X. Wang, M. Liserre, X. Lu and S. Engelken, "Grid-forming converters: an overview of control approaches and future trends," in *2020 IEEE Energy Conversion Congress and Exposition (ECCE)*, Detroit, MI, USA, 2020.

[13] Z. Shuai, Y. Sun, Z. J. Shen, W. Tian, C. Tu, Y. Li and X. Yin, "Microgrid stability: Classification and a review," *Renewable and Sustainable Energy Reviews,* vol. 58, pp. 167-179, 2016.

[14] E. Karfopoulos and N. Hatziargyriou, "Distributed Coordination of Electric Vehicles Providing V2G Services," *IEEE Transactions on Power Systems,* vol. 31, no. 1, pp. 329 - 338, January 2016.

[15] X. Meng, J. Liu and Z. Liu, "A Generalized Droop Control for Grid-Supporting Inverter Based on Comparison Between Traditional Droop Control and Virtual Synchronous Generator Control," *IEEE Transactions on Power Electronics,* vol. 34, no. 6, pp. 5416 - 5438, 2019.

[16] S. Giacomuzzi, M. Langwasser, G. De Carne, G. Buja and M. Liserre, "Smart transformer-based medium voltage grid support by means of active power control," *CES Transactions on Electrical Machines and Systems ,* vol. 4, no. 4, pp. 285 - 294, 2020.

[17] L. F. Costa, G. De Carne, G. Buticchi and M. Liserre, "The Smart Transformer: A solid-state transformer tailored to provide ancillary services to the distribution grid," *IEEE Power Electronics Magazine,* vol. 4, no. 2, pp. 56-67, June 2017.

[18] M. Liserre, G. Buticchi, M. Andresen, G. De Carne, L. F. Costa and Z.-X. Zou, "The Smart Transformer: Impact on the Electric Grid and Technology Challenges," *IEEE Industrial Electronics Magazine,* pp. 46-58, 22 June 2016.

[19] L. Zheng, A. Marellapudi, V. R. Chowdhury, N. Bilakanti, R. P. Kandula, M. Saeedifard, S. Grijalva and D. Divan, "Solid-State Transformer and Hybrid Transformer With Integrated Energy Storage in Active Distribution Grids: Technical and Economic Comparison, Dispatch, and Control," *IEEE Journal of Emerging and Selected Topics in Power Electronics,* vol. 10, no. 4, pp. 3771-3787, August 2022.

[20] O. S. Neffati, S. Sengan, K. D. Thangavelu, S. D. Kumar, R. Setiawan, M. Elangovan, D. Mani and P. Velayutham, "Migrating from traditional grid to smart grid in smart cities promoted in developing country," *Sustainable Energy Technologies and Assessments,* vol. 45, 2021.

[21] R. Rosso, X. Wang, M. Liserre, X. Lu and S. Engelken, "Grid-Forming Converters: Control Approaches, Grid-Synchronization, and Future Trends—A Review," *IEEE Open Journal of Industry Applications,* vol. 2, pp. 93-109, 2021.

[22] J. Jia, G. Yang and A. H. Nielsen, "A Review on Grid-Connected Converter Control for Short-Circuit Power Provision Under Grid Unbalanced Faults," *IEEE Transactions on Power Delivery,* vol. 33, no. 2, pp. 649-661, 2018.

[23] A. Ramy and T. O'Donnel, "Analysis and mitigation of harmonic resonances in multi–parallel grid–connected inverters: A review," *Energies,* p. 5438, 27 July 2022.

[24] P. D. Burlacu, L. Mathe, M. Rejas, H. Pereira, A. Sangwongwanich and R. Teodorescu, "Implementation of fault tolerant control for modular multilevel converter using EtherCAT communication," in *2015 IEEE International Conference on Industrial Technology (ICIT)*, Seville, Spain, 2015.

[25] S. Bayhan and K. Hasan, "Sliding-Mode Control Strategy for Three-Phase Three-Level T-Type Rectifiers With DC Capacitor Voltage Balancing,," *IEEE Access,* vol. 8, pp. 64555-64564, 2020.

[26] L. Vancini, M. Mengoni, G. Rizzoli, L. Zarri and T. Alberto, "Voltage Balancing of the DC-Link Capacitors in Three-Level T-Type Multiphase Inverters," *IEEE Transactions on Power Electronics,* vol. 37, no. 6, pp. 6450-6461, 2022.

[27] K. Sun, X. Wang, Y. W. Li and F. Nejabatkhah, "Parallel Operation of Bidirectional Interfacing Converters in a Hybrid AC/DC Microgrid Under Unbalanced Grid Voltage Conditions,," *IEEE Transactions on Power Electronics,* vol. 32, no. 3, pp. 1872-1884, 2017.

[28] R. Billinton and N. A. Ronald, Reliability evaluation of engineering systems, vol. 792, New York: Plenum press, 1992.

[29] H. Wang and F. Blaabjerg, "Power Electronics Reliability: State of the Art and Outlook," *IEEE Journal of Emerging and Selected Topics in Power Electronics,* vol. 9, no. 6, pp. 6476 - 6493, December 2021.

[30] S. Rahimpour, H. Tarzamni, N. V. Kurdkandi, O. Husev, D. Vinnikov and F. Tahami, "An Overview of Lifetime Management of Power Electronic Converters," *IEEE Access,* vol. 10, pp. 109688-109711, 2022.

[31] W. Zhang, D. Xu, P. Enjeti, H. Li, J. Hawke and H. Krishnamoorthy, "Survey on Fault-Tolerant Techniques for Power Electronic Converters," *IEEE Transactions on Power Electronics,* vol. 29, no. 12, pp. 6319 - 6331, December 2014.

[32] X. J. Yi, J. Shi and M. Hui-Na, Goal Oriented Methodology and Applications in Nuclear Power Plants, London: Elsevier, 2019.

[33] F. Richardeau and T. T. L. Pham, "Reliability Calculation of Multilevel Converters: Theory and Applications," *IEEE Transactions on Industrial Electronics ,* vol. 60, no. 10, pp. 4225 - 4233, 2013.

[34] J. Poon, P. Jain, I. Konstantakopoulos, C. Spanos, S. K. Panda and S. Sanders, "Model-Based Fault Detection and Identification for Switching Power Converters," *IEEE Transactions on Power Electronics,* vol. 32, no. 2, pp. 1419 - 1430, 2017.

[35] S. Rahimpour, H. Tarzamni, N. V. Kurdkandi, O. Husev, D. Vinnikov and F. Tahami, "An Overview of Lifetime Management of Power Electronic Converters," *IEEE Access,* vol. 10, pp. 109688 - 109711, 2022.

[36] M. Malinowski, K. Mozdzynski, T. Gajowik and S. Stynski, "Fault Tolerant Smart Transformer in Distributed Energy Systems," in *NEIS 2019; Conference on Sustainable Energy Supply and Energy Storage Systems*, Hamburg, Germany, 2019.

[37] M. Takongmo, C. Zhang, S. Wdaan, W. Telmesani, D. Yapa and J. Salmon, "Parallel-Connected Voltage Source Converters With a DC Common Mode and an AC Differential Mode PWM Filter," *IEEE Transactions on Power Electronics,* vol. 38, no. 3, pp. 3664-3675, 2023.

[38] M. Priya, P. Pathipooranam and K. Muralikumar, "Modular-multilevel converter topologies and applications–a review.," *IET Power Electronics,* vol. 12, no. 2, pp. 170-183, 2019.

[39] Z. Dong, R. Ren and F. Wang, "Development of High-Power Bidirectional DC Solid-State Power Controller for Aircraft Applications," *IEEE Journal of Emerging and Selected Topics in Power Electronics,* vol. 10, no. 5, pp. 5498-5508, 2021.

[40] B. Wei, J. M. Guerrero, J. C. Vasquez and X. Guo, "A Circulating-Current Suppression Method for Parallel-Connected Voltage-Source Inverters With Common DC and AC Buses," *IEEE Transactions on Industry Applications,* vol. 53, no. 4, pp. 3758-3769, July-Aug 2017.

[41] M. Lu, X. Wang, P. C. Loh and F. Blaabjerg, "Interaction and aggregated modeling of multiple paralleled inverters with LCL filter," *IEEE Energy Conversion Congress and Exposition (ECCE),* pp. 1954-1959, 2015.

[42] F. Cecati, M. Andresen, R. Zhu, Z. Zou and M. Liserre, "Robustness Analysis of Voltage Control Strategies of Smart Transformer," *IECON 2018 - 44th Annual Conference of the IEEE Industrial Electronics Society,* pp. 5566-5573, 2018.

[43] A. Adib, F. Fateh and B. Mirafzal, "A Stabilizer for Inverters Operating in Grid-Feeding, Grid-Supporting and Grid-Forming Mode," in *IEEE Energy Conversion Congress and Exposition (ECCE)*, Baltimore, MD, USA, 2019.

[44] Y. Li, D. M. Vilathgamuwa and P. C. Loh, "Microgrid power quality enhancement using a three-phase four-wire grid-interfacing compensator," *Applications, IEEE Transactions on Industry,* vol. 41, no. 6, pp. 1707-1719, 2005.

[45] A. K. Jindal, A. Ghosh and J. Avinash, "Interline Unified Power Quality Conditioner," *IEEE Transactions on Power Delivery,* vol. 22, no. 1, pp. 364-372, 2007.

[46] M. Sędłak, Czterogałęziowe przekształtniki trójpoziomowe dla energetyki odnawialnej. Analiza, modulacja i sterowanie, Warszawa: Politechnika Warszawska, 2014.

[47] K. Ndirangu, H. D. Tafti and J. Fletcher, "Impact of Grid Voltage and Grid-Supporting Functions on Efficiency of Single-Phase Photovoltaic Inverters," *IEEE Journal of Photovoltaics,* vol. 12, no. 1, pp. 421-428, 2022.

[48] D. Rathnayake, M. Akrami, C. Phurailatpam, S. Hadavi, G. Jayasinghe, S. Zabihi and B. Bahrani, "Grid Forming Inverter Modeling, Control, and Applications," *IEEE Access,* vol. 9, pp. 114781-114807, 2021.

[49] W. Alhosaini, F. Diao, M. H. Mahmud, Y. Wu and Y. Zhao, "A Virtual Space Vector-Based Model Predictive Control for Inherent DC-Link Voltage Balancing of Three-Level T-Type Converters," *IEEE Journal of Emerging and Selected Topics in Power Electronics,* vol. 9, no. 2, pp. 1751-1764, 2021.

[50] . A. Tarique, Z. Lin, M. Waseem and S. Liu, "Review on optimization methodologies in transmission network reconfiguration of power systems for grid resilience," *International Transactions on Electrical Energy Systems,* vol. 31, no. 3, 2020.

[51] W. Yao, J. Liu and Z. Lu, "Distributed Control for the Modular Multilevel Matrix Converter," *Transactions on Power Electronics,* vol. 34, no. 4, pp. 3775-3788, 2019.

[52] Y. Wei Li, "Control and Resonance Damping of Voltage-Source and Current-Source Converters With LC Filters," *IEEE Transactions on Industrial Electronics ,* vol. 56, no. 5, pp. 1511 - 1521, 2009.

[53] H. Yang, H. Lin, Y. Lu and X. Wang, "A multi-resonant PR inner current controller design for reversible PWM rectifier," in *Twenty-Eighth Annual IEEE Applied Power Electronics Conference and Exposition (APEC)*, Long Beach, CA, USA, 2013.

[54] C. Xie, X. Zhao, K. Li, J. Zou and J. Guerrero, "A New Tuning Method of Multiresonant Current Controllers for Grid-Connected Voltage Source Converters," *IEEE Journal of Emerging and Selected Topics in Power Electronics,* vol. 7, no. 1, pp. 458-466, 2019.

[55] M. Merai, M. W. Naouar, I. Slama-Belkhodja and E. Monmasson, "Grid connected converters as reactive power ancillary service providers: Technical analysis for minimum required DC-link voltage," *Mathematics and Computers in Simulation,* vol. 158, pp. 344-354, 2019.

[56] F. Hassan, A. Kumar and A. Pati, "Recent Advances in Phase Locked Loops for Grid Connected Systems: A Review," in *IEEE Delhi Section Conference (DELCON)*, Delhi, 2022.

[57] A. Akhavan, H. R. Mohammadi and J. M. Guerrero, "Modeling and design of a multivariable control system for multi-paralleled grid-connected inverters with LCL filter," *International Journal of Electrical Power & Energy Systems,* vol. 94, pp. 354-362, 2018.

[58] T. D. Busarello, J. A. Pomilio and M. G. Simoes, "Design Procedure for a Digital Proportional-Resonant Current Controller in a Grid Connected Inverter," in *IEEE 4th Southern Power Electronics Conference (SPEC)*, Singapore, 2018.

[59] S. Bacha, I. Munteanu and A. I. Bratcu, Power Electronic Converters Modeling and Control, London: Springer-Verlag, 2014.

[60] H.-S. Kim, M.-H. Ryu, J.-W. Baek and J.-H. Jung, " High-Efficiency Isolated Bidirectional AC–DC Converter for a DC Distribution System," *Power Electronics, IEEE Transactions on,* vol. 28, pp. 1642-1654, 2012.

[61] T. Ericsen, "Power Electronic Building Blocks-a systematic approach to power electronics," in *2000 Power Engineering Society Summer Meeting (Cat. No.00CH37134)*, Seattle, 2000.

[62] H. Ginn, N. Hingorani, J. Sullivan and R. Wachal, "Control Architecture for High Power Electronics Converters," *Proceedings of the IEEE,* vol. 103, no. 12, pp. 2312-2319, 2015.

[63] J. Robert, J.-P. Georges,, E. Rondeau and T. Divoux, "Minimum cycle time analysis of Ethernet-based real-timeprotocols," *International Journal of Computers, Communications and Control,* vol. 7, no. 4, pp. 743-757, 2012.

[64] P. Danielis, J. Skodzik, V. Altmann, E. B. Schweissguth, F. Golatowski, F. Timmermann and J. Schacht, "Survey on real-time communication via ethernet in industrial automation environments," in *Proceedings of the 2014 IEEE Emerging Technology and Factory Automation (ETFA)*, Barcelona, Spain, 2014.

[65] M. Wollschlaeger, T. Sauter and J. Jasperneite, "The Future of Industrial Communication: Automation Networks in the Era of the Internet of Things and Industry 4.0," *IEEE Industrial Electronics Magazine,* vol. 11, no. 1, pp. 17-27, 2017.

[66] J. H. Fey, F. Hinrichsen, G. Carstens and R. Mallwitz, "Development of a Modular Multilevel Converter Demonstrator with EtherCAT Communication," in *IEEE 13th International Conference on Compatibility, Power Electronics and Power Engineering (CPE-POWERENG)*, Sonderborg, Denmark, 2019.

[67] T. Maruyama and T. Yamada, "Communication architecture of EtherCAT master for high-speed and IT-enabled real-time systems.," in *2015 IEEE 20th Conference on Emerging Technologies & Factory Automation (ETFA)*, Luxembourg, 2015.

[68] P. D. Burlacu, L. Mathe, M. Rejas, H. Pereira, A. Sangwongwanich and R. Teodorescu, "Implementation of fault tolerant control for modular multilevel converter using EtherCAT communication," in *2015 IEEE International Conference on Industrial Technology (ICIT)*, Seville, 2015.

[69] S. Rahimpour, H. Tarzamni, N. V. Kurdkandi, O. Husev, D. Vinnikov and F. Tahami, "An Overview of Lifetime Management of Power Electronic Converters," *IEEE Access,* vol. 10, pp. 109688-109711, 2022.

List of Figures

List of tables